INFORMATION TO USERS

This manuscript has been reproduced from the microfilm master. UMI films the text directly from the original or copy submitted. Thus, some thesis and dissertation copies are in typewriter face, while others may be from any type of computer printer.

The quality of this reproduction is dependent upon the quality of the copy submitted. Broken or indistinct print, colored or poor quality illustrations and photographs, print bleedthrough, substandard margins, and improper alignment can adversely affect reproduction.

In the unlikely event that the author did not send UMI a complete manuscript and there are missing pages, these will be noted. Also, if unauthorized copyright material had to be removed, a note will indicate the deletion.

Oversize materials (e.g., maps, drawings, charts) are reproduced by sectioning the original, beginning at the upper left-hand corner and continuing from left to right in equal sections with small overlaps.

ProQuest Information and Learning
300 North Zeeb Road, Ann Arbor, MI 48106-1346 USA
800-521-0600

Solvent Extraction and Liquid Membrane Separation of Rhodium

by

Seyed N. Ashrafizadeh

Department of Mining and Metallurgical Engineering

McGill University

Montreal, Quebec, Canada

July 1996

A thesis submitted to the Faculty of Graduate Studies and Research in partial fulfillment of the requirements for the degree of Doctor of Philosophy

In the name of God, the Compassionate, the Merciful

And Say: My Lord! Let my entry be by the gate of truth and honour, and likewise my exit by the gate of truth and honour: and grant me from thy presence an authority to aid (me).

The Glorious Qur'an (17. 80)

To those who gave up all, that we may thrive today

ABSTRACT

The aim of this work was to develop a viable solvent-extraction based system for the separation of rhodium (Rh) from aqueous chloride solutions. Ultimately, two different systems were developed. Kelex 100, a commercially available derivative of 8-hydroxyquinoline, was used as the extractant reagent in both of these systems. One of the systems involved the supported liquid membrane (SLM) extraction of Rh. In this system a very thin microporous "Gore-Tex" polymer sheet, impregnated with an organic solution of Kelex 100, served as the SLM. The other system involved the conversion of the chloro-complexes of Rh to bromocomplexes prior to their solvent extraction with Kelex 100.

The results of the lab-scale experiments using a SLM of Kelex 100 having a surface area of 44 cm^2 are reported. The optimum conditions for Rh permeation were found as a feed solution of 2.5 M HCl and a strip solution of 0.1 M HCl. The SLM was quite stable at the optimum conditions with no sign of organic loss or membrane deterioration after 72 hours of operation. It was determined that the HCl activity gradient across the membrane acts as the driving force that "pumps" the non-aquated Rh chlorocomplexes against their concentration gradient. The mechanism of Rh permeation was the ion-pair formation between the protonated Kelex 100 and $RhCl_6^{3-}$ complexes. The rate of Rh permeation was in the order of 10^{-6} $mol.m^{-2}.s^{-1}$. The mechanism of HCl and H_2O permeation, which were co-extracted along with Rh chlorocomplexes, were found to be the hydration of protons at the low feed acid region and the formation of microemulsions at the high feed acid region. The permeated acid and water were separated from the SLM receiving phase by contacting the latter phase with an organic solution of trioctylamine (TOA). The chlorocomplexes of Rh(III) and acid are readily extracted to the TOA organic phase and subsequently subjected to differential stripping with a concentrated solution of Cl^- and a mild NaOH solution, respectively. By interfacing the TOA solvent extraction with the SLM of Kelex 100 highly concentrated solutions of Rh (at least 10 times the initial concentration) and raffinates essentially free of rhodium were produced.

The UV-Visible investigations revealed that the bromocomplexes of Rh undergo aquation to a much lesser extent than that of the chlorocomplexes. The chlorocomplexes of Rh were converted to bromocomplexes by precipitating first the $Na(NH_4)_2Rh(NO_2)_6$ salt and subsequently dissolving that in an HBr solution. The newly formed bromocomplexes of Rh(III) responded very favorably to extraction with Kelex 100. Relatively high distribution coefficients, about 20, and very steep extraction isotherms were generated. The freshly loaded Kelex 100 organic was efficiently stripped upon contact with a strip solution of 6-8 M HCl and a contact time of 10-12 hours. The developed system shows high promise from a practical implementation point of view.

RÉSUMÉ

Le but de cette étude était de développer un système d'extraction par solvant pour la séparation du rhodium, à partir de solution aqueuse de chlorure. A la fin, deux systèmes ont été developpés. Kelex 100, un dérivé du 8-hydroxyquinoline qui est disponible commercialement, a été utilisé pour ces deux systèmes. Le premier système emploie une membrane liquide supporté (MLS) pour extraire le rhodium. Le MLS était une très mince feuille, microporeuse de "Gore-Tex" polymère, impregnée de Kelex 100. L'autre système utilise la conversion des chlorocomplexes du rhodium en bromocomplexes avant l'extraction par solvent avec le Kelex 100.

Les résultats des experiences de laboratoire avec le MLS, ayant une aire de surface de 44 cm^2, sont rapportés. Les conditions optimal pour la perméation du rhodium sont une solution d'alimentation de 2.5 M HCl, et une solution de ré-extraction de 0.1 M HCl. Le MLS été trouvé être stable, montrant aucun signe de perte d'organique ou de déterioration après 72 heures d'opération. Il a été déterminé que c'est de gradient d'activité du HCl qui cause la mobilité des complexes non-hydraté du rhodium à travers le MLS. Le méchanisme de transfert est la formation de paire. d'ions entre le Kelex 100 protoné et le rhodium. La vitesse de perméation du rhodium est d'a peu près 10^{-6} $mol.m^{-2}.s^{-1}$. Le méchanisme de perméation du HCl et du H_2O implique l'hydration des protons à de basses acidités et la formation de microemulsions à de hautes acidités. L'eau et l'acide ont étés séparer de la solution de ré-extraction à l'aide d'une solution organique d'amine trioctyl (TOA). L'acide et les chlorocomplexes du rhodium ont été extrait avec le TOA et ensuite re-extrait avec une solution de NaOH et une de chlore concentré, respectivement. En inter façant l'extraction par solvant avec le TOA et le MLS, des solutions concentrés en rhodium (au moins 10 fois plus que la solution initiale) ont été obtenues.

La spéctroscopie UV-Visible a révelé que les bromocomplexes du rhodium sont moins suseptible de formé des complexes avec H_2O que les chlorocomplexes. Ces derniers sont donc convertis en bromocomplexes en precipitant $Na(NH_4)_2Rh(NO_2)_6$ et ensuite en dissouant ce dernier dans une solution de HBr. Les bromocomplexes répondent bien envers d'extraction avec le Kelex 100. De haut coefficient de distribution (à peu près 20) et un bon isotherme d'extraction ont été génerés. Le Kelex 100 a été éfficacement re-extrait sur contact avec une solution de 6-8 M HCl, pendant 10-12 heures. Ce système montre une grande promesse vis-à-vis l'implémentation practique.

ACKNOWLEDGEMENTS

This research would not be complete without recognizing the contributions of several individuals whose names do not appear on the title page. I am especially indebted to:

- My supervisor, Professor George P. Demopoulos, for his enthusiasm, interest, encouragement, criticism and useful suggestions throughout the course of this work.

- Professor I.S. Butler of the Department of Chemistry, McGill University, for his points on Coordination Chemistry and UV-Visible spectroscopy; Professor T. van de Ven and his research group of the Department of Chemical Engineering, McGill University, for their help in conducting light scattering measurements; and Professor B.E. Mann of Department of Chemistry, Scheffild University, for discussions on NMR spectroscopy.

- W.L. Gore & Associates, Inc., for providing the GORE-TEX polymer membranes; WITCO Co. for supplying Kelex 100; and the Natural Sciences and Research Council of Canada for partial financial support.

I gatefully acknowledge the department secreterial staff, Carol Rousseau and Jeanne Gould, for their assistance; Jean Dumont, Nabil Habib, and Ed Siliauskas of the Department of Chemical Engineering for their help with experimental supplies and technical assistance; Elyse Benguerel for translating the abstract into French and proofreading part of the thesis; my fellow graduate students in the hydrometallurgy group and in Workman Wing, Aloysio, David, Raff, Terry, and Shang for their friendship; and especially my good friends Mohammad K. Khoshkbarchi and Elias El-Ammouri for their encouragement, and many fruitful discussions.

I would like to extend my appreciation to the Ministry of Culture and Higher Education of the Islamic Republic of Iran for making my postgraduate studies possible.

Lastly but far from least, I am indebted to my wife, Z. Alavi, for her support, understanding, and patience during a time of unusual neglect; and to my lovely little sons, Mehdi and Masoud, who have also been patiently awaiting my "return".

TABLE OF CONTENTS

CHAPTER 4 The Rh(III)-HCl-Kelex 100 Solvent Extraction System

CHAPTER 5 Extraction of Rh Chlorocomplexes and Acid Through a Supported Liquid Membrane of Kelex 100

CHAPTER 6 Extraction and Separation of HCl and Rh(III) from the SLM Strip Solution with Trioctylamine

CHAPTER 7 Formation of Rhodium Bromocomplexes and Their Extraction with Kelex 100

LIST OF FIGURES

LIST OF TABLES

NOMENCLATURE

Abbreviations

AA	Atomic Absorption Spectroscopy
A/O	Aqueous/Organic Volume Ratio
ELM	Emulsion Liquid Membrane
HLB	Hydrophilic Lipophilic Balance
ID	Internal Diameter
IX	Ion Exchange
LM	Liquid Membrane
MIBK	Methylisobutylketone
PGM	Platinum Group Metals
PM	Precious Metals
PP	Polypropylene
PTFE	Polytetrafluoroethylene
PVDF	Polyvinylidenefluoride
R-HQ	R-Substituted 8-Hydroxyquinoline
8-HQ	8-Hydroxyquinoline
SLM	Supported Liquid Membrane
SX	Solvent Extraction
TBP	Tributylphosphate
TOA	Tri-n-octylamine
TOPO	Trioctylphosphine oxide
W/O	Water in Oil Emulsion
— (overbar)	Organic Phase Characteristics

Nomenclature

a	Activity
B	Parameter of Meissner Equation
C	Concentration, mole/L
D	Diffusion Coefficient, m^2/s
D	Distribution Coefficient (defined in the text; Eq. 4.8)
J	Rate of Permeation, $mole/m^2.s$
I	Ionic Strength, molality
K	Chemical-Reaction Equilibrium Constant
k	Mass Transfer Coefficient, m/s
k	Chemical-Reaction Rate Constant
M	Molarity, mole/L
m	Molality, mole/kg solvent
n	Number of moles
P	Permeation Coefficient, m/s
ppm	Part per million, mg/L
q	Parameter of Meissner Equation
r	Radius of the Diffusing Species, m
S	Surface Area, m^2
t	Time, s
T	Absolute Temperature, K
V	Volume, m^3
W	Molecular Weight, kg/kg-mole
x	Distance, m
Y	Enrichment Factor (defined in the text; Eq. 2.14)

Greek Letters

Γ	Reduced Activity Coefficient
Γ^*	Parameter of Missner Equation
γ	Activity Coefficient in Molality Scale
Δ	Gradient of the Property
δ	Thickness, m
ε	Porosity (surface area of pores/suface area of membrane), %
τ	Tortuosity (length of pores/thickness of membrane), m/m
ρ	Density, g/cm^3
Ψ	Solvent Association Factor, $m^4/K.s^2$
η	Viscosity, kg/m.s
κ	Boltzmann Constant, 1.380662×10^{-23} J/molecule.K

Subscripts

a	Aqueous Stagnant Layer
B	Base
b	Bulk
f	Feed
i	Interface
m	Membrane
O	Overall
o	Organic Phase
r	Reaction
s	Strip
sol	Solvent
°	Initial Value
+	Cation
−	Anion
±	Mean Value

CHAPTER 1

INTRODUCTION

1.1 INTRODUCTION

Rhodium (Rh) is one of the platinum group metals (PGM) which include Pt, Pd, Ru, Rh, Ir, and Os. Pt and Pd are the primary PGM and Ru, Rh, Ir, and Os are the secondary PGM. Together with gold and silver, the PGM form the family of precious metals (PM). Since the PGM occur together along with base metals, it is important to devise techniques to separate them and to purify and recover each of the metals separately. According to Grant (1990), amongst the separation processes applied for the PGM, development of a viable separation process for rhodium is one of the most difficult aspects in the refining industry of the precious metals.

Separation and recovery of Rh, like other PGM, has traditionally been achieved through a series of precipitation-dissolution steps followed by calcination to produce pure metal or sponge (Ohrbach, et al., 1988). This traditional method, however, is no longer considered efficient in terms of the degree of separation, yields and complexity of operation. To meet today's challenges, the PGM industry has largely abandoned the inefficient classical technique and is adopting modern separation methods. The main advantages of such new processes are considered to be lower lock-up of valuable metal inventory due to reduced overall processing time, improved primary yields, reduced process recycles, flexibility and versatility, and capability for continuous operation and process control (Demopoulos, 1986). Among the available separation methods, solvent extraction has proved to be a most suitable and powerful technique.

At McGill University, extensive research in the area of PGM separation has been carried out over the past decade with the aim of developing viable solvent-extraction-based methods. Throughout that research, oxine derivatives (substituted 8-hydroxyquinolines (R-HQ)) have been the extractants of choice. This, in part, has led to the development of a Pt/Pd separation process involving two possible flowsheets (Demopoulos et al., 1987a & b; Coté et al., 1993). As an extension of this work, the solvent extraction (SX) of Rh (III) with R-HQ derivatives and, in particular Kelex 100, was investigated. Direct solvent extraction of Rh(III) with Kelex 100 resulted in very low distribution coefficients (Benguerel et al., 1994). This situation arises mainly because of the complex chemistry of Rh in chloride-containing aqueous solutions. In other words, the complexes formed by Rh(III) undergo aquation and lose their affinity towards the organic extractant. Consequently, conventional solvent extraction, which has been implemented for the recovery of the other PGM, cannot be applied to the direct separation-recovery of Rh from chloride-based solutions.

As a means of overcoming the inefficiency of conventional SX, a novel "catalyzed" SX approach (based on the addition of $SnCl_2$ as an activator) was recently investigated for the recovery of Rh (III). This new system, which is still under critical examination, has been the subject of a recent patent (Demopoulos et al., 1993) and a Ph.D. thesis (Benguerel, 1996). The system, however, is characterized by very complex activation, extraction and stripping chemistry and, as such, imposes significant challenges for implementation in industry.

As a radical departure from the conventional SX-approach, it was decided to examine the potential of using the new method of liquid membrane to address the Rh separation problem. This thesis is the product of this line of investigation.

1.2 THE LIQUID MEMBRANE TECHNIQUE

The liquid membrane (LM) separation technique, first developed by Li (1968), effectively combines into one step the two stages of the solvent extraction process, i.e., solvent extraction and solvent stripping. There are effectively two types of liquid membrane-based separation systems; the Emulsion Liquid Membrane (ELM) system and the Supported Liquid Membrane (SLM) one.

The emulsion liquid membrane system consists of an emulsion, of water-in-oil (W/O) type, stabilized by the aid of a surfactant and dispersed in an external aqueous feed solution (Miesiac et al., 1993). Thus, the extraction process proceeds between the two aqueous phases through the membrane organic phase. The membrane phase contains emulsifier(s) to stabilize the W/O emulsion as well as the appropriate metal extractant, i.e., the metal carrier. The emulsion liquid membrane is thus prepared by first emulsifying the internal (receiving) aqueous phase into the organic solvent and then dispersing this emulsion in the feed (external) aqueous phase. In this way, the three-liquid-system is supported by an emulsion stabilized with the aid of appropriate surface active reagents (for this application called emulsifiers).

In the case of the so-called supported liquid membranes, thin layers of organic solutions containing the extractant reagent are immobilized on microporous inert substrates interposed between the two aqueous solutions and play the same role as the emulsion (Danesi, 1984). The substrates can be in the form either of flat sheets forming the divider in a multi-compartment cell, or of hollow fibers with porous walls packed into modules.

According to proponents of LM technology, liquid membrane extraction, in which the extraction and stripping operations are combined in a single process, has advantages over conventional solvent extraction. Conventional SX is well known as an effective method for the separation and concentration of metal species on an industrial scale. This technique, however, requires a large number of stages in a series of mixer-settlers in order to achieve high purification levels. Another limitation in traditional SX is that a large inventory of solvent and carrier is required. On the other hand, liquid membranes provide a maximum driving force for the transportation of extracted solutes and, as such they have in principle the potential to compete favorably with multistage SX flow diagrams. Furthermore, the organic phase is merely a short-time mediator and hence its capacity is not a very important characteristic. The latter reduces the solvent inventory requirement and thus the capital cost. It also allows the use of expensive and highly selective extractants, which otherwise would be uneconomic in SX, thus rendering this technology more attractive (Flett, 1992). Consequently, the LM process is capable of giving a higher degree of concentration of metal ions in fewer stages while maintaining the high selectivity of the SX. On the other hand, conventional SX can better handle the presence of fine solids or co-extraction of impurities via incorporation of scrubbing procedures.

1.3 THE SCOPE OF THIS WORK

The principal objective of the present work has been to investigate the feasibility of employing liquid membranes to the separation-recovery of rhodium – a metal that has defied all efforts at direct liquid-liquid extraction from chloride solutions (the typical solutions found in the precious metal refining industry). For this investigation, Kelex 100 – an alkylated 8-hydroxyquinoline – was chosen as the metal carrier in liquid membrane. As part of this investigation, the interfacial chemistry of the Rh(III)-HCl-Kelex 100 system was studied, the mass transfer characteristics of Rh(III) complexes across the selected

SLM were established, and finally a conceptual SLM-SX flowsheet for the separation/recovery of rhodium was determined. Moreover, during the course of this investigation, an altogether novel approach to the separation of Rh was identified based on the conversion of the Rh(III) chlorocomplexes to bromocomplexes and the extraction of the latter by solvent extraction using Kelex 100.

The whole this body of research work is presented in this thesis according to the following division in chapters:

Chapter 1 offers a broad introduction into the thesis subject-matter. The objectives and the structure of the thesis are also presented.

Chapter 2 is an extensive literature review of the subject. In this chapter, the traditional methods of separation and recovery of Rh along with the particular chemistry of Rh complexes and recent efforts which have been made to develop modern flowsheets are reviewed. Various technical aspects of liquid membranes are also reviewed, and the important issues encountered in LM technology such as stability, membrane structure and properties, and process modeling and implementation discussed.

Chapter 3 gives a description of the experimental methodology. This includes materials and methods, the experimental set up for both SX and LM experiments and the analytical methods.

In Chapter 4, the aqueous and interfacial chemistry of the Rh/Kelex 100 system is examined from the standpoint of SX of rhodium. In particular the microemulsion-bearing organic phase of Kelex 100 is characterized and the role of W/O microemulsion formation in promoting aquation of rhodium chlorocomplexes is elucidated.

In Chapter 5, the general transport behavior of Rh complexes through the SLM of Kelex 100 is presented, and the transport rates of $RhCl_6^{3-}$, H_2O, and HCl reported. The mechanism of Rh(III) transport through the SLM is fully investigated and the parameters affecting the kinetics of the transport critically discussed.

In Chapter 6, the extraction of HCl and Rh from the SLM strip liquors by trioctylamine is studied as a means of improving the efficiency of the SLM system. Based on the findings of this study, an appropriate flowsheet is advanced for the extraction and separation of rhodium via the interfacing of the SLM system with a conventional SX one. In the same chapter, the aquation of the chlorocomplexes of rhodium is investigated with the aid of UV-Visible spectroscopy.

In Chapter 7, the conversion of the Rh(III) chlorocomplexes to bromocomplexes as an avenue of rendering Rh extractable via conventional solvent extraction with Kelex 100 is described. A conceptual flowsheet of high promise for the precious metal industry is presented.

Chapter 8 completes the thesis with a list of the most important overall conclusions, claims to original contributions to knowledge, and recommendations for future work.

CHAPTER 2

Literature Review

2.1 RHODIUM: NATURAL OCCURRENCE, PRODUCTION, AND APPLICATIONS

Rhodium was discovered by the English chemist William H.Wollaston in 1814 (Benner et al., 1991) and was given its name from the Greek word for rose because of the red color of its trivalent cation salt. Rhodium and other members of platinum group metals are very rare; their concentration in the earth's crust has been estimated by Goldschmidt (1937) to be in the order of 0.001 g/ton (ppm). Even in platinum-rich deposits (e.g., the Merensky Reef in Transvaal, South Africa) where the PGM concentration is several thousand times higher than elsewhere, the latter reaches only 10 ppm. PGM occur in nature associated with the major base metals, iron, copper, nickel, cobalt and a wide range of minor elements such as lead, tellurium, selenium and arsenic. According to Cabri and Naldrett's scheme (1984), the PGM deposits can be classified into two major groups: sulphide association and oxide-silicate association. The sulphide association group is further subgrouped into PGM dominant vs. Ni-Cu dominant. In a different classification, the PGM occurrence is grouped either as native alloys in placer deposits or as lode deposits associated with copper and nickel (Loebenstein, 1985).

About 98% of the world's PGM production comes from three major sources: the Merensky Reef and UG2 gigantic layers of the Bushveld complex in South Africa (50%), the Noril'sk region deposits in former U. S. S. R. (43%), and a minor portion comes from Sudbury, Ontario as a by-product of the Ni-Cu operations of INCO and Falconbridge (Postle et al., 1986). In fact all Soviet (former USSR) and Canadian PGM production is by-product from Ni-Cu mining. Meanwhile, most of the western world's PGM production comes from mines owned by one of the 5 companies, i.e., Rustenburg Platinum Mines, Impala Platinum, Western Platinum, INCO, and Falconbridge. Another significant

portion of the annual production of platinum metals comes from secondary sources including jewelry, laboratory equipment, spent catalysts, old dental alloys, etc., plus sweepings and spillage from refiners and electroplaters. To give an idea about the annual production and consumption of PGM, it is worth mentioning that US consumption in 1994 was about 2.5 million troy ounces, which was equal to about 23% of the total world production (i.e., 10.6 million troy ounces) (Cowley, 1995). Most of the output of the platinum metals find applications in a variety of industries, notably in electrical, chemical and metallurgical engineering, rayon, and glass industries; the luxury applications consume less than a quarter of the total. The very high melting points of these metals and great resistance to corrosion are the factors responsible for much of the industrial demand.

In particular, the variety of numerous applications that Rh itself has found is notable. In addition to its major use for alloying with platinum, rhodium finds application as a coating material because of the hardness and luster of its surface. The plated surface is ideal for the finish of high quality scientific instruments. Rhodium protects metal surfaces of precision apparatuses in corrosive media, such as those used for the measurement of physical constants of corrosive liquids. Another example is the rhodium-plated electrical contacts which are extremely free from contact resistance and find application in components for radio- and audio- frequency circuits. In another application, rhodium compounds have become the catalyst of choice in various industrial and laboratory scale organic reactions (Dickson, 1985). The range of such important organic synthesis reactions is immense, and due to the widespread use of PGM in heterogeneous catalysis, the preparation of different types of catalysts such as extremely small size colloidal particles (Boutonnet et al., 1982) has attracted much interest. But overall, it is the catalytic converter industry (a means of reducing the toxicity of vehicle exhaust gases (Bolinski, 1991)) which has been the largest user of Rh and PGM since the beginning of the 1980's (Carson, 1989). According to Cowley (1995), in 1994 alone, autocatalysts consumed about 30% of the total PGM demand. This is equal to more than 90% of total Rh production in 1994. However, recovery of the PGM from the scrapped converters may also be viewed as a substantial secondary resource. With regard to Rh's high value (i.e.,

about $5000-6000/oz in 1990 and $1000/oz in 1994), which according to Cowley (1995) has almost always been the most expensive element of PGM, and substantial demand in the market, the need to develop an efficient recovery process for Rh remains of great importance.

2.2 BASIC PHYSICAL AND CHEMICAL CHARACTERISTICS OF RHODIUM

Rhodium like other platinum metals, belongs to group VIII in the 6th transition period of the periodic Table. The characteristic feature of Rh, and other platinum metals, is the filling of the 5d electron orbitals in the presence of one "s" electron in the higher (6s) electron orbital. Like all the elements of the 5th and 6th periods, the characteristics of Rh are very different from that of group VIII elements of the 4th period. On the other hand, rhodium has similar chemical properties to the other platinum metals. This has been attributed to the similarity of the configurations of the outer electron subshells in the atoms and the effective atomic radii of the platinum metals. The strongest similarity, however, is observed with iridium, which is located in the same column, while marked differences distinguish rhodium from its adjacent elements, i.e., ruthenium and palladium (Ginzburg et al., 1975).

The physical properties of Rh, though not the main concern of this study, along with its atomic characteristics are listed in Table 2.1 and discussed briefly. Due to the low specific gravity, in comparison with the platinum metals of the 6th period, Rh is classified as a light platinum metal. Similar to osmium, Rh is very hard and brittle and this results in a very low mechanical working performance, however it has the highest thermal and electrical conductivities among the platinum metals. Also, due to the possession of high ionization potential, Rh is very resistant to many chemical reagents at room temperature, such as acids, bases, and the most active nonmetals. Rhodium has a high ability to maintain a low and stable contact resistance owing to the freedom from oxidation films on the surface. For the same reason, the reflectivity of rhodium surfaces is quite high and rhodium is widely used as a durable, highly reflecting surface material (Benner et al., 1991).

Table 2.1: Physical Properties and Atomic characteristics of Rh†

Physical Properties		Atomic Characteristics	
Density	12.41	Atomic number	45
Color	Grayish/Silver white	Configuration of outer electron subshells	$4d^8\ 5s^1$
Specific heat (Cal/g.°C)	0.0591	Atomic weight	102.91
Thermal conductivity [0-100 °C] (cal/cm.sec.°C)	1.50	Number of unpaired electrons	3
Melting point (°C)	1967	Atomic volume ($Å^3$)	8.29
Boiling point (°C)	3827	Effective atomic radius (Å)	1.345
Lattice structure	F.C.C.	Effective ionic radius (Å)	$Rh^{III} = 0.65$
Lattice parametr [20 °C] (Å)	$a = 3.8031$	Ionization potential (V)	$Rh^{III} = 31.05$
Electrical resistivity at 0°C (μΩ.cm)	4.33	Characteristic oxidation state	III
Brinell hardness	100-120	Coordination number	6

†Data from: Ginzburg et al., 1975; Benner et al., 1991.

The main oxidation state of Rh is +III although +I and others are known to exist but at a much lesser extent. This characteristic of having multiple oxidation states is a common feature of all transition elements including the PGM. Furthermore, owing to their large charge, small ionic radii and presence of unfilled "d" orbitals, the platinum metals often form complexes. In fact, all of their compounds in solution, including simple compounds (oxides, halides, etc.), are converted to complex ions. Therefore, the entire analytical chemistry of platinum metals is based on their coordination compounds (Ginzburg et al., 1975).

Rhodium (III) readily forms octahedral complexes, as do most "d^6" configurations, with anions, halides, and oxygen-containing ligands. In fact, six coordination with octahedral geometry is the most widely distributed and encountered of all coordination numbers and, is the most stable configuration for six mutually repelling charges of the same sign (Butler and Harrod, 1989). Accordingly, Rh(III) forms a large number of various octahedral complexes including cationic, neutral, and anionic. The latter complexes, along with the various inorganic and organometallic compounds of Rh, are extensively studied and described in comprehensive texts (Wilkinson, et al., 1987). From that, a number of remarks have been highlighted by Cotton and Wilkinson (1980). One is that the Rh(III) complexes are fairly simple in their magnetic and spectral properties and indeed all

compounds of rhodium (III), are diamagnetic. As well, the cationic and neutral complexes of Rh(III) are generally kinetically inert, while its anionic complexes are usually labile. Also, it has been found that the anionic complexes of rhodium are more labile than those of other PGM.

One characteristic of the compounds of the transition elements that sets them apart from the elements of the main group is their color. As a rough rule, most compounds of the transition elements are colored, whereas most of those of the main groups are not (Cotton and Wilkinson, 1980). This has been attributed to the unfilled d-orbitals of the transition metal ion complexes. As it is described by Butler and Harrod (1989), the energy required to excite an electron in these complexes from a "t_{2g}" to an "e_g" orbital (in octahedral complexes) is often in the range of energy of visible light. Absorption of light can, therefore, induce these electronic transitions, and the colors of many of the metal ion complexes arise from this effect. Different complexes exhibit different absorptivities (required energy to cause the transition) and thus, different colors of the absorbed light. Being a transition element, Rh is not an exception. The visible spectra of Rh(III) complexes in general exhibit two absorption bands toward the blue end of the visible region (see Table 2.2), which are responsible for the characteristic orange, red, yellow, or brown colors of rhodium (III) compounds. This characteristic of the Rh(III) complexes, which is very similar to that of Co(III), has been widely used in the identification of the latter compounds, as is discussed in the following sections.

2.2.1 The Aqueous Chloride Chemistry of Rh(III)

Interest in the solution chemistry of rhodium(III) complexes has grown considerably as a result of the rapid increase in the use of rhodium in catalytic processes and the economic necessity of its recovery. In particular, the chemistry of Rh(III) complexes in chloride media has been the subject of research. Chloride media serve as the background for the majority of Rh feed solutions in the industrial recovery processes. Also, chloride is the preferred media to carry out almost all reactions which take place in analytical chemistry for separation and determination of Rh complexes (Ginzburg et al., 1975).

Regarding the octahedral structure of Rh(III), six chloride ions are supposed to participate in the formation of the hexachlororhodate complex, i.e., $RhCl_6^{3-}$. However, a study of the rhodium (III) chloride complexes reveals that a variety of rhodium chloro/aquo complexes exist in solution. In other words, under ordinary conditions the complex chlorides are slowly converted to aquochlorides in aqueous solutions, i.e., the molecules of water are substituted with chloride ions in the inner coordination sphere of the Rh(III) complexes:

$$RhCl_6^{3-} + nH_2O \leftrightarrow RhCl_{(6-n)}(H_2O)_n^{(3-n)-} + nCl^- \quad (2.1)$$

The aquation, therefore, leads to the formation of a variety of complexes, ranging from the fully aquated hexaaquorhodate, i.e., $Rh(H_2O)_6^{3+}$, to the non-aquated hexachlororhodate, i.e., $RhCl_6^{3-}$, all of which co-exist in aqueous solutions.

A number of studies have investigated the aquation of Rh(III) chlorocomplexes in hydrochloric acid or chloride-containing solutions (Swaminathan and Harris, 1966; Pavelich and Harris, 1973). Meanwhile, various techniques have been employed to separate and identify the chloro/aquo complexes. Wolsey et al. (1963), and Palmer and Harris (1974) took advantage of the slow kinetics of the $RhCl_{6-n}(H_2O)_n^{(3-n)-}$ system and applied an ion-exchange technique to separate all ten possible species, including geometric isomers. Another effort was carried out by Carr et al. (1987) who continued the previous work of Mann and Spencer (1982) on ^{103}Rh NMR spectroscopy to identify the above mentioned complexes. According to these authors, each particular complex exhibits a distinct and separated NMR signal. The latter signals are excellent tools to identify the complexes and follow the separation procedures. The assignments of Carr et al. (1987) for $RhCl_{6-n}(H_2O)_n^{(3-n)-}$ isomers are presented in Table 2.2.

Furthermore, the visible spectra of Rh solutions have been also thoroughly studied (Wolsey et al., 1963; Bridges and Chang, 1967; Work and Good, 1970; Pavelich and Harris, 1973; Palmer and Harris, 1975) and the absorption bands, in complement with IR and Raman spectroscopy, have been found as another tool to identify the various Rh complexes. As the relative abundance of chloro/aquo complexes changes, the color of the solution varies from yellow to various shades of red and brown. This variation in the color, in turn, causes the absorption bands to shift to another wavelength, accordingly. The band wavelength for different Rh(III) chloro/aquo complexes are given in Table 2.2.

Table 2.2: Chemical Shifts δ (^{103}Rh) (ppm), and UV-Visible Absorption Bands of $RhCl_{6-n}(H_2O)_n$ Complexes in Solution

Complex	δ (^{103}Rh) (ppm) †		UV/visible Absorption Bands ‡	
	(3 °C)	(35 °C)	λ_{max} (nm) (ε)	λ_{max} (nm) (ε)
$[RhCl_6]^{3-}$	8001	8075	518 (111.5)	411 (93.8)
$[RhCl_5(H_2O)]^{2-}$	8235	8298	507 (72.8)	402 (73.4)
cis-$[RhCl_4(H_2O)_2]^-$	8486	8541	492 (101)	392 (113)
trans-$[RhCl_4(H_2O)_2]^-$	8561	8620	484 (99.6)	384 (78.2)
fac-$[RhCl_3(H_2O)_3]$	8753	-----	474 (68.3)	376 (93.5)
mer-$[RhCl_3(H_2O)_3]$	8817	8870	471 (77.1)	370 (71.6)
cis-$[RhCl_2(H_2O)_4]^+$	9088	9142	450 (~68)	355 (~72)
trans-$[RhCl_2(H_2O)_4]^+$	9153	9208	450 (64.9)	349 (49.5)
$[RhCl(H_2O)_5]^{2+}$	9445	9503	395 (57.9)	323 (32.5)
$[Rh(H_2O)_6]^{3+}$	9866	9931	396 (62.0)	311 (67.4)

†Data from: Carr et al., 1987. ‡Data from: Wolsey et al., 1963; Bridges and Chang, 1967; Pavelich and Harris, 1973; Palmer and Harris, 1975.

2.2.2 Distribution of Rh(III) Chlorocomplexes

In order to develop a separation process for Rh(III) complexes, it is first necessary to identify all present rhodium complexes, as well as their relative abundance, in solution. It should be noted that different chloro/aquo complexes which exist in aged Rh solutions may undergo ligand substitution at different rates and thus exhibit different extractabilities against any solvent extraction or ion exchange reagent. Therefore, it is only by acquiring information on the characteristics of Rh species in the feed solution that one may devise an appropriate separation technique. Such information is provided by a "rhodium-chloride" speciation diagram.

Speciation diagrams are based on stability constants of all species present in a particular solution. These stability constants are calculated based on data obtained from analytical techniques such as polarography, potentiometric titration, high voltage electrophoresis, and ion exchange. Due to the complexity of these analytical methods, the determination of stability constants has been found not to be only tedious but also problematic in terms of reliability of the obtained data. In the case of Rh, as it is pointed out by Benguerel et al. (1996), there exists only one set of experimental data – polarographic measurements – provided by Cozzi and Pantani (1958) out of which the stability constants for the chloro/aquo complexes of Rh can be calculated at ambient temperature. Because different

researchers have used different techniques of data analysis to determine the stability constants, a considerable discrepancy is observed from one group's speciation diagram to another's. Benguerel et al. (1996) have critically reviewed all of these contradictory speciation calculations and have attempted to refine them by resorting to the use of activities and rate data. In addition to Cozzi and Pantani (1958) a number of other groups have reported on experimentally determined stability constants of a number of complexes (but not all of them) at both ambient and elevated temperatures (Sillen, 1964; Robb and Harris, 1965; Robb and Steyn, 1967; Sillen, 1971).

The speciation diagram calculated by Cozzi and Pantani (1958) is shown in Figure 2.1. In the original version of Cozzi and Pantani's diagram, the relative abundance of the complexes are plotted vs mean activity of HCl (a_{HCl}). This, apparently, makes difficult the use of the diagram at high HCl concentrations, i.e., the region of interest to PGM refiners, since at that region deviations from activity are great. For that reason, Benguerel et al. (1996) replotted the diagram using the original data and including a concentration scale at the x-axis margin which makes the diagram much more user friendly (Figure 2.1).

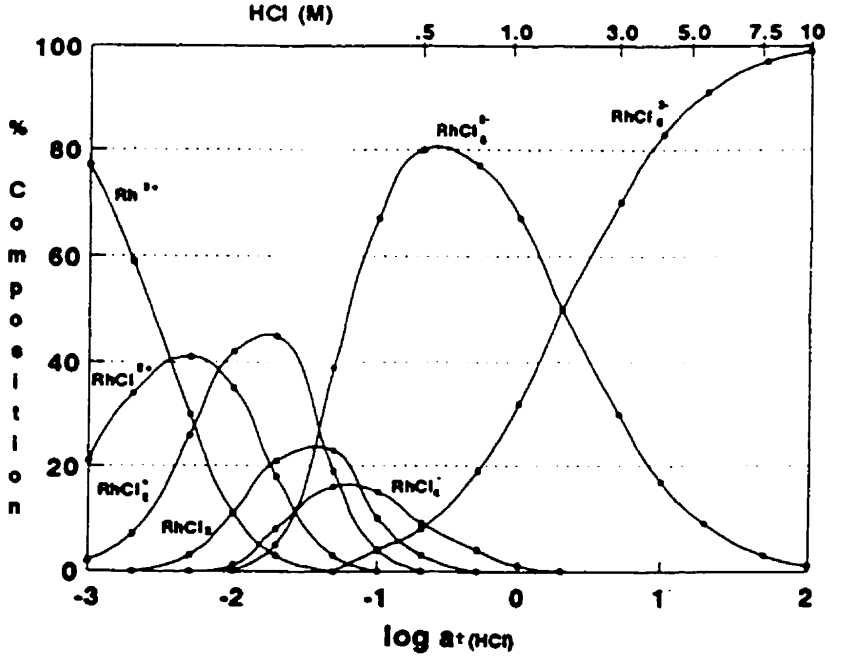

Figure 2.1: Cozzi and Pantani Rhodium-Chloride Speciation Diagram, Reproduced by Benguerel et al. (1996)

Mihailov et al. (1974) reanalysed the stability constants obtained by Cozzi and Pantani (1958) using a mathematical model (Mihailov, 1974) to treat the polarographic data. However, their constructed diagram is unreliable as it predicts the $RhCl_6^{3-}$ species to predominate even at very low chloride concentrations - a prediction totally in fault when compared to experimental observations.

Through a further attempt, Benguerel et al. (1996) constructed another speciation diagram which is based on the kinetics of exchange between the Cl^- and H_2O ligands, rather than the thermodynamic stability constants. Regarding the fact that at high chloride ion concentrations the most abundant species in solution are $RhCl_4(H_2O)^-$, $RhCl_5(H_2O)^{2-}$, and $RhCl_6^{3-}$, these authors constructed their diagram for chloride concentrations higher than 0.5 M and considered only the latter three anionic species. Furthermore, they realized that the kinetic rate-constants for the first and second aquation/anation reactions (Mihailov et al., 1974; Robb and Harris, 1965) can be used to predict the thermodynamic stability constants after a suitably long period of time (i.e. at $-d[RhCl_n]/dt = 0$). Consequently, from these "kinetic-based" stability constants, they constructed a "kinetic" speciation diagram. Benguerel et al. (1996) also realized that the activity of water is considerably lower than one in concentrated HCl media (Meissner, 1980) and its influence on the aquation of $RhCl_6^{3-}$ cannot be ignored. Therefore, they modified further their diagram by taking into account the activity of water in the formulation of the equilibrium and rate equations. The obtained speciation diagram, which is presented in Figure 2.2, appears to be more realistic in predicting the relative abundance of the two most important (from an industrial process point of view) chlorocomplexes of Rh(III), i.e., $RhCl_5(H_2O)^{2-}$ and $RhCl_6^{3-}$. Thus the point of transition from $RhCl_5(H_2O)^{2-}$ predominance to $RhCl_6^{3-}$ predominance is calculated to be at about 5 M HCl as opposed to 2 M HCl calculated by Cozzi and Pantani (1958).

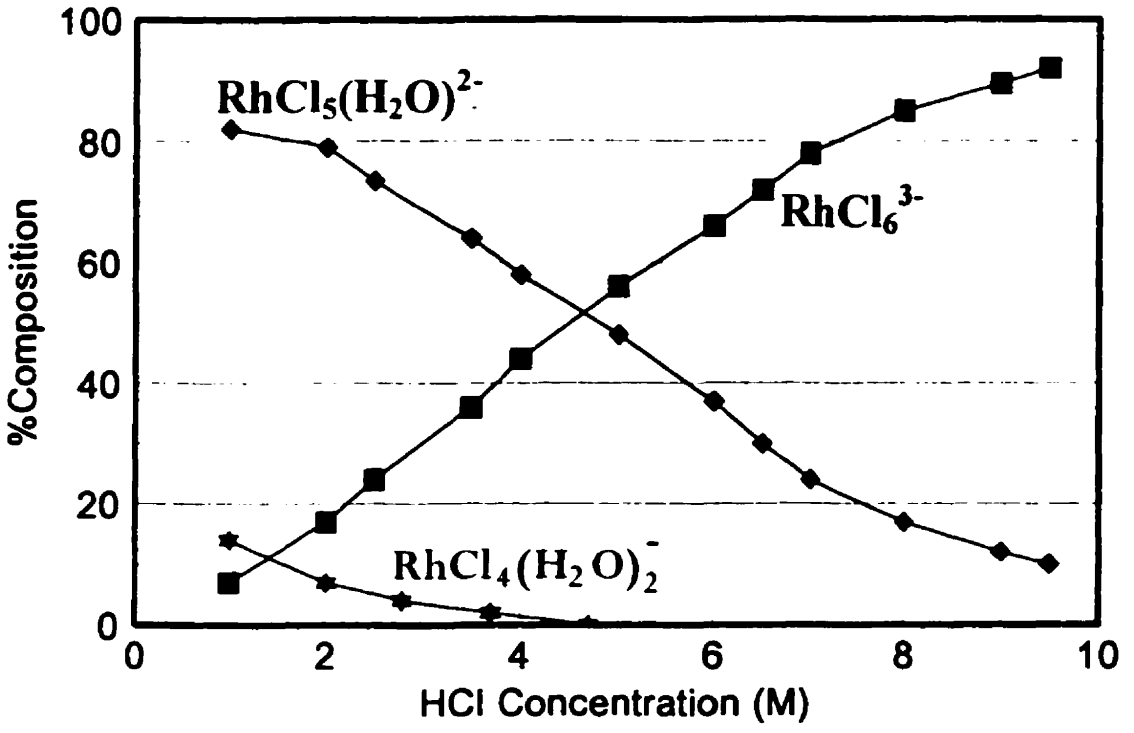

Figure 2.2: Kinetic-Based Rhodium-Chloride Speciation Diagram Constructed by Benguerel et al. (1996)

2.2.3 Attempts to Quantify the Aquation of Chlorocomplexes

Clearly, there remains much uncertainty in affirming the exact speciation of rhodium in chloride solutions due to the scarcity of data and the necessary assumptions which must be made to extrapolate data to other concentrations and temperature ranges. However, from the reported stability constants, collected by Benguerel et al. (1996), one may easily realize that, as a general trend, the aquation process depends primarily on the chloride ion concentration; the pH and temperature of the solution are two other variables which affect the aquation, though to a lesser degree. To this end, in an effort to remove or at least to alleviate, this uncertainty, in the course of this project it was also attempted to establish the presence of the major chlorocomplexes (penta- and hexa-) of Rh(III) and somehow quantify the aquation process at different conditions.

Two different methods were examined: NMR spectroscopy (Mann, 1982) and ion selective electrode (ISE) measurements (Khoshkbarchi and Vera, 1995). As previously

described, NMR spectroscopy is an excellent tool to identify the various chlorocomplexes through the assignment of a characteristic chemical shift for each particular complex (see Table 2.2). However, it appeared very difficult to apply the same technique for speciation purposes, i.e., for quantification purposes. The reason is the very large amount of spectrometer time required to make the method quantitative (Mann, 1995). The chloride ion selective electrode method (ISE) was also employed with the hope of measuring the amount of exchanged chloride ions with water molecules, as a result of the aquation reaction (reaction (2.1)). With such a method, one may determine the extent of aquation which takes place at each particular chloride concentration, and thus the relative abundance of aquated and non-aquated complexes. The latter method also failed to quantify the aquation reaction since the amount of exchanged chloride ions, which was the subject of measurement, in most cases was negligible in comparison with the background chloride concentration. As a result of that, the measurements were within the range of experimental error and hence inaccurate.

However, UV-Visible absorption spectrophotometry proved a useful means of verifying the reliability of the various speciation diagrams. This technique, which will be discussed later in more detail, distinguishes the dominant complexes based on the difference in the color of the aquated complexes of rhodium (orange-peach) and that of hexachlororhodate (cherry-red). Such semi-quantitative spectrophotometric analysis seems to confirm the predictions of Benguerel et al.'s (1996) speciation diagram (Figure 2.2) which is based on the kinetic data and considers the activities of Cl^- and H_2O.

Apparently, the presence of varying amounts of mixed aquo/chloro complexes at practical conditions causes problems when devising a solvent extraction-based separation scheme. Indeed, the solvent has to be capable of extracting, at least in part, species containing H_2O in their inner coordination sphere and this is most likely the reason why many of the processes outlined below were doomed to fail as a feasible separation process for rhodium. Before reviewing these schemes, the classical practice of Rh recovery from a PGM containing feed solution is reviewed.

2.3 THE GENERAL PGM SEPARATION APPROACH

Traditionally the refining of platinum group metals involved their separation after dissolution in oxidizing chloride leach liquors followed by a series of precipitation/re-dissolution steps adapted from analytical chemistry methods (Hampel, 1954). This refining approach was universally practiced until about the middle 1970s. Since then, most major refiners have modernized their processes by implementing more efficient separation schemes based on the technique of solvent extraction (Harris, 1993). Although the full details of such commercial operations are usually well-guarded secrets, nevertheless to date at least the main features of three of these processes from INCO, Matthey Rustenburg (now AMPLAT) , and LORNHO have been published (Harris, 1993). As a typical example of a modern PGM refining flowsheet, the one assumed to be used by INCO Ltd. at Acton, U.K. (Grant, 1990), is shown in Figure 2.3.

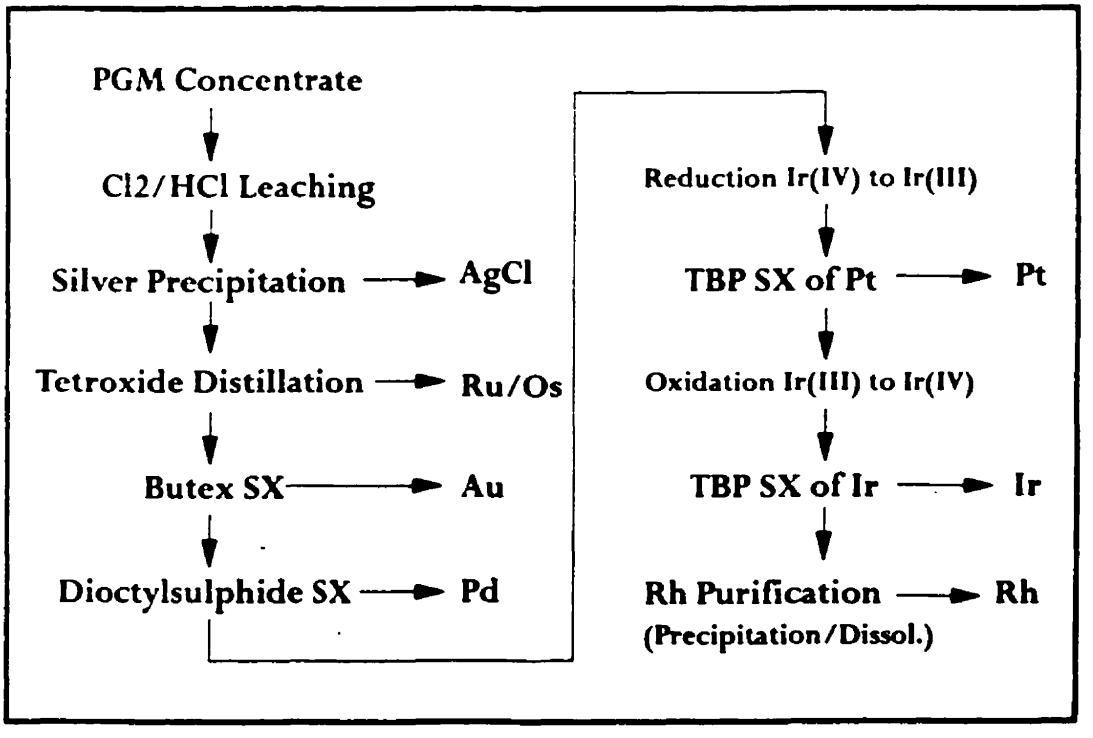

Figure 2.3: INCO Solvent Extraction Flowsheet for PGM Refining
(Reported by Grant, 1990)

As a common feature, all these flowsheets invariably end up with rhodium as the last metal to be recovered/refined. The Rh feed solution contains substantial amounts of impurities including precious metals (Pt and Ir), base metals (Cu, Zn, Fe, Ni, etc.), and metalloids (As, Se, Sb, Te, Bi). The amount of each impurity varies and depends mostly on the original source of the feed (i.e., gold mine bullion, silver refinery anode mud, or base metal processing) and the flowsheet of PGM recovery. Among all of the impurities, separation of iridium, due to its similar properties with Rh, has been reported to be a rather complicated issue.

2.3.1 Classical Rhodium Refining Practice

Even in the modern flowsheets, the recovery scheme for rhodium has remained almost unchanged over the years and rhodium is still recovered through a complicated series of precipitation/re-dissolution steps which is highly time consuming and inefficient. Apparently, this is attributed to the complex chemistry of Rh and its previously mentioned tendency to form a variety of chloro/aquo complexes in aqueous chloride solutions (Benguerel et al., 1996).

The classical flowsheet for rhodium recovery and purification (Thorpe, 1956) is shown in Figure 2.4. In this flowsheet, the chloride Rh solution is first heated to boiling and treated with sodium nitrite until the color changes to yellow. This treatment converts the Rh(III) aquo-chlorocomplexes into double nitrites, $Rh(NO_2)_6^{3-}$, which are extremely stable to hydrolysis. As a result of this stability, base metals can be largely removed selectively from the solution as hydroxides or basic salts, by neutralization and precipitation with $NaOH/Na_2CO_3$. After filtration the solution is cooled, treated with sodium sulphide, and set aside to allow the sulphides of the other platinum metals and of lead to separate out (Thorpe, 1956). After settling, the clear liquor is decanted through a filter and the sulphide precipitate returned to an earlier stage of the refining process for recovery of its precious-metal content. The rhodium is precipitated then as ammonium rhodonitrite

$Na(NH_4)_2[Rh(NO_2)_6]$ through the slow addition of an excess of saturated ammonium chloride solution. This precipitation step is partially selective over the other PGMs which may be present in the Rh solution. After settling for 1 hour, the crystals are collected, washed with cold water, and dissolved by boiling with 1:4 hydrochloric acid. The resulting chlororhodate ($RhCl_6^{3-}$) solution is reconverted into double nitrite and the whole process is repeated several times until the required degree of purity is attained. Once the ammonia-nitrite rhodium complex is of acceptable purity, the final dissolution in hydrochloric acid is followed by the precipitation of rhodium with ammonia to give $(NH_4)_3[RhCl_6]$. The final step (Ryan, 1968) involves the addition of formic acid to form the Rh black precipitate. The separated solid is collected on a filter, washed, and ignited in a muffle furnace at 1000 °C, under a reducing hydrogen atmosphere.

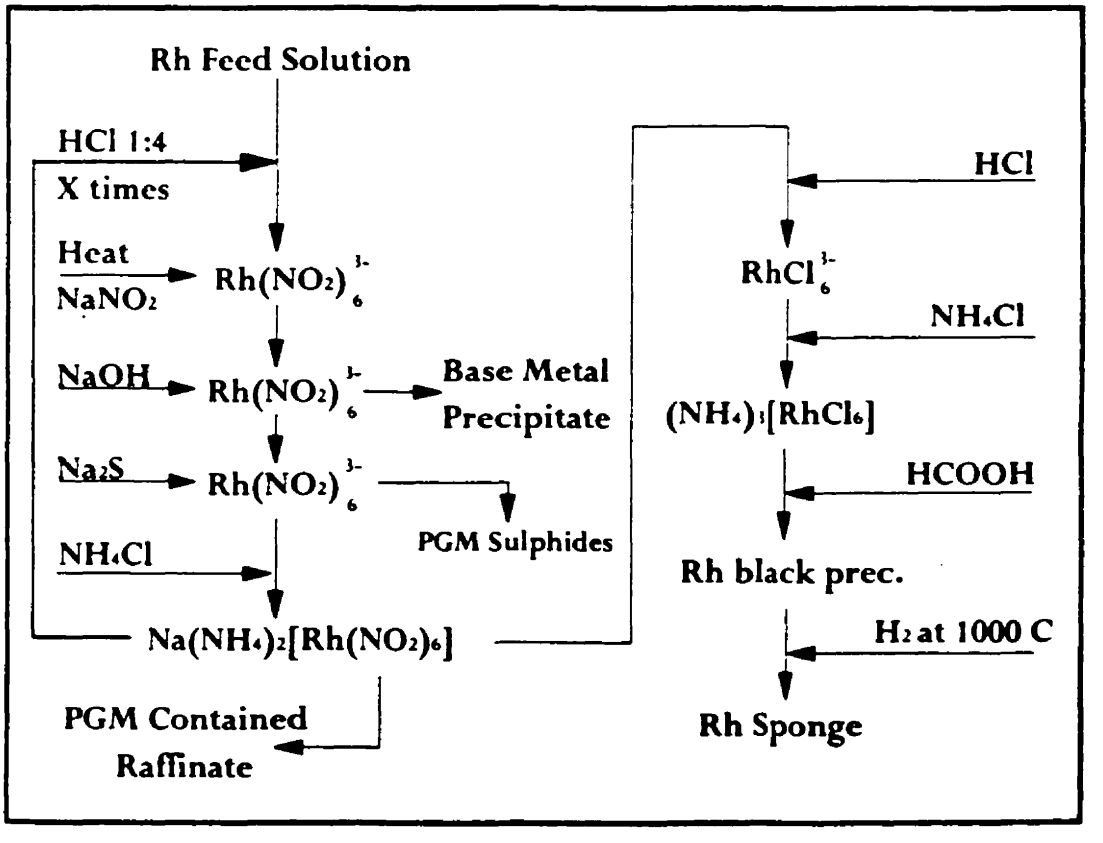

Figure 2.4: Classical Flowsheet for Rh Refining and Recovery

2.3.2 Solvent Extraction Processes for PGM Refining

At this point, it is useful to remark some general features of the liquid ion exchange-based processes applied in PGM refining. Solvent extraction has been extensively used in the precious metal refining applications and there are many documented examples in the literature (Mooiman, 1993). In the SX of precious metals, there have always been concerns with extractant stability. That is obviously due to the catalytic nature of precious metals which promotes oxidation and, therefore, causes the reagent to undergo degradation (Harris, 1993). For a majority of extractants applied for PGM recovery from chloride-based solutions, selectivity is largely based on the charge and size of the chloroanion. Larger PGM anions are more readily extracted than the ionic base metal species. This leads to the selectivity of the extractants for the PGM over base metals. Charge considerations also lead to differences in the extractability of the various PGM chloroanions – the lower the anion charge the more readily extracted the anion. For instance, the order of extraction for the anion exchanger types of extractants is most commonly found as: $AuCl_4^- > PtCl_6^{2-} \approx IrCl_6^{2-} > PdCl_4^{2-} > RhCl_6^{3-} \approx IrCl_6^{3-}$ (Mooiman, 1993). This might be attributed, in part, to the steric effects, i.e., the difficulty in packing three organic molecules around a single anion.

The extractants that have been used in PGM refining so far can be basically classified into three major categories: a) solvating extractants like long chain alcohols, ethers, and tributyl phosphate; b) coordinating extractants like oximes or dialkyl sulphides; and c) anion exchange extractants like long chain alkyl amines. From the latter, amines have received considerable attention and have been practiced in numerous instances in the area of precious metal refining. Also amines have been extensively investigated for their performance in Rh refining. These investigations, along with those involving Rh extraction with other extractants, are reviewed in the next sections.

2.3.3 Solvent Extraction of Rh(III) with Amine Extractants

One of the most important category of organic compounds that exhibit appreciable basicity, is the family of amines. An amine has the general formula of RNH_2, R_2NH, or R_3N which is respectively called primary, secondary, and tertiary, according to the number of the R groups attached to the nitrogen atom. Simply, amines are ammonia in which one or more hydrogen atoms have been replaced by the organic R groups, the latter can be any alkyl or aryl group. The nitrogen forms "sp^3" orbitals which are directed to the corners of a tetrahedron. Three of these orbitals overlap "s" orbitals of hydrogen or carbon; the fourth contains an unshared pair of electrons. The tendency of nitrogen to share this pair of electrons underlies the entire chemical behavior of amines; their basicity.

$$\underset{\text{stronger base}}{RNH_2} + H_3O^+ \rightarrow \underset{\text{weaker base}}{RNH_3^+} + H_2O \qquad (2.2)$$

It is convenient to compare basicities of amines by measuring the extent to which they accept hydrogen ions from water; the equilibrium constant for this type of reaction is called a basicity constant, $\mathbf{K_b}$.

$$RNH_2 + H_2O \leftrightarrow RNH_3^+ + OH^- \qquad (2.3)$$

$$K_b = \frac{[RNH_3^+][OH^-]}{[RNH_2]} \qquad (2.4)$$

Each amine has its characteristic $\mathbf{K_b}$; the larger the $\mathbf{K_b}$, the stronger the base. Aliphatic amines of all three classes have $\mathbf{K_b}$'s of about 10^{-3} to 10^{-4} (Morrison and Boyd, 1992); they are somewhat stronger bases than ammonia ($\mathbf{K_b} = 1.8 \times 10^{-5}$). Aromatic amines, on the other hand, are considerably weaker bases than ammonia, having $\mathbf{K_b}$'s of 10^{-9} or less.

The basicity of amines though should be compared with the stability of their respective ions; the more stable the ion relative to the amine from which it is formed, the more basic the amine. From an electronic structural point of view, one can consider that an alkyl group pushes electrons toward nitrogen, and thus makes the fourth pair more available for sharing with an acid (Morrison and Boyd, 1992). The low basicity of aromatic amines, in comparison with the aliphatic ones, is due to the fact that the amine is stabilized by

resonance to a greater extent than is the ion. In other words, one can say that aniline is a much weaker base than ammonia because the fourth pair of electrons is partly shared with the ring and is thus less available for sharing with a hydrogen ion; the tendency for the $-NH_2$ group to release electrons to the aromatic ring makes the ring more reactive toward electrophilic attack; at the same time this tendency necessarily makes the amine less basic.

Due to their basicity, all types of amines in acidic media become protonated:

$$\overline{R_3N} + HCl \leftrightarrow \overline{[R_3NH^+]Cl^-} \quad (2.5)$$

$$3\overline{[R_3NH^+]Cl^-} + MCl_6^{3-} \leftrightarrow \overline{[R_3NH^+]_3MCl_6^{3-}} + 3Cl^- \quad (2.6)$$

The extraction of PGM from acidic solutions is thus effected through an anion exchange between the protonated amine and the anionic species of the platinum metals (Eq. 2.6). The quaternary amines constitute, however, exception to the above rule since the latter possess a permanent positive charge so the extraction reaction is a simple ion exchange. Regarding the order of basicity, the order of the extraction of anionic PGM species by the various types of amines is as follows: quaternary > tertiary > secondary > primary (Dhara, 1984). Similar considerations hold for different aromatic amines such as pyridine, quinoline, etc., and reasonably explain the behavior of the aromatic amines which readily undergo deprotonation and release protons upon contact with aqueous solutions of low acidity (Dhara, 1984).

The extraction of rhodium with amines is generally favoured at low acidity and low chloride concentration. For instance, it has been shown that Rh is only significantly extracted (but still not adequately from an industrial point of view) by tri-n-octylamine at 0.1 M HCl (Khattak and Magee, 1969). This can be easily explained by considering reactions 2.5 and 2.6. It is clear that the extraction of the precious metal species is an ion-pair formation between protonated amine and the anionic complex of the metal. If the concentration of chloride ion is too high, then its replacement by the metal complex will become increasingly difficult and the extraction degree will drop. On the other hand, the low concentration of chloride and proton favours the formation of mixed aquo/chloro complexes (specially in the case of Rh) which are less extractable.

The highly basic quaternary ammonium chloride extractants perform successful extraction of PGM, i.e., more than 80% at some adjustable conditions (Work and Good, 1970). However, the problem encountered with the use of this type of amines is the non-efficient stripping. It is believed that the anionic rhodium species undergo rapid dimerization, or possibly polymerization, in the loaded organic phase. The newly formed dimers, $Rh_2Cl_9^{3-}$, are so strongly bound to the organic ammonium cations that they get "locked-up" in the organic phase and stripping becomes impossible. The results of a recent work on Rh extraction with pyridine derivatives showed encouraging extraction of up to 85% of a 3 g/L Rh solution at 3 M HCl, while the selectivity over base metals has been also reported as satisfactory (Inoue et al., 1993). Similar results were reported by Wang et al. (1988). However, the same problem of non-efficient stripping once more coined the latter works as "unsuccessful". In addition to the above mentioned shortcomings of amines, in the case of Rh separation, the problem of selectivity over other PGM and base metals is also significant.

2.3.4 Solvent Extraction of Rh with Extractants Other than Amines

Several groups have investigated solvent extraction systems of Rh(III) using different extractants than amines. For instance, the extraction of rhodium in its cationic form, $Rh(H_2O)_6^{3+}$, has been examined using the cation exchanger extractant dinonylnaphthalene sulfonic acid (Khan and Morris, 1967; Knothe, 1979). Other instances include amides, TBP, TOPO, and various phosphinic and phosphonic based extractant systems. All these systems, which are well summarized by Benguerel et al. (1996), have resulted in various degrees of success, in terms of extraction and separation of rhodium. However, these systems cannot be used "as-designed" for industrial purposes because of the procedures required in the preparation of the feed solutions prior to extraction – most of these systems were developed for analytical purposes.

2.3.5 Ion Exchange (IX) Processes for Rh Refining

There has been some work carried out with ion exchange (IX) with the aim of developing a viable system for industrial rhodium recovery applications. The fundamentals of the separation of rhodium from the other PGM using ion exchange techniques has been described in review papers (Beamish, 1967; Al-Bazi and Chow, 1984). Several resin type ion exchangers including strong base anion exchange resins, thiourea based resins, polyurethane foams, and some cation exchange resins have been investigated (Dhara, 1993). However, similar to solvent extraction, most of the reported ion exchange systems suffer from their lack of selectivity for rhodium over other PGM and their lack of ease of back-extraction.

Recently, IBC Advanced Technologies of Orem, has developed a new series of ligands called SuperLig™. These molecules which are based on crown ethers work on the principle of molecular recognition technology (MRT). The functional molecule is designed and synthesized, in order to selectively bind a specific metal species by carefully considering its geometry, size, charge, and coordination affinity (Breuning et al., 1990). The process, therefore, would appear to be more of a chromatographic technique rather than ion exchange, but it operates very similar to ion exchange processes.

This new generation of ion exchangers offers very good selectivity for Rh and Ir over base metals at higher chloride concentrations (4 M), where dominant species are hexachloro iridium and rhodium complexes. The process also provides the unique advantage of the potential application at the head of the PGM flowsheet rather than at the end. These ligands, therefore, present an alternate recovery scheme to be considered in precious metals processing, and there do appear to be some advanced attempts of implementing this new technology to precious metal refineries in Japan and South Africa (Harris, 1993). There are, however, some problems or concerns with the implementation of this technique

for Rh recovery purposes. For instance, it appears that the presence of both platinum and lead causes problems, and two different SuperLig™ resins have to be used to effect complete recovery and purification, resulting in several stages somewhat analogous to the classical scheme (Ichiishi et al., 1992). Other potential problems may be the use of somewhat exotic and expensive elution reagents as well as the long-term stability of the silica-gel based support material.

2.3.6 Attempts at McGill to Develop Modern Schemes for Rhodium Recovery

At McGill University, extensive research has been conducted over the past decade in the area of SX of precious metals using 8-hydroxyquinoline derivatives (R-HQ). A part of this continuing research has focused on developing a SX-based recovery process for rhodium, using Kelex 100. Since direct extraction of Rh(III) by Kelex 100 proved impossible – the distribution coefficients obtained for aged rhodium solutions were lower than 0.5 (Benguerel et al. (1994) – the research focused first on "activation" of rhodium prior to its extraction. Thus Benguerel et al. investigated a new approach based on the activation of the basically "solvent-extraction-inert" mixed aquochloro complexes, namely $RhCl_5(H_2O)^{2-}$, via the formation of extractable complexes with the aid of $SnCl_2$ (Demopoulos et al., 1993; Benguerel and Demopoulos, 1993). The stannous chlorocomplexes of Rh, which form upon interaction of Rh(III) complexes with Sn(II) in aqueous chloride solutions, respond so well to the Kelex 100 organic phase that very high distribution coefficients (> 100) for a single contact of less than 1 min are achieved. However, in spite of this high extraction efficiency, the stripping seems to be more complicated. As it has been reported, stripping of Rh from the organic is possible only for organics loaded with a feed having a Sn:Rh ratio ≥6:1 (Benguerel and Demopoulos, 1993; Benguerel et al., 1995). This will, in turn, impose some limitations on process performance variables and make the obtainment of concentrated strip solutions of Rh very difficult. More recent work, not published as yet, has shown stripping of Rh from the Sn(II)-Rh(III)-loaded organic phase to be possible even at lower Sn/Rh ratios, i.e., around 3 to 4.

In this case a reductive stripping medium is used; Na_2SO_3/HCl. However, the problem of obtainment of concentrated strip solution even with this medium persists.

Regarding the difficulties and shortcomings encountered in the course of previous attempts in developing a viable separation process for Rh(III) complexes, it was decided to explore the application of liquid membranes for this duty. The investigations on the capabilities of this new technology, particularly the SLM technique, is the subject of a major part of this thesis. However, a second approach was also conceived which seems to offer less complexity, from a practical point of view, than the liquid membranes. This newly conceived route to rhodium recovery/refining makes use of the bromide chemistry of Rh(III) complexes and solvent extraction with Kelex 100.

Since the latter work of Benguerel et al. (1995) and all the investigations described in this thesis were carried out, almost invariably, using the commercial extractant Kelex 100 – a 7-substituted 8-hydroxyquinoline – it is considered appropriate to introduce this family of extractants and to review their applications in various metal extraction processes.

2.4 8-HYDROXYQUINOLINE EXTRACTANTS

Oxine, also called 8-hydroxyquinoline (8-HQ) or 8-quinolinol, has a particular ability to form stable chelate complexes with a number of metallic ions. This ability of oxine was recognized a long time ago and extensive reviews have described the physical, chemical, and spectroscopic properties of 8-HQ and its various derivatives (Hollingshead, 1954; Sillen and Martel, 1979). Lix 26[1] and Kelex 100[2], alkylated derivatives of 8-hydroxyquinoline, are the two best known, and commercially available, members of this family which have been used in the solvent extraction industry as metal extractants.

[1]Proprietary product of Henkel Corp.
[2]Proprietary product of WITCO Chemical Co.

The structure of Kelex 100, a 7-substituted alkyl derivative of 8-hydroxyquinoline, is presented in Figure 2.5. However, it should be remarked that commercial extractants are often mixtures of structural and positional isomers as well as by-products. The main component of Kelex 100 produced before 1976 by Ashland Chemical was 7-(1-vinyl-3,3,5,5-tetramethylhexyl)-8-hydroxyquinoline (Ashbrook, 1975a; b). Ashbrook did not report the full list of components present in that extractant except that he identified the main component in Kelex 100 as about 77.7%, 8-hydroxyquinoline of 3.7%, and the remainder was reported to be unknown viscous fluorescent material.

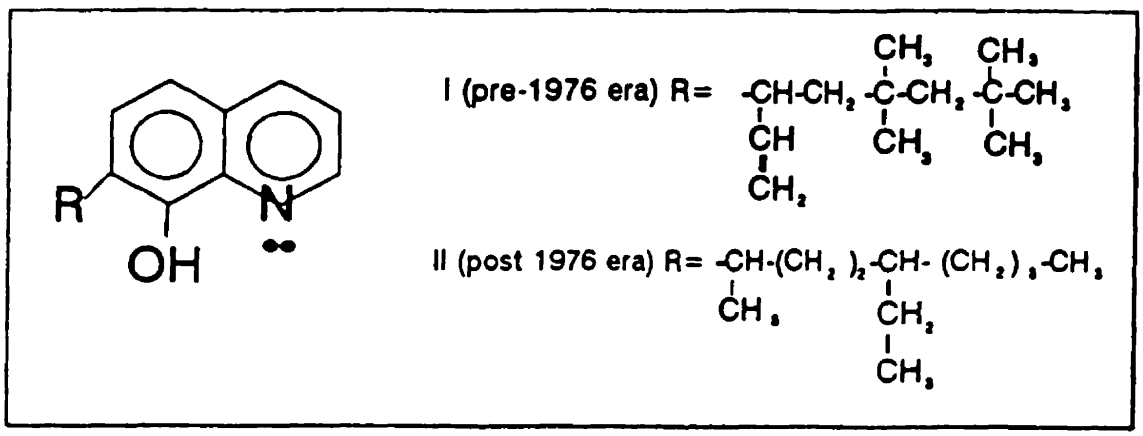

Figure 2.5: Chemical Structure of Kelex 100

In 1976, the manufacturing process of Kelex 100 was changed and Sherex Chemical Company (effective Sept. 1992 WITCO Chemical Company) became the producer. The main component of post-1976 Kelex 100 is 7-(4-ethyl-1-methyloctyl)-8-hydroxyquinoline. Demopoulos and Distin (1983) identified the composition of Kelex 100 (post-1976) by gas chromatography (GC) and mass spectroscopy (MS). According to these authors, Kelex 100 contains 82% of the active component, 1% 7-(2-ethylhexyl)-8-quinolinol, 0.5% 7-(4-ethyl-1-methyloctyl-1-ene)-8-quinolinol, 8% 9-ethyl furoquinoline, 4.5% 8-methyl-9-

(2-ethylhexyl)furoquinoline, and 0.5% 8-methyl-9-(2-ethylhexyl) dihydrogenated furoquinoline. Gareil et al. (1989) using liquid chromatography (LC) and MS analysed the Kelex 100 composition and confirmed most of the components that had been previously identified by Demopoulos and Distin (1983) with the exception of 9-ethyl furoquinoline. However, they also identified as well a ketone and two alcohols.

2.4.1 Extraction of Precious Metals with Kelex 100

Initially Kelex 100 was developed specifically to compete with the hydroxyoxime group of extractants for copper extraction (Budde and Hartlage, 1972). However, the commercial application of Kelex 100 to the copper industry faced problems due to two principal reasons. One was the poor selectivity over Fe(III) (Fleming et al., 1980) and the other was the considerable degree of acid extraction via protonation during stripping (Hartlage et al., 1975).

In spite of those shortcomings, Pouskouleli and Demopoulos (1985) were the first researchers who recognized that alkylated derivatives of 8-HQ have good extractive properties for chlorocomplexes of precious metals. Thus they successfully applied Kelex 100 to effect the co-extraction of Au(III), Pt(IV) and Pd(II). Later, the use of Lix 26 was proposed as the preferred reagent since it was found to exhibit higher solubility for the extractable Pt(IV) species than Kelex 100 (Pouskouleli et al., 1987). Isomerism of the R group in the Lix 26 molecule was taken as responsible for its superior performance. The latter work of Pouskouleli and Demopoulos resulted in developing a process flowsheet for the co-extraction of Pt(IV)/Pd(II) followed by differential stripping, using Lix 26 (Demopoulos, et al., 1987a; b) as the extractant. The reactions by which 7-substituted 8-hydroxyquinolines (R-HQ) were found to work were the following:

(i) Protonation of the extractant

$$\overline{R-HQ} + HCl \leftrightarrow \overline{R-H_2Q^+Cl^-} \qquad (2.7)$$

(ii) Extraction of Pd(II) via chelation

$$PdCl_4^{2-} + 2(\overline{R-H_2Q^+Cl^-}) \leftrightarrow \overline{Pd(R-Q)_2} + 4H^+ + 6Cl^- \quad (2.8)$$

(iii) Extraction of Pt(IV) via ion-pair formation

$$PtCl_6^{2-} + 2(\overline{R-H_2Q^+Cl^-}) \leftrightarrow \overline{PtCl_6^{2-}(R-H_2Q)^+_2} + 2Cl^- \quad (2.9)$$

Differential stripping was accomplished by water stripping (pH>2) of $PtCl_6^{2-}$ followed by HCl (6M) stripping of $PdCl_4^{2-}$.

Through a further attempt, Demopoulos and researchers from the German chemical company Schering AG synthesized and tested a novel 8-HQ derivative, TN 1911, which appeared to outperform Kelex 100 and LIX 26 (Demopoulos et al., 1989). In contrast to all other reagents used in the past, TN 1911 had been specifically designed for PGM separation. At a preliminary assessment, the new extractant offered the advantages of faster kinetics, higher metal loading capacity and higher separation factor in comparison to Lix 26. Following that, Schering AG synthesized some more 8-HQ derivatives, called TN 2181, TN 2221, and TN 2336. The only difference in the structure with Kelex 100 and the TN family of reagents, whose production in large quantities never materialized for a number of reasons, is in the R group. The R group had different spatial orientation (conformation) and a saturated or an unsaturated chain of various lengths. Coté and Demopoulos (1993) thoroughly characterized the latter extractants and examined their behavior in Pt/Pd extraction circuits (Coté and Demopoulos, 1994a; b).

In addition to the TN reagents, a higher purity Kelex 100 product, called Kelex 100S, was also produced by Schering AG. A purity of 90% was claimed for this product while no information on the method of preparation or its composition was revealed. Coté and Demopoulos (1993) using the copper loading method, reported the active component of Kelex 100 and Kelex 100S to be 78% and 88%, respectively. However, Haesebroek (1991) claimed improved properties for Kelex 100S compared to Kelex 100, especially in its long-term stability against oxidation in alkaline media, Dziwinski et al. (1995) reported that Kelex 100S is of similar purity as that of distilled Kelex 100. Based on their

identification, except for the rate of phase separation, there is no clear reason for the superiority in performance or properties of Kelex 100S over distilled Kelex 100.

In conclusion, 8-HQ derivatives possess the unique property to act as both chelating and ion-pair forming reagents, when in protonated form. This property has been considered as the key factor for the success of 8-HQ derivatives in the solvent extraction of precious metals (Demopoulos, 1986). Regarding the failure of all previous Rh SX attempts with different extractants, it was, indeed, this promising feature of Kelex 100 which prompted its use in the present research.

2.5 LIQUID MEMBRANE TECHNIQUE

Membrane separations have evolved into an expanding and diverse field. There are now numerous types of membranes, various applications, and certain uses which have attained commercial success. As defined by Noble (1987), a membrane can be viewed as a semi-permeable barrier between two phases which prevents the intimate contact. This barrier which restricts the movement of molecules across it in a very specific manner can be solid, liquid, or even a gas. The semi-permeable nature is essential to ensuring that a separation takes place.

Liquid membranes are homogeneous, non-porous membranes, where the solute is dissolved at one side of the membrane and released at the other side. The driving force is given by different mechanisms at both interfaces. Although many membrane-based separation processes suffer from low transport rates resulting from low diffusivities in porous solid media, liquid membranes offer much higher transport rates because of the low viscosity of the membrane. Liquid membranes, over the past ten or fifteen years, have attracted the attention of many research groups from all over the world (Boyadzhiev, 1990). There have been many attempts to develop liquid membrane systems, but only two methods have been developed to a reasonable level: emulsion liquid membrane (ELM) and supported liquid membrane (SLM).

2.5.1 Emulsion Liquid Membrane (ELM) System

Emulsion liquid membranes are prepared by dispersing a primary emulsion – usually of water-in-oil type – in a second aqueous phase. The primary emulsion itself is prepared by emulsifying the internal (receiving) aqueous phase in the liquid membrane phase. The liquid membrane, which consists of a low viscosity diluent incorporating a surfactant (to stabilize the primary emulsion) and an extractant reagent, separates the two aqueous phases. (Figure 2.6). Except for some characteristic differences, the ELM can be regarded as a variation of the conventional solvent extraction process. One of these differences is that the extractant concentration in the membrane phase may be much lower than that of solvent extraction (about 1-4%), and because of this low concentration no modifiers may be needed.

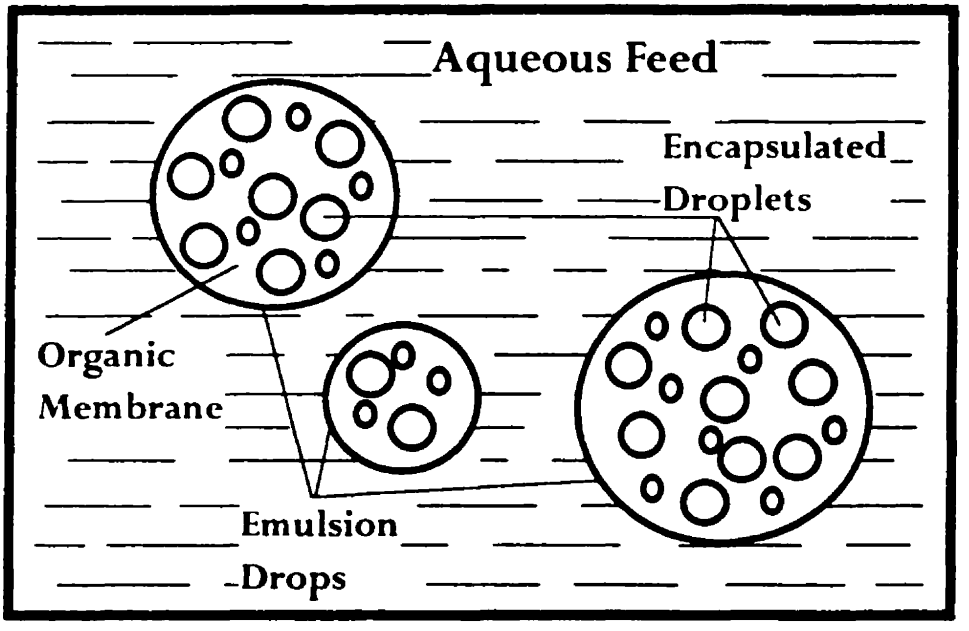

Figure 2.6: Schematic of an Emulsion Liquid Membrane (ELM) System

The main advantage of ELM over other membrane processes is the very large inner interfacial area of the emulsion (more than 10^6 m^2/m^3 emulsion) which provides very high transport rates for the permeant. This huge surface area is due to the tiny size of the dispersed droplets. The diameter of an emulsion drop varies between 0.1-2 mm and the diameter of the dispersed droplets between 0.5 and 10 μm (Cahn and Li, 1974). However,

as a main drawback, the emulsion drop is not able to keep its initial form and undergoes some changes during its contact with the external feed. This "instability" results mostly from two major effects. One is the break-up of the dispersed droplets and release of the internal receiving phase. The other is swelling of the emulsion droplets by water transport from the outer to the inner aqueous phase. The main cause of swelling is the presence of the extractants and surfactants which both act as water carriers (Wiencek and Qutubuddin, 1992b). As a very unfavorable consequence, the swelling often prevents highly concentrated solutions being obtained. Wiencek and Qutubuddin (1992a) applied the microemulsion liquid membrane technique as a solution to swelling problem and claimed several advantages, such as faster rate of separation, lower leakage, and ease of demulsification, for the latter process over ELM.

The surfactant is the most important component of the ELM system. It not only determines the stability of the emulsion but also influences a number of other parameters like viscosity and water solubility of the liquid membrane. While a proper amount of surfactant is required to obtain the appropriate stability, the applied surfactant often exhibits a high mass transfer resistance since it occupies the interfacial surface and confines the available surface for the metal extractant. On the other hand, the highly stable emulsions exhibit difficulties in the demulsification stage which is the final recovery step (Goto et al., 1989). Therefore, the choice of an appropriate emulsifier system is of vital importance. Szymanowski and Sobczynska (1992) introduced different systems of emulsifier selection based on the *hydrophilic lipophilic balance (HLB)* concept. According to the most conventional HLB scale, i.e., Griffin scale, different types of surfactants including anionic, cationic, amphoteric and non-ionic surfactants have HLB values between 0 to 20. Those showing HLB values lower than 10 exhibit hydrophobic character while those of HLB values above 10 are of a hydrophilic character. Apparently, an emulsifier system, containing either a single or a combination of surfactants, should exhibit an HLB value in the middle of the range (0-20) to satisfy both hydrophobic and hydrophilic characters.

Many surfactants which have been introduced in literature have the capability to be employed as an emulsifier (either singly or as mixtures) in the ELM system. Examples are the application of Span 80 (sorbitan monooleate) for phenol extraction by Cahn and Li (1974), ECA 4360 (polyamine) for zinc extraction by Draxler and Marr (1986), ECA 5025 and Emery DNP-8 for copper extraction by Wiencek and Qutubuddin (1992b), Brij 92 (polyoxyethylene-2-oleyl-ether) for the extraction of lanthanum and neodymium by Milanova et al. (1993), and amphoteric surfactants for copper extraction by Nakashio et al. (1990). From these, the application of Span (Span 20, 40, 60, 80, 85) and Tween (Tween 20, 40, 60, 65, 80, 85) surfactants as commercially-available standard emulsifiers is noticeable.

In terms of industrial development, ELM technology has only been tested at the pilot plant level. As remarked by Marr et al. (1990), the first efforts in this direction were made in the USA where at least a pilot plant for the recovery of a number of metals in the 1970s (Bock and Valiant, 1982) is known to have been run. This process development activity was later curtailed due to unfavorable metal (especially uranium) prices. In the 80's the commercial development efforts were renewed mostly driven from the surge of environmental research, i.e., recovery of heavy metals from industrial effluents. This has led to the construction of an industrial ELM plant in an Austrian viscose company for zinc at a rate of 100 m^3 h^{-1} for a 0.5 g/l Zn effluent (Ruppert et al., 1988). Reported by the same research group, ELM has also been successfully tested on a pilot-plant scale for the extraction of zinc, copper, cadmium, lead, tungsten, and chromium. These modest industrial achievements in the ELM technology have been significantly hampered since a fire that destroyed the Austrian ELM zinc plant.

In the course of the present thesis research, most of the above mentioned emulsifiers were extensively employed and examined for their stability and performance. The objective was to obtain a satisfactory ELM system to effect the separation of chlorocomplexes of

Rh(III), from a strong HCl feed (4 M) into a dilute HCl (0.1 M) receiving phase, using Kelex 100 as the membrane carrier. The results, which are not reported here, showed a consistent lack of stability which led to fast de-emulsification. It was after this unfortunate observation that it was decided to investigate the SLM system.

2.5.2 Supported Liquid Membrane (SLM) System

Supported liquid membranes can be obtained when a rigid porous substrate is filled with an organic solution of the extractant. In this technique, very thin porous polymer sheets are used as the substrate. The oleophilic properties of the polymer keep the organic liquid in the pores and prevent both aqueous solutions from direct contact (Figure 2.7).

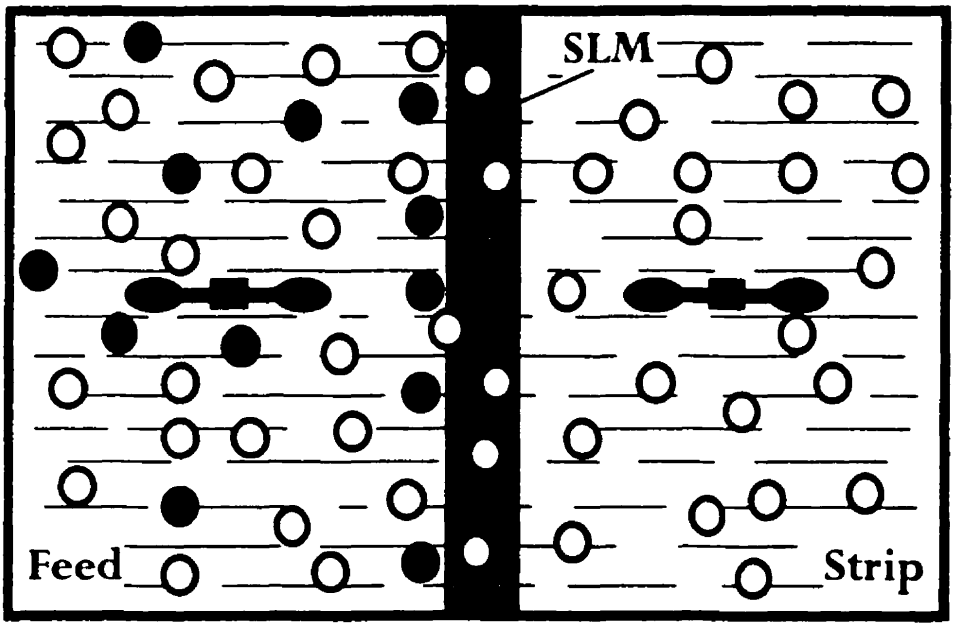

Figure 2.7: Schematic of a Supported Liquid Membrane (SLM) System

The material and structure of the substrate play an important role in the performance of SLM. Polymeric structure variables such as pore size, porosity, tortuosity, thickness, and hydrophilicity are key elements which determine not only the rate of permeation but also the stability of the membrane. The structure properties, however, depend on the type of

polymer material and the particular process through which the membrane support has been produced. Although the details of such processes for the production of microporous membranes are commercial secrets, three major processes, i.e., Celgard, phase inversion, and sintering, have been reported (Lloyd, 1985).

2.5.3 Material and Structure of the Support

In the Celgard process, semicrystalline films or fibers are extruded from the polymeric melt and porosity is induced by simply stretching the finished articles in the solid state. As noted by Kesting (1985), in many respects the *Celgard* process represents the ideal manufacturing process for microporous membranes, although the process is limited to certain slitlike pore sizes – generally 0.2 μm in length and 0.02 μm in width. The *phase inversion* process, on the other hand, refers to the process by which a polymer solution inverts into a swollen three dimentional macromolecular network or gel. In producing membranes by the *sintering* process, finely divided particles are heated to a temperature at or below the melting range of the material. As the exterior surface of the particles softens or melts, capillary pressure tends to rearrange the solid particles and ultimately ends with the formation of bridges and pores. Sintering is largely restricted to polymers with a flexible configuration. The sintering of PTFE membranes, called Gore-Tex process, takes place at 327 °C followed by a uniaxial or biaxial stretching. The Gore-Tex process is versatile and capable of producing membranes within a wide range of pore-size and porosity. The Gore-Tex membranes represent the most chemically inert and hydrophobic synthetic polymeric membranes and are unique in their ability to filter organic solutions and hot organic acids and bases (Kesting, 1985).

The microporous membranes have been made from polypropylene (PP), polytetra fluoroethylene (PTFE), and polyvinylidene fluoride (PVDF) materials. Polypropylene, the polymer chosen for extensive commercialization, is among the lowest-cost membrane

substances and is available in a large number of specialty grades. Furthermore, production rates are believed to be high (Kesting, 1985). The major manufacturers of microporous membranes are: Hoechst Celanese (Charlotte, NC) manufacturer of different types of Celgard (PP) membranes; W.L. Gore and Associates (Elkton, MD) manufacturer of the Gore-Tex (PTFE) membranes; Millipore (Bedford, MA) manufacturer of different types of (PVDF) and (PTFE) membranes under the commercial names of Durapore and Fluoropore; and Enka AG (Germany) manufacturer of the ACCUREL (PP) membranes.

Table 2.3: Characteristics of Commercial Polymer Microporous Membranes

Membrane	Material	Thickness δ (μm)	Pore Size (μm)	Porosity ε (%)	Tortuosity[a] (τ)	Supplier	Reference
Accurel 2E-PP	PP	130-170	0.2	75		Enka AG	Zha et al., 1995
K-100	PTFE	–	0.02	NA		–	"
Durapore GVWP	PVDF	110	0.22	70		Millipore	"
Celgard 3501	PP[b]	25	0.075 x 0.2	45		Hoechst Cel.	"
Durapore GVHP	PVDF[b]	110	0.22	75	1.67	Millipore	Zha et al., 1994
Celgard 2500	PP	25	0.075 x 0.25	45	2.25	Hoechst Cel.	"
Celgard 2400	PP	25.4	0.02	38	2.96	"	Prasad et al., 1986
Celgard 2500	PP	25.4	0.04	45	2.23	"	"
Goretex 1	PTFE	50.8	0.02	50	1.82	W.L. Gore	"
Goretex 2	PTFE	63.5	0.2	78	1.21	"	"
Fluoropore FP-045	PTFE	80	0.45	74	NA	Sumitomo	Akiba & Hashimoto (1985)
Gore-Tex TA-001	PTFE[c]	400	2.0	50	2.3	Junkosha	Teramoto & Tanimoto (1983)
KPF-400	PP[c]	33	0.135	45	3.6	Mitsubishi	"
—	PP[c]	300	NA	70	4.5	Asahi Kasei	"
Durapore FHLP	PTFE	60	0.50	85	–	Millipore	Deblay et al., 1991

a) measured by authors; **b**) hydrophilic polymer; **c**) hollow fibers

Celgard membranes are available in both film and hollow-fiber forms. Celgard 2400 and Celgard 2500 are hydrophobic films with effective pore size (pore-width dimention) of 0.02 and 0.04 μm, respectively. The corresponding hydrophilic (surfactant-containing) grades are Celgard 3400 and Celgard 3500. The two hydrophobic microporous hollow-fiber grades, Celgard X-10 and X-20, differ in porosity (20 and 40%, respectively) but not in effective pore size (0.03 μm). Celgard X-10 is available in 100, 200, and 240 μm ID, and 25 μm wall thickness. Gore-Tex membranes are also among the most important porous membranes. A very wide range of properties, i.e., pore size from 0.02 to 15 μm and porosity from 50 to 98%, afforded by this type of membranes is one of their advantages over other commercially available microporous membranes. A list of membranes, that had been employed by a number of researchers, mostly for metal separation purposes, along with their characteristic parameters are given in Table 2.3.

2.6 GENERAL FEATURES OF SLM

The unique advantages of this method over conventional solvent extraction and ELM are the possibility of using small amounts of expensive, tailor-made extractants, to achieve high separation and concentration factors on one hand and avoid phase mixing and emulsion formation on the other. However, SLM, similarly to ELM, has some major shortcomings of its own as well. These are:

1. Fouling: fouling is any unwanted coating of the membrane surface which has as result diminishing mass transfer fluxes and deteriorating separation performance. This problem includes the loading of reagent with impurities, solid deposition, and gel formation.

2. Scrubbing: scrubbing is a very common practice in conventional SX used to reject any co-extracted impurities and thereby to increase the selectivity of the separation process. In the case of liquid membranes, the lack of such an efficient stage is a major stumbling block in the industrial application of liquid membranes.

3. Low interfacial area: SLM provides much less interfacial area, in comparison with ELM, for the contact of the phases. This shortcoming, however, has been considerably removed by the application of hollow fiber modules which offer a relatively high surface in a very compact volume[3]. Kiani et al. (1984) have compared as an example the overall rate of extraction of acetic acid with MIBK, between a hollow fiber system and a perforated column. Due to the large *dispersion surface area per unit equipment volume* afforded in hollow fiber systems (16370 to 32742 m^2/m^3), these authors concluded that the overall rate of extraction by hollow fiber modules should be at least several times greater than that for the conventional perforated column systems.

4. Low transport rate: in spite of the very thin porous polymers used as the support, the total mass flux across the membrane is still low. Further attempts to reduce the membrane thickness increase the risks of mechanical rupture. Furthermore, that will accelerate the dissolution of the organic liquid filling the pores into both aqueous flows across the membrane. The latter problem of wash out of liquid membrane, which is in fact considered as the main cause of instability in the SLM technique, is discussed in more detail in the following section.

2.6.1 Life Time and Stability of SLM

As mentioned above, membrane instability, i.e., bleeding of the liquid organic from the pores of the support, constitutes one of the major drawbacks of SLM (Danesi, 1986; Tanigaki et al., 1988; Baker and Blume, 1990). The SLM system is composed of two elements: the support and the liquid membrane (LM). In order to obtain a stable SLM system, the compatibility of these two elements under practical operating conditions is of vital importance. The stability of the membrane has been defined in different terms in the

[3]As far as industrial application of SLM is concerned this seems to depend on the successful development of commercial hollow fiber modules or other type of membrane contactors. As a pioneer in this area, Hoechst Celanese Corporation has recently commercialized a new generation of modules (15 ft^2 interfacial surface area in a module of 2.5"ϕ×8") and given more promise for future developments.

literature. A general definition, which incorporates almost all means of instabilities, has been made (Deblay et al., 1991) based on the selectivity of the SLM during the operation; "A stable membrane maintains its initial selectivity constant". Except for the cases of chemical instability due to the chemical reactions with the extractant, i.e., lock up, degradation, etc., as long as the liquid membrane remains immobilized in the microporous support, the selectivity and permeability remain constant with time. This period of time is called the "life time" of the SLM and is a function of several factors.

The membrane may become unstable due to some factors such as hydrostatic pressure gradient, agitation and hydrodynamic regimes. This type of physical instability happens when the external forces exceed the capillary forces which keep the LM in the pores of the support. On the other hand, in the SLM system sufficient agitation of the feed and strip solutions is required in order to decrease the thickness of the boundary layer, between the membrane and the bulk solutions, and thereby increase the mass transfer rate. Prasad et al. (1986) examined the application of pressure gradient as an alternative to agitation. According to these authors, the latter may prove counterproductive causing instability to increase. Another type of instability may also occur due to the physicochemical phenomena which might take place during the process. Protonation of the extractant, i.e., hydrophilization of the extractant (Neplenbroek et al., 1992b), reverse micelle and microemulsion formation (Deblay et al., 1991), water transport through the membrane, and emulsion formation due to the induced shear forces by agitation (Neplenbroek et al., 1992c) are reported as some of these phenomena.

Apparently, all these types of instabilities are related to both process variables (i.e., agitation speed, viscosity of LM, acidity of the phases, chemistry of the reagents, etc.) and the support properties (i.e., hydrophilicity, thickness, network structure, etc.). For instance, Zha et al. (1992) studied the maximum pressure gradient that a supported liquid membrane can tolerate before becoming unstable. They realized that the *critical displacement pressure* is related to the membrane maximum pore size, pore structure,

interfacial tension of fluids, and contact angle. These authors finally concluded that a membrane with a morphology having a less connected network and shrap pore edges affords higher stability.

2.6.2 Methods to Increase SLM Stability and Membrane Contactor Design

Many attempts have been made to increase the life time and the stability of the SLM. These efforts can be categorized in three different approaches. The first approach involves the simple replacement (continuous or intermittent) of the lost liquid membrane with fresh organic (Danesi and Rickert, 1986; Nakano et al., 1987; Klein and Schneider, 1987). Teramoto and Tanimoto (1983) used the same method to regenerate the membrane pores in a hollow fiber system. Such methods all use the principle of supplying new carrier to the membrane rather than preventing loss of the liquid membrane. This method is questionable for both environmental and economic reasons.

The second approach aims to prevent the loss of liquid membrane from the pores of the support. One way to achieve this goal, which has been undertaken by researchers of "The Center for Membrane Technology" at the University of Twente (the Netherlands), includes homogeneous gelation of the substrate using PVC (Neplenbroek, 1989). Although the applied gelatin layer promotes the stability of the SLM it causes a drastic decrease in the rate of permeation (i.e., down to about 65% of the uninhibited mode) (Bromberg et al., 1992; Wijers et al., 1994). Another method which has been considered for the prevention of LM loss is sandwiching the hydrophobic support by two hydrophilic protection layers. Neplenbroek (1989) used interfacial polymerisation, to form via polycondensation a hydrophilic layer at the interface of the two immiscible phases. As a result of that, the stability of the SLM increased while the rate of permeation more or less remained the same, depending on the type of interfacial polymer formed.

The third approach that has been proposed to increase the stability of the SLM is to radically change the configuration of the membrane contactor itself. According to this approach, the organic no longer remains stationary in the pores of the support. Instead, the organic and aqueous phases are contacted through a hydrophilic or a hydrophobic microporous membrane. Boyadzhiev (1990), who has worked on the development of this alternative membrane configuration for some 15 years has called this process "liquid film pertraction" (LFP). In this technique, parallel hydrophilic supports are employed to separate the aqueous flows from the organic flow (Figure 2.8). In this way, the organic is not stagnant in the pores of the support, but rather forms a thin film which counter currently flows through the channel between the hydrophilic supports. As one of the potential advantages of this process, in addition to enhanced stability, Boyadzhiev mentioned the possibility of incorporating a scrubbing stage in the circulation path of the organic phase.

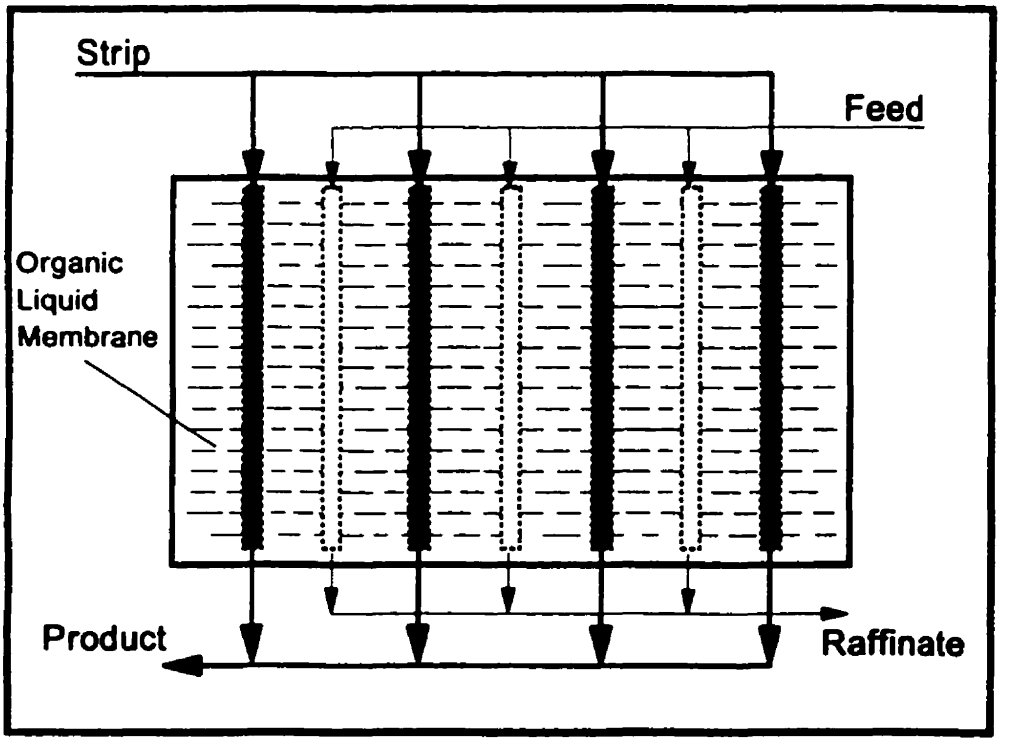

Figure 2.8: Schematic Representation of Liquid Film Pertraction Adapted from (Boyadzhiev, 1990)

A superficially similar approach with that used in LFP has been applied to develop an alternative solvent extraction process called *solvent extraction with immobilized interfaces*, or equivalently *dispersion-free solvent extraction*. This method involves the solvent extraction of a solute from an aqueous phase into a solvent (moving in the countercurrent direction) through a microporous hydrophobic or hydrophilic membrane. In a second stage, the loaded organic is brought into contact through a similar membrane with a strip aqueous phase. In other words, this method is not a truely LM technique since does not involve the coupling of extraction and stripping into a single stage. As such, the dispersion-free SX process does not offer the unique advantage that characterizes liquid membranes, i.e., the operation of powerful driving forces suitable for the treatment of very dilute solutions. Nevertheless, this method offers a number of advantages such as less extractant loss, independent variation in phase flow rates, avoidance of flooding, loading and sweeping, no need for density differences between the aqueous and organic phases, and high contact area per unit volume of equipment (Prasad et al., 1986; Prasad and Sirkar, 1990). This method like any other membrane method, though, is very sensitive to the presence or formation of solid particles which leads to membrane blockage.

2.6.3 Mechanism of Metal Transport through SLM

In general, liquid membrane is a concentration-driven separation process. As such the process can be *facilitated* by maximizing the concentration gradient of the diffusing species across the membrane. This can be achieved by two different methods.

One method of *facilitated transport* is the minimization of the permeant concentration in the receiving phase by reacting the diffusing species with some other constituent in the latter phase. The product of this reaction is insoluble in the membrane phase and thus incapable of diffusing back through the membrane. For instance, in the removal of phenol from an aqueous feed, the phenol diffuses through a hydrocarbon membrane to a receiving phase of caustic solution (Matulevicius and Li, 1975). The phenol reacts with caustic to

form sodium phenolate which is insoluble in the hydrocarbon membrane and hence cannot diffuse back into the feed. In this way, the concentration of phenol in the receiving phase is kept low, thus, facilitating its passage through the membrane.

The second method of *facilitated transport*, so called *coupled transport*, has been mainly used for metal extraction purposes. In this case, the transport rate of the diffusing species across the membrane is accelerated by incorporating a metal extractant, i.e., a metal *carrier* in membrane terminology, in the membrane phase. The mechanism of coupled transport through SLM is schematically described in Figure 2.9. In the case of *co-transport* mechanism (Figure 2.9(a)), the carrier reagent forms a complex with the metal species at the feed interface and carries the latter across the membrane to the strip interface. While in the case of *counter-transport* (Figure 2.9(b)), the transfer of the metal ionic species is counterbalanced by an equivalent transport of similar ionic charges in the reverse direction. Comparison of these transport mechanisms with conventional solvent extraction mechanism of metal extraction quickly reveals that the co-transport mechanism corresponds to the ion-pair formation mechanism and the counter-current transport to the compound or inner-sphere complex formation mechanism.

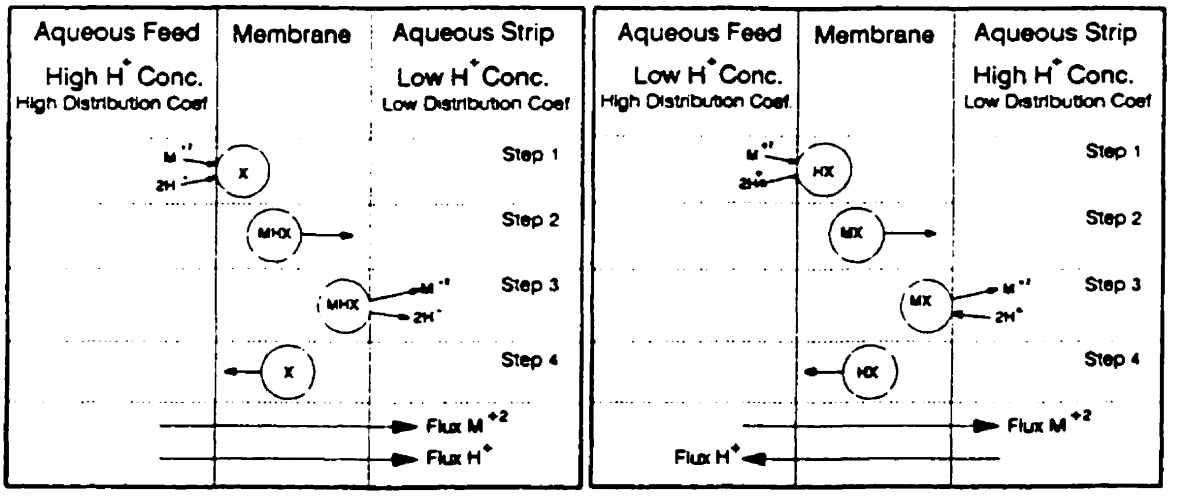

(a) Co-Transport Mechanism (b) Counter-Transport Mechanism

Figure 2.9: Coupled Transport of Metal Species through Liquid Membranes

Apparently, in this coupled transport mechanism, the concentration gradient of the metal species across the membrane is no longer the driving force. However, pH, counterion concentration-gradient, or any other expedient which assures a large chemical potential gradient between the two opposite sides of the membrane, can be used as the driving force for this permeation process. From this schematic description of coupled transport it follows that metal species can be transported across the membrane against their concentration gradient. This type of "uphill" transport will continue until all the metal species which can permeate the SLM have been transferred from the feed to the strip side, providing the driving force of the process is kept positive. This situation often occurs in practice when the concentration of the chemicals responsible for the driving force is continuously adjusted to keep it constant. It follows that in a SLM permeation process, very high concentration factors can be obtained by using a volume of the strip solution which is much lower than that of the feed solution. Moreover, by choosing a very selective carrier high separation factors can be also achieved.

2.6.4 Equations Describing the Supported Liquid Membrane Transport

Many attempts have been made to develop mathematical models of the liquid membrane transport process. In the area of separation of metal species, efforts have been devoted to work out a simple model which, in terms of a few and independently measurable variables, could describe quantitatively the permeation process of metal species through SLM (Danesi, 1984). Two principal approaches have been applied to modeling liquid membrane processes (Kremesec, 1981).

The approach which is mainly used for ELM process, *integral approach*, considers the three liquid-phase system as a closed multiphase system and therefore takes into account the processes and changes in all three liquids (Boyadzhiev et al., 1977). The other, *differential approach*, which is commonly used in the modeling of separations by SLM, considers only the phenomena occurring in the bulk or at the surfaces of the membrane. According to this approach, the overall rate of mass transfer is controlled by any of the

diffusion or chemical-reaction resistances raised in the aqueous stagnant layers adjacent to the membrane or in the organic within the membrane. The resistance-in-series method is also adopted to formulate this model of the permeation process.

In order to develop the differential model, it is first necessary to identify the various steps which characterize the transport of metal species through SLM. These steps are schematically described with the help of Figure 2.10 (Danesi et al., 1981). Step 1: The metal species diffuse from the bulk of the feed into the feed-SLM interface. Step 2: The diffused metal species react with the metal carrier at the feed-SLM interface (the counterbalanced ions are released into the feed solution or the counterions accompany the metal species into the membrane, in counter-transport and co-transport, respectively). Step 3: The metal-carrier complex diffuses across the membrane because of its favorable concentration gradient. Step 4: At the SLM-strip solution interface the metal-carrier complex undergoes a reverse reaction and releases the metal species and accompanying

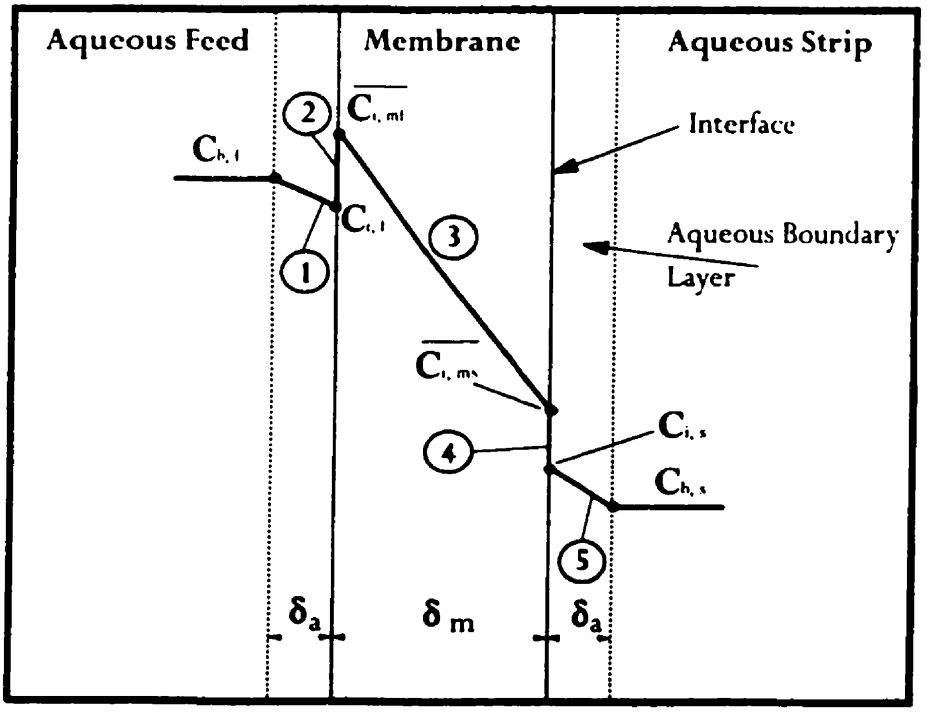

Figure 2.10: Schematic Representation of the Stepwise Processes Controlling Membrane Permeability (Adapted from Danesi et al., 1981)

ions into the aqueous strip solution (the counterbalanced- and counter-ions are exchanged). Step 5: The permeated metal species diffuse from SLM-strip interface into the bulk strip phase. There is, however, a complementary step which accomplishes the return of the free carrier from the SLM-strip interface to the SLM-feed interface. However, since in most cases it is presumed that free carrier diffuses much faster than the metal-carrier complex the role of this step in the whole permeation process is neglected.

When the metal distribution ratio ($\overline{C}/C$) at the membrane-strip interface is lower than that at the membrane-feed interface, the continuous transport through the membrane takes place. The steady-state overall membrane flux can be derived by applying Fick's diffusion law. Fick's first law states that the rate of diffusion (dn/dt) of a solute across an area (S), known as diffusive flux (J), is calculated as follows:

$$J = (dn/dt) = -D_m S(dC/dx) \tag{2.10}$$

where (dC/dx) is the concentration gradient of the solute across the distance "dx" and "dn" is the amount of solute (in moles) passing across the membrane in time "dt". D_m is the diffusion coefficient that accounts for the environment of a specific membrane.

In the study of SLM it is convenient to use the parameter "flux" to describe the complex process of the permeation of the solute through an SLM. In measurable terms, it is best to express flux as the decrease in the concentration "C " of the solute in the feed solution with time "t".

$$J = \frac{-dC}{dt}(V/S) \tag{2.11}$$

where "V " is the volume of the feed solution and "S" is the surface area of the support. The permeation coefficient "P" is then defined as:

$$P = \frac{J}{C} = \frac{-dC/C}{dt}(V/S) \tag{2.12}$$

This equation can be integrated to

$$\ln\frac{C}{C_o} = \frac{-PS}{V}t \tag{2.13}$$

where C_o is the initial feed concentration. The permeation coefficient, P, is a very useful term to report the permeation rate of the metals particularly when several metal species are present in the solution (Barnes et al., 1995). Another useful parameter is the enrichment factor of the metal species since the application of SLM is often aimed at the enrichment of a solute. Sato et al. (1990) defined the enrichment factor, Y, of a species as the ratio of the concentration of the species in the stripping solution, C_s, to its initial concentration in the feed solution, $C_{o,f}$.

$$Y = C_s / C_{o,f} \tag{2.14}$$

In order to develop a mathematical expression to predict the SLM permeation behavior, though, a phenomenological analysis of the SLM system is required. As mentioned earlier, a permeating species experiences five different resistances in passing through an SLM (see Figure 2.10). At steady-state condition, the regional flux through these steps are equal to the overall flux through the membrane, i.e., $J = J_1 = J_2 = J_3 = J_4 = J_5$. Accordingly, five equations can be derived to correlate the overall flux with the individual mass transfer coefficients "k" and the respective concentration gradients acting across each region. By rearranging these equations, one finally obtains a single expression which correlates the flux "J" with an overall mass transfer coefficient "k_O" and the measurable concentrations of the feed or strip solutions (Ho and Sirkar, 1992). The overall mass transfer coefficient incorporates a combination of individual mass transfer coefficients and some independently-measurable parameters such as metal distribution ratios and chemical reaction constants. These parameters can be determined through various independent experiments and be applied in the latter expression.

As a general trend in literature, the situation has always been simplified by neglecting one or more of the above five resistance terms. It is notable that steps 1, 3, and 5 represent diffusive resistances while steps 2 and 4 account for the resistances of the interfacial chemical reactions. Apparently, if the resistance of one of these steps is negligible in

comparison to the others, the overall flux is not controlled by the resistance raised through that step and thus the respective term can be neglected. For instance, Danesi (1984) considered only steps 1 to 3 as the rate controlling steps and derived the following equation:

$$P = \frac{J}{C} = \frac{\mathbf{k}_r}{\mathbf{k}_r(\delta_a/D_a) + (\delta_m/D_m)} \tag{2.15}$$

where $\mathbf{k}_r$ is the interfacial chemical reaction constant, δ_a is the thickness of the aqueous stagnant layer adjacent to the membrane, δ_m is the thickness of the liquid membrane, D_a and D_m are the diffusion coefficients in the aqueous layer and the organic liquid membrane, respectively.

Another instance is the derivation made by Zha et al. (1995) who neglected the reaction resistances at both interfaces and expressed the permeation rate as:

$$J_A = k_O\left(C_f - \frac{\mathbf{D}_s}{\mathbf{D}_f}C_s\right) \tag{2.16}$$

$$\frac{1}{k_O} = \frac{1}{k_f} + \frac{1}{\mathbf{D}_f k_m} + \frac{\mathbf{D}_s}{\mathbf{D}_f k_s} \tag{2.17}$$

where k_O is the overall mass transfer coefficient, C_f and C_s are the concentration of metal in the feed and strip solutions, k_f, k_s, and k_m are individual mass transfer coefficients in the feed, strip, and membrane solutions, respectively. The terms $\mathbf{D}_s$ and $\mathbf{D}_f$, the distribution coefficients at the interfaces on the feed side and the strip side, are conventionally given by

$$\mathbf{D}_f = \overline{C_{f,i}}/C_{f,i} \tag{2.18}$$

$$\mathbf{D}_s = \overline{C_{s,i}}/C_{s,i} \tag{2.19}$$

The overbar refers to the respective concentrations in the organic phase and the subscript "i" denotes the interface. Meanwhile, the intrinsic diffusive resistance of the membrane ($1/k_m$) can be explicitly expressed as:

$$\frac{1}{k_m} = \frac{\delta_m \tau}{D_m \varepsilon} \tag{2.20}$$

where δ_m is the thickness of the membrane, τ is tortuosity of the pores, and ε is the porosity of the membrane. In the cases that molecular parameters are available from the literature, Wilke-Chang correlation can be used to calculate D_m (Deblay et al., 1991);

$$D_m = 1.17\times10^{-16}\frac{T(\Psi_{sol}M_{sol})^{0.5}}{\eta_{sol}\tilde{V}^{0.6}} \quad (m^2/s) \qquad (2.21)$$

where T is the absolute temperature, Ψ_{sol} the solvent association factor, M_{sol} the solvent molecular weight, η_{sol} the solvent viscosity, and $\tilde{V}$ the molar volume of the solute at normal boiling point. Neplenbroek et al. (1992c) used Stokes-Einstein equation to correlate the diffusion coefficient in the membrane, Dm, with the viscosity of the liquid membrane;

$$D_m = \frac{\kappa T}{6\pi r \nu} \qquad (2.22)$$

where κ stands for the Boltzmann constant, T is the absolute temperature, r is the radius of the diffusing species and ν is the kinematic viscosity of the liquid.

From the above discussion, it follows that a phenomenological model can be developed through a detail analysis of the permeation process of a given solute. This model provides an expression for the flux of the permeant which incorporates geometrical, chemical, and diffusive terms. However, it should be emphasized that when aqueous film diffusion, interfacial chemical reactions, and membrane diffusion simultaneously control the membrane permeability, explicit solutions for the membrane flux lead to not-easy-to-solve mathematical complexities (Danesi et al., 1981). Further limitations to the development of theoretical treatments is associated with the very scanty information which might be available on the rate and mechanisms of chemical reactions occurring at liquid membrane-aqueous interfaces. Due to the latter complications, in some cases the general permeation behavior of the SLM against the variables of the system has been examined and only an empirical relation is provided. This empirical relation correlates the rate of the permeation with the main variables of the system such as the concentration of the carrier, and that of acid, base, metal ion, etc. (Saito, 1991; 1993).

CHAPTER 3

Experimental

3.1 INTRODUCTION

The experiments conducted in the course of this project can be categorized into two groups, i.e., solvent extraction and liquid membrane experiments. In the solvent extraction of Rh species part, three types of experiments were conducted; (i) SX from chloride solutions with Kelex 100, (ii) with trioctylamine, and (iii) SX from bromide solutions with Kelex 100. The organic phase of Kelex 100 was also characterized in order to explain some of the observations obtained through this part of the experiments. In the liquid membrane section, a major part of the work was devoted to the permeation behavior of chlorocomplexes of rhodium and HCl through the SLM. Due to the variety of the experiments, the general description of the experimental and analytical methods are provided in this chapter and the details of the procedures, where necessary, are given in the respective sections.

3.2 MATERIALS AND REAGENTS

HCl, NaOH, and $LaCl_3$ were of reagent grade from Canlab (Mississauga, Ont.). Trioctylamine[1] (TOA) from Aldrich (Milwaukee, WI) and reagent grade of chloride salts, i.e., NH_4Cl, NaCl, KCl, $MgCl_2$, from Anachemia (Montreal, Que.) were used. Sodium hexachlororhodate(III) hydrate ($Na_3RhCl_6.xH_2O$), rhodium(III) bromide ($RhBr_3.2H_2O$), and standard Rh solution obtained from Aldrich (Milwaukee, WI). Kelex 100, supplied by WITCO (Dublin, OH), was used as extractant. This reagent has an average molecular weight of 299 and a purity and density in the vicinity of 80-85% and 1 g/mL, respectively. A more detailed description of this reagent was given in chapter 2. Kerosene which was

[1]MW: 353.68; purity: 98%; d: 0.809; bp: 365 °C.

obtained from Fisher Scientific (Nepean, Ont.) was used as diluent and tridecanol (Harcros Chemicals) was added as phase modifier. Karl Fischer titrant, AQUASTAR Comp 5 (pyridine free), and solvent (1-propanol) were obtained from BDH Inc (Ville St-Laurent, Quebec). Distilled water, which was deionized to a minimum resistance of 1 megohm/cm, was used for preparation of aqueous solutions.

3.3 EXPERIMENTAL PROCEDURES

The preparation procedure of aqueous and organic solutions in both solvent extraction and liquid membrane experiments was similar. The aqueous solutions were prepared by weighing appropriate amounts of Rh salt and dissolving it in previously prepared HCl/H_2O, or HBr/H_2O, solutions. Extra amounts of Cl^- or Br^- if required were added to the aqueous phases in the form of salts. In the cases that aged Rh solutions were required, the aqueous solutions were left to rest at room temperature for the desired period of time.

Organic solutions of Kelex 100 were prepared by diluting the latter in kerosene. Tridecanol was always added as phase modifier in order to improve the organic properties and prevent third phase formation. The preparation of the organic solutions, however, consisted of a purification stage of the "as received" extractant. This involved contacting the prepared organic solution with an equal volume of 4 M HCl aqueous solution for five minutes to wash out all of the acid-soluble organic compounds. The acidified organic phase was then subjected to four 5-minute contacts with distilled water at an aqueous to organic volume ratio (W/O) of one, which removed all of the organic-phase acidity.

For SX applications, the relative percent composition, in a volume basis, of the organic solutions were either 2, 5, and 93% (v/o), or 5, 5, and 90% (v/o) of Kelex 100, tridecanol, and kerosene, respectively (These correspond to approximately 0.056 and 0.14 M of extractant and 0.21 M of alcohol). While for the LM applications, the latter were X, X, and (100-2X) v/o, mostly 25, 25, and 50 v/o of Kelex 100, tridecanol, and kerosene, respectively. (The 25, 25 v/o composition corresponds to approximately 0.70 M extractant and 1.0 M tridecanol solution).

Organic solutions of trioctylamine (TOA) were also prepared by diluting this extractant in kerosene and adding tridecanol as phase modifier (due to the high purity of TOA, it was used "as received"). The relative percent composition was 5 , 5, and 90% of TOA, trioctylamine and kerosene, respectively (these correspond to 0.115 M trioctylamine and 0.21 M tridecanol). Experiments throughout this project were almost always carried out at room temperature (23±2 °C). In some cases, the Rh solutions were heated at elevated temperatures, i.e., 70-80 °C, for a period of time using a thermostated water bath.

3.3.1 Solvent Extraction Experiments

All of the tests were performed using either 125-mL separatory funnels or 50-mL cylindrical glass jars fixed to a Burrell automatic wrist action shaker (Model 75). Due to the substantial value of Rh, the volume of the aqueous solution was kept to a minimum and, in general, 15-mL samples were used in the contact experiments. The W/O volume ratio, unless otherwise indicated, was one. Samples of the aqueous feed and raffinate were kept for the Rh content analysis and the organic solutions were kept for water content measurements.

3.3.2 Organic Phase Characterization

The water content of the organic phase, mg (H_2O)/mL (of sample), was determined by the Karl Fischer titration method (Ashrafizadeh, 1992; Goklen, 1986) using an automatic Schott Gerate Titrator (Model T80/50). The results of the Karl Fischer measurements were verified using some organic solutions of known water content. These samples were prepared by injecting specified amounts of water into the organic phase. In all cases, the Karl Fischer readings were accurate to ±2%. Viscosity measurements were performed in a thermostated bath, at 25 °C, by using an Ubbleohde Viscometer (Fisher Scientific). Interfacial tension measurements were conducted on a "surface tensiomat" tensiometer from Fisher Scientific. Refractive indices were measured by an Abbe-3L refractometer from Milton Roy Company (Rochester, NY, USA).

Dynamic light scattering experiments were conducted by using a vertically polarized 50 mW He-Ne laser source from Spectra Physics. The scattering plane was perpendicular to the incident light polarization and the incident wavelength was 632.8 nm. A commercial goniometer PCS (Brookehaven Instruments BI-2030) was used to measure the scattered light at 90°. A refractive index matching bath of filtered decalin (0.22 μm) surrounded the scattering cell and its temperature was controlled at 25±0.1 °C. The autocorrelation functions were analysed using the cumulant method (Berne and Pecora, 1976). The micellar diameter of the organic-phase *water in oil (W/O)* microemulsions was measured for an organic solution containing 5 v/o (i.e., ~0.14 M) Kelex 100. Due to the intensive labour required, no extrapolation for diluted Kelex 100 solutions was made.

3.3.3 SLM Experiments

SLM experiments were carried out in a two-compartment cell schematically shown in Figure 3.1. The apparatus was composed of an inner plexiglass vessel held vertically in a Pyrex crystallizing dish (125 x 65) as the outer container. A membrane with an effective surface area of 44 cm^2 (7.5 cm in diameter) separated the two parts while being sealed with a Viton (acid resistant) gasket. Two different structure hydrophobic microporous polymers (polytetrafluoroethylene (PTFE)), supplied by W. L. Gore & Associates under the commercial name of 4C5 GORE-TEX, were used as membrane support. One of the polymer materials had pore size of 0.45 μm, thickness of 57 μm, and porosity of 75.9%. The other had pore size of 0.20 μm, thickness of 20 μm, and porosity of 66.8%. Agitation was provided by using a magnetic stirrer for the feed and a cylindrical Teflon impeller for the strip solution. The latter had been used previously (Mihaylov, 1991) in a solvent extraction kinetic study as a part of a rotating diffusion cell (RDC).

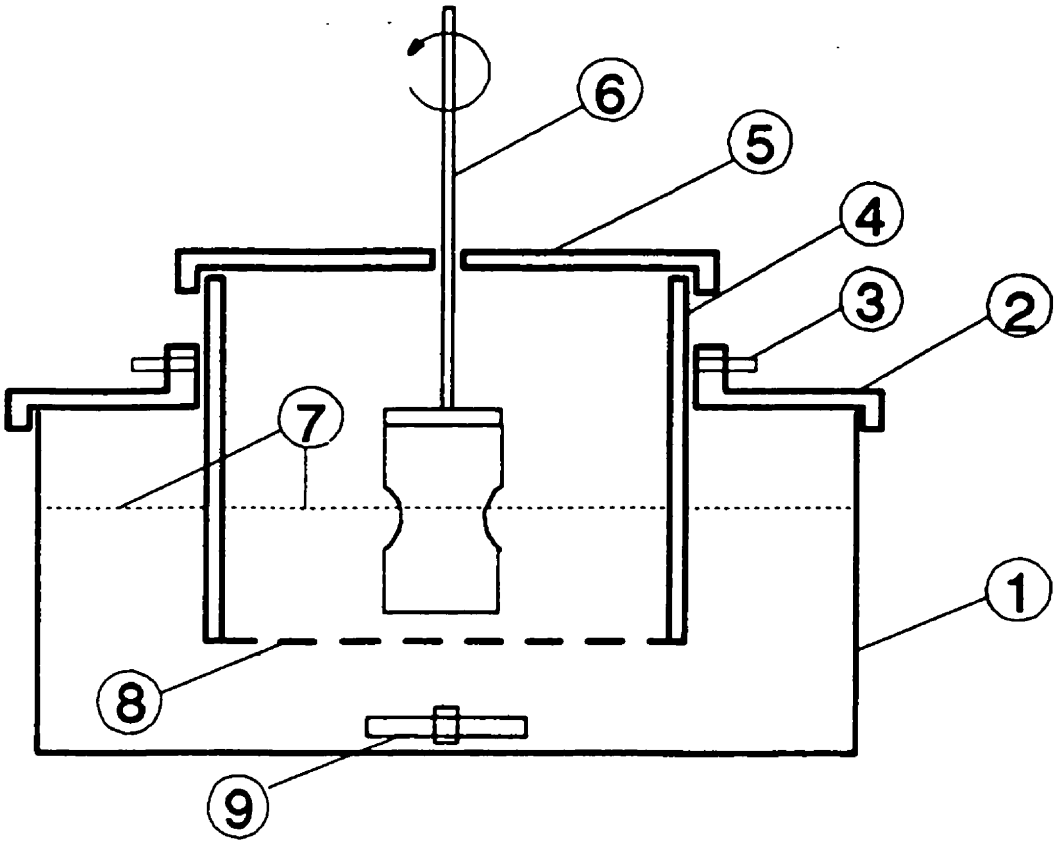

1. Feed Container
2. Feed Container Cap
3. Height Adjust Pin
4. Strip Container
5. Strip Container Cap
6. Turbine Agitator
7. Aqueous Levels
8. Membrane
9. Stirrer

Figure 3.1 SLM Apparatus

The SLMs were prepared by soaking the polymeric support for 10-15 hours into the liquid membrane solution, then letting it drip for a few minutes before placing it in the cell. The feed and strip containers were filled with previously prepared feed and strip solutions, according to the required specifications, always at a volume ratio of 200 mL to 20 mL, respectively. Except for the experiments devoted to measuring the extraction of water, the duration of the vast majority of tests was one hour. For the case of water-extraction experiments, due to the volumetric measurement of the strip phase, it was required to run the experiments for a longer period of time in order to achieve higher quantities of extracted water and thus to decrease the error introduced in the volumetric determination. For this reason a period of six hours was chosen for that set of experiments.

The experiments were conducted at constant feed and strip acidity. This was almost satisfied for the feed which contained a high volume and a relatively high acid concentration. However, for the strip solution, the co-extracted acid caused the pH of the strip solution (pre-fixed at pH=1) to change. Therefore, a solution of 10 M NaOH was used to neutralize the extracted acid and maintain the pH at one. This was done every 30 minutes. In this way, it was assured that the variation in the pH of the strip solution was almost negligible. For the cases where accurate volume measurements were necessary, the amount of added NaOH was taken into account. For the metal content analysis, aliquots of 1 mL were taken from feed and strip solutions, before and after each run. Rhodium permeation tests were conducted in a very broad range of feed, strip, and membrane conditions while the permeation of other metals was investigated only for a very confined range of variables.

3.4 ANALYTICAL PROCEDURES

Acidity of the feeds and raffinates in SX and the strip solutions in LM experiments were determined through a standard acid-base titration. Titrations were performed manually using 0.1 M NaOH and phenolphthalein as the end-point indicator. The pH measurements were performed with a PHM 84 Research pH meter from Radiometer Copenhagen in

combination with an ORION ROSS pH electrode. The fast response, stability, accuracy, and reproducibility were of primary importance in performing pH measurements in the region of pH 1-2 and the precision was ±0.01 in that pH scale.

The Rh concentrations in the feed and strip solutions were determined by atomic absorption spectroscopy on an spectrophotometer Model 357 from Instrumentation Laboratory Inc. All the samples and the AA standards were diluted to the linear region using 1.4 M HCl. A drop of 100 g/L $LaCl_3$ was added to all samples and standards to minimize the effect of sodium on the Rh determinations. A nitrous oxide-acetylene flame was used rather than the more common air-acetylene flame (Griffith, 1967). The amount of Rh extracted into the organic phase and the percent extraction was calculated as the difference in Rh concentration between the feed and the raffinate. The calculation takes into account the amount of water which moves from the original aqueous phase to the organic phase, using a small computer program reported in a previous work (Ashrafizadeh et al., 1993).

As an alternative to atomic absorption (AA) measurements, UV-Visible Spectroscopy was also recognized as an appropriate technique to measure the concentration of the Rh complexes in different aqueous solutions. A UV-Visible spectrophotometer model Cary 1 from Varian Australia Pty Ltd. was used for this matter. The absorption spectra of the Rh solutions at the visible region (300-900 nm) were found to exhibit a correlation between the absorption peak and the concentration of the solution (Figure 3.2). Furthermore, for each particular concentration of chloride in the background solution, the peak shifts to another wavelength, while still remaining proportional to Rh concentration (Figure 3.3). This observation prompted the establishment and use of the calibration curves to measure the concentrations of Rh in different solutions (Appendix A; Figures A-1 to A-6). Therefore, the *"peak vs. concentration"* calibration curves, which are prepared against the AA measurements, provide a non-destructive and on-line technique which is very useful particularly in handling the SLM experiments.

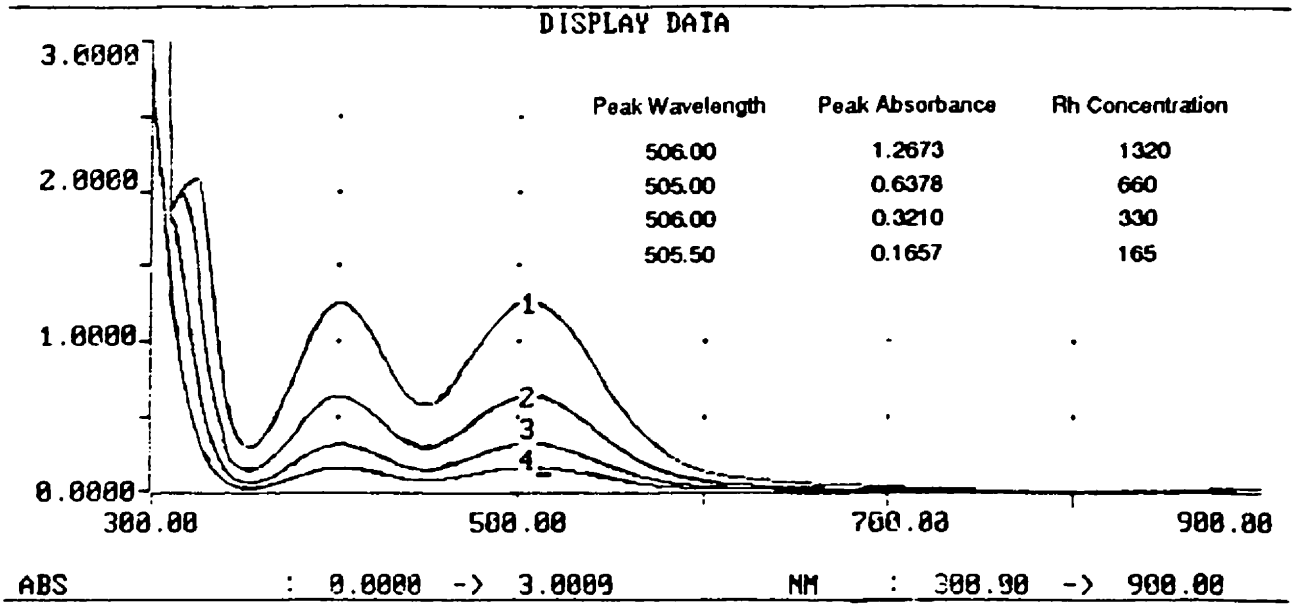

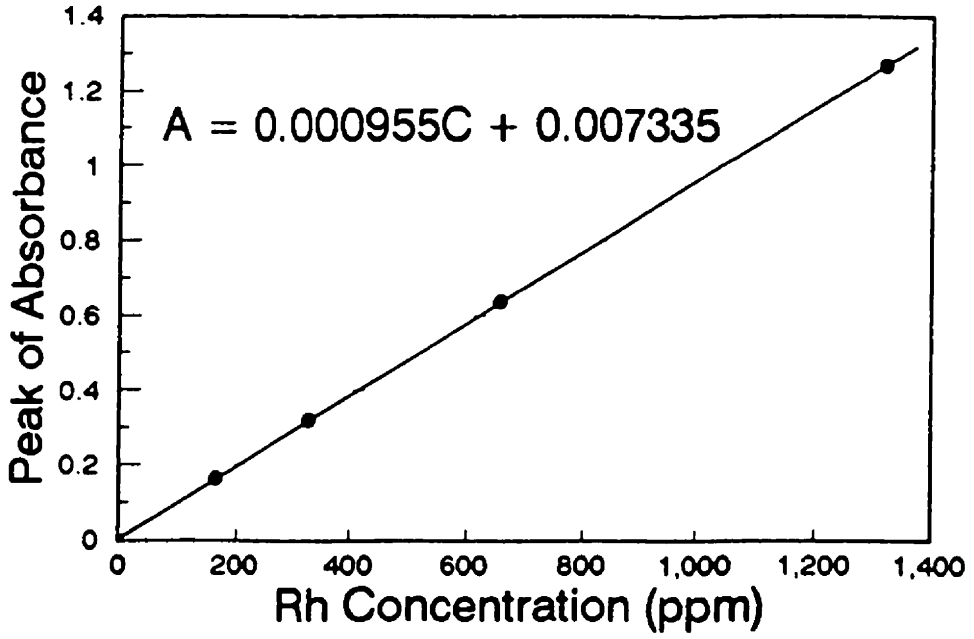

Figure 3.2: Absorption Spectra and Calibration Curve for Aged Rh Solutions of 2.5 M HCl

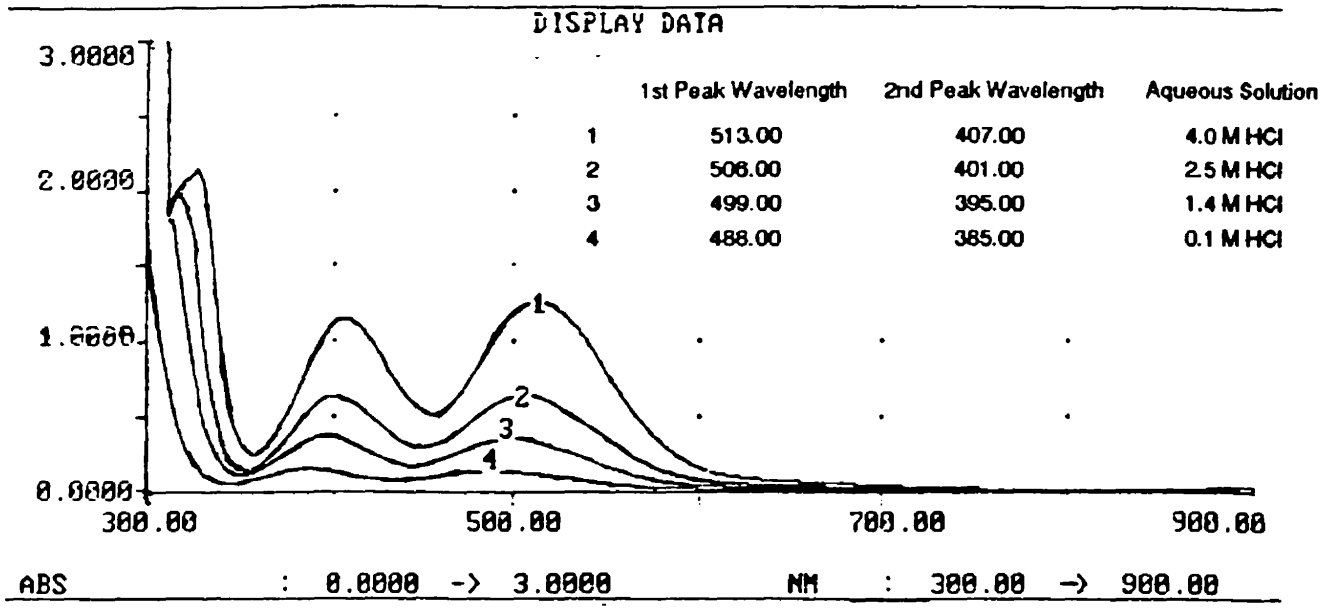

Figure 3.3: Absorption Spectra for Aged Rh Solutions at Different HCl Concentrations.

The results of the SX experiments are always reported as percent extraction or as distribution coefficient (**D**) of the metal species. The rate of water, acid, and Rh transport through the membrane were determined for the initial stage of the transport process and expressed as moles of transported species per unit area (geometric) of the SLM per unit time, i.e., $mol.s^{-1}.m^{-2}$. For instance, the flux of Rh through the SLM is given by:

$$J = \left(\frac{d[Rh]_{f,t}}{dt} \right)_{t=0} \frac{V_f}{S} \qquad (3.1)$$

where V_f is the volume of the feed solution and S refers the surface area of the SLM. The rate of Rh extraction was determined by monitoring the change in Rh concentration of both aqueous phases, i.e., feed and strip solutions. The reported rate is, though, an average of these two obtained values. The same procedure was used to report the rate of acid permeation while for the rate of water transport the volumetric measurements were directly used to calculate the flux. The calculations take into account the volume changes due to the transport of water. Solvent extraction and SLM experiments were performed more than once and the reproducibility was always within ±5%.

CHAPTER 4

The Rh(III)-HCl-Kelex 100 Solvent Extraction System[1]

4.1 INTRODUCTION

4.1.1 Aquation and Extraction of Rhodium

The extent to which a metal ion is extracted from an aqueous into an organic phase is the result of many factors. One of these factors is the amount of water which accompanies the metal complex. This water favors the solubility of the metal complex into the aqueous phase and disfavors its solubility in the organic phase. In the case where the metal ion is fully coordinated , i.e., all its coordination sites are occupied by ligand donor atoms, the water will form the outer-sphere of the complex by means of solvation (hydration). In this case the water molecules interact with the complex but not directly with the cation (Martell, 1971). However, for metal ions with high coordination numbers, i.e., ≥ 6, the water may exist in the inner-sphere of the complex (aquation). Both types of water association with inorganic complexes may have a suppressing effect on the extraction of the metal complexes but it is the latter type, i.e., aquation, which causes the most serious problems. In the latter case, different procedures and techniques may be applied to dehydrate the metal complexes prior to extraction (anation). For instance, one possible way is to replace the residual inner-sphere water by a neutral organophilic ligand (Choppin, 1992). This ligand exchange reaction is characterized by an equilibrium constant, **K**, defining the thermodynamic feasibility, and $\mathbf{k_1}$ and $\mathbf{k_2}$, forward and backward exchange reaction-rate constants, which define the kinetic feasibility:

---

[1]The material presented in this chapter constitutes the subject-matter of a recent publication: S.N., Ashrafizadeh, and G.P., Demopoulos, Formation of W/O Microemulsions in the Extraction System Rh(III)-HCl-Kelex 100 and Its Impact on Rh(III) Distribution, *J. Colloid Interface Sci.*, **173**, 448-459, 1995.

$$M(H_2O)_x^{m+} + L \leftrightarrow M(H_2O)_{x-1}L^{m+} + H_2O \quad (4.1)$$

As a general observation, aquation is very frequent in transition metals and it is more noticeable for base metals (Cotton and Wilkinson, 1980), rare earths metals (lanthanides) (Choppin, 1992), and specifically for platinum group metals (Griffith, 1967). The anionic complexes of secondary PGM (Ir, Rh, Ru, Os) extensively undergo aquation. The extent of aquation varies considerably with the oxidation state of the metal, the trivalent metals form the most extensive aquated complexes (Stern, 1981). Previous investigations on the aquation behavior of Rh(III) chlorocomplexes and the generated speciation diagrams, which were extensively reviewed in Chapter 2, confirm the substantial aquation of the latter complexes in chloride media.

$$RhCl_6^{3-} + wH_2O \leftrightarrow RhCl_{(6-w)}(H_2O)_w^{(3-w)-} + wCl^- \quad (4.2)$$

Benguerel et al. (1994) examined the extraction of Rh(III) complexes by Kelex 100, from hydrochloric acid solutions. According to these authors, a limited amount of Rh(III) of less than 40% is extractable with Kelex 100. The following mechanism was proposed to account for the extraction of Rh(III):

$$\overline{R-HQ} + H^+ + Cl^- \leftrightarrow \overline{R-H_2Q^+Cl^-} \quad \text{(protonation)} \quad (4.3)$$

$$RhCl_6^{3-} + 3(\overline{R-H_2Q^+Cl^-}) \leftrightarrow \overline{RhCl_6^{3-}(R-H_2Q^+)_3} + 3Cl^- \quad \text{(ion-pair formation)} \quad (4.4)$$

where R-HQ stands for the alkylated 8-hydroxyquinoline extractant, Kelex 100. Regarding the very low distribution coefficient obtained, these investigators postulated that only the non-aquated complex, i.e., $RhCl_6^{3-}$, is extracted and aquation has been mentioned as the most important parameter in hindering the quantitative extraction of rhodium (Benguerel et al., 1994; 1996).

In this chapter the aquation and interfacial chemistry of Rh(III) in the extraction system Rh(III)-HCl-Kelex 100 are studied in an effort (i) to substantiate the previous claim of Benguerel et al. (1994) and (ii) to unblock, if possible, the problematic extraction of rhodium.

4.1.2 Microemulsion Formation in the Organic Phase

In spite of the extensive investigations dealing with alkylated 8-hydroxyquinolines (R-HQs), and specifically with Kelex 100, a gap of information exists on the structure of the organic phase, i.e., the intramolecular relations between diluent, extractant, modifier (alcohol), extracted metal, and probable solubilized water molecules into the organic phase. Apart from the systematic work of Tondre (Boumezioud et al., 1989; Tondre and Boumezioud, 1989; Kim and Tondre, 1989; Tondre and Caanet, 1991; Tondre et al., 1991; Ismael and Tondre, 1992) on the micellization behavior of Kelex 100, which deals with the kinetics and the rate of metal complexation in the aqueous phase, only sporadic references on the aggregation behavior of R-HQs in the organic phase can be found in the published literature. The work of Tondre et al. has dealt with the solubilization behavior of Kelex 100 into the aqueous micelles of a second surfactant. These investigators have attempted to develop a new technique to enhance and control the rate of reaction between metal ions and the extractant by solubilizing the extractant into the aqueous phase.

On the other hand, in the present project the main attention is paid to the aggregation behavior of Kelex 100 inside the organic phase. In the past some investigations in this regard involving 8-hydroxyquinoline-based extractants have been published. For example, the formation of microemulsions in the mixed Kelex 100/Versatic 911 extractant system has been demonstrated to enhance the extraction kinetics of Ga(III) from caustic solutions (Bauer et al., 1981; Fourré et al., 1983; Bauer et al., 1989). Similar observations were reported for the extraction of nickel (Haraguchi and Freiser, 1983) and lanthanides (Yamada and Freiser, 1981) with 7-substituted 8-hydroxyquinolines. In the present work the formation of W/O microemulsions in the Kelex 100-alcohol-HCl system is investigated in order to study the impact these organic aggregates might have on the extraction system.

4.2 EXPERIMENTAL INVESTIGATIONS

4.2.1 The Effect of Aquation/Anation on Rh Extraction

Aged (2-week) Rh(III) solutions of varying concentrations of H^+ and Cl^- were contacted with Kelex 100-based solutions to study the distribution-extraction behaviour of rhodium. Typical extraction results are plotted in Figure 4.1. All these data were produced by applying 3 min. contact time as this has been found previously to be adequate to reach equilibrium in the given system (Benguerel et al., 1994). One curve gives distribution coefficient, **D**, versus acidity (solid), and the other one (dotted) represents **D** versus Cl^- concentration while the acidity had been kept constant. The latter set of experiments was conducted by keeping the acidity at 0.7 M HCl and increasing the Cl^- concentration by introducing $MgCl_2$ to the system. As it is shown, the first curve reaches a maximum at about 2.5-3 M of HCl and then drops drastically. While the dotted curve, which has a lower maximum, shows that Cl^- at high concentrations does not suppress extraction to the same extent with HCl. The slight decrease in extraction at high Cl^- concentration, is attributed to Le Chatelier's principle (see reaction (4.4)) On the other hand in lower concentrations of Cl^- the amount of extraction increases by Cl^- concentration. This can be attributed first to the suppression of the aquation process (reaction (4.2)), and second to the increased activity of H^+ (Jansz, 1983) which further promotes the protonation of extractant molecules (i.e., reaction (4.3)). Similar to Cl^-, the H^+ ion also exhibits two opposite effects on extraction. In the low acid region due to increased protonation of the extractant molecules (reaction (4.3)), it promotes extraction. However further increase of H^+ ion concentration beyond 4 M has an unfavorable effect on extraction. The origin of the latter effect is not clear. One cause for this effect might be the formation of the neutral chlororhodic acid, $H_3RhCl_6^0(aq)$,

$$RhCl_6^{3-} + 3H^+ \leftrightarrow H_3RhCl_6^0(aq) \qquad (4.5)$$

which is not extractable by ion-pair formation. A similar behavior was observed in the case of Pt(IV) extraction from chloride solutions, by extractants similar to Kelex 100, by Coté and Demopoulos (1994).

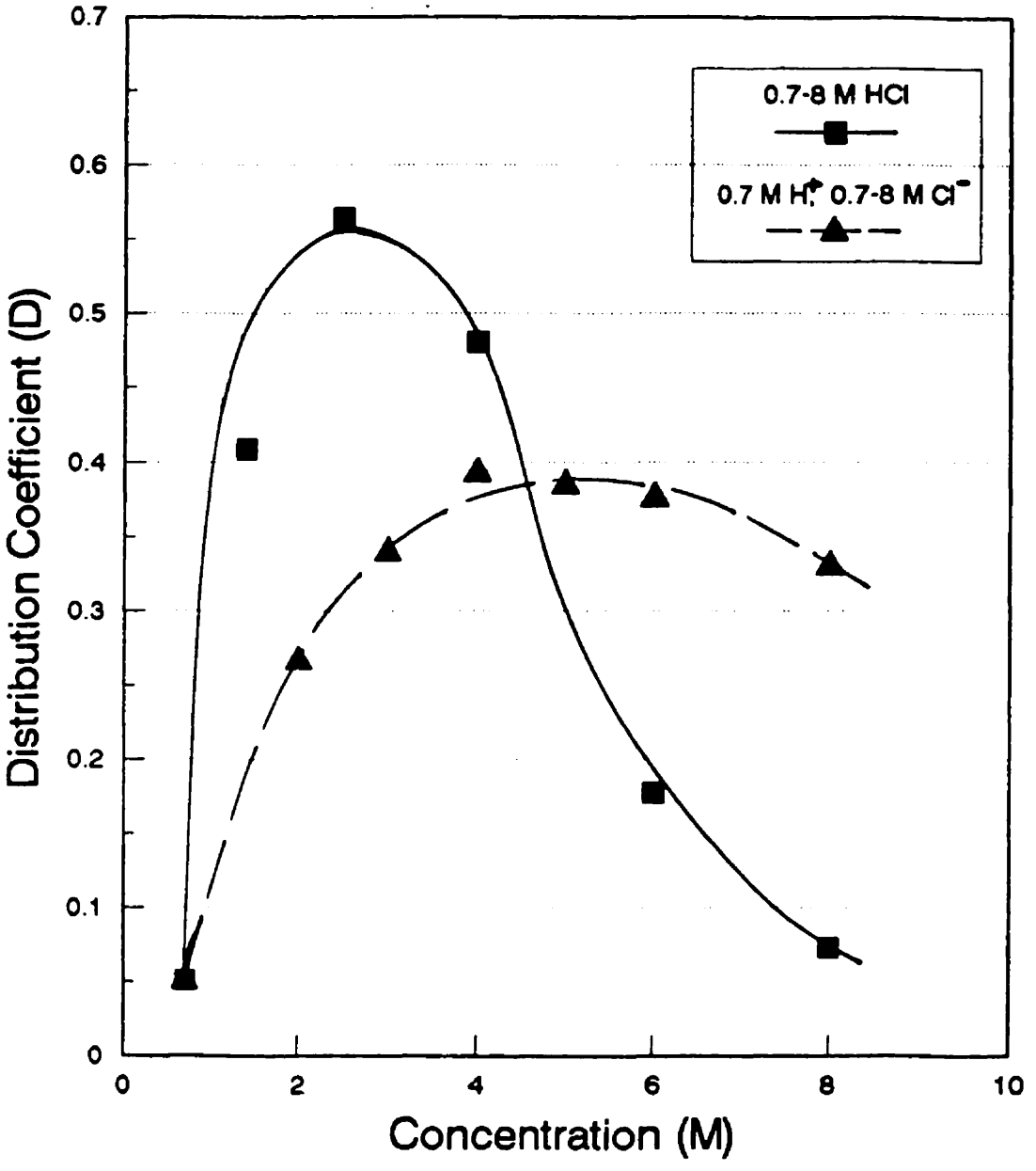

Figure 4.1: Effect of HCl and/or Cl^- Concentration on Extraction

(O: 5 v/o Kelex 100; 5 v/o tridecanol; 90 v/o kerosene, A: 0.7-8 M H^+ & Cl^-; 500 mg/L Rh; 2-week aged, contact time (CT): 3 min)

Due to the importance of aquation, the equilibrium and kinetics of this reaction were examined on an experimental basis. The kinetics of aquation (aging) was investigated through two different sets of experiments. In one set of experiments an organic phase of 2 or 5 v/o of Kelex 100 (0.056 or 0.14 M, respectively) was contacted with aqueous phases of different ages; fresh, 2-hr, 1-day, 3-day, 1-week, and 2-week. Five consecutive contacts with fresh organic solutions were performed for each aqueous solution. The results of one set of experiments with 5 v/o of Kelex 100, are shown in Figure 4.2. The results of this figure clearly demonstrate that the amount of Rh extracted in a single contact strongly depends on the age (i.e., on the degree of aquation) of the aqueous feed. However, upon consecutive contacts with fresh portions of organic solvent, the cummulative amount of Rh extracted tends to reach the same level (≅ 85-90% after five contacts). This then raised the question of whether it would be possible, after each contact, to separate the two phases, let the aqueous phase re-equilibrate (i.e., regenerate $RhCl_6^{3-}$ –see reaction (4.2)) and then recontact with the partially loaded organic phase. The results of this series of tests for a re-equilibration time of 10 minutes are shown in Table 4.1. It can be clearly seen that while the cumulative extraction of Rh increased when fresh solvent was used the same did not happen when the same organic was used.

Table 4.1: Cumulative Rh Extraction After Reequilibration of the Aqueous Phase with the Same or Fresh Organic Phases

	same organic %Rh Extracted		fresh organic %Rh Extracted	
contact	each contact	cumulative	each contact	cumulative
1	33	33	33	33
2	0	33	33	54.65
3	0	33	33	69.46
4	0	33	33	79.43
5	0	33	33	86.14

O: 5 v/o Kelex 100 (0.14 M); 5 v/o tridecanol (0.21 M); 90 v/o kerosene.
A: 4 M HCl Rh solution, 2-week aged; CT = 3 min; Reequilibration Time = 10 min.

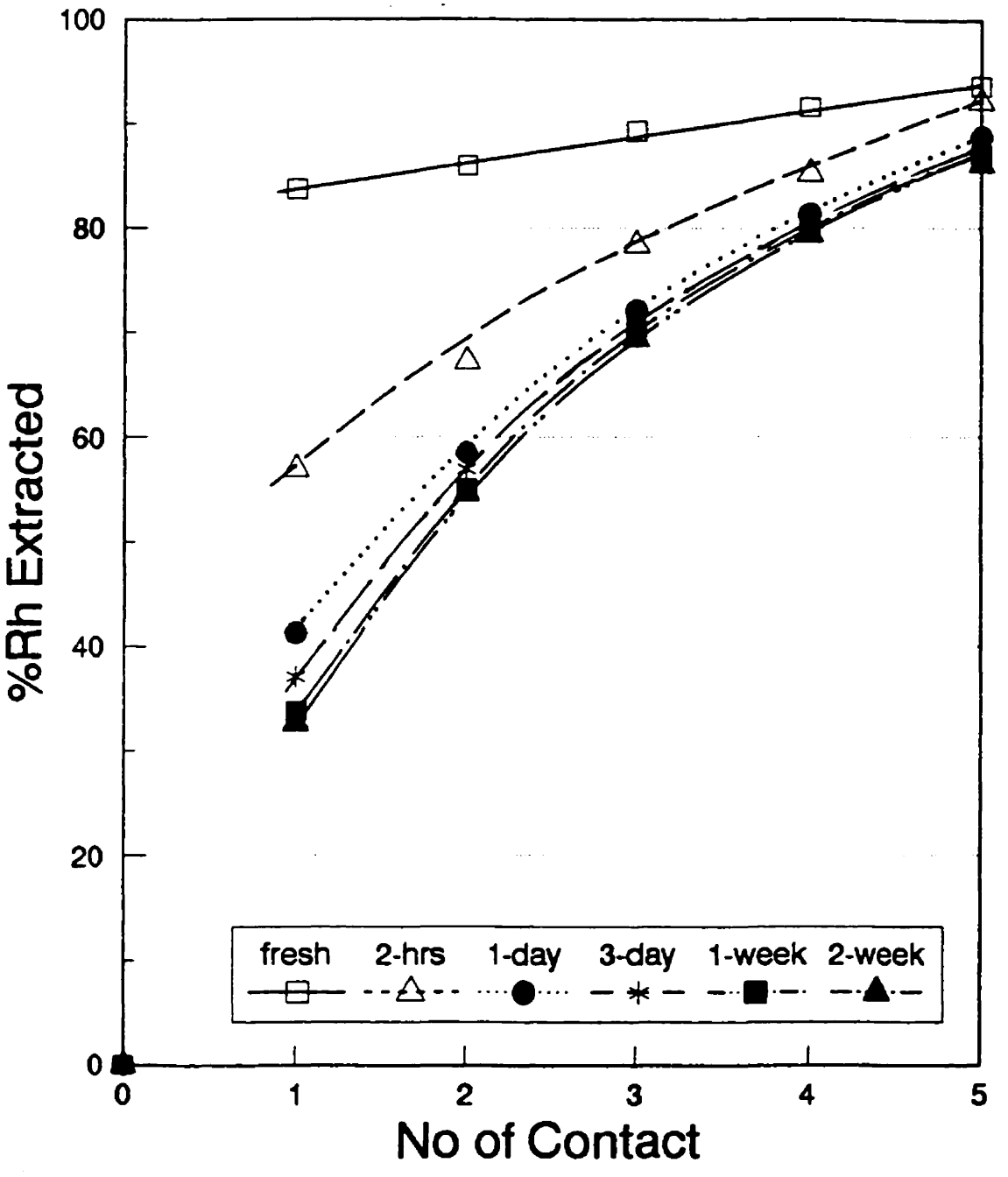

Figure 4.2: Cross-Current Extraction of Rh as a Function of Aqueous Solution Age

(O: 5 v/o Kelex 100; 5 v/o tridecanol; 90 v/o kerosene, A: 4 M HCl; 400 mg/L Rh, CT for each contact 3 min)

At this point it was decided to study the effect of aging (aquation) simultaneously to extraction. To this end, freshly prepared solutions were brought in immediate contact with the organic solution and continuously mixed together for 30 hours. After regular periods samples were withdrawn for measuring the distribution of Rh. The results are shown in Figure 4.3. The interesting point here is that despite the fast and high degree of extraction obtained after the first few minutes, rhodium was found to go back to the aqueous phase as time elapsed. In other words it seems that aquation continues to occur even when most of the Rh is in the organic phase. This phenomenon has not been previously reported and an effort will be made, later in this chapter, to explain it on the basis of microemulsion formation.

The effect of aging-aquation on extraction is further manifested with the results of Figure 4.4. As shown, aquation severely suppresses the extraction of rhodium and for an aged solution, the distribution coefficient is less than one. Similar findings were reported by Benguerel et al. (1994).

The kinetics of the anation process (the reverse of reaction (4.2)) was also investigated. Two different aqueous solutions of Rh of 4 and 1.4 M HCl were contacted with an organic phase of 5 v/o Kelex 100. Five consecutive contacts with fresh organic solutions were made for each aqueous solution. Three different time intervals (i.e., reequilibration times) of 3 min, 2-3 hours, and 2-3 days were imposed between consecutive contacts. The results which are shown in Figure 4.5 indicate that for 4 M HCl the re-equilibration time makes no difference. However, for 1.4 M HCl extraction is promoted by longer reequilibration time intervals. In other words, for the former case the anation process reaches equilibrium in 3 minutes, while for the latter the kinetics are slower. This observation has not been made before.

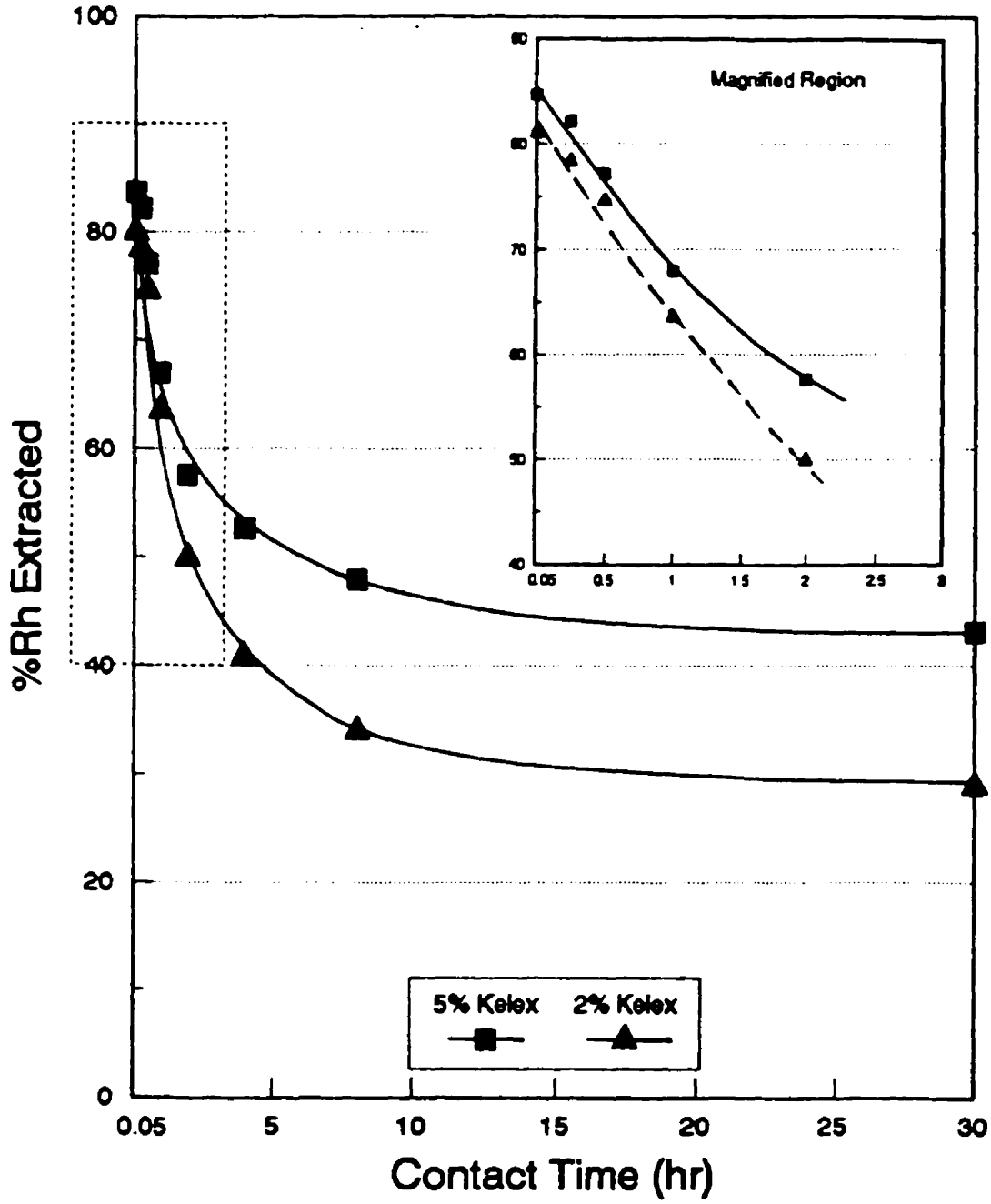

Figure 4.3: %Rh Extraction For a Freshly Prepared Solution as a Function of Contact Time

(O: 2 v/o or 5 v/o of Kelex 100; 5 v/o tridecanol; kerosene,

A: fresh; 4 M HCl; 400 mg/L Rh)

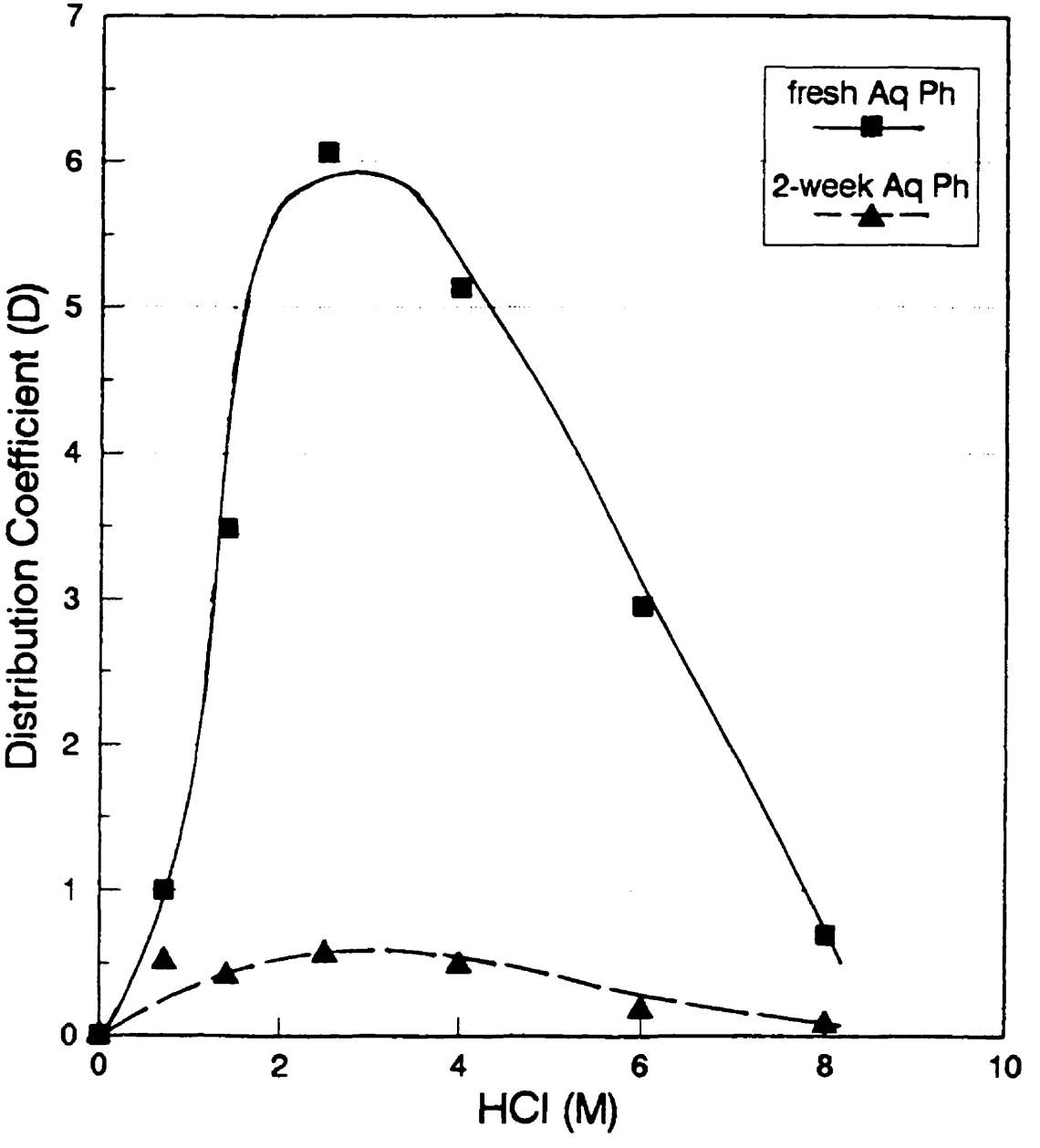

Figure 4.4: Effect of Aging on Extraction

(O: 5 v/o Kelex 100; 5 v/o tridecanol; 90 v/o kerosene,

A: different acidities; 500 mg/L Rh, CT: 3 min)

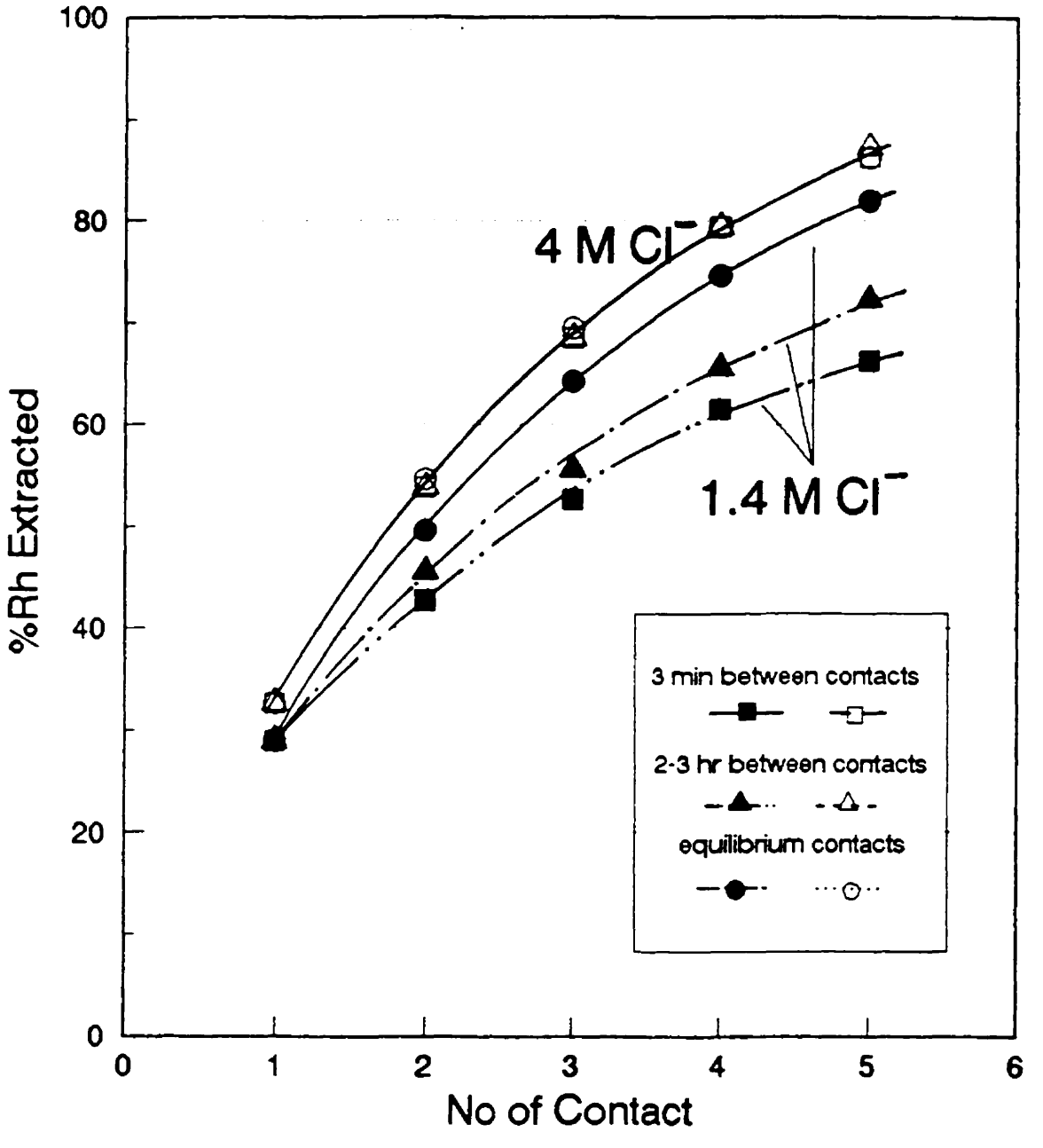

Figure 4.5: Cross-Current Extraction of Rhodium as a Function of Inter-Contact Re-Equilibration Time at Two Chloride Concentrations

(O: 5 v/o Kelex 100; 5 v/o tridecanol; 90 v/o kerosene,

A: 4 or 1.4 M HCl; 500 mg/L Rh; 2-week aged, CT: 3 min)

4.2.2 The Effect of System Parameters on Rh Extraction

The effect of Kelex 100 concentration on Rh extraction is depicted in Figure 4.6. Apparently, extraction increases with Kelex 100 concentration.

In another series of tests the effect of varying the phase volume ratio on rhodium extraction was investigated. The results which are shown in Figure 4.7, indicate that as the O/A ratio increased the amount of Rh extraction increased as well; this was more pronounced for the aged aqueous solutions. The Kelex 100 concentration effect (Figure 4.6) and the O/A effect (Figure 4.7) on Rh extraction raises the question of whether the extra rhodium extracted is in the form of the aquated complexes, i.e., $RhCl_5(H_2O)^{2-}$, previously thought (Benguerel et al., 1994) not to be extractable. This question is to be answered later on in section 4.3.1.

The amount of alcohol in a solvent of 5 v/o Kelex 100 (~ 0.14 M) was varied from 5 to 20 v/o (0.21 to 0.84 M). The results which are presented in Table 4.2 show a decrease in the amount of Rh extraction at high alcohol concentrations. At the same time the amount of water uptake was found to decrease (see Table 4.2) at very high alcohol concentrations. The latter phenomenon is further discussed in the next section (4.3). Finally the effect of the nature of the diluent on extraction was investigated by using three different solvents: kerosene, Solvesso 150 (a commercial aromatic solvent), and toluene. The results showed practically no difference in the degree of Rh extraction.

To evaluate the effect of temperature on extraction, some experiments were performed at 60 °C. The results, which are not presented here for the sake of brevity, showed that at 60 °C the amount of extraction dropped drastically. This is believed to be due in part to the acceleration of the aquation process upon temperature elevation (Benguerel et al., 1996) and in part to the exothermic nature of ion-pair forming solvent extraction systems (Coté and Demopoulos, 1994).

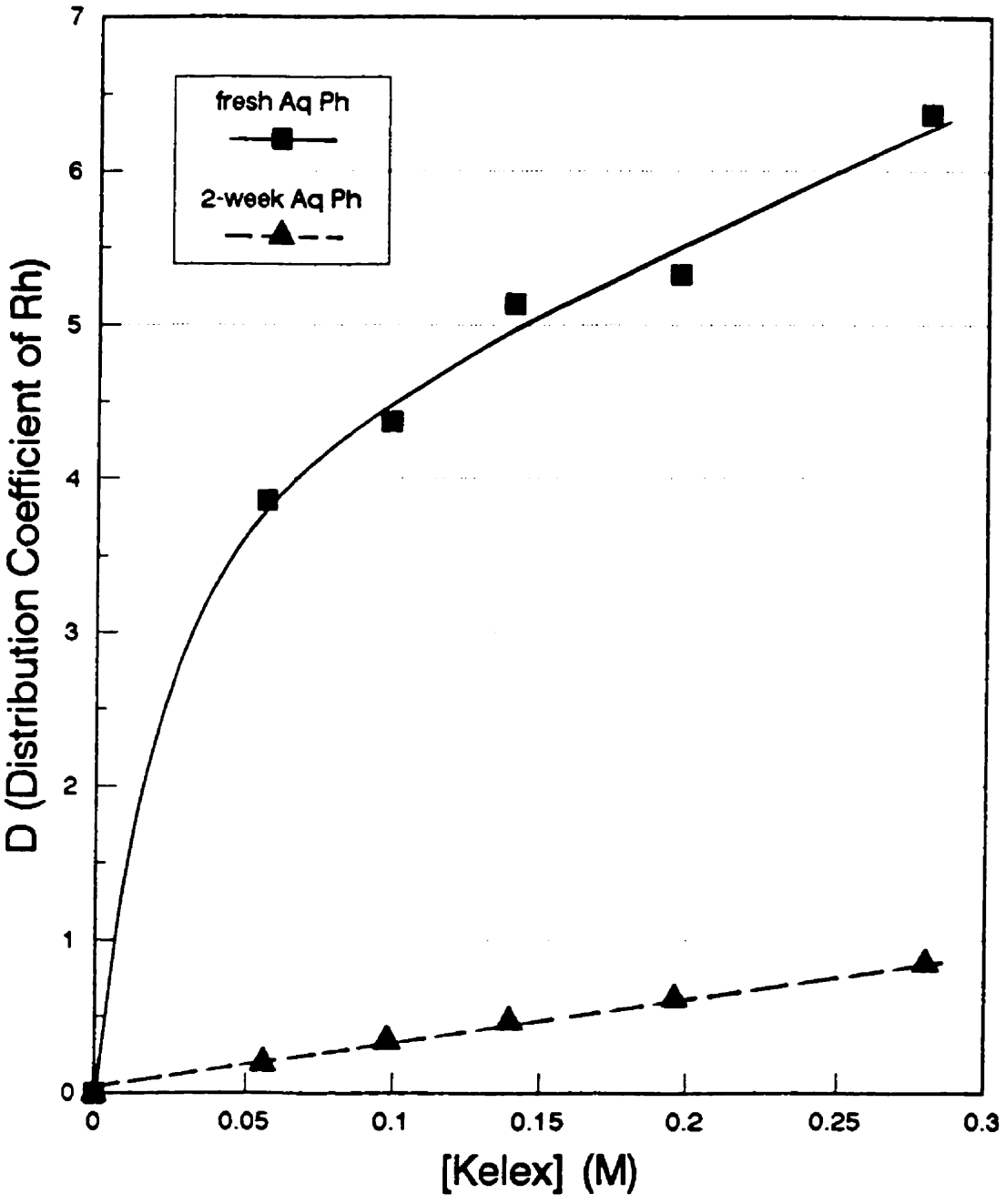

Figure 4.6: Effect of Kelex 100 Concentration on Extraction

(O: X v/o Kelex 100; X v/o tridecanol; [100-2X] v/o kerosene,

A: 4 M HCl; 500 mg/L Rh, CT: 3 min)

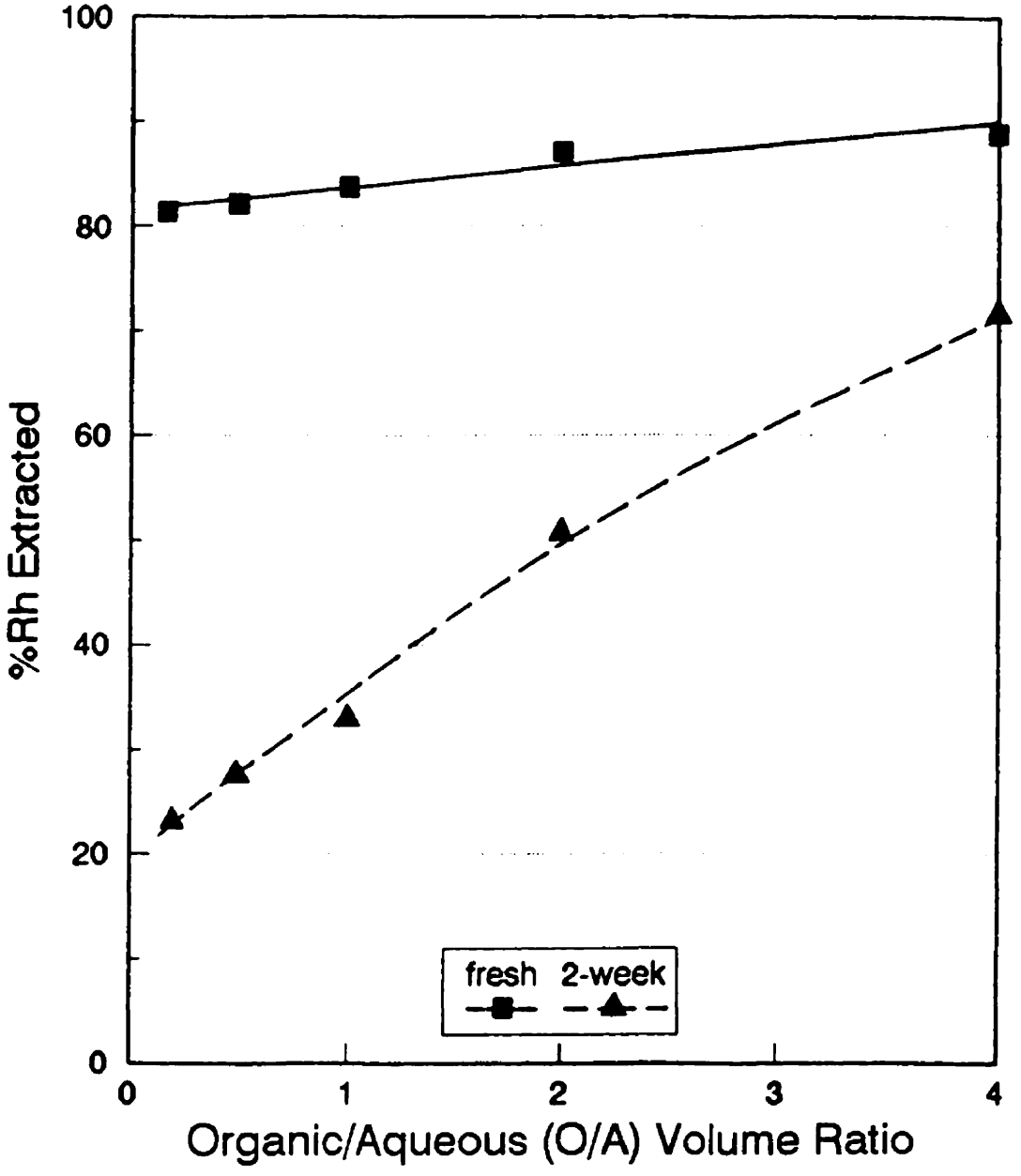

Figure 4.7: Effect of O/A Ratio on Extraction

(O: 5 v/o Kelex 100; 5 v/o tridecanol; 90 v/o kerosene,

A: 4 M HCl; 500 mg/L Rh, CT: 3 min)

Table 4.2: Effect of Tridecanol Concentration on Rh Extraction and Water Uptake

tridecanol (v/o)	%Rh Extraction	mol H2O/L org.
5 (0.21 M)	30.65	0.337
8 (0.33 M)	30.60	0.328
10 (0.42 M)	30.55	0.311
15 (0.63 M)	29.66	0.270
20 (0.84 M)	26.73	0.250

O: 5 v/o Kelex 100 (0.14 M); A: 1.4 M HCl Rh solution, 2-week aged.

4.2.3 The Microemulsion Structure of Kelex 100 and Its Influence on Rh Extraction

The main aim of this part of the work was to answer the following questions: Is the limited extraction of Rh associated with the formation of the aquated complexes, and if so how does the transfer of water in the organic phase impact on the distribution of Rh? To answer these questions it was necessary to study the internal structure and composition of the organic phase. The major findings of this investigation are reported below.

An organic solution of 5 v/o Kelex 100 was contacted with aqueous solutions of different acidities (no Rh). After phase separation the water uptake and viscosity of the organic phase were measured. Also, the interfacial tension of the organic-aqueous interface was determined. Finally, dynamic light scattering experiments were conducted on the organic phase to detect and measure the size of the formed aggregates.

The water uptake results are shown in Figure 4.8. As can be seen from these results, the water uptake increases with the acidity of the aqueous phase. In particular, three different zones can be observed. The first zone exhibits initially a modest increase up to 0.7 M HCl

and then a sharp increase up to about 1.7-2 M HCl. The second zone (2-10 M HCl) starts with an inflection up to 4 M HCl and is followed by a linear increase in water uptake with acidity. Although this increase continues for acidities above 6 M HCl it should be mentioned that the water uptake data for this upper range (> 6 M HCl) might not be fully reliable. This is due to the chemical reaction between Karl Fischer titrant and solubilized acid, which results in higher readings. At very high acidities, i.e., > 10 M, the extractant, possibly due to degradation which is known to occur (Coté, 1994), seems to extract less water.

At this point it is interesting to correlate the amount of water uptake to the amount of acid extracted inside the organic phase. The extraction of HCl by Kelex 100 as a function of aqueous HCl concentration is shown in Figure 4.9. The reported data in Figure 4.9 have been corrected for the extraction of acid by the co-surfactant, tridecanol. According to this figure Kelex 100 becomes fully protonated ($[HCl]_o/[Kelex\ 100]=1$) at >2.5 M HCl (aq). This agrees with the value (≥2.0 M HCl) reported by Coté and Demopoulos (1993; 1994) for the system Kelex 100-tridecanol-Solvesso 150. The acid extracted in excess of $[HCl]_o/[Kelex\ 100]=1$ may be assumed to be due to solubilization in the W/O microemulsion formed inside the organic phase (the amount of acid extracted via the protonation of the alcohol has already being taken into account). The corresponding water extraction vs aqueous HCl concentration is shown in Figure 4.10. It is interesting to note the similarity of the two extraction curves, i.e., the water extraction curve and the acid extraction curve. A closer look, though, of the water/acid extraction data in the form $[H_2O]_o/[HCl]_o$ vs aqueous acidity, reveals the picture depicted in Figure 4.11. It is seen that the ratio $[H_2O]_o/[HCl]_o$ decreases with increasing acidity. This may very well be related to the activity of water, which is known to decrease with increasing HCl concentration (Zemaitis et al., 1986). As a result of that less water is associated via hydration with the extracted protons: $H_3O^+(H_2O)_n$. Similar conclusions have been drawn by Osseo-Asare for the TBP-HCl-H_2O system (Osseo-Asare, 1991).

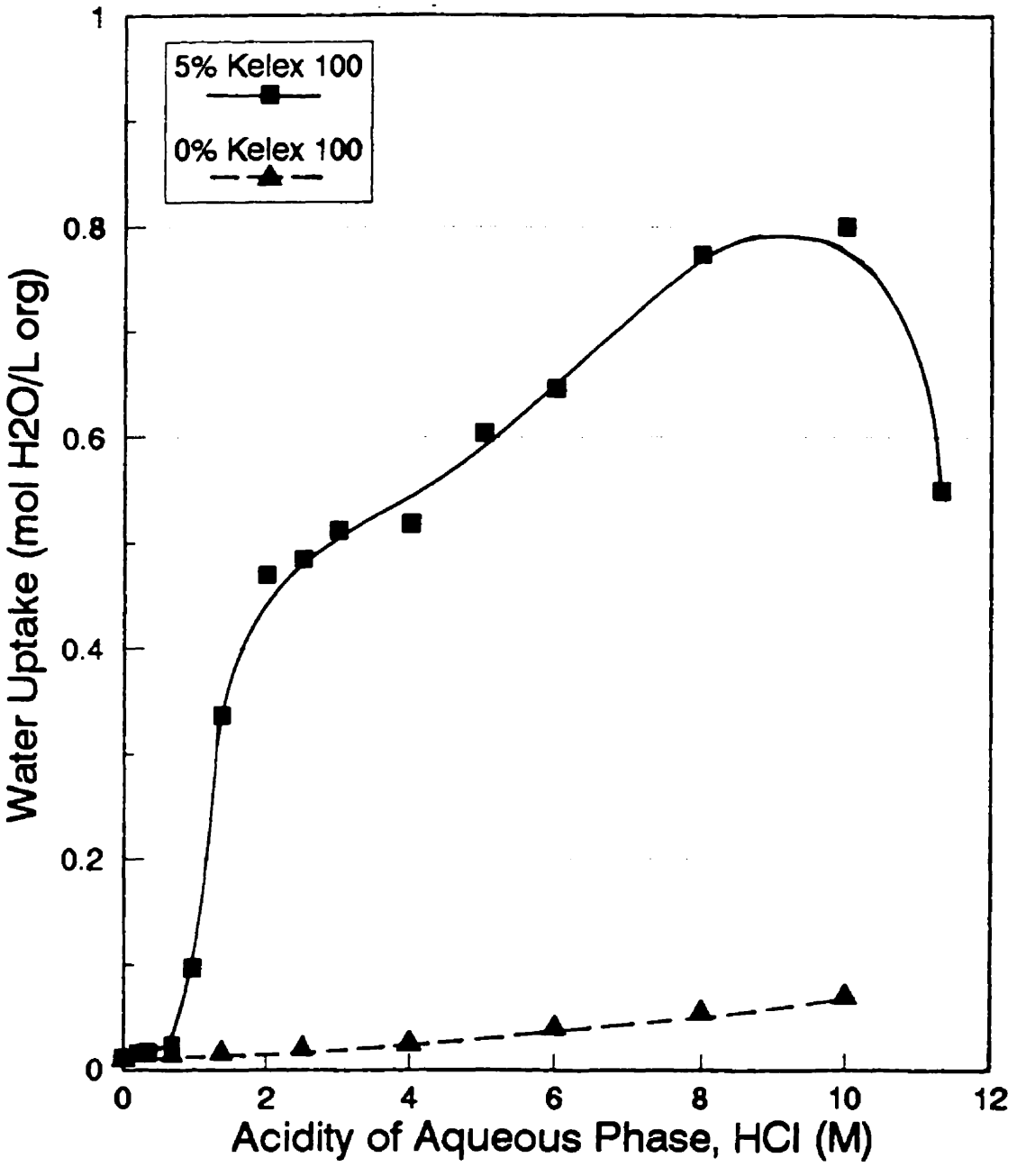

Figure 4.8: Effect of Acidity on Water Uptake by the Organic Phase

(O: 5 v/o Kelex 100; 5 v/o tridecanol; 90 v/o kerosene,

A: 0-10 M HCl (No Rh), CT: 3 min)

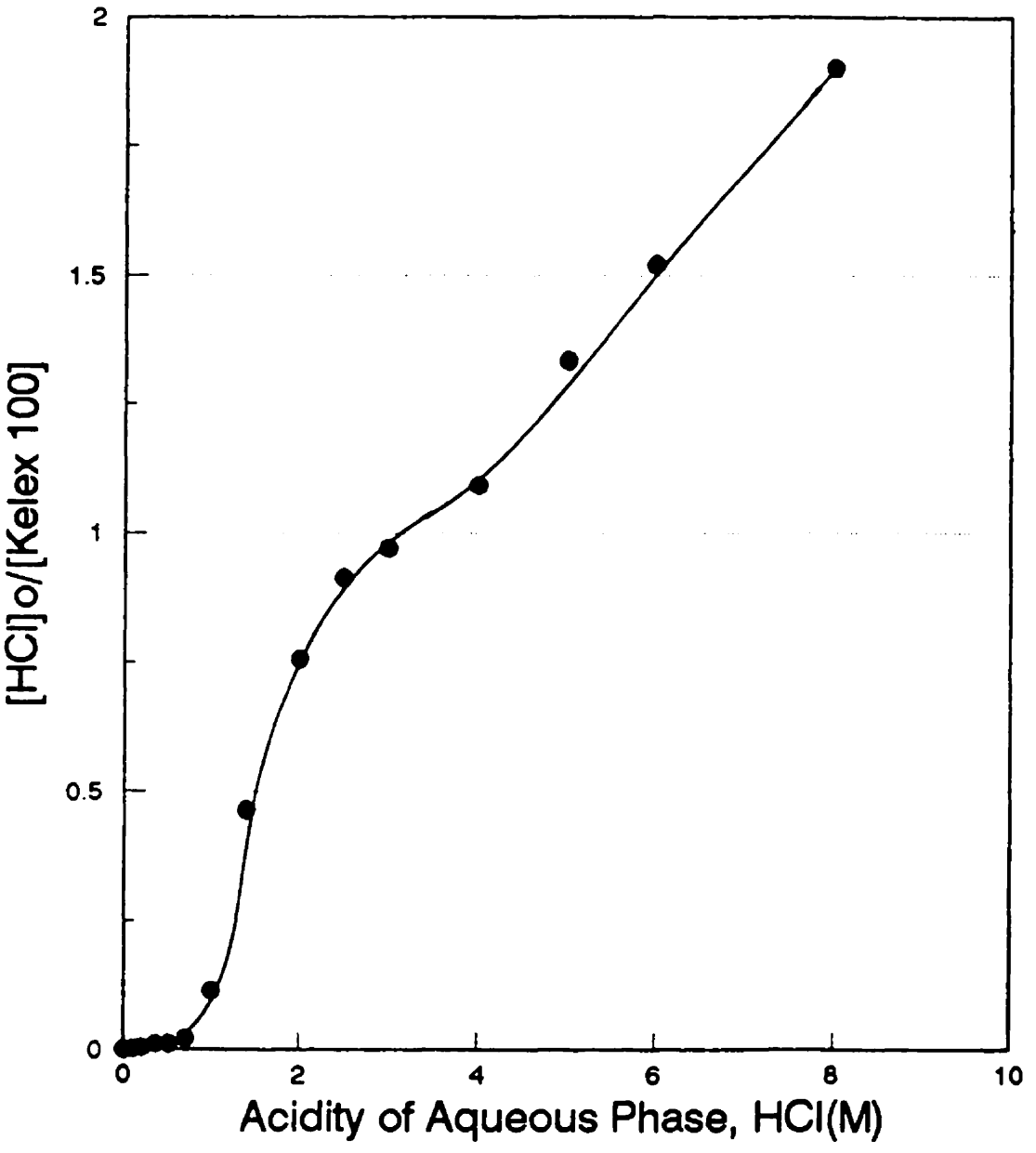

Figure 4.9: The Extraction of Acid by Kelex 100

(O: 5 v/o Kelex 100; 5 v/o tridecanol; 90 v/o kerosene, A: 0-8 M HCl)

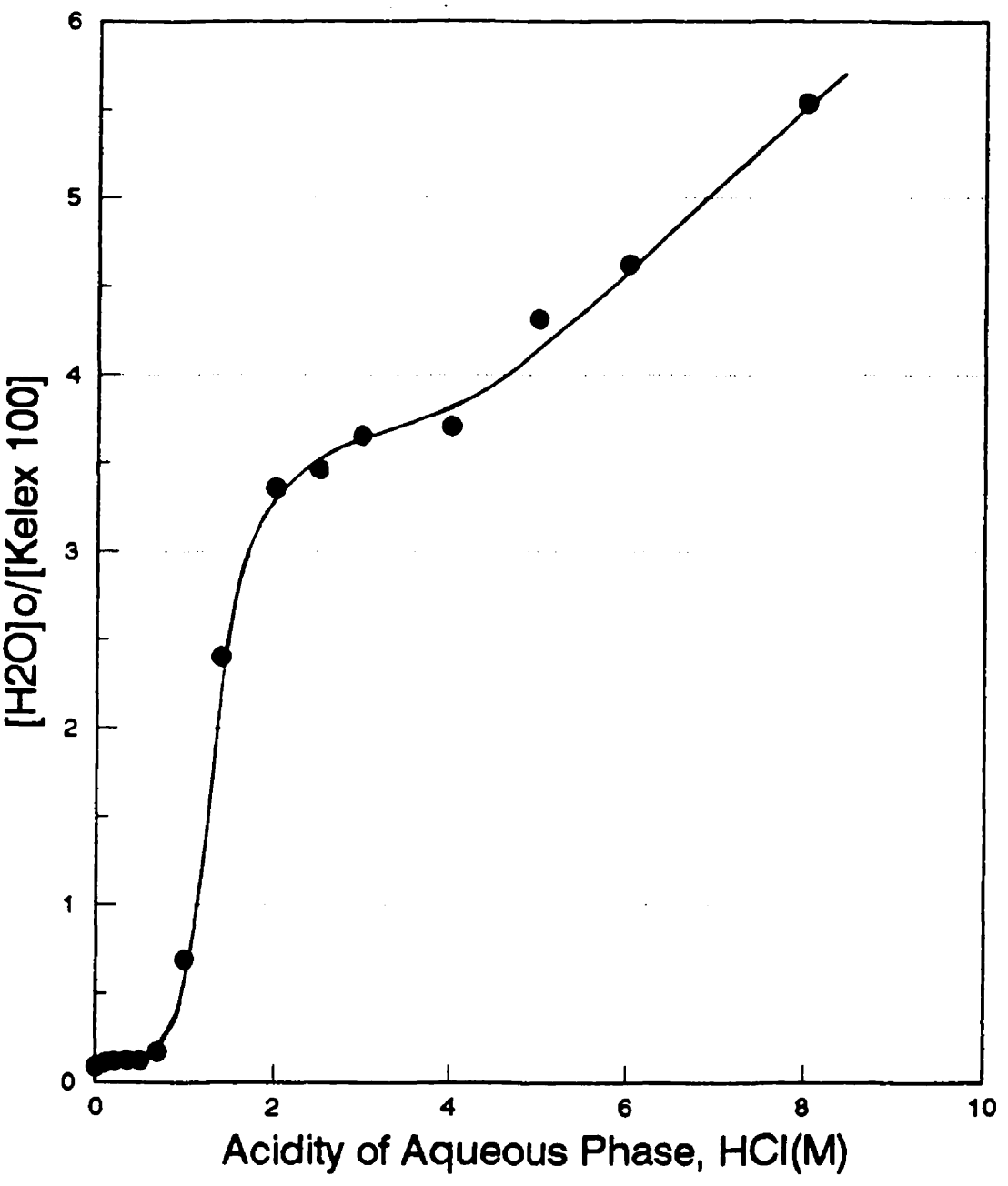

Figure 4.10: The Extraction of Water by the Organic Phase as a Function of Aqueous HCl Concentration

(O: 5 v/o Kelex 100; 5 v/o tridecanol; 90 v/o kerosene, A: 0-8 M HCl)

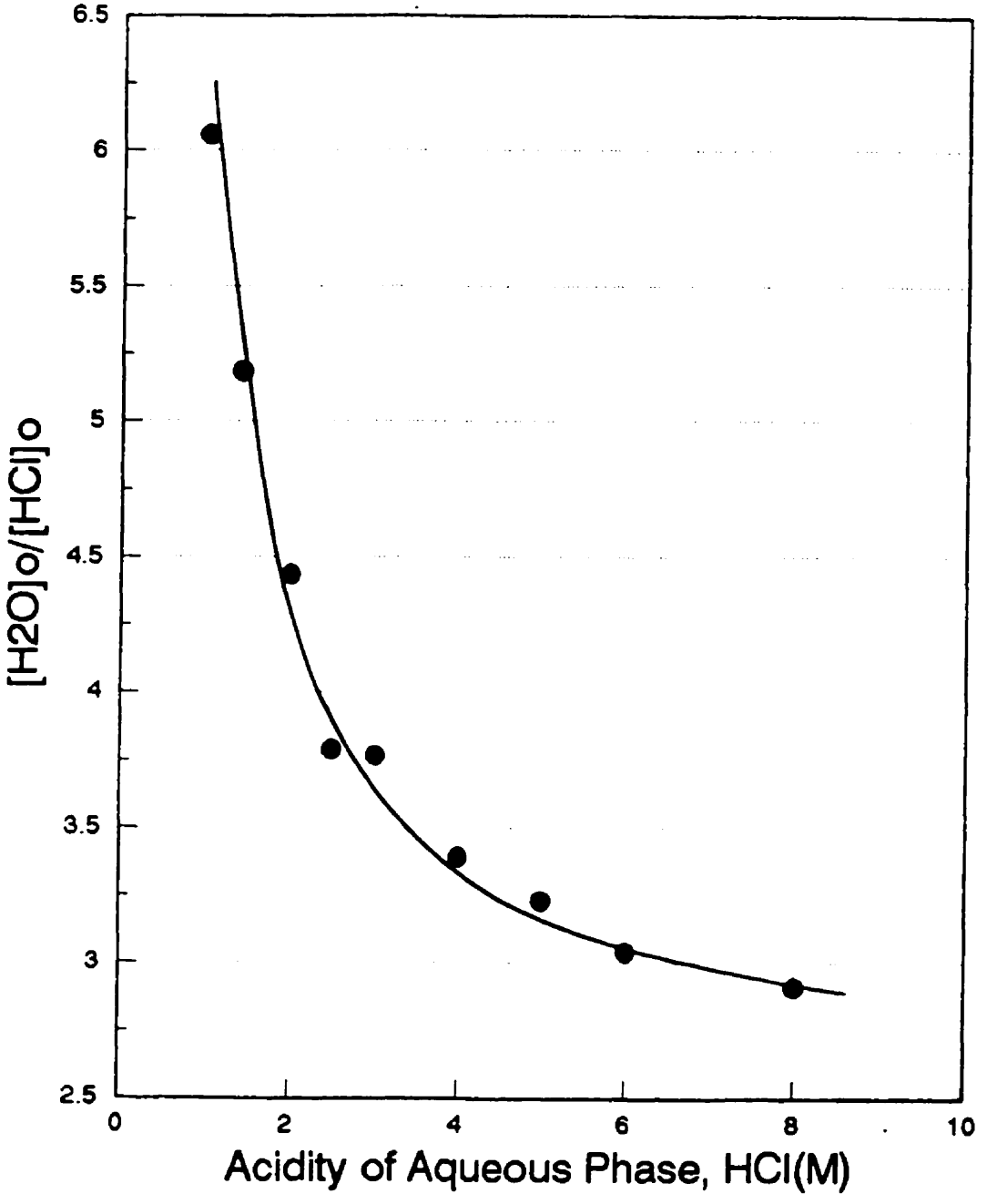

Figure 4.11: Co-Extraction of Acid and Water into the Organic Phase as a Function of Aqueous Phase Acidity

(O: 5 v/o Kelex 100; 5 v/o tridecanol; 90 v/o kerosene, A: 0-8 M HCl (No Rh))

The effect of alcohol on water uptake was investigated in two different ways. First, for an organic phase of 0 v/o extractant, the amount of water uptake is almost negligible for the range of acidity up to 4 M (Figure 4.8). However, for higher acidities, > 4 M, the water uptake data exhibit a modest increase. This observation is also in agreement with acid extraction results involving tridecanol reported by Coté and Demopoulos (1994) and confirmed in the present work. Second, the amount of water uptake for an organic phase of 5 v/o of extractant and different concentrations of alcohol in contact with a solution at a moderate acidity (1.4 M HCl) show a decrease for higher alcohol concentrations (Table 4.2). Although the alcohol itself does not absorb any water for acidities up to 4 M HCl, nevertheless it is well known that it acts as co-surfactant in W/O microemulsion formation (Khoshkbarchi and Vera, 1995). In this regard, then, the amount of water solubilized in the microemulsion-containing organic phase is expected to increase up to a certain critical alcohol concentration and thereafter to decrease, as reported in some other W/O microemulsion systems (Leung and Shah, 1987; Krei and Hustedt, 1992). It appears in the present system (i.e., 5 v/o or 0.14 M Kelex 100) the 5 v/o tridecanol (0.21 M) concentration is already above that critical alcohol level after which water solubilization decreases. The latter might be the result of effective solvation of the protonated molecules of the extractant ($R\text{-}H_2Q^+Cl^-$) by the excess alcohol molecules causing their removal from the W/O interphase and the subsequent partial destabilization or shrinkage of the W/O microemulsions.

Viscosity measurements are reported in Figure 4.12 as a function of water uptake. As shown, the viscosity increases with the water uptake up to 0.45-0.5 (mol H_2O/L org) and subsequently reaches a plateau at $\cong$0.6 (mol H_2O/L org). This sharp increase in viscosity appears to be related to the onset of formation of the W/O microemulsion state while the extra water uptake beyond that region does not increase the viscosity considerably.

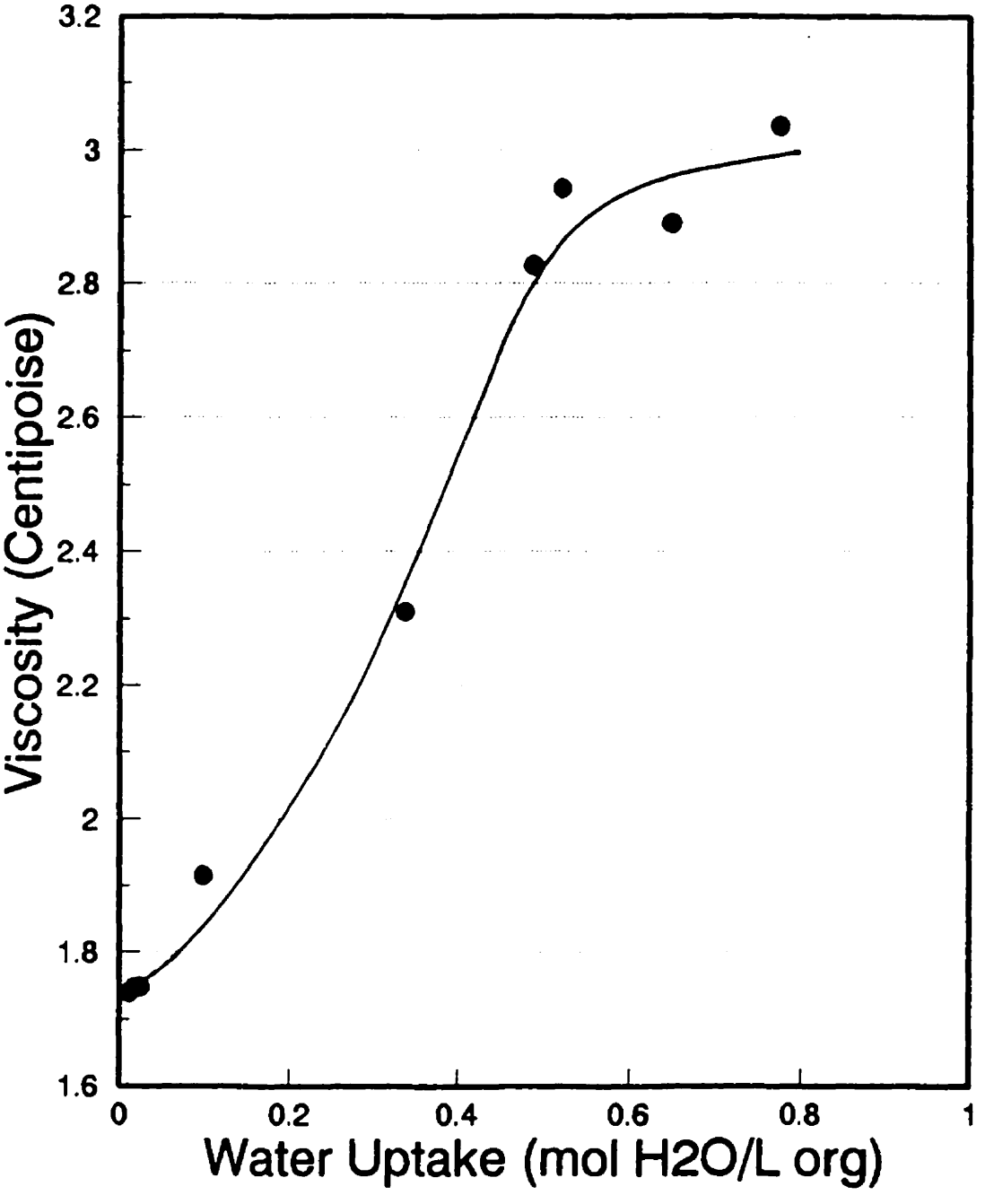

Figure 4.12: Viscosity of the Organic Phase as a Function of Water Uptake

(O: 5 v/o Kelex 100; 5 v/o tridecanol; 90 v/o kerosene,

A: 0-8 M HCl (No Rh), CT: 3 min)

Interfacial tension data and light scattering measurements are presented in Figure 4.13. Interfacial tension, which is high for low aqueous-phase acidities, drastically decreases for aqueous phases of about 0.7 M acidity. For higher acidities it becomes much lower and for acidities more than 4.0 M it is near zero. As light scattering data show, there is no detectable aggregate for the aqueous-phase acidities of 0.7 M. But for the higher acidities, the existence of such aggregates is obvious. The size of these so-called reverse micelles, or microemulsions, remains practically constant in the region 1.4-8.0 M of aqueous-phase acidity at 10 nm of micellar diameter, and this size agrees with reported data in literature (Kotlarchyk et al., 1982).

Similar measurements of water uptake, viscosity, interfacial tension, and light scattering for organic solutions which were aged for two weeks after contact with acidic solutions (without Rh) were also conducted. The results showed these parameters to remain almost constant with aging time. This observation seems to confirm the stability of the protonated extractant and the formed microemulsions.

In conclusion, organic solutions of Kelex 100-tridecanol-kerosene in contact with HCl (>1.0 M) aqueous solutions form W/O microemulsions in the organic phase. These microemulsions solubilize considerable amounts of water in the organic phase, causing an increase in viscosity. Solubilization of water into the organic phase is associated with the lowering of the interfacial tension. Similar observations have been made by other investigators (Calvarin et al., 1992). The solubilization of water by means of microemulsions is clearly confirmed by the light scattering measurements.

4.3 INTERPRETATION OF THE RESULTS

First the extraction data will be discussed from a macroscopic equilibrium point of view and then the interfacial chemistry of the system will be discussed in light of the organic-phase physicochemical property measurements made.

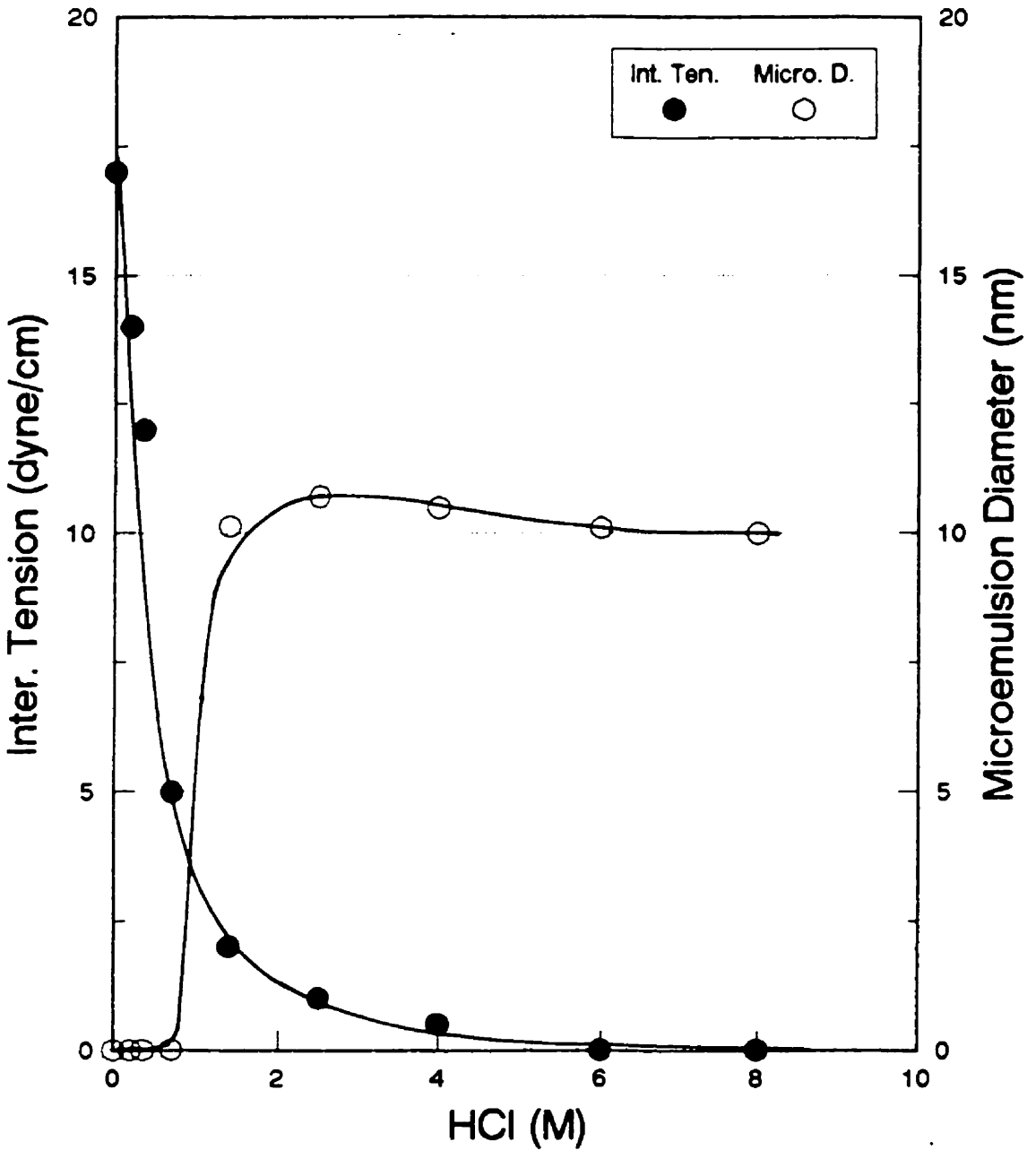

Figure 4.13: Interfacial Tension Between Aqueous and Organic Phases and Light Scattering Measurements of W/O Microemulsions

(O: 5 v/o Kelex 100; 5 v/o tridecanol; 90 v/o kerosene,

A: 0-8 M HCl solutions (No Rh))

4.3.1 View I: Distribution Equilibria

The aquation process is generally represented by reaction (4.2). However, according to previous studies (Benguerel et al., 1994; 1996) the most abundant species of Rh(III) in the HCl media are $RhCl_6^{3-}$ and $RhCl_5(H_2O)^{2-}$; i.e., the aquation process is limited to the following reaction:

$$RhCl_6^{3-} + H_2O \leftrightarrow RhCl_5(H_2O)^{2-} + Cl^- \tag{4.6}$$

Benguerel et al. (1994) postulated that only $RhCl_6^{3-}$ is extractable and its extraction occurs via ion-pair formation (reaction (4.4)). However, these authors did not examine the effect of Kelex 100 concentration and organic/aqueous ratio. Since in the present study it was found that Rh(III) extraction increases with both of these parameters (Figures 4.6 and 4.7) it was of interest to examine whether the assumptions made (i.e., that $RhCl_5(H_2O)^{2-}$ is inextractable) by the previous investigators are still valid. The equilibrium constant for reaction (4.4) is given by

$$K_4 = \frac{[\overline{RhCl_6^{3-}(R-H_2Q^+)_3}][Cl^-]^3}{[RhCl_6^{3-}][\overline{R-H_2Q^+Cl^-}]^3} \tag{4.7}$$

and the distribution coefficient, **D**, by

$$\mathbf{D} = \frac{[\overline{RhCl_6^{3-}(R-H_2Q^+)_3}]}{[RhCl_6^{3-}]+[RhCl_5(H_2O)^{2-}]} \tag{4.8}$$

but

$$K_6 = \frac{[RhCl_5(H_2O)^{2-}][Cl^-]}{[RhCl_6^{3-}][H_2O]} \tag{4.9}$$

so **D** can be rewritten

$$\mathbf{D} = \frac{[\overline{RhCl_6^{3-}(R-H_2Q^+)_3}]}{[RhCl_6^{3-}]+K_6\dfrac{[RhCl_6^{3-}][H_2O]}{[Cl^-]}} \tag{4.10}$$

which eventually becomes

$$\mathbf{D} = \frac{K_4[\overline{R-H_2Q^+Cl^-}]^3[Cl^-]^{-2}}{[Cl^-]+K_6} \tag{4.11}$$

or

$$\log \mathbf{D} = \log K_4 + 3\log[\overline{R-H_2Q^+Cl^-}] - 2\log[Cl^-] - \log([Cl^-]+K_6) \tag{4.12}$$

Equation (4.12) can explain the results of Figure 4.6, since **D** (or equivalently percentage extraction) increases as $[\overline{R-H_2Q^+Cl^-}]$ (i.e., the concentration of the protonated Kelex 100) increases. On the other hand an analysis of the O/A results (Figure 4.7) on the basis of **D** (Table 4.3) suggests (within experimental error) the above analysis and assumptions hold as well.

Table 4.3: The Effect of A/O on D
(Analysis of the Data of Figure 4.7 For 2-week Aged Solutions).

A/O Ratio	1	2	4
%Extraction	33	50	70
D	0.50	0.50	0.58

4.3.2 View II: Microemulsion Formation

One of the most important findings of the current project is the quantification of the formation of some kind of aggregation in the organic phase, composed of Kelex 100, alcohol, water, and acid molecules. Based on the experimental findings of this work and the relevant published literature (Osseo-Asare, 1991; Nai-Fu, 1992; Bhattacharyya and Ganguly, 1987) a physicochemical model to describe the organic phase structure is proposed.

According to this model the protonated extractant molecules ($R\text{-}H_2Q^+Cl^-$) act as strong amphiphiles and carry H_2O with them due to the formation of W/O microemulsions (Figure 4.14). Water is transferred within the organic phase in part due to its chemical

association (hydration) with the protons ($H_3O^+(H_2O)_n$) (Bockris and Reddy, 1970) and in part due to its physical solubilization within the W/O microemulsions. The role of the alcohol is to stabilize the microemulsion structure.

For a solvent of 5 v/o Kelex 100 (0.14 M) in contact with 4 M HCl the water uptake is measured to be 0.52 M (There was negligible amount of water extracted by the modifier or the diluent, hence all this water uptake is due to Kelex 100). Meanwhile, the organic-phase water and metal loading ratios are calculated to be $[H_2O]/[Kelex] \cong 4$, $[Kelex]/[Rh] \cong 30$. In other words there is a huge excess of extractant and water dissolved in the organic phase to accommodate the quantitative extraction of the strongly hydrophilic Rh(III) species. Nevertheless, this did not occur as witnessed in the previous work of Benguerel et al. (1994) and in the present study. The mystery remains then as to why Rh(III) is not fully extracted despite the extensive formation of "W/O" microemulsions in the organic phase. No doubt the presence of water inside the inner coordination sphere of Rh(III) must be held responsible for this behavior despite the fact that the exact mechanism is not clearly understood.

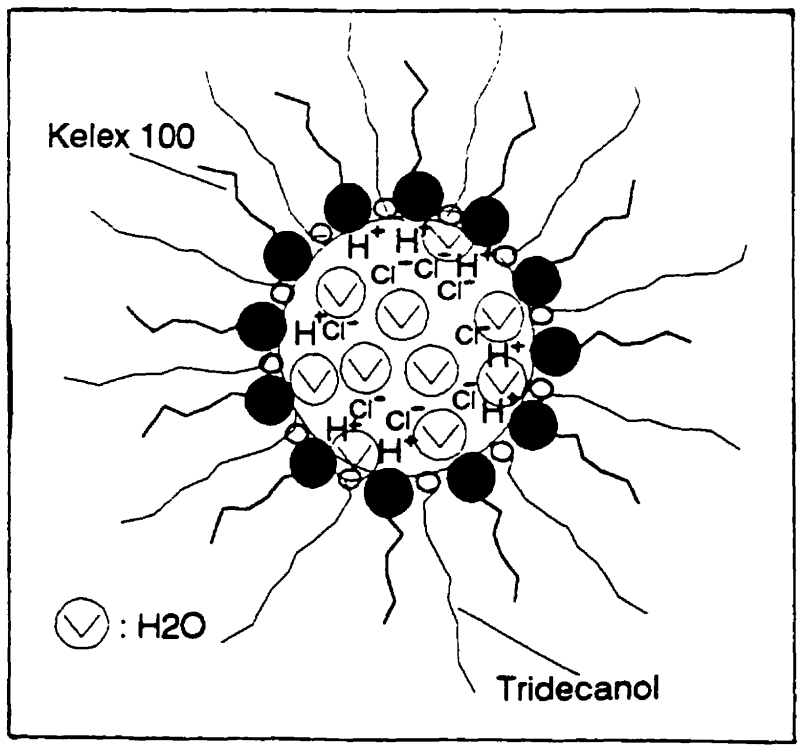

Figure 4.14: Proposed Structure of the Organic-Phase Aggregates.

Finally the inability of the same organic phase to extract additional Rh(III) after re-equilibration of the aqueous phase (Table 4.1), despite the fact that the anation reaction is very fast (Figure 4.5), must be attributed again to the microemulsion formation inside the organic phase. Thus any newly formed $RhCl_6^{3-}$ (upon re-equilibration) will be quickly extracted during the subsequent contact but it will equally quickly undergo aquation (by the water present inside the microemulsions) and thereby return back in the aqueous phase. In conclusion, therefore, any effort to enhance the extraction of Rh(III) from chloride solutions by a conventional solvent extraction approach is doomed to fail.

4.4 SUMMARY

1. Aging of aqueous chloride solutions of Rh(III) leads to formation of aquo-chloro complexes of Rh(III), e.g., $RhCl_5(H_2O)^{2-}$, which are not extractable by ion-pair forming extractants like protonated Kelex 100.

2. Even if Rh(III) is extracted from a fresh aqueous solution (apparently as $RhCl_6^{3-}$) it still goes back into the aqueous phase due to aquation, which continues to occur inside the bulk of the organic phase.

3. This phenomenon is attributed to the formation of W/O microemulsions inside the organic phase when the latter is contacted with concentrated HCl media.

4. The formation of microemulsions consisting of protonated Kelex 100-tridecanol-acid-water was confirmed experimentally. The microemulsion water pools were found to have a 10-nm diameter in the whole acid range and the ratio H_2O/HCl/Kelex 100 at 2 and 6 M HCl to be 4/1/1 and 4.5/1.5/1, respectively. In other words with increasing HCl concentration the relative ratio of $[H_2O]_o/[HCl]_o$ decreases but without this to be translated to a change in the micellar diameter.

CHAPTER 5

Extraction of Rhodium Chlorocomplexes and Acid Through a Supported Liquid Membrane of Kelex 100[1]

5.1 INTRODUCTION

In a detailed study of the interfacial chemistry of the Rh(III)-HCl-Kelex 100 system, presented in the previous chapter, it was demonstrated that W/O microemulsions form inside the organic phase and "catalyze" the aquation of Rh(III), thus making nonfeasible the development of a conventional solvent extraction system for Rh(III) (i.e., the D remains always low, <1). Therefore, alternative approaches have to be found to effect its separation. One possible alternative is to use a liquid membrane technique to permit the continuous transfer of the extractable $RhCl_6^{3-}$ complex from the feed aqueous phase to a receiving phase through an organic membrane of Kelex 100. Of course, this approach implies that upon withdrawal of the non-aquated Rh species the aqueous feed will undergo reequilibration, thus producing more of the nonaquated complexes by shifting the aquation-anation reaction towards anation.

[1]The material presented in this chapter constitutes the subject-matter of a recent publication: S.N., Ashrafizadeh, and G.P., Demopoulos, Extraction of Rhodium Chlorocomplexes and Acid through a Supported Liquid Membrane of Kelex 100, *Sep. Sci. Technol.*, **31**(7), 895-914, 1996.

Indeed, it is the object of the present work to investigate the feasibility and viability of the transport of Rh(III) complexes through a liquid membrane containing Kelex 100 in a kerosene medium. To this end, first, various combinations of available surfactants (Draxler and Marr, 1986; Miesiac et al., 1993) were applied in order to obtain a suitable emulsion liquid membrane (ELM) system. The results, which are not reported here, failed consistently to show satisfactory stability. By contrast, the supported liquid membrane (SLM) system behaved in a very stable and reproducible manner, thus justifying continuation of the investigation.

In this chapter, the supported liquid membrane is employed to effect the separation of Rh chlorocomplexes from hydrochloric acid solutions. The mechanism of acid, water, and Rh permeation through the SLM is investigated and the driving force for this permeation process identified. Optimum conditions for the transport of Rh species are determined and possible approaches to suppress the co-extraction of acid and water outlined. Under optimum conditions the membrane was found to be very stable for at least a period of 72 hours while the rate of extraction was found to be well comparable with other SLM systems.

5.2 RESULTS AND DISCUSSION

Description of the SLM apparatus and its operation along with details on experimental procedure and analysis, are given in Chapter 3. The only point worth mentioning here is that throughout this chapter the concentration of Rh is reported in ppm (mg/L). This is done, for simplicity, due to the low concentrations used. Concentrations of Rh in ppm are converted to molarity by multiplying by 0.97×10^{-5}.

5.2.1 Membrane Selection

As described in the last chapter, Kelex 100 tends to extract in a reversible manner a certain fraction of Rh (III) (the nonaquated complex $RhCl_6^{3-}$) from chloride solutions (D<0.5) via protonation (step 1) and ion-pair formation (step 2):

Step 1: Protonation

$$\overline{R-HQ} + H^+ + Cl^- \leftrightarrow \overline{R-H_2Q^+Cl^-} \qquad (5.1)$$

Step 2: Ion-pair formation

$$RhCl_6^{3-} + 3\overline{R-H_2Q^+Cl^-} \leftrightarrow \overline{RhCl_6^{3-}(R-H_2Q^+)_3} + 3Cl^- \qquad (5.2)$$

The extraction reaction (5.2) can be easily reversed upon contact of the loaded Kelex 100 with a dilute acid solution of pH ≥ 1. It was thought, therefore, that upon combining together extraction and stripping in the form of an SLM system, a quantitative transfer of rhodium from an impure dilute solution into a purified concentrated strip solution could be achieved. It was thought so because the aquation-anation reaction of Rh(III) (reaction (5.3)) is relatively fast (see the results of Chapter 4):

$$RhCl_6^{3-} + H_2O \leftrightarrow RhCl_5(H_2O)^{2-} + Cl^- \qquad (5.3)$$

To this end, a Kelex 100-based SLM system was designed and tested. During the first stage of the work the concentration of Kelex 100 (in mixture with tridecanol and kerosene), type of support, and agitation regime were selected by measuring acid permeation rates. In this part of the work the stability of the membrane was studied as well.

Agitation

The effect of agitation on the rate of acid extraction was first examined through a set of experiments, using 0.45 μm Gore-Tex membrane as support and a LM of 25 v/o (0.7 M) of Kelex 100. The results, which are summarized in Table 5.1, exhibit an increase in the rate of acid extraction upon increasing the agitation speed from the low to the intermediate agitation range. However, an almost negligible increase was observed upon any further increase of the agitation speed. Moreover, it can be seen that an increase in the agitation speed of the strip side has a more pronounced effect than that of the feed side. In other words, the rate of acid transport seems to be controlled by boundary layer resistance of the the strip phase, rather than that of the feed phase. As a precaution against loss of membrane stability, the intermediate range of agitation speed (100 rpm) was chosen for the rest of the experimental work.

Table 5.1: Effect of Agitation Speed on Rate of Acid Permeation

Feed Agitation Speed (rpm)	Strip Agitation Speed (rpm)	J_{acid} (mol/s.m^2)
50	50	1.68×10^{-4}
100	100	1.85×10^{-4}
150	150	1.90×10^{-4}
50	100	1.83×10^{-4}
100	50	1.71×10^{-4}

Support: 0.45 μm Gore-Tex.

LM: 25, 25, 50 v/o; Kelex 100, Tridecanol, Kerosene.

Feed: 200 mL 2.5 M HCl.

Strip: 20 mL (initial) 0.1 M HCl.

Support Structure

To investigate the effect of support pore size on the performance of the SLM system, two Gore-Tex polymer sheets were tested at different LM concentrations of Kelex 100. The results of these tests, summarized in Table 5.2, show the identical performance of the two supports (0.2 and 0.45 μm pore size). It must be mentioned here that the membrane with the smaller pore size had a smaller thickness, and this perhaps had compensated for any decrease in permeation rate as a result of the pore size. For the subsequent series of tests, the membrane of 0.45 μm pore size was retained and used, since it possesses a higher durability and thus a higher mechanical strength.

Table 5.2: Effect of Support Pore Size on Rate of Acid Permeation

	J_{acid} (mol/s.m^2)	
Kelex v/o	0.2 μm pore size	0.45 μm pore size
15	1.392×10^{-4}	1.396×10^{-4}
20	1.790×10^{-4}	1.786×10^{-4}
25	1.831×10^{-4}	1.850×10^{-4}

Support: Gore-Tex.

LM: X, X, (100-2X) v/o; Kelex 100, Tridecanol, Kerosene.

Feed: 200 mL 2.5 M HCl.

Strip: 20 mL (initial) 0.1 M HCl.

Kelex 100 Concentration

The rate of acid extraction was found to increase with Kelex 100 concentration and eventually to reach a plateau at about 0.7 M (25 v/o) Kelex 100 (Figure 5.1). This concentration of Kelex 100 was chosen to conduct the remaining SLM experiments. Apparently, higher concentrations result in a very viscous liquid membrane which imposes resistance on the transport process. Another interesting observation worth mentioning is the behavior of the SLM when LM does not contain the carrier (i.e., zero v/o Kelex 100). In this case, the support was soaked in a pure kerosene solution. The impermeability of the SLM shows that, even if all the Kelex 100 contents are lost, the support is capable of partitioning the two aqueous phases due to its inherent hydrophobicity, and thus diffusion in an unwanted direction can be prevented.

SLM Stability

To examine the stability of the SLM system and also to determine whether its performance is reproducible under the fixed experimental conditions (i.e., 0.45 μm Gore-Tex; 25 v/o Kelex 100; 100 rpm agitation speed), two sets of experiments were conducted in which the change of Rh concentration in two similar feed solutions was measured as a function of time. In the first experiment, the SLM was periodically (every 3 hours) replaced with a fresh one; whereas in the second, the same SLM was used throughout its entire duration. The results, which are shown in Figure 5.2, indicate a very similar trend for both systems, an observation which suggests that the SLM remained stable for the duration of the test (70 hours). The same figure serves to demonstrate the separation capability of the present SLM process as it achieves more than 90% Rh extraction and subsequent concentration of the extracted Rh values in the low volume (feed volume/strip volume = 10) strip solution.

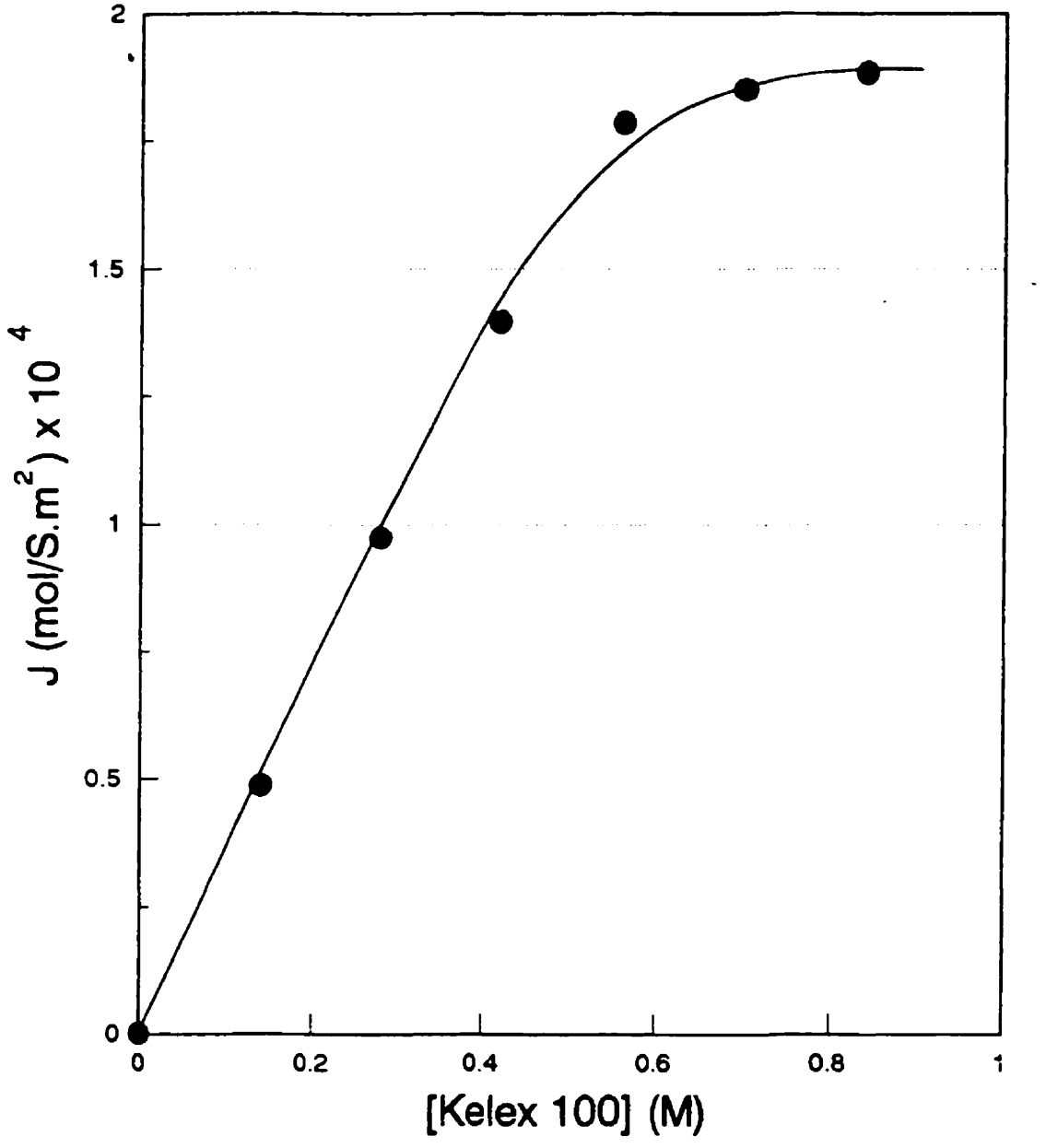

Figure 5.1: Effect of Carrier Concentration on Rate of Acid Permeation

(Support: 0.45 μm Gore-Tex; LM: X v/o Kelex 100, X v/o tridecanol, (100-2X) v/o kerosene; Feed: 200 mL 2.5 M HCl; Strip: 20 mL 0.1 M HCl)

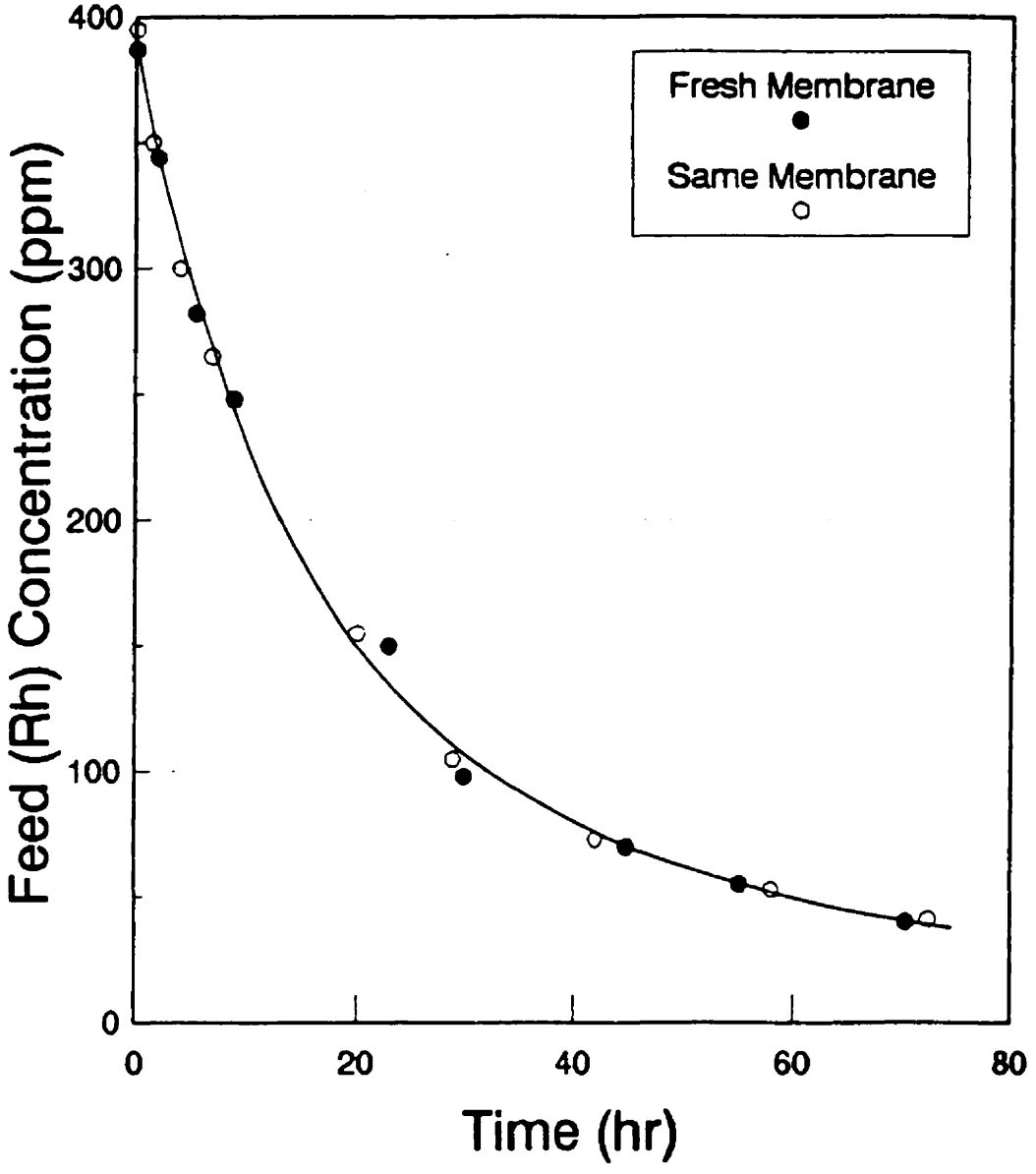

Figure 5.2: Stability of SLM vs Operation Time (Support: 0.45 μm Gore-Tex; LM: 25 v/o Kelex 100, 25 v/o tridecanol, 50 v/o kerosene; Feed: 200 mL 2.5 M HCl, 400 ppm Rh, 2-week aged; Strip: 20 mL 1.5 M NaCl at pH=1)

5.2.2 Permeation of Acid

As previously discussed, acid (HCl) and water are co-extracted along Rh (III) with the Kelex 100 organic phase. Acid is extracted via the protonation of Kelex 100 (eq. (5.1)) while water is extracted through hydration at the low acid region and through the formation of W/O microemulsions in the loaded organic phase at elevated acid concentrations (≥ 0.7 M HCl). Both of these co-extracted components have negative consequences on the SLM process of Rh. Permeation of acid, itself, causes two kind of problems. First, it increases the acidity of the strip phase, and thus causes a decrease in the HCl concentration gradient. This results in a loss of driving force and stoppage of metal transfer, unless the extracted acid is neutralized. Second, it produces a buildup of chloride ion concentration in the strip phase. Consequently, it further complicates the Rh extraction process, as will be shown below.

In Figure 5.3, the rate of acid extraction is plotted against feed acidity. The rate increases sharply with the feed acidity up to about 2 M HCl, followed by a plateau region up to 4 M HCl. Beyond that acidity, the rate again increases with feed acidity. This behavior is quite similar to that of the solvent extraction process (Chapter 4), and it might be interpreted as follows. The sharp increase at lower acidities is due to an increase in the protonation of the extractant molecules (eq. (5.1)). However, since the protonation of the extractant is supposed to be completed at 2.5-3 M HCl (see Chapter 4), any further increase in the feed acidity at the plateau region does not significantly promote the acid extraction. At higher acidities, the mechanism of acid extraction changes, and W/O microemulsions are believed to be responsible for this extra acid uptake (see Chapter 4).

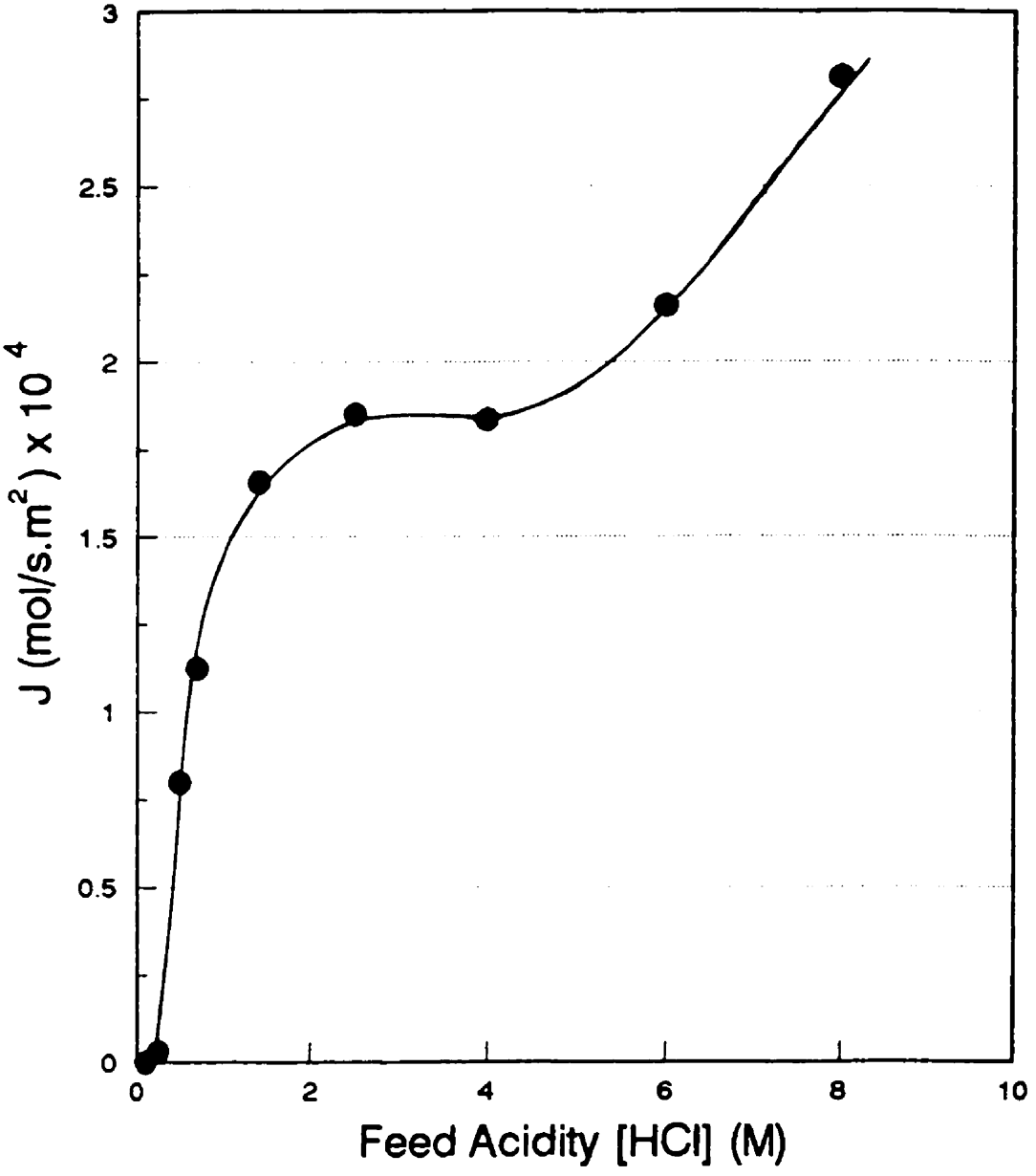

Figure 5.3: Effect of Feed Acidity on Rate of Acid Permeation

(Support: 0.45 μm Gore-Tex; LM: 25 v/o Kelex 100, 25 v/o tridecanol, 50 v/o kerosene; Feed: 200 mL different [HCl]; Strip: 20 mL 0.1 M HCl)

The effect of the strip phase acid concentration on the rate of acid extraction is depicted in Figure 5.4. As shown, the rate of extraction is not sensitive to small increases in the strip acidity (0.1 to 0.2 M HCl). However, at higher acidities it sharply decreases with the acidity of the strip phase.

One of the variables that had to be considered in the SLM system under investigation was the amount of salt in the feed and strip solutions. The salt (NaCl) is accumulated in the strip solution as a result of the neutralization of the co-extracted acid with NaOH. On the other hand, NaCl may be present in the feed solution either as a component of the original industrial solution or, again, as a result of the adjustment of acid with NaOH. The effect of NaCl accumulation in the strip solution on acid extraction is shown in Figure 5.5. It is clear that, as the salinity of the strip solution increases, the rate of acid extraction drops drastically. This negative effect of strip solution salinity on acid extraction is attributed to the effect [Cl^-] has on the activity of HCl (a_{HCl}) as well as on the individual H^+ ion activity (Jansz, 1983). As a result of the increasing a_{HCl} of the strip solution with increasing [NaCl], the acid activity gradient decreases or, equivalently, the driving force for acid extraction decreases. For exactly the same reasons, an increase in the salinity of the feed solution is observed to increase the rate of acid extraction, as indicated in Figure 5.6.

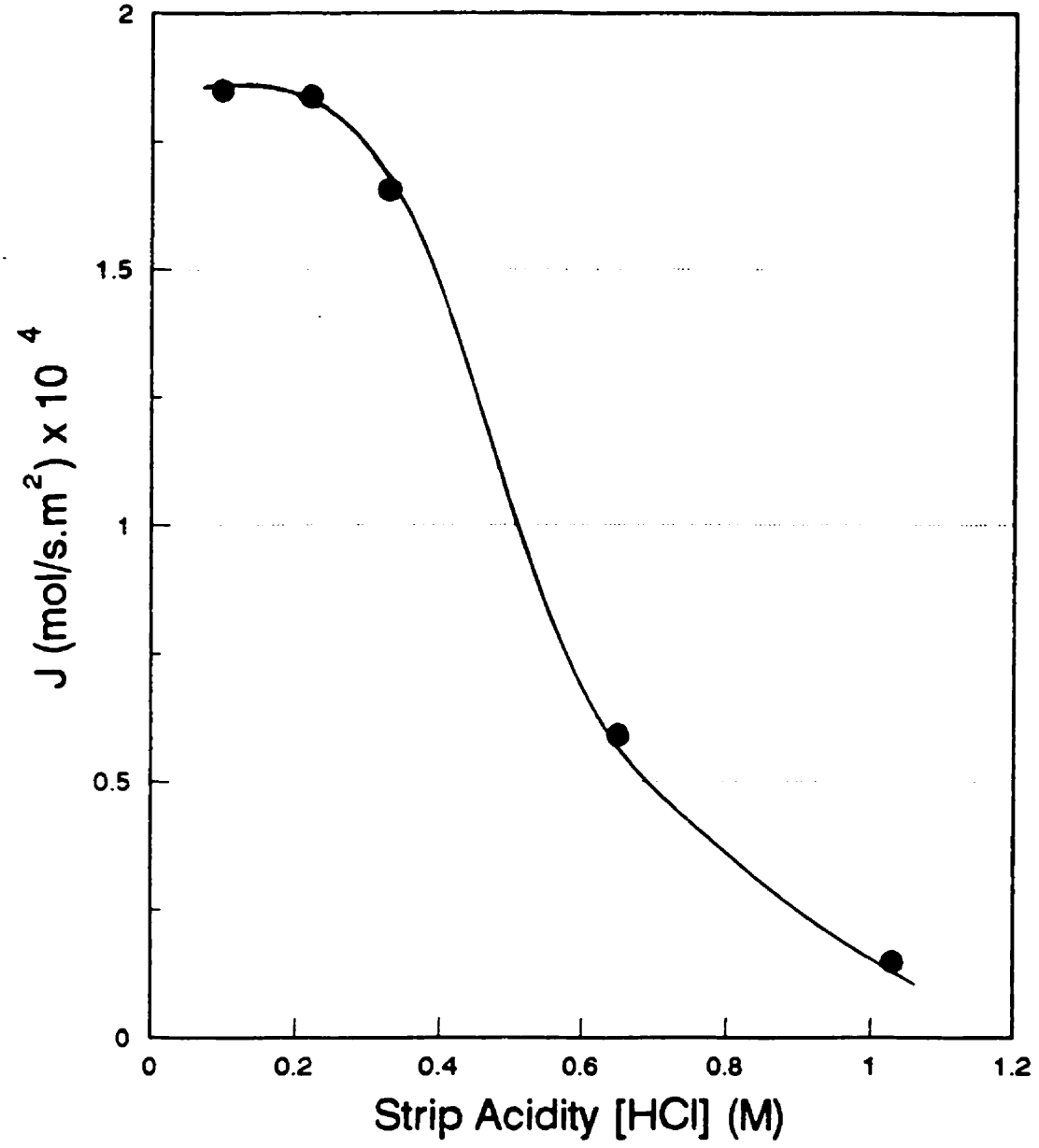

Figure 5.4: Effect of Strip Acidity on Rate of Acid Permeation

(Support: 0.45 μm Gore-Tex; LM: 25 v/o Kelex 100, 25 v/o tridecanol, 50 v/o kerosene; Feed: 200 mL 2.5 M HCl; Strip: 20 mL different [HCl])

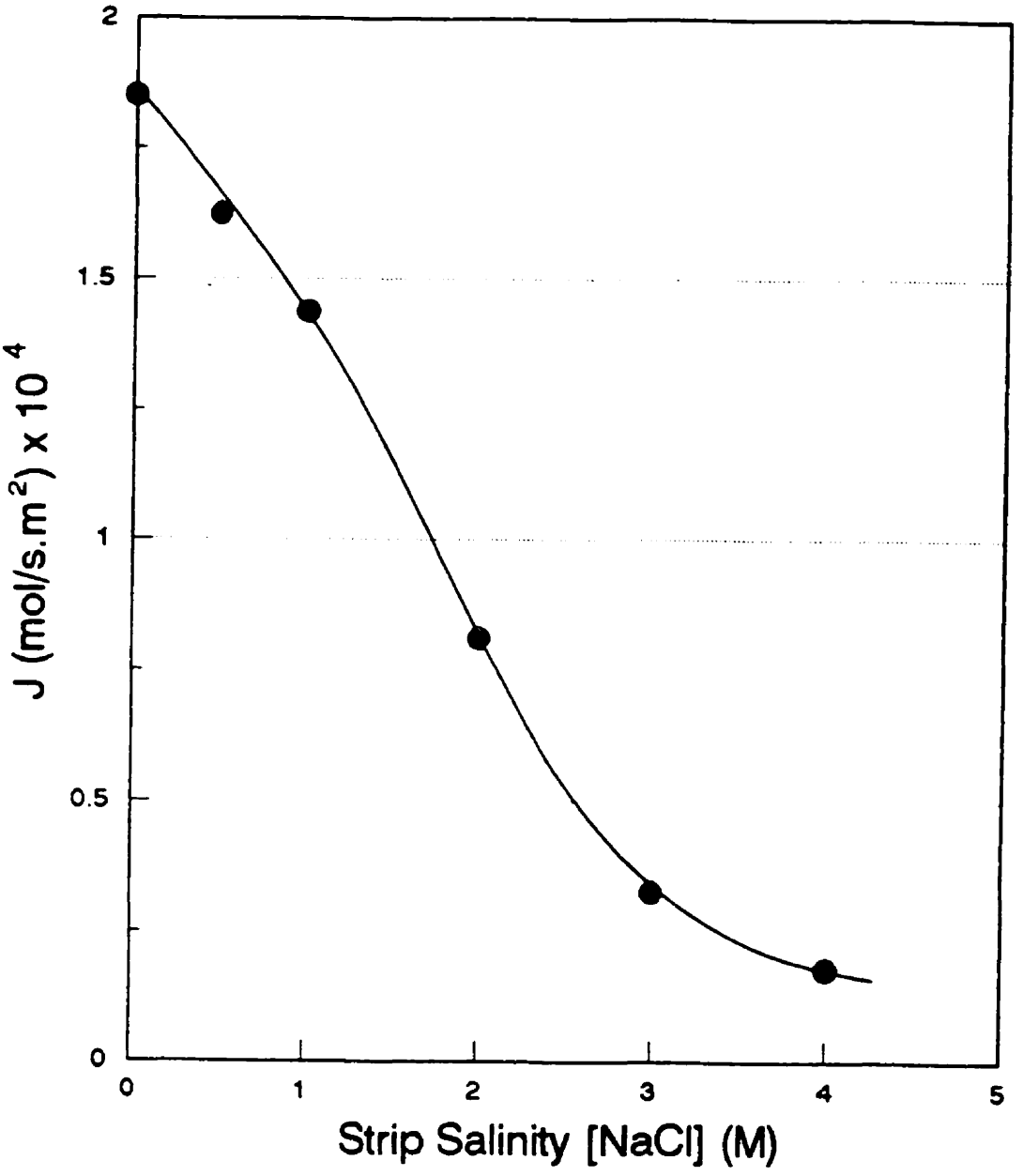

Figure 5.5: Effect of Strip Salinity on Rate of Acid Permeation

(Support: 0.45 μm Gore-Tex; LM: 25 v/o Kelex 100, 25 v/o tridecanol, 50 v/o kerosene; Feed: 200 mL 2.5 M HCl; Strip: 20 mL different [NaCl] at pH=1)

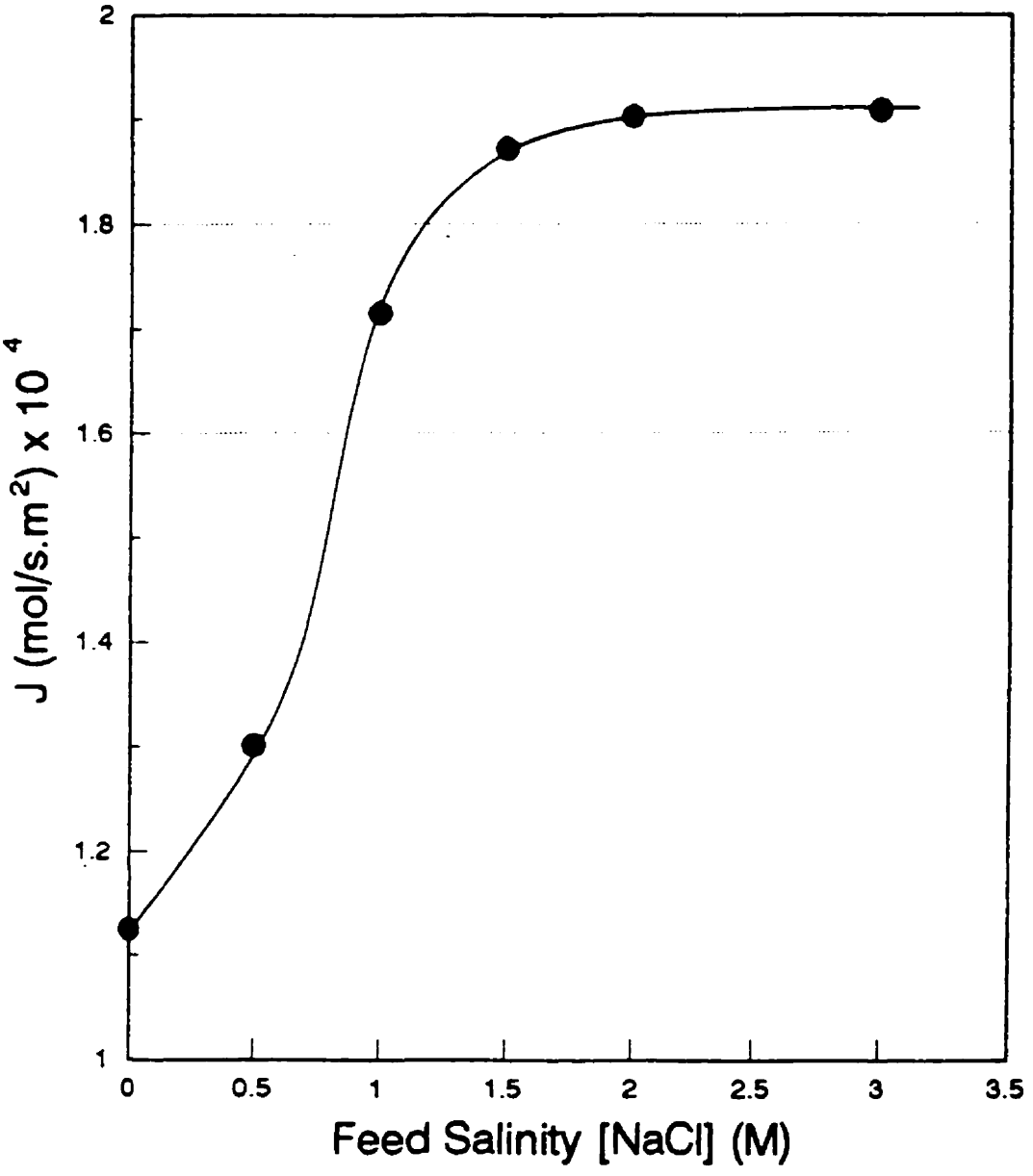

Figure 5.6: Effect of Feed Salinity on Rate of Acid Permeation

(Support: 0.45 μm Gore-Tex; LM: 25 v/o Kelex 100, 25 v/o tridecanol, 50 v/o kerosene; Feed: 200 mL 0.7 M HCl & different [NaCl]; Strip: 20 mL 0.1 M HCl)

5.2.3 The Role of HCl Activity

In order to demonstrate further the significance of acid activity (as opposed to simple acid concentration) as the true driving force, not only for the transport of acid but also for the transport of metal species across the membrane, the following analysis is presented.

The mechanism of acid permeation through SLM is schematically shown in Figure 5.7. The free extractant (X) at the membrane/feed interface being first protonated with protons (H^+) forms the ion-pair with chloride ions (or similarly with anionic metal chlorocomplexes). The ion-pair diffuses through SLM due to the concentration gradient across the membrane and undergoes dissociation by reaching the downstream interface. The free extractant, however, moves in reverse direction of the ion-pair due to an opposite concentration gradient to that of ion-pair across the membrane. As reversible reactions, both ion-pair formation/dissociation and transport through the SLM might take place in opposite directions, and thus the net rate is considered as the result of this permeation process. The ion-pair formation- and dissociation-rate constants are denoted by 1 and 2 in the feed side and by 3 and 4 in the strip side.

In order to have a net acid permeation (r_A) into strip solution there should be a concentration gradient of ion-pair (i.e., X-H-Cl) across the membrane. In other words, the relation $r_1 > r_3$ or, equivalently, $(\mathbf{a}_H \times \mathbf{a}_{Cl})_f > (\mathbf{a}_H \times \mathbf{a}_{Cl})_s$ must hold. Therefore, the rate of acid permeation is a function of the gradient of the activity products ($\mathbf{a}_H \times \mathbf{a}_{Cl}$) across the membrane. It should be emphasized that the latter relation is held only at the lower range of acid and salt concentrations, where the extractant molecules are not saturated with protons and where the permeation process is not controlled by diffusion through the membrane. To demonstrate the latter dependency, the activity of HCl solutions at different molalities are calculated and presented in Appendix B.

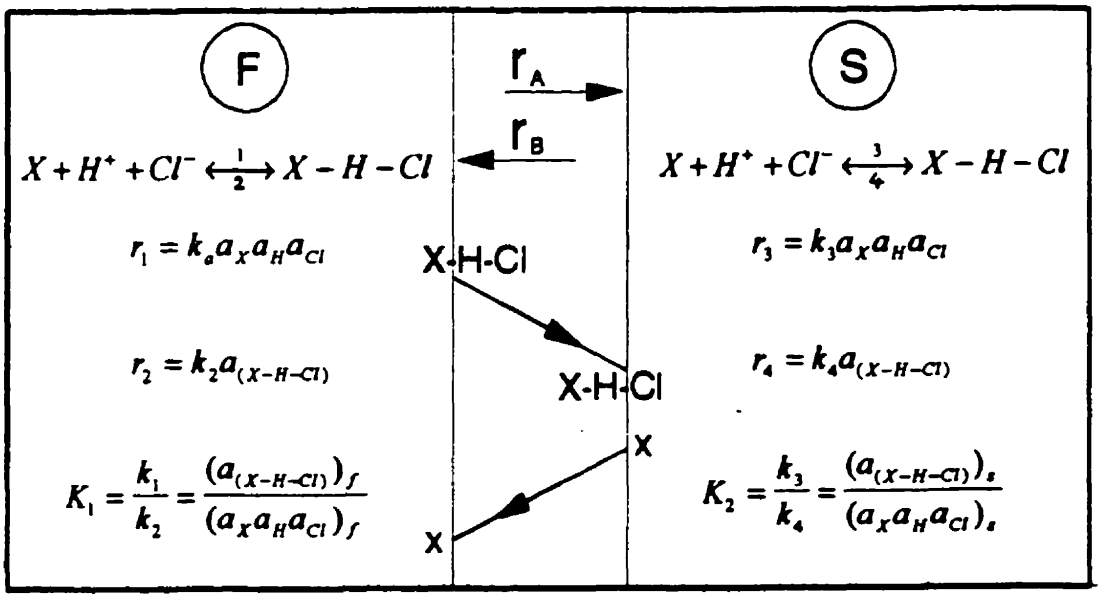

Figure 5.7: Schematic Presentation of SLM Permeation Mechanism

The activity of HCl and the activity of its constituent ions in the presence and absence of salt (NaCl) were determined using literature data (Robinson and Stokes, 1959) and the Meissner's method (1980). The activity data were calculated as a function of feed and/or strip acidity, or salinity, for similar cases discussed through Figures 5.3 to 5.6. These calculations are described in detail in Appendix B. In all cases, the activity of HCl across the membrane, as the main driving force, shows a trend very similar to that of rate of acid permeation. For instance, the activity gradient, i.e., $\Delta a_{HCl} = (a_{HCl})_{feed} - (a_{HCl})_{strip}$ (Figure 5.8), shows a direct correlation with the rate of acid permeation versus feed acidity (Figure 5.3). In other words, the rate of acid permeation is a function of the HCl activity gradient (Δa_{HCl}) across the membrane. As well, by increasing the strip acidity, the activity gradient decreases, i.e., $(a_{HCl})_{strip}$ increases (Figure 5.9), similarly to the decrease of the rate of acid permeation with strip acidity (Figure 5.4). Similar trends are found with the effect of salt on acid activity and acid permeation and so on. These additional activity estimations are given in Appendix B.

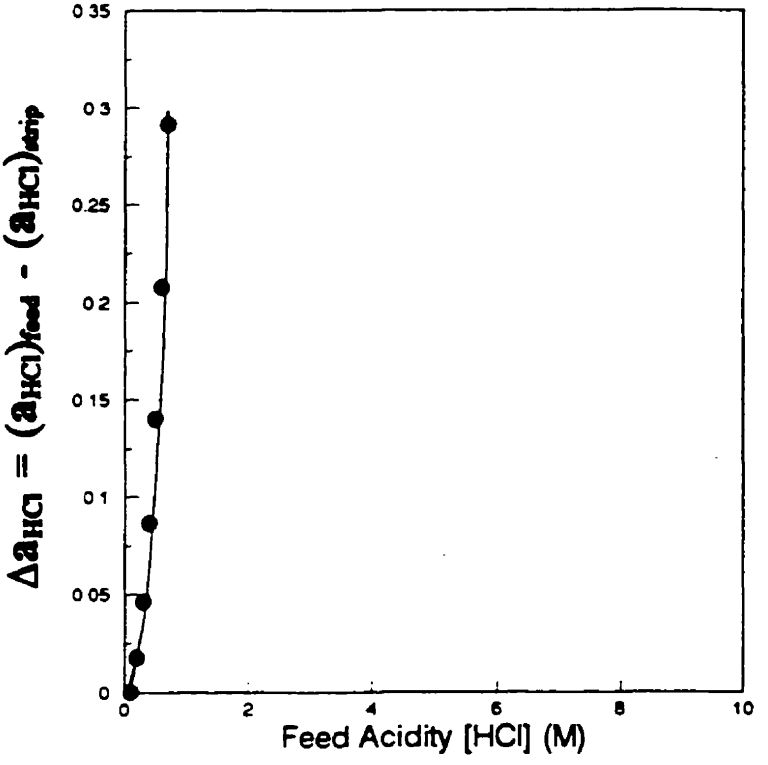

Figure 5.8: Activity Gradient of HCl Across SLM vs Feed Acidity

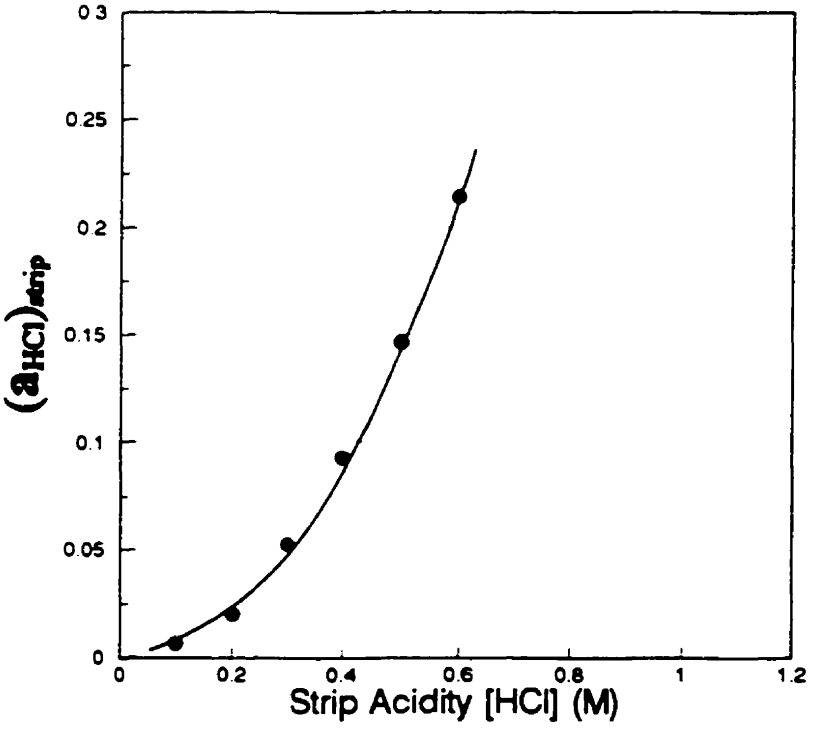

Figure 5.9: Activity of HCl in SLM Strip Phase vs Strip Acidity

Figure 5.10 depicts the transfer of acid from a feed solution with low acid concentration (0.7 M HCl / 3.3 M NaCl; the acid concentration was kept constant throughout the whole experiment) towards a strip solution whose acidity progressively increased from 0.1 M to 2.2 M, at which point equilibrium was reached. In other words, in this case acid was transferred from the feed phase to the receiving phase against the apparent acid concentration gradient. This is because a positive acid activity gradient (Δa_{HCl}) was operating due to the high salt concentration (3.3 M NaCl) of the feed phase. This was confirmed by estimating the activities of acid at the equilibrium point (a feed of 0.7 M HCl and 3.3 M NaCl vs. a strip solution of 2.2 M HCl). The estimated activity values are given in Table 5.3. As shown, the system reaches its equilibrium when a_{HCl} is equal across the SLM or, equivalently, when the activity gradient (Δa_{HCl}) becomes zero. This experiment proves beyond doubt that the true driving force of the SLM process investigated here is the HCl activity gradient across the membrane.

Table 5.3: Estimations of Acid Activities - Re Experiment of Fig. 5.10

Feed	Strip	
0.7 M HCl & 3.3 M NaCl	[HCl] (M)	$a_{H^+} \times a_{Cl^-}$
$a_{H^+} = 1.835$ ‡	1.0	† 0.795
$a_{Cl^-} = 3.609$ ‡	1.5	† 2.081
$a_{H^+} \times \alpha_{Cl^-} =$ **6.623** ‡	2	† 4.796
	2.2	† **6.569**
	2.5	† 10.301
$a_{H^+} \times a_{Cl^-} =$ **6.646** *	**2.25**	* **6.545**

(†) From Tables 2 & 3 of Reference (Jansz, 1983).

(‡) From Figures 7 & 8 of Reference (Jansz, 1983).

(*) Meissner method; see Appendix B for details.

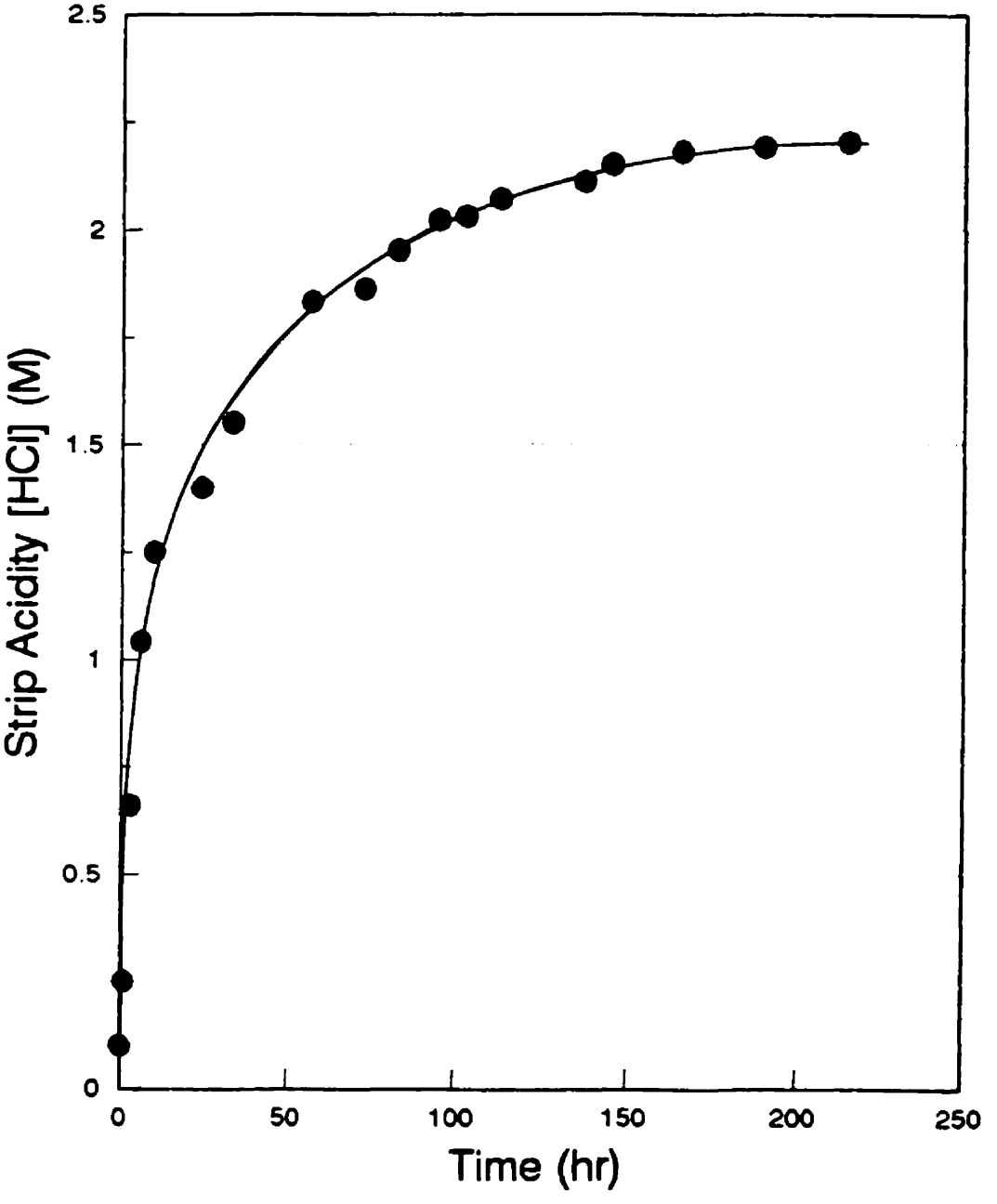

Figure 5.10. Build-up of Strip Acid Concentration with Time

(Support: 0.45 μm Gore-Tex; LM: 25 v/o Kelex 100, 25 v/o tridecanol, 50 v/o kerosene; Feed: 200 mL 0.7 M HCl & 3.3 M NaCl; Strip: 20 mL initially 0.1 M HCl)

5.2.4 Permeation of Water

The permeation of water through the membrane creates problems in the effort to obtain a concentrated Rh strip solution due to the dilution brought about. It was shown previously that, in a conventional solvent extraction system, Kelex 100 extracts water along with acid. The co-extraction of water with acid has been confirmed in the present SLM system as well. Some measured water transport rates[2] are given along with the corresponding acid transport rates in Table 5.4.

Table 5.4: Rates of Water and Acid Permeation through SLM

Expt.	Feed		Strip		J_{Water}	J_{Acid}	J_W/J_A
#	HCl (M)	NaCl (M)	HCl (M)	NaCl (M)	(mol/s.m^2)	(mol/s.m^2)	
1	0.7	0.0	0.1	0.0	1.30×10^{-4}	1.15×10^{-4}	1.13
2	0.7	3.0	0.1	0.0	1.38×10^{-4}	1.90×10^{-4}	0.73
3	0.7	0.0	0.1	0.5	1.35×10^{-4}	--	--
4	2.5	0.0	0.1	0.0	2.92×10^{-4}	1.85×10^{-4}	1.60
5	2.5	2.0	0.1	0.0	2.70×10^{-4}	--	--
6	2.5	0.0	0.1	2.0	3.20×10^{-4}	0.80×10^{-4}	4.00

Support: 0.45 μ Gore-Tex.

LM: 25, 25, 50 v/o; Kelex 100, Tridecanol, Kerosene.

Feed: 200 ml different M HCl & NaCl.

Strip: 20 ml (initial) at different M HCl & NaCl.

[2]It must be stated here that due to difficulties in the measurement of water transport rates, the reported data should be viewed as approximations, with a relative rather than absolute value.

The permeation of water is seen to be low when the feed acidity is low (0.7 M). However, higher water transport rates are observed with 2.5 M HCl feed. This drastic increase in water transport seems to relate to the mechanism of water extraction (see Chapter 4). Thus, at low acid concentration (0.7 M) water is extracted through partial hydration of the protonated Kelex 100 molecules. On the other hand, at acidities above 0.7 M HCl, W/O microemulsions form which make the transport of larger quantities of water through the organic phase possible. Finally, the variable ratio of J_{water} / J_{acid} at the range of high feed acidity (expt. 4 vs expt. 6) can be at least partly explained on the basis of higher water activity gradient as a result of the higher level of salinity in the strip phase.

5.2.5 Permeation of Rh(III) Chlorocomplexes

In Section 5.2.1, the results of a typical Rh-SLM extraction test were presented in the form of a graph (Fig. 5.2) giving the variation of Rh(III) concentration in the feed phase with time (up to 70 hr). For the subsequent work on the kinetics of Rh(III) transport, the initial rate (defined as the concentration drop after one hour – see Chapter 3) was measured under a variety of conditions. The results obtained are presented in this section. The mechanism of Rh(III) transport is discussed in Section 5.2.6.

The effect of agitation speed on the initial rate of Rh permeation is shown in Table 5.5. It can be seen the rate to increase by increasing the agitation speed with more pronounced being the effect of the agitation speed in the strip phase. This trend resembles the one observed with the permeation of acid (Table 5.1). For the remainder of the tests, 100-rpm agitation speed on both sides of the membrane was chosen. With this speed the plateau of rate vs. rpm has been practically reached for the feed/membrane interface. For the membrane/strip interface, the plateau had not been completely reached at 100 rpm, but in order to avoid problems with the stability of the membrane no higher speed was applied.

Table 5.5: Effect of Agitation Speed on Rate of Rh Permeation

Feed Agitation Speed (rpm)	Strip Agitation Speed (rpm)	J_{Rh} (mol/s.m^2)
50	50	2.43×10^{-6}
100	100	2.62×10^{-6}
150	150	2.71×10^{-6}
50	100	2.55×10^{-6}
100	100	2.62×10^{-6}
150	100	2.65×10^{-6}
100	50	2.48×10^{-6}
100	100	2.62×10^{-6}
100	150	2.69×10^{-6}

Support: 0.45 μm Gore-Tex.
LM: 25, 25, 50 v/o; Kelex 100, Tridecanol, Kerosene.
Feed: 200 mL 2.5 M HCl; 400 ppm Rh, 2-week aged.
Strip: 20 mL (initial) 0.1 M HCl.

The effect of Kelex 100 concentration on the rate of the permeation of rhodium is illustrated with the results of Figure 5.11. The rate increases with Kelex 100 concentration, reaching a maximum-plateau rate at 0.7 M (25 v/o) Kelex 100. This trend fully agrees with the corresponding acid permeation profile (Figure 5.1). The data of Figure 5.11 are re-plotted in Figure 5.12 in a log-log scale. A first order dependency is obtained. This suggests that the rate controlling step involves the protonated Kelex 100 ($R\text{-}H_2Q^+Cl^-$) molecule.

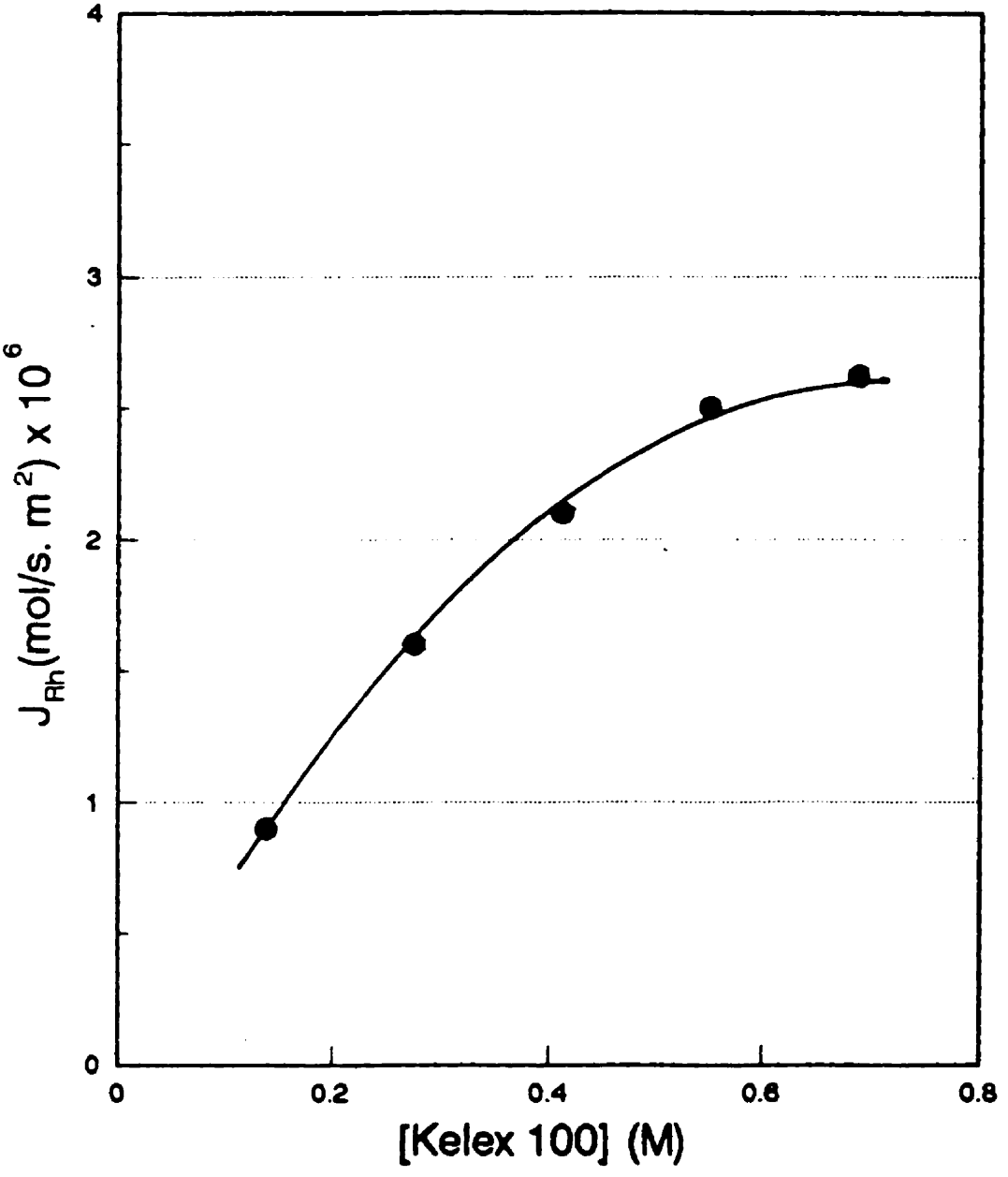

Figure 5.11: Effect of Kelex 100 Concentration on Rate of Rh Permeation (Support: 0.45 μm Gore-Tex; LM: x v/o Kelex 100, x v/o tridecanol, kerosene; Feed: 200 mL 2.5 M HCl, 400 ppm Rh, 2-week aged; Strip: 20 mL 0.1 M HCl)

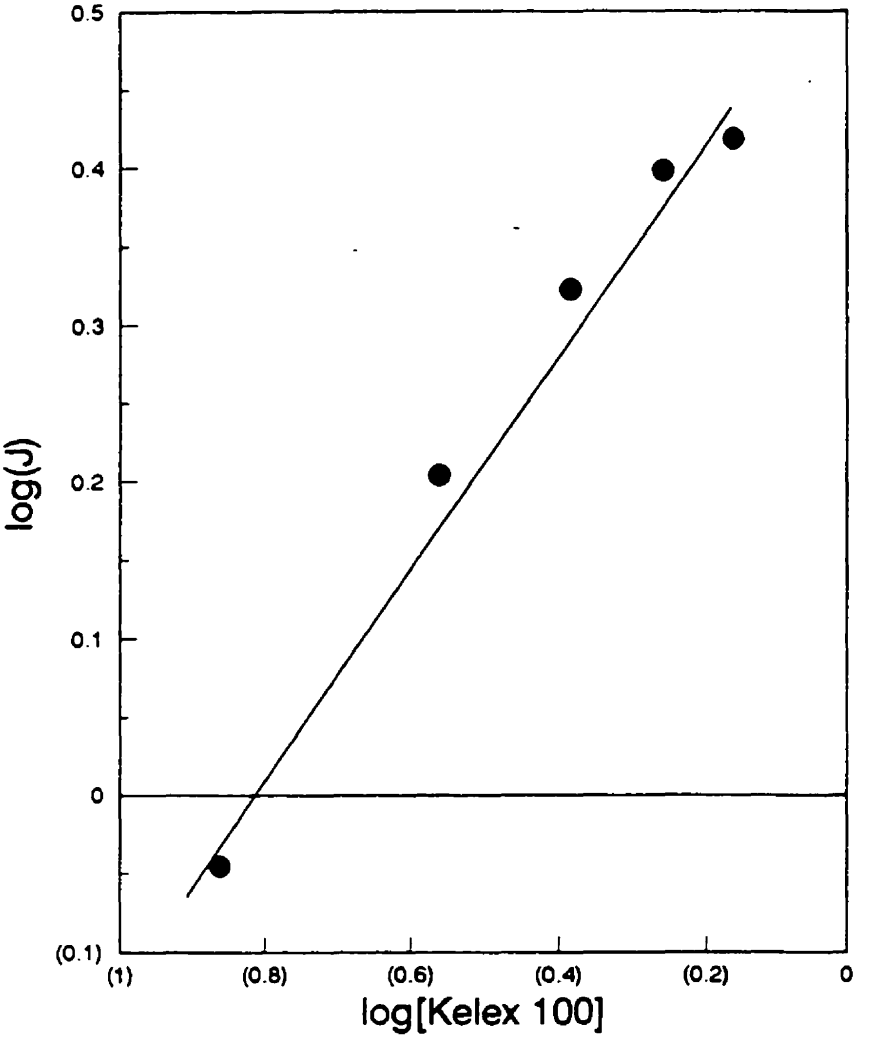

Figure 5.12: Re-Plot of the Data of Figure 5.11 in a Log-Log Scale

The effect of feed Rh concentration on the rate of Rh permeation is shown in Figure 5.13. The data apparently obey a first order relationship ($J=k_O C_{Rh}$). The first order dependency on rhodium feed concentration was also determined by analyzing tha data of Figure 5.2 via the integration method. The first order plot is shown in Figure 5.14. While the rate of rhodium permeation is directly dependent on the level of rhodium concentration in the feed phase the same is not true for the strip phase. Thus, as one can see in Figure 5.15, build up of Rh concentration in the strip solution (up to 6 times the concentration of rhodium in the feed solution) has no effect on rhodium permeation kinetics.

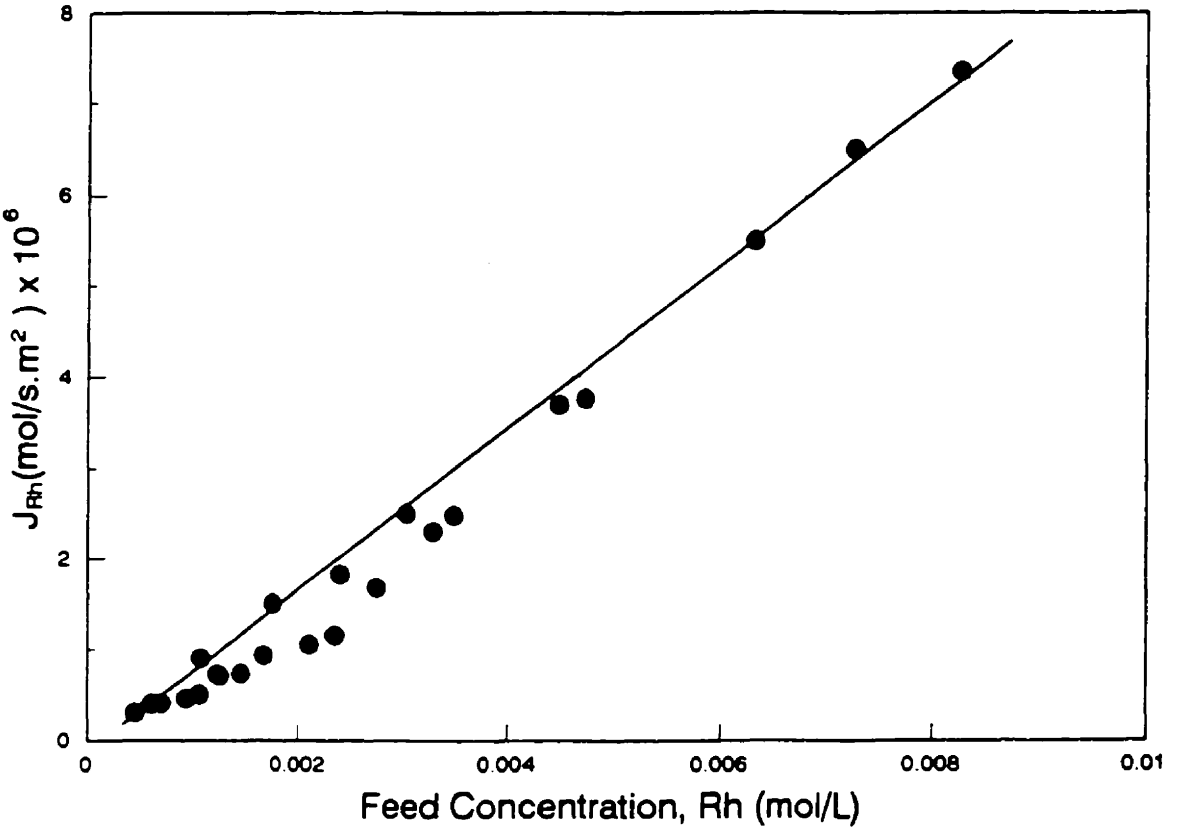

Figure 5.13: Effect of Feed Rh Concentration on Rate of Rh Permeation

(Support: 0.45 μm Gore-Tex; LM: 25 v/o Kelex 100, 25 v/o tridecanol, 50 v/o kerosene; Feed: 200 mL 2.5 M HCl, different [Rh], 2-week aged; Strip: 20 mL 0.1 M HCl)

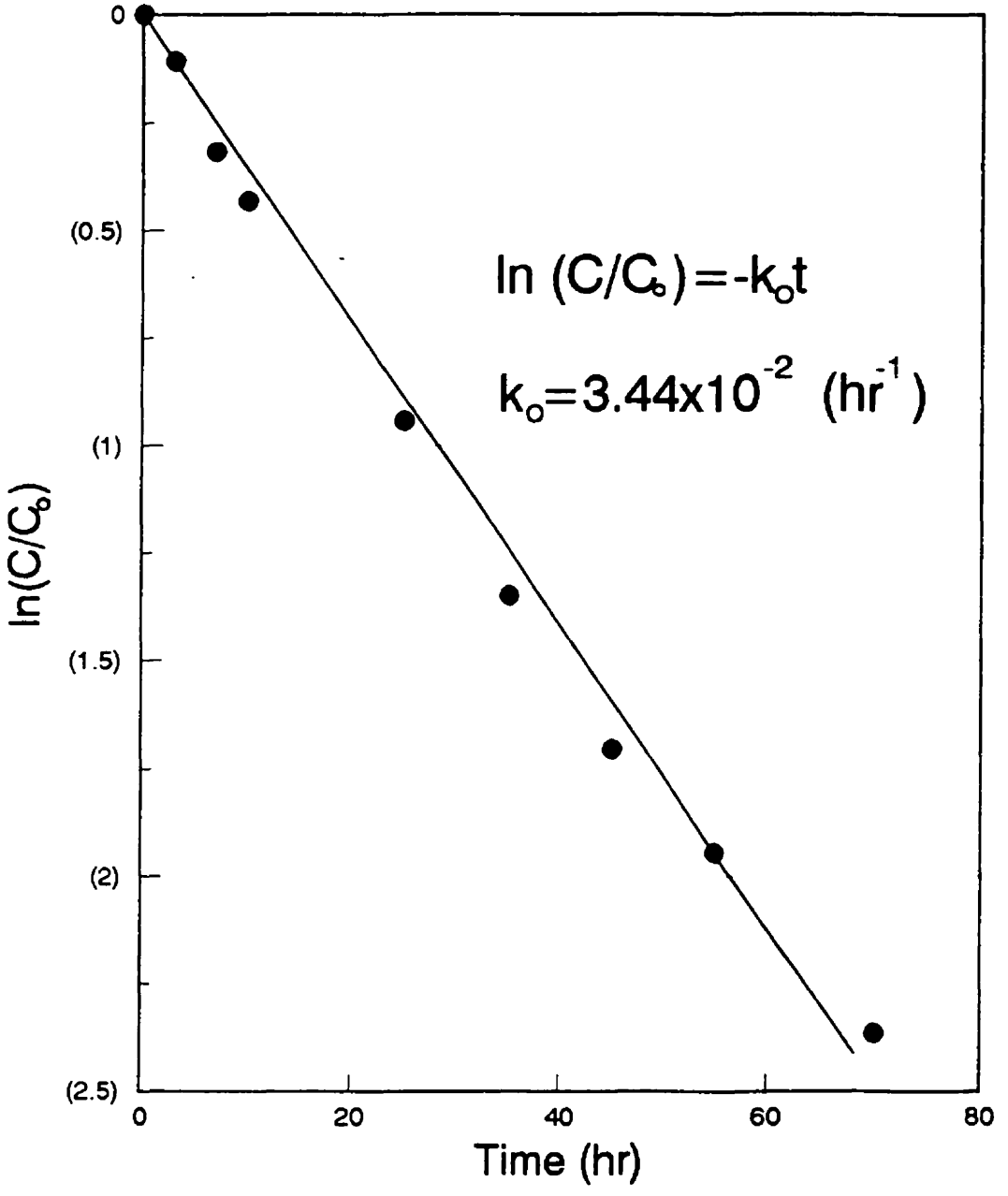

Figure 5.14: Re-Plot of the Integrated Data of Figure 5.2

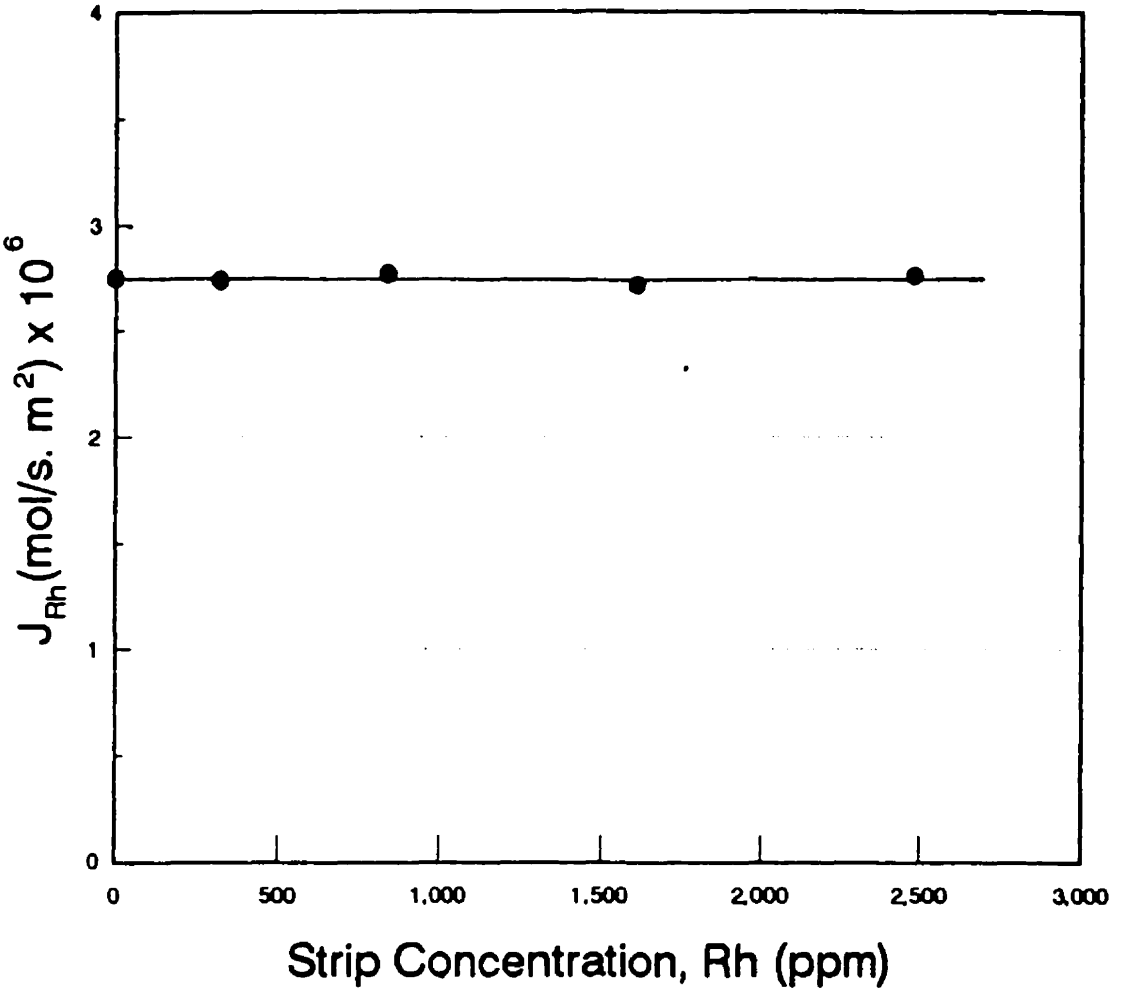

Figure 5.15: Effect of Strip Rh Concentration on Rate of Rh Permeation

(Support: 0.45 μm Gore-Tex; LM: 25 v/o Kelex 100, 25 v/o tridecanol, 50 v/o kerosene; Feed: 200 mL 2.5 M HCl, 400 ppm Rh, 2-week aged; Strip: 20 mL 0.1 M HCl)

The effects of other variables on the rate of Rh permeation through the Kelex 100-based SLM are depicted in Figures 5.16 through 5.19. First, the effect of feed acidity on the rate of Rh permeation is presented. As one can see in Figure 5.16, the rate of permeation increases with feed acidity up to about 2 to 2.5 M HCl, where it reaches a plateau and falls off thereafter with any further increase in the feed acidity. The initial increase is attributed primarily to the increased protonation, eq. (5.1), of Kelex 100 and, secondarily, to an increase of the relative ratio $RhCl_6^{3-}/RhCl_5(H_2O)^{2-}$ via the suppression of aquation (eq. (5.3)). On the other hand, the decrease in the latter stage is attributed to the suppression of the ion-pair formation reaction (eq. (5.2)), at high chloride concentrations. A similar observation can be made with respect to the effect which the NaCl content of the feed (1.4 M HCl) had on the rate of Rh extraction (Figure 5.17). Again the plateau is reached almost within the same region, i.e., 2 to 2.5 M total Cl^-, followed by a decrease at higher chloride concentrations. It is interesting to note that the maximum in Figure 5.16 corresponds to the initial plateau of the HCl extraction kinetic curve (see Figure 5.3). This plateau, reached at about 2 to 3 M HCl, relates to the complete protonation of Kelex 100 (see Figure 4.9). The extra acid extracted beyond that acid concentration level – i.e., beyond 2 to 3 M HCl as mentioned earlier (see Chapter 4) – is attributed to the formation of W/O microemulsions, which apparently do not relate to rhodium extraction. There is a similar correspondence between the observed maximum rate of rhodium permeation at 2.4 M total Cl^- (Figure 5.17) and the maximum rate of HCl extraction (refer to Figure 5.6).

The effects of strip solution acidity and salinity on the transport of rhodium are depicted in Figures 5.18 and 5.19. One can see that the rate of Rh permeation decreases linearly, though at a moderate degree with both strip acidity and salinity. This might be interpreted in terms of the possible effect [HCl] and [NaCl] have on the activity of acid ($\mathbf{a}_{HCl} = \mathbf{a}_{H^+}\ \mathbf{a}_{Cl^-}$) (refer to section 5.2.3), which, in turn, effects the rate of acid permeation and, eventually, the dependent rate of Rh extraction.

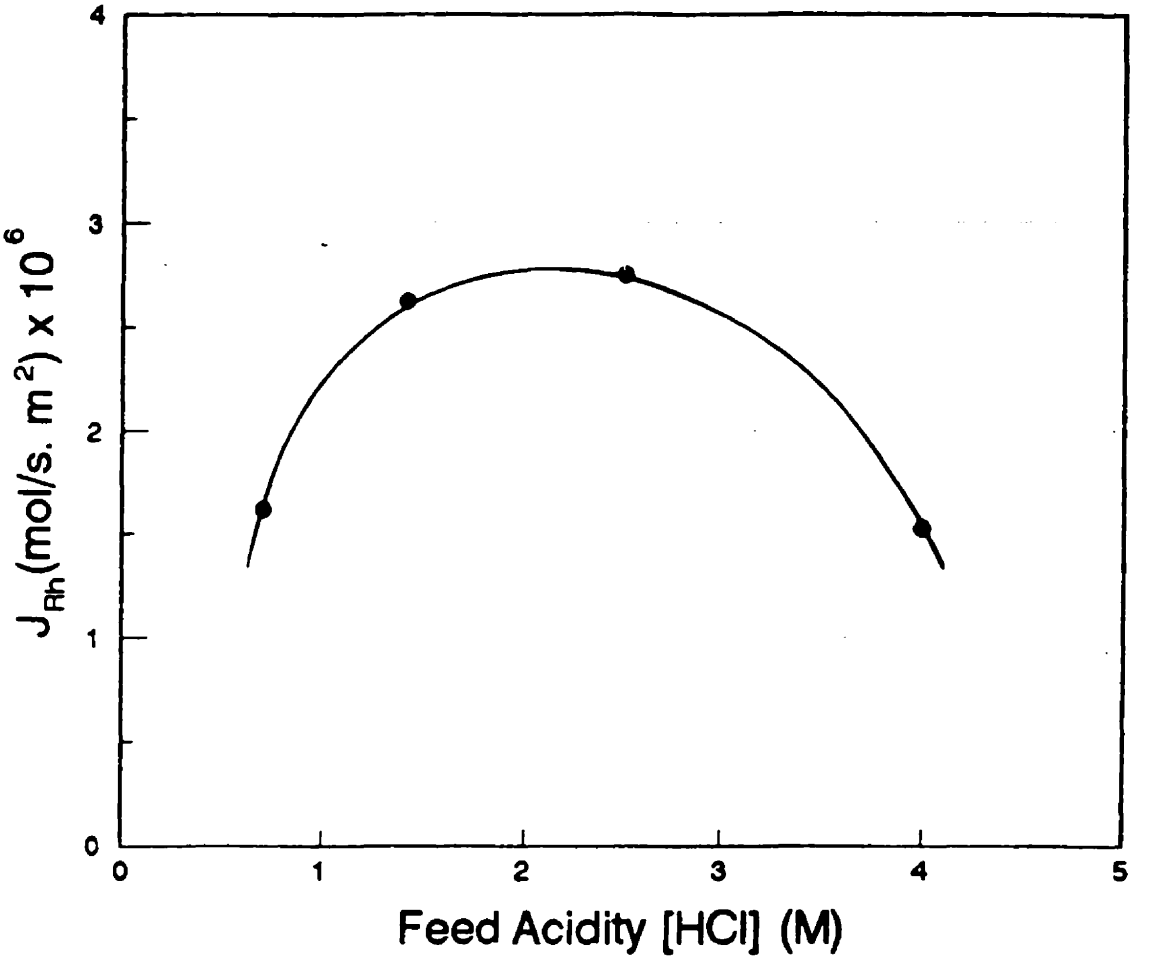

Figure 5.16: Effect of Feed Acidity on Rate of Rh Permeation (Support: 0.45 μm Gore-Tex; LM: 25 v/o Kelex 100, 25 v/o tridecanol, 50 v/o kerosene; Feed: 200 mL different [HCl], 400 ppm Rh, 2-week aged; Strip: 20 mL 0.1 M HCl)

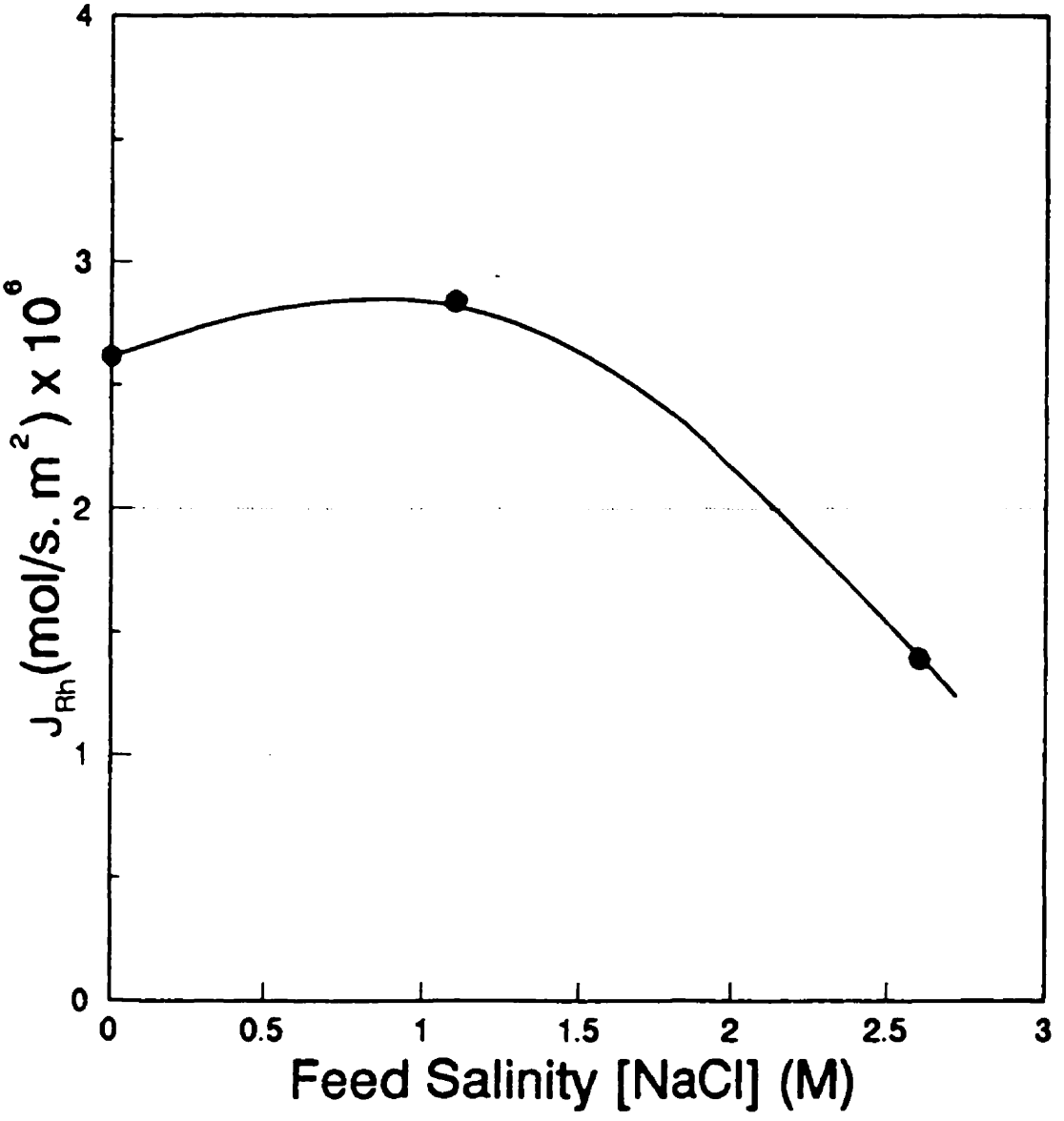

Figure 5.17: Effect of Feed Salinity on Rate of Rh Permeation

(Support: 0.45 μm Gore-Tex; LM: 25 v/o Kelex 100, 25 v/o tridecanol, 50 v/o kerosene; Feed: 200 mL 1.4 M HCl, 400 ppm Rh, 2-week aged, different [NaCl]; Strip: 20 mL 0.1 M HCl)

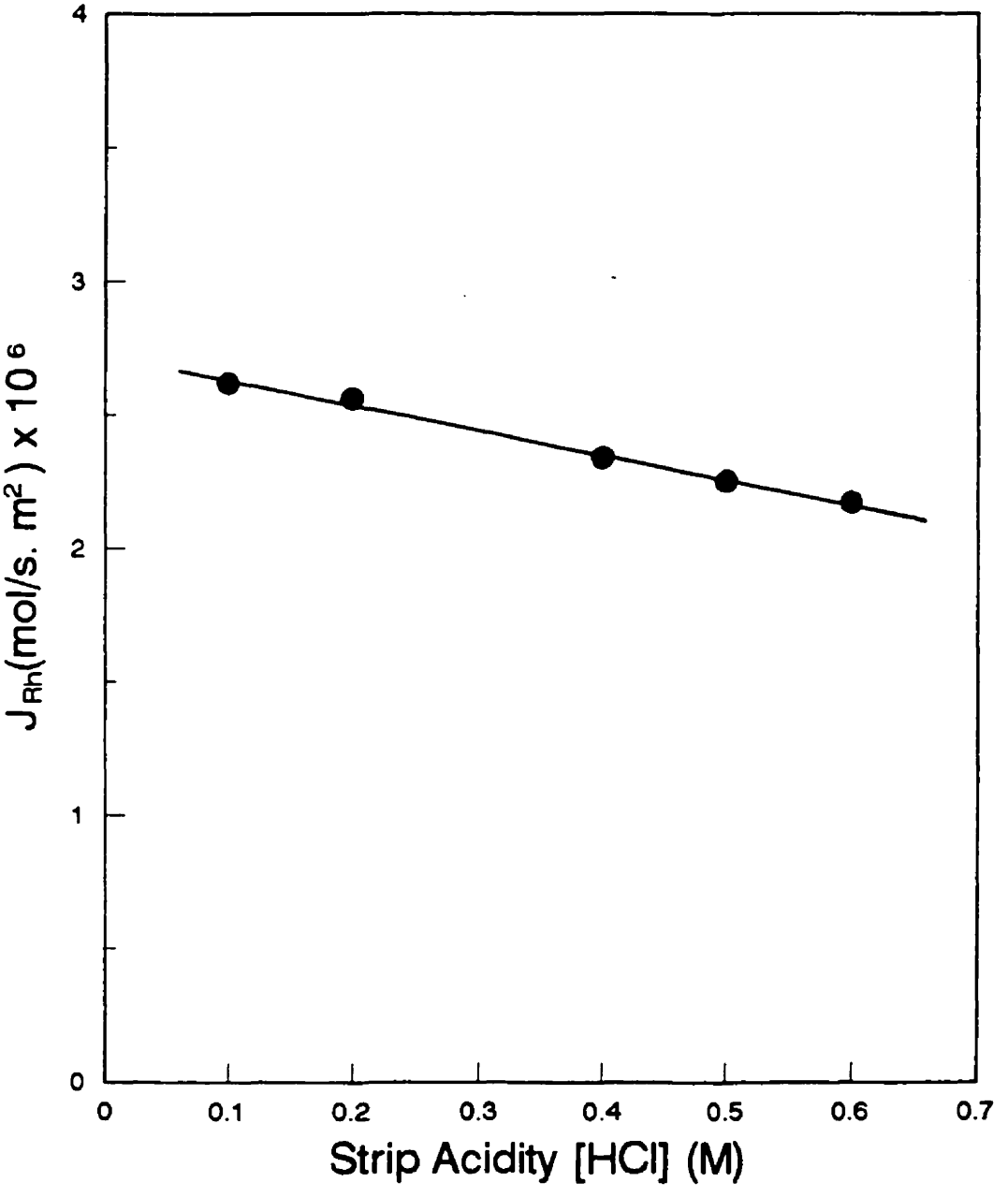

Figure 5.18: Effect of Strip Acidity on Rate of Rh Permeation (Support: 0.45 µm Gore-Tex; LM: 25 v/o Kelex 100, 25 v/o tridecanol, 50 v/o kerosene; Feed: 200 mL 2.5 M HCl, 400 ppm Rh, 2-week aged; Strip: 20 mL different [HCl])

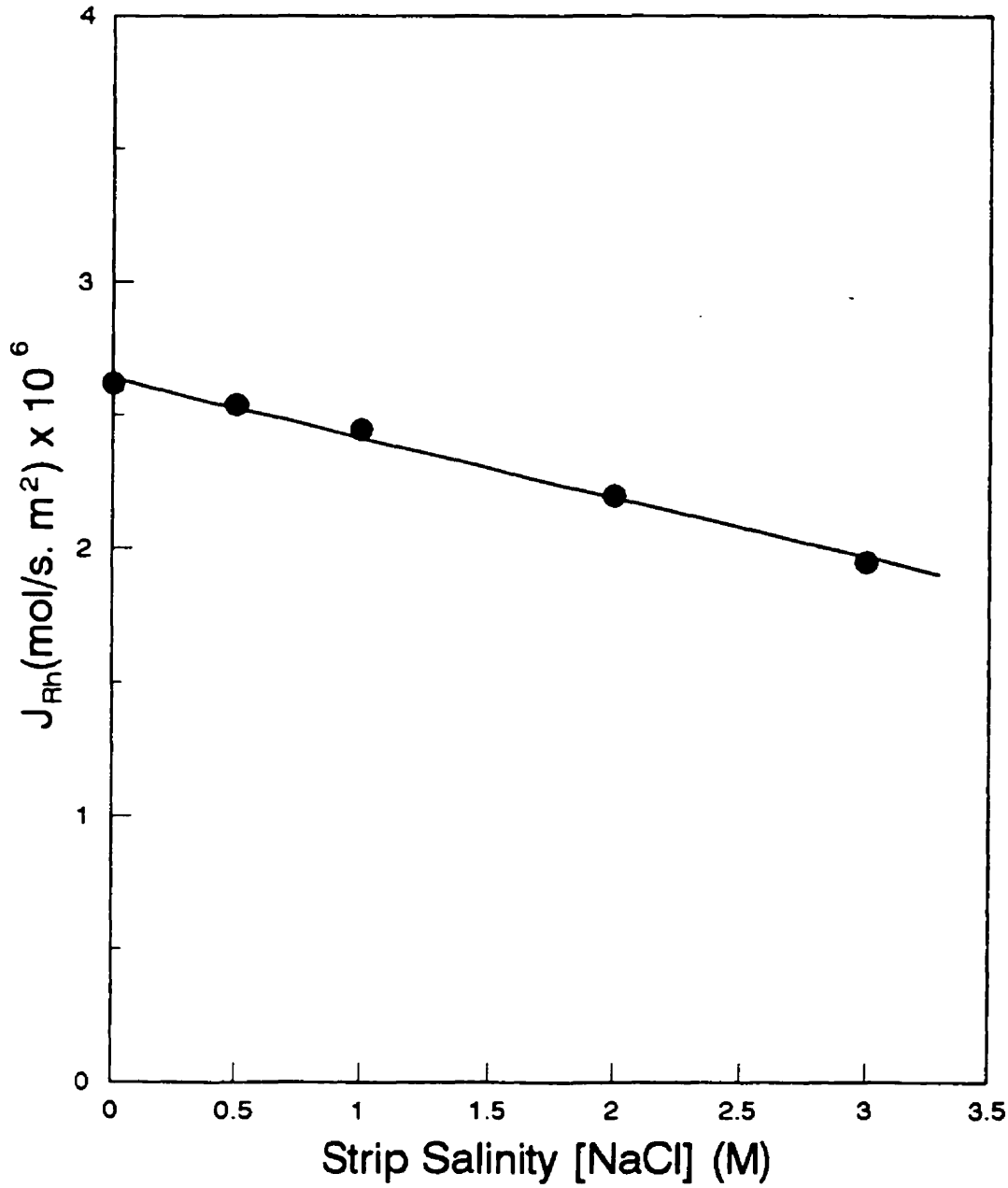

Figure 5.19: Effect of Strip Salinity on Rate of Rh Permeation (Support: 0.45 μm Gore-Tex; LM: 25 v/o Kelex 100, 25 v/o tridecanol, 50 v/o kerosene; Feed: 200 mL 1.4 M HCl, 400 ppm Rh, 2-week aged; Strip: 20 mL different [NaCl] at pH=1)

Comparison of the relative magnitude of the rates of acid (and water) extraction with the rate of rhodium permeation shows the former to be 100 times higher than the latter. The rates of Rh extraction (in the order of 10^{-6} $mol.s^{-1}.m^{-2}$) compare very well with other reported rates of similar SLM systems. The rates of metal transport ($mol.s^{-1}.m^{-2}$) for some of these systems, which operate with the same ion-pair mechanism, at almost comparable metal feed concentrations are reported here for comparison – i.e., 1.50×10^{-8} for Pu(IV) (Shukla et al., 1992), 1.75×10^{-6} for Cd(II) (Saito, 1991), 4.90×10^{-11} for Zn(II) (Saito, 1992), 9×10^{-6} for Pt(IV) (Fu et al., 1995a). The latter SLM systems are all HCl based except that for Pu(IV) which is HNO_3 based.

Nevertheless, the extraction of acid is of concern, due to the dilution brought to the strip phase, on the one hand and the reduction it brings to the rate of Rh extraction as a result of Cl^- build-up in the strip phase, on the other. For example, after operating the SLM system for 70 hours with an initial 10/1 aqueous feed to strip solution volumetric ratio (feed: 400 ppm Rh/2.5 M HCl; strip: 0.1 M HCl), a strip solution containing 2100 ppm Rh was produced while the raffinate concentration of Rh was 40 ppm. This gives a concentration ratio of about 5 as supposed to the expected one of 10, if no acid and water co-extraction had taken place. Interfacing the SLM system with an acid extraction process is investigated in Chapter 6 as a means of overcoming this negative effect.

5.2.6 Mechanism of Rh(III) Transport

The mechanism of Rh permeation through the SLM is very similar to that of chloride ions (i.e., ion-pair formation between protonated Kelex 100 and Rh species). In fact, the carrier for both species is the protonated extractant; and, therefore, the chloride ions and anionic $RhCl_6^{3-}$ species compete with each other to take this shuttle and become permeated. Therefore, the proton activity gradient, or acid activity gradient, remains to serve as the main driving force for the transport of Rh species. The difference in the permeation rate of

chloride ions and that of Rh species can be attributed to several factors. First, there is a huge difference in the concentration of the latter species in the feed solution (HCl concentration is in the vicinity of 2.5 M, while the concentration of Rh is somewhere in the range of 4×10^{-3} M). Second, the diffusivity of ion-pairs in the LM solution might be significantly different. This is attributed to the size and geometry of the ion-pairs and the fact that each Rh complex forms the ion-pair with three protonated Kelex 100 molecules as opposed to that of chloride ions, which form a smaller ion-pair with only one protonated Kelex 100 molecule. This analysis seems to explain the observed difference in the rates of Rh transport relative to the rates of acid (or equivalently Cl^-) permeation (about 100 times difference).

The analysis of the rhodium permeation kinetics is made on grounds similar to those of Zha et al. (1994) for the analogous SLM system of gallium transport through a SLM of Kelex 100. The analysis is based on the resistance-in-series kinetic model (Danesi et al., 1981) schematically presented in Figure 2.10, and re-drawn in Figure 5.20.

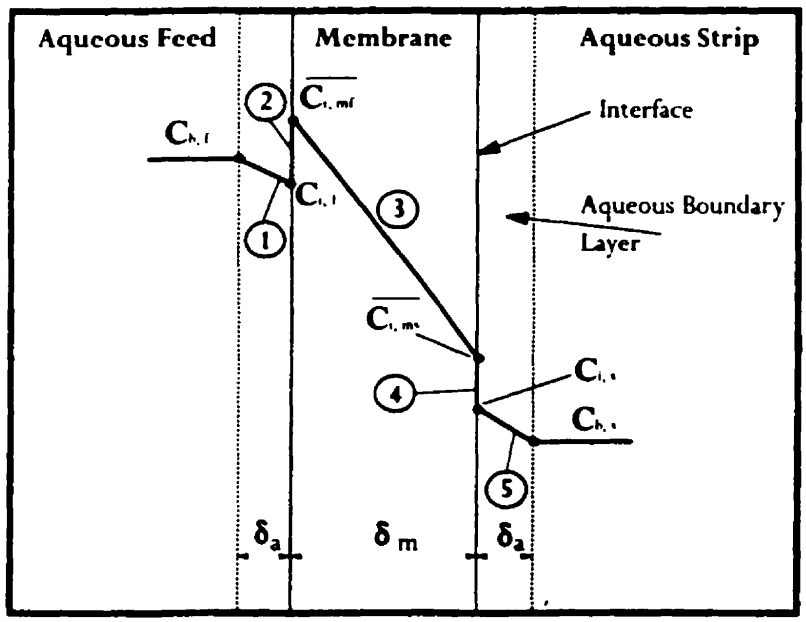

Figure 5.20:Schematic Representation of the Membrane Permeation (Re-Drawn of Figure 2.10; Adapted from Danesi et al., 1981)

By neglecting the reaction resistances at both interfaces, i.e., assuming very fast chemical reactions[3], and by assuming that the diffusion of the free extractant molecules (in the reverse direction of metal transport) is much faster than the metal complex in the membrane phase, the resistance-in-series model gives the following expression for the mass transport rate of metal:

$$J = k_O(C_f - \frac{\mathbf{D}_s}{\mathbf{D}_f} C_s) \tag{5.4}$$

where k_O is the global mass transfer coefficient and incorporates a summation of three contributions:

$$\frac{1}{k_O} = \frac{1}{k_f} + \frac{1}{\mathbf{D}_f k_m} + \frac{\mathbf{D}_s}{\mathbf{D}_f k_s} \tag{5.5}$$

where k_f, k_m, and k_s are local mass transfer coefficients in the feed, membrane, and strip solutions, respectively. $\mathbf{D}_f$ and $\mathbf{D}_s$ are also defined as distribution coefficients of metal species at feed and strip interfaces, respectively:

$$\mathbf{D}_f = \overline{C_{f,i}} \Big/ C_{f,i} \tag{5.6}$$

$$\mathbf{D}_s = \overline{C_{s,i}} \Big/ C_{s,i} \tag{5.7}$$

In the present system, the second term in Equation 5.4 (i.e., $\frac{\mathbf{D}_s}{\mathbf{D}_f} C_s$) can be considered negligible for two reasons. First, the distribution coefficient at the strip interface ($\mathbf{D}_s$) is almost zero (the loaded Kelex 100 organic upon contact with 0.1 M HCl strip solution is completely stripped). Second, as mentioned earlier, the concentration of Rh in the strip phase (C_s) was found not to affect the rate of permeation (see Figure 5.15). This is apparently due to the fact that the true driving force for Rh permeation is the proton activity gradient and not the metal concentration gradient. As a result of these considerations, Equation 5.4 may be simplified to:

[3]This is a valid assumption, since no inner-sphere complex is involved but ion-pair formation.

$$J = k_O C_f \tag{5.8}$$

where

$$\frac{1}{k_O} = \frac{1}{k_f} + \frac{1}{\mathbf{D}_f k_m} \tag{5.9}$$

$1/k_f$ is also negligible since it was shown that the increase in agitation speed did not increase the rate of permeation. Considering at the same time that $\mathbf{D}_f$ is almost constant (for constant $[Cl^-]_f$ and $[R\text{-}H_2Q^+Cl^-]_{org}$ – which is the case here), one may infer that the total mass transfer resistance ($1/k_O$) is directly dependent only on the resistance in the membrane ($1/k_m$). The linear dependency of the rate on Rh feed concentration, predicted by Eq. 5.8, is confirmed by the data of Figs. 5.12 and 5.13. Meanwhile, through the slope of "J vs. C_f" curve, the mass transfer coefficient (k_O) is found to be 0.909×10^{-3} m/s.

5.3 SUMMARY

A supported liquid membrane technique utilizing Kelex 100 as the carrier has been successfully applied to the separation of Rh from a hydrochloric acid solution. The non-aquated chlorocomplexes of Rh(III) are transported through the membrane via the formation of ion-pairs with protonated extractant molecules. The main driving force for this extraction process is the acid activity gradient across the membrane. Acid and water are co-transported along with the Rh species via protonation of the extractant and the possible formation of W/O microemulsions. The rate of acid and water extraction is about 100 times that for Rh when the concentration of Rh is about 400 ppm. The main resistance in the transport of Rh is postulated to be the diffusion step inside the liquid membrane. The rate of acid extraction can be substantially reduced by using a strip solution containing a high salt (NaCl) concentration. However, this may slow down the Rh extraction rate. At optimum conditions – i.e., a feed solution of 2.5 M HCl and a strip solution of essentially zero salt concentration and pH=1 – the rate of Rh extraction is in the order of 10^{-6} $mol.s^{-1}.m^{-2}$, which compares very well with other analogous systems described in the literature.

CHAPTER 6

Extraction and Separation of HCl and Rh(III) from the SLM Strip Solution with Trioctylamine[1]

6.1 INTRODUCTION

The significant co-extraction of acid and water along with the chlorocomplexes of Rh through the SLM of Kelex 100 (Figure 6.1), described in the last chapter, constitute a drawback for the operation of the SLM system. The permeated water, has as a result, to dilute the SLM receiving (strip) phase, while the permeated acid aggravates the problem further, since upon its neutralization with a strong base it produces water as well as a salt build-up in that phase. Even if the dilution of the SLM product solution by the co-extracted water is neglected, the accumulation of Cl^- ions into that phase suppresses the permeation of the Rh species (Figure 5.18) and tends to slow down and reverse the extraction process. After evaluating a number of possible approaches to the solution of this problem, it was decided to evaluate the potential of using tri-n-octylamine (TOA) solvent extraction in order to remove the co-transported HCl from the rhodium-bearing solutions generated by the SLM process (Figure 6.1).

The extraction of inorganic acids by various amines has been described in the literature in several instances (Teramoto et al., 1981; Cox and Flett, 1983; Baird et al., 1987; Eyal et al., 1993;). Trioctylamine (TOA), a well known amine with the molecular formula of

[1]The material presented in this chapter constitutes the subject-matter of the following publication: S.N., Ashrafizadeh, and G.P., Demopoulos, Extraction and Separation of HCl and Rh(III) with Trioctylamine, *J. Chem. Tech. Biotechnol.*, 1996 (in press).

$(CH_3\text{-}(CH_2)_7)_3N$, MW = 353.68, was chosen as the preferred amine in this work since it offers a number of advantages such as negligible solubility in the aqueous phase, high boiling point, low density (0.809) (Lide, 1993), and low cost and wide availability. The present work differs from previous studies involving the extraction of acids with amines, since it describes the removal of HCl in the presence of Rh(III). In particular, the role of salt (Cl^-) concentration and age of solution in suppressing the co-extraction of Rh(III) has been investigated in the present work and the main features of a novel selective acid removal process scheme described.

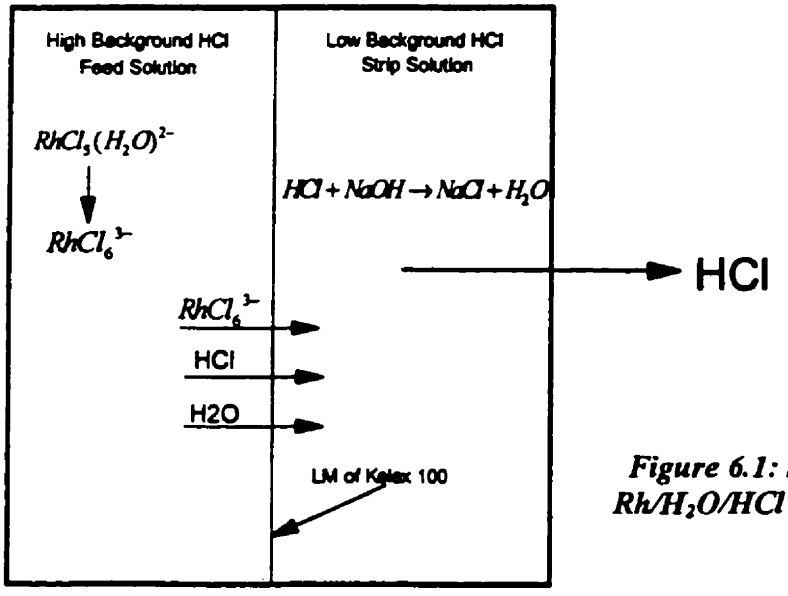

Figure 6.1: Schematic Presentation of $Rh/H_2O/HCl$ Permeation through SLM

6.2 ACID EXTRACTION WITH TOA

First the extraction of HCl from Rh-free solutions was investigated. Aqueous solutions of varying HCl concentrations were contacted with 5 v/o (0.115 M) trioctylamine organic solutions in the absence and presence of salt (Cl^-). The results of these acid extraction experiments are tabulated in Table 6.1. The same results are presented in the form of acid extracted per mole of TOA also in Figure 6.2. Quantitative extraction of HCl at a molar ratio $[HCl]_o/[TOA]$ of approximately one was obtained even at raffinate acidities as low as 0.1 M. This occurred even in the presence of a high background salt concentration (3 M Cl^-).

Table 6.1: Acid Extraction by TOA as a Function of Aqueous Feed Acidity

$[Salt]_{Feed}$ = 0 M			$[Salt]_{Feed}$ = 3 M		
Feed Acidity (M)	Raffinate Acidity (M)	Extracted Acid (M)	Feed Acidity (M)	Raffinate Acidity (M)	Extracted Acid (M)
0.1	0.010	**0.090**	0.098	6.5×10^{-3}	**0.097**
0.2	0.085	**0.115**	0.190	7.33×10^{-2}	**0.117**
0.3	0.182	**0.118**	0.283	0.167	**0.116**
0.4	0.285	**0.115**	0.370	0.255	**0.115**
0.5	0.380	**0.120**	0.472	0.355	**0.117**
1.0	0.883	**0.117**	0.930	0.815	**0.115**
2.0	1.870	**0.130**	1.870	1.750	**0.120**

A: H_2O/HCl ; H_2O/HCl/3 M NaCl or NH_4Cl.
O : 5 v/o Trioctylamine (**0.115 M**); 5 v/o Tridecanol (0.21 M); 90 v/o Kerosene.
A/O = 1; CT = 3 min.

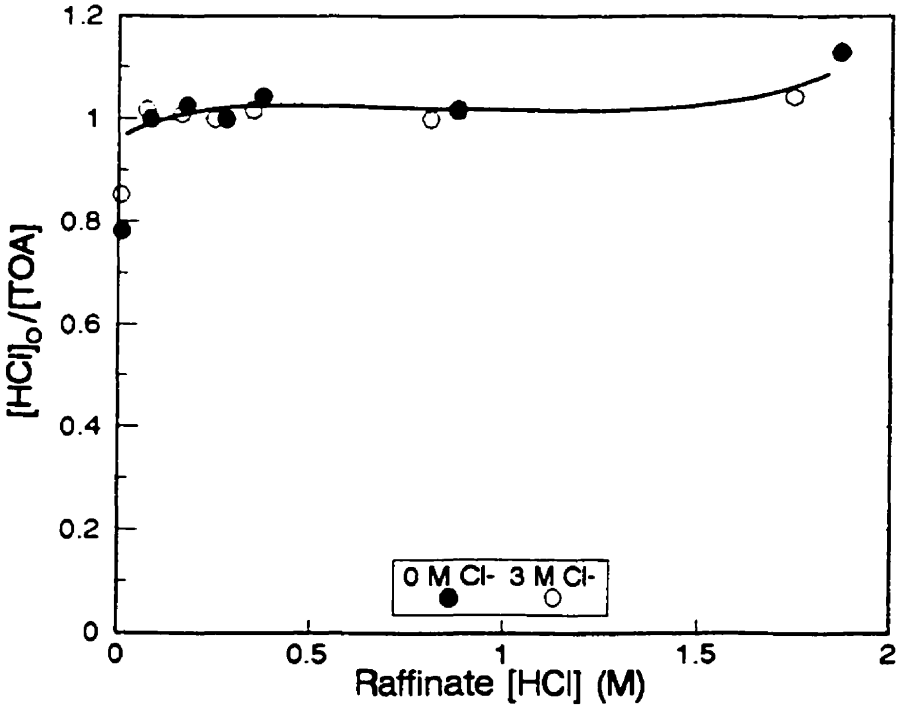

Figure 6.2: [HCl]$_o$/[TOA] versus Aqueous Phase Acidity
(A: H_2O/HCl, H_2O/HCl/3 M NaCl or NH_4Cl; O: 5 v/o TOA, 5 v/o tridecanol, kerosene; A/O: 1; CT: 3 min)

The acid extraction performance of the amine, upon repeated recycling, was subsequently evaluated. The acid-loaded organic was first stripped in one contact with 1 M NaOH, and then washed twice with distilled water, before it was used again for acid extraction. As one can see from the results of Table 6.2, the amine solvent showed no signs of loading-capacity loss or degradation after a series of five cycles. In addition, phase separation was fast and clean.

Table 6.2: Effect of Recycling on Acid Extraction by TOA

No. of Cycle	Extracted Acid (HCl) [M]	
	$[Salt]_{Feed}$ = 0 M $(pH)_{Feed}$ = 0.710	$[Salt]_{Feed}$ = 3 M $(pH)_{Feed}$ = 0.412
1	0.115	0.114
2	0.117	0.116
3	0.120	0.117
4	0.116	0.115
5	0.115	0.116
6	0.117	0.117

A: 0.3 M HCl ; 0.3 M HCl and 3 M NaCl or NH_4Cl.
O: 5 v/o Trioctylamine (**0.115 M**); 5 v/o Tridecanol (0.21 M); 90 v/o Kerosene.
A/O = 1; CT = 3 min.

6.3 WATER EXTRACTION WITH TOA

The organic solutions containing alcohols and/or basic extractants upon contact with acidic solutions usually extract substantial amounts of water. This matter was discussed in Chapter 4 and is well described in the literature (Osseo-Asare, 1991). In this regard, it was thought appropriate to examine the water uptake behavior of the TOA organic phase, as

well. A similar organic solution with that of the acid extraction experiments, 0.115 M (5 v/o) TOA, was contacted with aqueous solutions of different acidities, i.e., 0.1 to 2 M HCl. The water-uptake results tabulated in Table 6.3 show that the amount of extracted water is considerable and is approaching the concentration of TOA, i.e., 0.115 M. This result confirms the capability of the TOA organic phase to extract water along with the acid. An average molar ratio of water/acid ≅ 0.85 was determined, which in effect corresponds to a theoretical ratio of HCl:H_2O equal to one. The exact mechanism of water uptake was not investigated in the present work. One possibility is that water is extracted along protons (i.e., acid) in the form of the hydronium ion (H_3O^+). Alternatively, in extrapolation from the previous study involving Rh(III)-HCl-Kelex 100 (Chapter 4), it may be postulated that the mechanism of water extraction is via the formation of W/O microemulsions; although in the latter case the ratio of H_2O/HCl was expected to be higher than one.

Table 6.3: Water Uptake by TOA at Various Feed Acidities

Initial Feed Acidity HCl (M)	Water Uptake (mol H_2O/L organic)		
	$[Salt]_{Feed}$ 0.0 (M)	$[Salt]_{Feed}$ 1.5 (M)	$[Salt]_{Feed}$ 3.0 (M)
0.1	0.085	0.077	0.070
0.2	0.105	0.095	0.089
0.3	0.107	0.096	0.088
0.4	0.108	0.094	0.085
0.5	0.115	0.106	0.095
1.0	0.103	0.101	0.100
2.0	0.102	0.100	0.104

A: H_2O/HCl/NaCl or NH_4Cl at different acidities.
O: 5 v/o Trioctylamine (**0.115 M**); 5 v/o Tridecanol (0.21 M); 90 v/o Kerosene.
A/O = 1; CT = 3 min.

6.4 RHODIUM EXTRACTION WITH TOA

According to the above reported results, TOA has the ability to withdraw the extra acid and water accumulated in the SLM strip solution (see the last chapter). However, the latter solutions contain Rh complexes, and this necessitates investigating the extraction behavior of TOA against the Rh complexes. The latter was investigated and Rh(III) was found to be extracted at various degrees, depending on the age of the solution and the concentration of Cl^- ion (Table 6.4). In agreement with previously reported studies (Fedorenko and Ivanova, 1965; Khattak and Magee, 1969), Rh extraction was favored (up to 90% in a single contact) whenever freshly prepared Rh solutions were used. However, Rh extraction dropped drastically with Cl^- concentration and age of the solution. Since industrial Rh solutions are of significant age and concentrated with Cl^-, it can be understood why amines or other similar basic extractants have not proven suitable as extractants for Rh (Benguerel et al., 1996). In the case presented in this chapter, though, the objective is not rhodium extraction but the opposite, – selective extraction of HCl from the SLM product phase. To this end, two alternative approaches to effect selective HCl removal were investigated: (i) suppression of Rh co-extraction, and (ii) co-extraction of Rh(III) along with HCl, followed by selective stripping.

6.5 SUPPRESSION OF RHODIUM EXTRACTION

The results of Table 6.4 clearly demonstrate that extraction of Rh(III) by TOA is suppressed by either a high Cl^- concentration (3 M) or by extended aging of the Rh feed solution or a combination of both.

Table 6.4: Effect of [Cl^-] and "Age" on Rh(III) Extraction by TOA

0.3 M HCl + [Cl^-] (M)	%Rh Extracted by TOA from Rh solutions of variable age				
	5 min	12 hr	24 hr	48 hr	60 hr
0.0	88.20	21.00	20.10	18.97	18.00
0.5	55.00	18.26	14.46	12.11	10.65
1.0	19.83	7.80	6.75	5.37	4.86
1.5	8.26	3.22	2.94	2.52	2.23
2.0	3.64	1.93	1.50	1.27	1.15
3.0	~ 0.00	~ 0.00	~ 0.00	~ 0.00	~ 0.00

A: 0.3 M HCl & different [NH_4Cl]; 500 ppm Rh added to solution as Na_3RhCl_6.
O: 5 v/o Trioctylamine (0.115 M); 5 v/o Tridecanol (0.21 M); 90 v/o Kerosene.
A/O = 1; CT = 3 min.

6.5.1 The Effect of Cl^- Concentration

The negative effect of high chloride concentration on Rh(III) extraction can be interpreted on the basis of Le Chatelier's principle. Rh(III) extraction can be represented, in analogy with the previously well-studied Rh(III)-HCl-Kelex 100 extraction system (Chapter 4; Benguerel et al., 1994), with the following ion-pair mechanism:

$$\overline{R_3N} + HCl \leftrightarrow \overline{R_3NH^+Cl^-} \qquad (6.1)$$

$$3(\overline{R_3NH^+Cl^-}) + RhCl_6^{3-} \leftrightarrow \overline{(R_3NH^+)_3RhCl_6^{3-}} + 3Cl^- \qquad (6.2)$$

To verify further whether the suppression of Rh(III) is solely the result of the high concentration of chloride ions, and not the result of any interaction between the Rh complexes ($RhCl_6^{3-}$) and the cations of the added chloride salt, the extraction behavior of

TOA against a number of chloride salts was examined. The salts tested were: KCl, NaCl, NH_4Cl, and $MgCl_2$. Invariably, all salts resulted in the same result, i.e., zero extraction at 3 M Cl^-; in other words, it was confirmed that the Cl^- concentration, and not the type of cation, is responsible for the suppression of Rh(III) extraction.

6.5.2 The Effect of Solution Age

It has been previously postulated (Chapter 4; Benguerel et al., 1994 and 1996) that aging relates to the conversion of the non-aquated hexachloro rhodium(III) complexes into the mixed aquo-chloro complexes:

$$RhCl_6^{3-} + H_2O \leftrightarrow RhCl_5(H_2O)^{2-} + Cl^- \qquad (6.3)$$

It is, indeed, this phenomenon of aquation that has been held responsible for the failure of Kelex 100 to extract Rh(III) quantitatively (Chapter 4). The results of Table 6.4 seem to suggest this to be the case as well with trioctylamine. The aquation of Rh(III) as a function of age and temperature was studied independently in order to provide experimental proof for the postulated suppression of Rh(III) extraction. The monitoring of the aquation process (reaction (6.3)) as a function of time, $[Cl^-]$, and temperature was done with the aid of UV-Visible spectroscopy. The results of this parallel study are summarized in Appendix C.

Based on the data of Table 6.4 and the discussion provided above and in Appendix C, it may be concluded that it is possible to effect selective extraction of HCl with TOA as long as a high Cl^- concentration is maintained in the feed solution. The required Cl^- concentration level can be lowered from 3 M down to 2 M or so if the solution is previously subjected to aging. The latter can be accelerated by heating (a few hours at 70 °C as opposed to a few days at ambient temperature). From the standpoint of the optimum operation of the SLM process (see Chapter 5) neither option is attractive, since on the one hand high Cl^- concentration retards significantly the permeation rate of rhodium (see Chapter 5), while on the other prolonged aging especially by heating is impractical.

6.6 CO-EXTRACTION OF HCL AND RHODIUM

The alternative approach investigated was co-extraction of Rh(III) along HCl followed by differential stripping. As the results of Table 6.4 show, the extraction of Rh(III) is high (90% in a single contact) when the solution produced by the SLM process is still fresh. Examination by UV-Visible spectroscopy of a Rh(III) SLM strip solution (0.1 M HCl) produced after 2-hours' operation of the SLM apparatus showed indeed that its characteristic absorption bands (Figure 3.3) at the same position as freshly prepared solutions (i.e., 509 and 404 nm, respectively), which are indicative of the presence of the non-aquated $RhCl_6^{3-}$ complexes. (For more details on the UV-Visible study of the aquation process refer to Appendix C.) Contact of the fresh SLM strip solution with TOA further confirmed the ability of the latter to co-extract Rh(III) and HCl.

The loaded organic with HCl and $RhCl_6^{3-}$ has been successfully subjected to differential stripping as follows: Rhodium was stripped first through one 3-min contact with an aqueous solution of 0.5 M HCl/3 M NaCl (reaction (6.4)), and the remaining acid-loaded organic was stripped through another 3-min contact with a dilute solution of 0.5 M NaOH (reaction (6.5)). Phase separation occurred without problems for both stripping media.

$$\overline{(R_3NH^+)_3RhCl_6^{3-}} + 3Cl^- \leftrightarrow 3(\overline{R_3NH^+Cl^-}) + RhCl_6^{3-} \qquad (6.4)$$

$$\overline{R_3NH^+Cl^-} + NaOH \leftrightarrow \overline{R_3N} + NaCl + H_2O \qquad (6.5)$$

The effectiveness of the 0.5 M HCl/3 M NaCl medium in stripping completely Rh(III) from the loaded TOA is illustrated by the results of Figure 6.3. According to these data, 100% stripping is possible in a single contact of 3-min, independently of the Rh concentration in the strip solution. At least a concentration ratio of 10 (5000 ppm of Rh in the strip solution vs. 450 ppm Rh in the loaded organic) is achievable without difficulty. On the other hand, tridecanol was found to have a modest effect on stripping performance (Figure 6.4). Nevertheless a minimum amount of tridecanol is needed (at least 1/1 ratio), otherwise phase separation is poor. A 2/1 (volume ratio) tridecanol/TOA ratio was determined as offering the best performance.

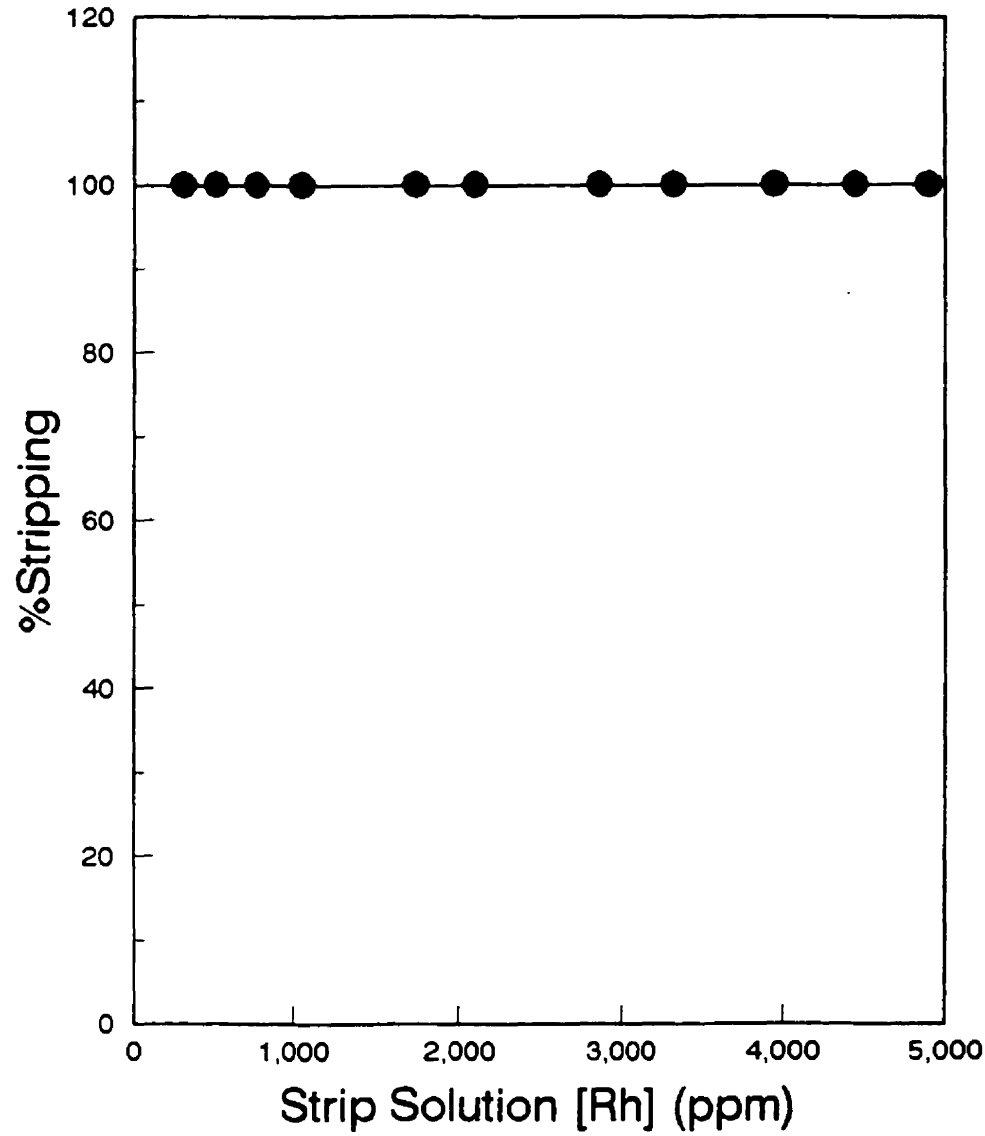

Figure 6.3: Stripping of Rh from TOA Organic vs Rh Concentration in the Strippant
(O: 5 v/o TOA, 10 v/o tridecanol, kerosene, 450 ppm Rh, 15-min aged;
A: 0.5 M HCl and 3 M NaCl, different [Rh]; CT: 3 min)

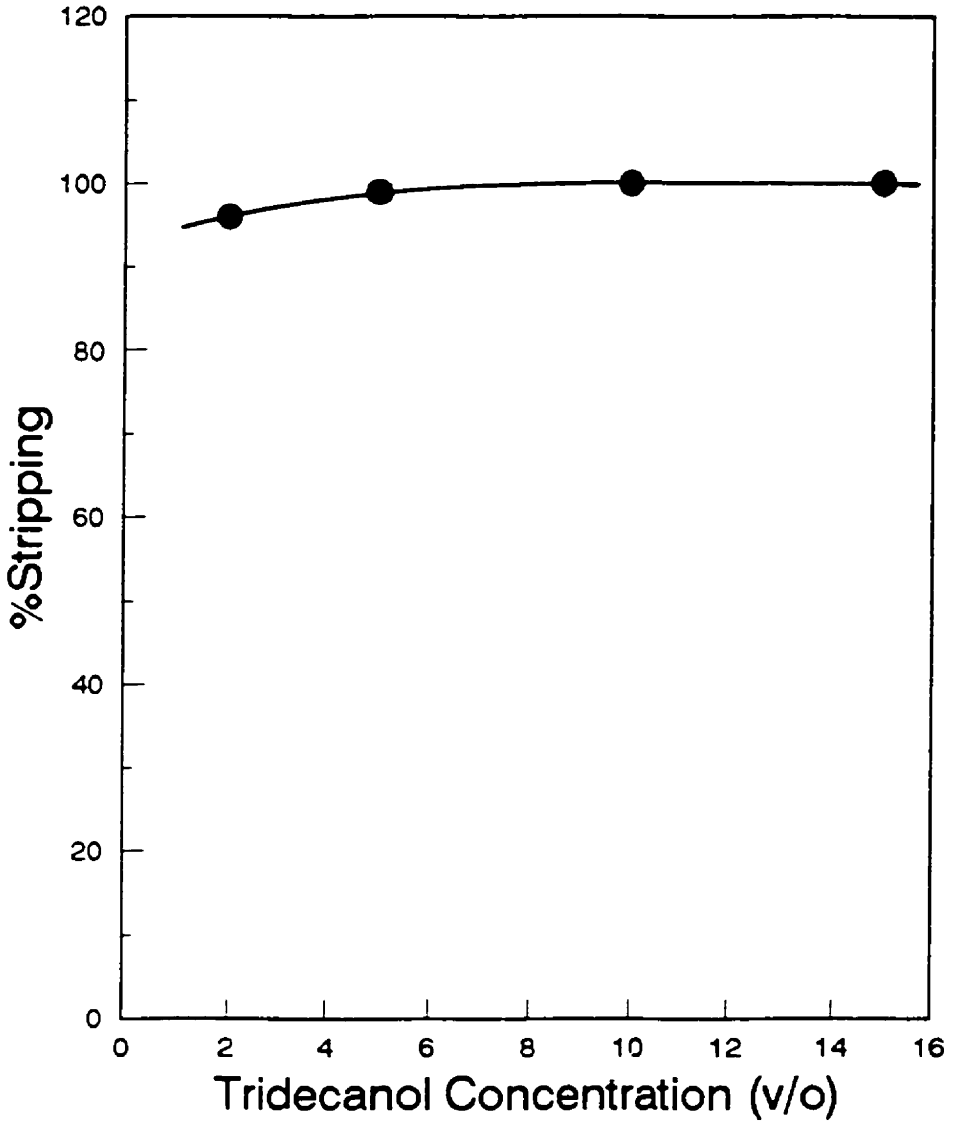

Figure 6.4: Effect of Tridecanol Concentration on Stripping of Rh
(O: 5 v/o TOA, x v/o tridecanol, kerosene, 450 ppm Rh, 15-min aged;
A: 0.5 M HCl and 3 M NaCl; CT: 3 min)

6.7 AN INTEGRATED CONCEPTUAL SLM FLOWSHEET

The flowsheet of Figure 6.5 is proposed on the basis of the findings of the present work. According to this flowsheet, the SLM system of Rh (Chapter 5) is interfaced with a TOA SX system through which the HCl co-transported with Rh through the supported liquid membrane is removed from the receiving SLM phase. In this way, the SLM operates at its maximum transfer rate of Rh without the need to neutralize the receiving phase. As explained earlier, along with HCl, $RhCl_6^{3-}$ is co-extracted with TOA, and this is preferentially stripped with a 0.5 M HCl/3 M NaCl medium followed by HCl stripping /neutralization with NaOH. By interfacing the SLM system with a downstream SX system, as described in Figure 6.5, the potential for achieving a higher concentration of Rh and better control of impurity carry-over exists. The SLM systems are known to suffer from their inability to accommodate scrubbing of impurities, a common practice in conventional SX circuits. In the combined SLM/SX circuit of Figure 6.5, scrubbing may be incorporated prior to and/or after stripping of rhodium from the loaded TOA organic phase with 0.5 M HCl/3 M NaCl. Such a scrubbing step can efficiently separate the other precious metals, as the latter require different strip solutions to be stripped (Fu et al., 1994; 1995a, b, and c).

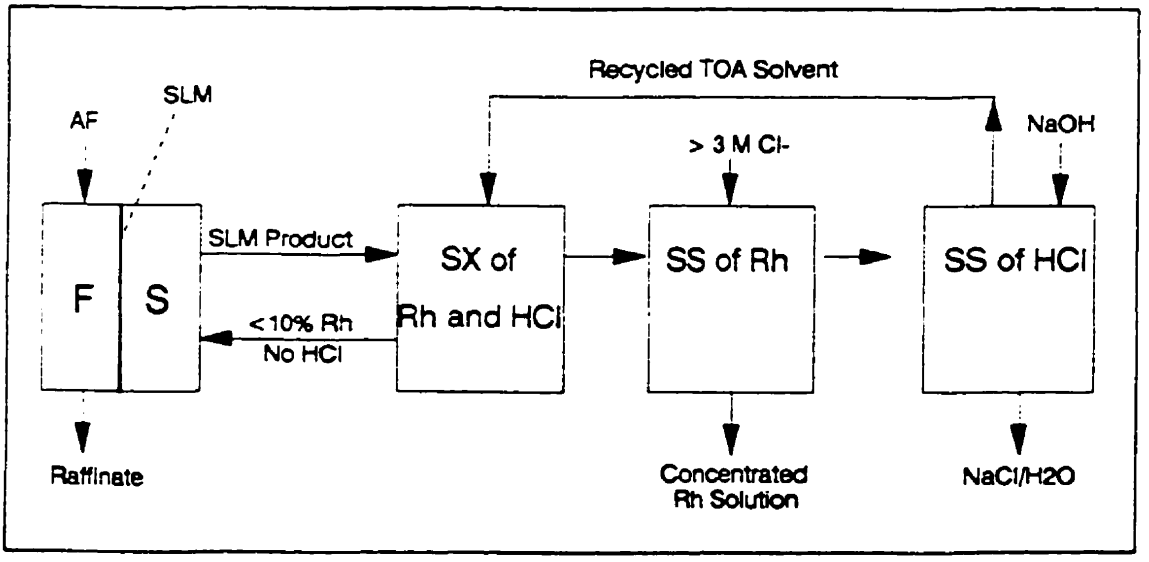

Figure 6.5: Combined SLM/SX Conceptual Rh Separation Flowsheet

The flowsheet of Figure 6.5 is redrawn in Figure 6.6 in order to show the incorporation of Hollow Fiber SLM (HFSLM) modules to effect the transfer of rhodium from a strong acidic Rh feed to an slightly acidic (0.1 M HCl) strip solution. The latter solution is periodically contacted with an amine (TOA) extraction system to remove the excess acid co-transported with rhodium. The TOA solvent extraction is followed by selective stripping of Rh and acid. A further improvement to the proposed flowsheet might be the use of liquid film pertraction (LFP) contactors (see Figure 2.8) instead of hollow fiber modules. Liquid Film Pertraction (LFP) (Boyadzhiev, 1990) involves the continuous counter-current flow of all three streams (i.e., feed, strip, and organic); thus offering a more elegant solution to the potential problem of impurity co-extraction and membrane blockage by fine particles or precipitates.

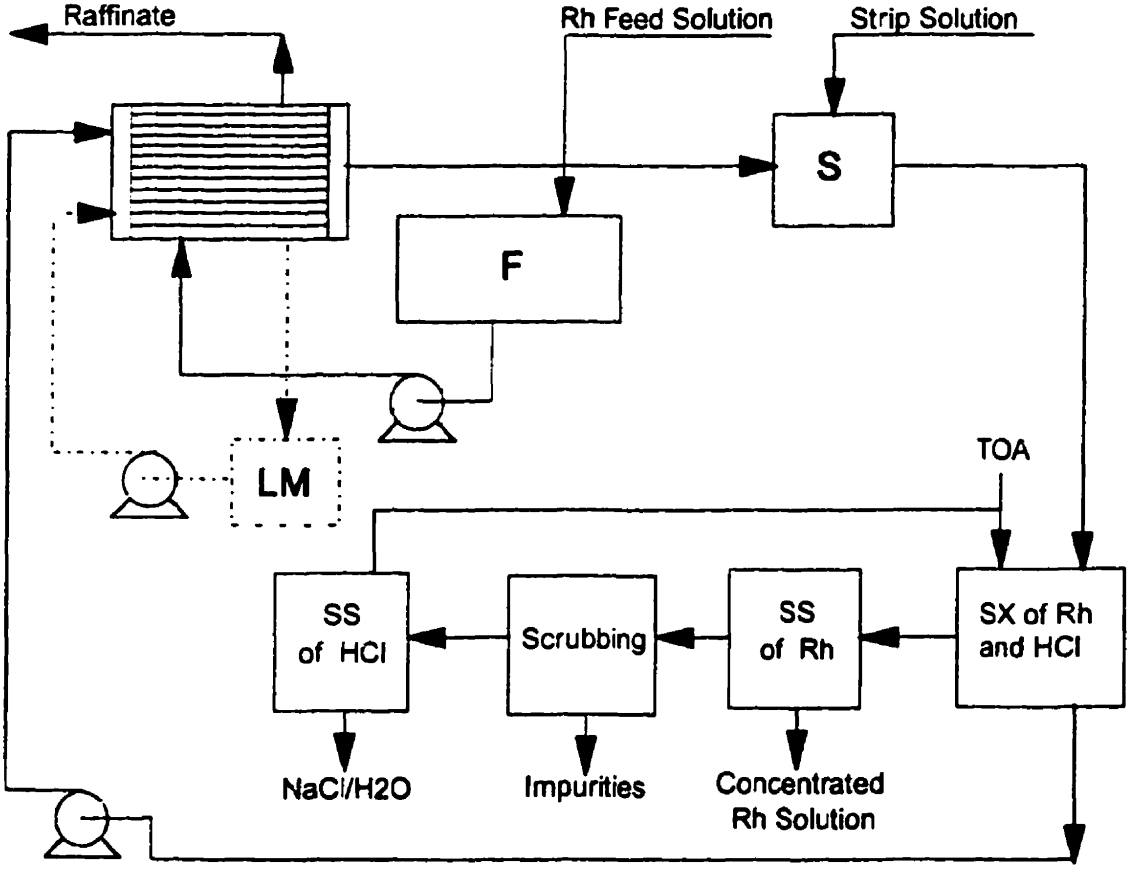

Figure 6.6: Conceptual Integrated Process Flowsheet for Rh

6.8 SUMMARY

It has been demonstrated that TOA is capable of readily and quantitatively extracting HCl from Rh(III)-containing chloride solutions at a molar ratio $[HCl]_o/[TOA]$ equal to one. Along HCl, H_2O was found to be co-extracted at a ratio of one – i.e., either in the form of H_3O^+ or in the form of a W/O microemulsion.

Rh(III) was found to be extracted significantly only if the solution was fresh (≤ 2-3 hours of age) and the Cl^- concentration low (0.2-0.3 M). Chloride ion concentration near 3 M or higher was found to suppress completely Rh(III) extraction. Similarly, prolonged aging suppressed Rh(III) extraction. The "aging" phenomenon was studied with UV-Visible spectroscopy and was attributed to the aquation of the $RhCl_6^{3-}$ complexes. From the standpoint of the optimum operation of the Rh SLM process developed and described in Chapter 5, it was concluded that co-extraction of Rh(III) and HCl from the SLM receiving phase with TOA offered the best overall performance (i.e., fast transfer rate for Rh(III) across the SLM, concentration of Rh(III)). Rh(III) was found to be selectively stripped with a solution of 0.5 M HCl/3 M Cl^- salt followed by stripping/neutralization of HCl with a mild NaOH solution.

By combining SLM with SX it has been shown that it is possible to overcome the drawbacks intrinsic to each of the two separation processes and to design integrated separation circuits for metals like Rh(III), which are difficult otherwise to extract (Benguerel et al., 1996). Thus in the proposed combined SLM/SX circuit, Rh(III) is extracted thanks to the powerful driving force of SLM, which overcomes the low distribution coefficient of Rh (<0.5), while SX makes possible the operation of the SLM at its highest transfer (production) rate due to the continuous removal of HCl (and Rh(III)) from the receiving phase. In addition, the interfacing of the TOA solvent extraction process with the SLM system renders possible, in principle, the control of impurity carry-over through the incorporation of scrubbing procedures.

CHAPTER 7

Formation of Rhodium Bromocomplexes and Their Extraction with Kelex 100

7.1 INTRODUCTION

As discussed in Chapter 4, due to its substantial aquation (aging) in typical chloride solutions, Rh(III) extraction by conventional SX contacting is very limited (**D** < 0.5). This problem was overcome when SLM contacting was employed instead (see Chapter 5). This was made possible due to the combined action of extraction and stripping. Thus, upon extraction-stripping of the extractable $RhCl_6^{3-}$ species, the non-extractable $RhCl_5(H_2O)^{2-}$ is converted to $RhCl_6^{3-}$ and extraction continues to completion. In addition to developing the SLM system described in Chapter 5, a parallel study was undertaken during the course of this work to see if aquation could be reversed or prevented by changing the chemistry of the Rh(III) chloride complexes. This study revealed that the aquation of Rh(III) in bromide solutions is substantially less, and this led to the elaboration of an alternative separation scheme for Rh(III). This scheme involves (i) precipitation of the double nitrite salt of Rh(III) from the original chloride solution (the same way this is done in the traditional refining process of rhodium; see Chapter 2), (ii) re-dissolution in an HBr medium, i.e., conversion of the Rh chlorocomplexes to bromide complexes, (iii) conventional SX of the $RhBr_6^{3-}$ species with Kelex 100.

In this chapter, first the bromide chemistry of Rh(III) is reviewed and the exchange of bromide with chloride ligands in the coordination sphere of Rh(III) investigated. The extent to which the bromocomplexes of Rh undergo aquation constitutes part of this investigation. Subsequent to that, the extraction and stripping behavior of the bromocomplexes of Rh(III) with an organic phase of Kelex 100 is fully examined. The stability of the Kelex 100 extractant against the acidic environment is studied and the performance of the regenerated extractant evaluated. Finally, a full extraction-stripping circuit for the separation/concentration of the Rh species from hydrochloric acid media is developed.

7.2 AQUEOUS BROMIDE CHEMISTRY OF RHODIUM(III)

Rhodium bromides have not been greatly studied. According to the limited number of published studies, the most common oxidation state of Rh in bromide solutions is III, similar to that of chloride solutions (Sidgwick, 1950). Rh(III) bromocomplexes are in general ionic species of octahedral structure very similar to that of chlorocomplexes, but with some distinct differences. For instance, while $Na_3[RhCl_6]$ is the most common salt among the Rh(III) chloride complexes, the equivalent $Na_3[RhBr_6]$ is not equally common. Instead, the binuclear type $M_3[Rh_2X_9]$ is much more common with the bromides. The formation of monomeric and polymerized complex ions is also equally characteristic of the complex bromides of several platinum metals. Water-soluble, simple bromides of platinum metals (MBr_2, MBr_3, MBr_4) are usually prepared by reacting hydrated metal oxides with hydrobromic acid (Claassen et al., 1961). Complex bromides of platinum metals are, prepared by dissolving simple bromides in hydrobromic acid. They may also be obtained by reacting the corresponding complex chlorides of the platinum metals with hydrobromic acid. Using this procedure, according to Ayres and Tuffly (1952), the complete removal of chlorine from platinum metal complexes may take place – except for platinum and palladium compounds, where the chlorides should first be heated with perchloric acid and then treated with hydrobromic acid. The same behavior was also reported by Cozzi and Pantani (1961), who claimed that the interaction of hexachlororhodate with HBr and/or NaBr produces several bromide complexes.

More recently, Mann and Spencer (1983) clearly confirmed this chloride-bromide substitution phenomenon through the identification of the various $[RhCl_{6-n}Br_n]^{3-}$ complexes with the aid of ^{103}Rh NMR spectroscopy. They demonstrated that solutions containing $[RhCl_{6-n}Br_n]^{3-}$ exhibit chemical shifts, δ (^{103}Rh), with the addition of varying concentrated mixtures of HCl and HBr (Table 7.1). In all cases, heating the solution at 80 °C for a period of 30 minutes has been found satisfactory for a complete replacement of Cl^- by Br^-, or vice versa. Bromide solutions of Rh(III), stabilized by heating, have a pink-violet and pink-greenish color at intermediate and high bromide concentrations, respectively (Ginzburg et al., 1975).

On the other hand, it appears that, similarly to chloride solutions, the aquation/anation reaction, i.e., reaction (7.1), occurs in bromide solutions as well:

$$RhBr_6^{3-} + nH_2O \leftrightarrow RhBr_{6-n}(H_2O)_n^{n-3} + nBr^- \qquad (7.1)$$

As a result of this stepwise reaction, a series of aquo/bromo complexes form in the solution. Stability constants for five rhodium(III) bromocomplexes at 25 °C have been calculated by Cozzi and Pantani on the basis of polarographic data, and the corresponding speciation diagram also provided (Cozzi and Pantani, 1961). The authors concluded that in the practical range of Br^- concentration the only available Rh(III) species are: $RhBr^{2-}$, $RhBr_2^+$, $RhBr_3^0$, $RhBr_4^-$, and $RhBr_5^{2-}$. These findings, however, cannot be considered reliable because of apparent errors associated with the applied electrode process (Ginzburg et al., 1975). Also, the absence of the hexabromorhodate, $RhBr_6^{3-}$, from the list of the complexes reported by Cozzi and Pantani is suspicious as it is known to form in 6 M HBr solutions upon prolonged boiling (Jorgensen, 1962), or to be the dominant species at 5M Br^- (Jorgensen, 1956). Despite the lack of reliable data on the stability constants of aquo/bromo complexes of rhodium(III), several studies have identified the latter complexes as well as the polynuclear bromide-bridged complexes of rhodium (III).

Table 7.1: ^{103}Rh Chemical Shifts and UV Absorption Bands of Different Aquo/Bromo and Chloro/Bromo Complexes

$[RhBr_n(H_2O)_{6-n}]^{3-n}$ Compounds			$[RhCl_{6-n}Br_n]^{3-}$ Compounds *	
Complex	$\delta(^{103}Rh)$ †	λ_{max}(nm) ‡	Complex	$\delta(^{103}Rh)$
$[Rh(H_2O)_6]^{3+}$	9880	396, 311	$[RhCl_6]^{3-}$	7985
$[RhBr(H_2O)_5]^{2+}$	9327	550, 454, 350	$[RhCl_5Br]^{3-}$	7848
trans-$[RhBr_2(H_2O)_4]^{1+}$	8928	483, 256	cis-$[RhCl_4Br_2]^{3-}$	7707
cis-$[RhBr_2(H_2O)_4]^{1+}$	8846	478, 208	trans-$[RhCl_4Br_2]^{3-}$	7712
mer-$[RhBr_3(H_2O)_3]$	8447	505, 256, 213	fac-$[RhCl_3Br_3]^{3-}$	7556
fac-$[RhBr_3(H_2O)_3]$	8347	--	mer-$[RhCl_3Br_3]^{3-}$	7561
t-$[RhBr_4(H_2O)_2]^{1-}$ (A)	8056	--	cis-$[RhCl_2Br_4]^{3-}$	7403
c-$[RhBr_4(H_2O)_2]^{1-}$ (A)	7962	--	trans-$[RhCl_2Br_4]^{3-}$	7409
$[RhBr_5(H_2O)]^{2-}$ (B)	7493	--	$[RhClBr_5]^{3-}$	7243
$[RhBr_6]^{3-}$ (C)	7007	562, 441, 340	$[RhBr_6]^{3-}$	7077
Dimers of (A)	7928			
Dimers of (B)	7384-7339			
Dimers of (C)	7070-6741			

Data From: † Read et al. (1992); ‡ Wilkinson et al. (1987); * Mann and Spencer (1983).

Read et al. (1992) identified all ten monomeric aquobromo rhodium(III) complexes, $[RhBr_{6-n}(H_2O)_n]^{(3-n)-}$ with $n = 0-6$, including the geometric isomers for $n = 2-4$, using ^{103}Rh NMR spectroscopy. The assignment of the cis- and trans-isomers of $[RhBr_2(H_2O)_4]^{+1}$, however, was made possible with the use of Raman spectroscopy. Their assignments, which are presented in Table 7.1, demonstrate a nephelauxetic dependence of the chemical shifts δ_{Rh} of these complexes – namely, a decrease in δ with an increase in the number of bromo ligands. These authors also realized that for solutions with a total Rh concentration $C_{Rh} > 0.5$ mol.L^{-1}, and with mole ratios of $n_{Br} / n_{Rh} = 3\text{-}8 / 1$, a complex of oligomeric aquobromo rhodate (III) species existed in the solution. They found that for

equilibrated solutions with similar mole ratios (n_{Br} / n_{Rh} ≈ 4/1) the complex distribution was dependent on the total Rh concentration. Upon dilution, the NMR measurements confirmed that the monomeric complexes were favored, thus indicating the presence of polynuclear Rh(III) bromide complexes. Consequently, Read et al. (1992) categorized the unassigned ^{103}Rh NMR signals into three distinct groups (A, B, and C in Table 7.1), with chemical shifts similar to those of the monomeric complexes $[RhBr_4(H_2O)_2]^{1-}$, $[RhBr_5(H_2O)]^{2-}$, and $[RhBr_6]^{3-}$, respectively; each group represented ^{103}Rh nuclei present in either mono-, di-, or tri-bromo bridged *dimers* with the same number of directly co-ordinated Br^- ligands, as in the "parent" monomeric species (see Table 7.1).

Several researchers have also identified the various aquobromo complexes of Rh(III) with the aid of UV-visible absorption bands in the absorption spectrum of the solutions containing the latter species (Wilkinson et al., 1987). The corresponding absorption bands (λ_{max}), which are presented in Table 7.1, exhibit a shift towards higher wavelengths with the increase in the number of Br^- ligands. This is consistent with the variation in the color of the solution from pink-violet towards cherry-red, as the complexes change from aquated towards nonaquated $RhBr_6^{3-}$. Due to the lack of reliable stability constants for bromo/aquo Rh (III) complexes, an effort has also been made in the course of this project to determine the extent to which bromocomplexes have been aquated using the latter UV-visible technique. The results of this investigation are discussed in the following sections.

7.3 FORMATION OF Rh(III) BROMOCOMPLEXES AND THEIR AQUATION

Before the experimental results on the formation and aquation of Rh(III) bromocomplexes are presented, it ought to be reported that similarly to the analysis of the Rh(III) chloride solutions (see Chapter 3) the concentration of Rh in the bromide solutions was determined with the aid of UV-Visible spectroscopy. Typical UV-Visible spectra and the corresponding calibration curve of Rh(III) bromide solutions (equilibrated, i.e., sufficiently aged) are shown in Figure 7.1.

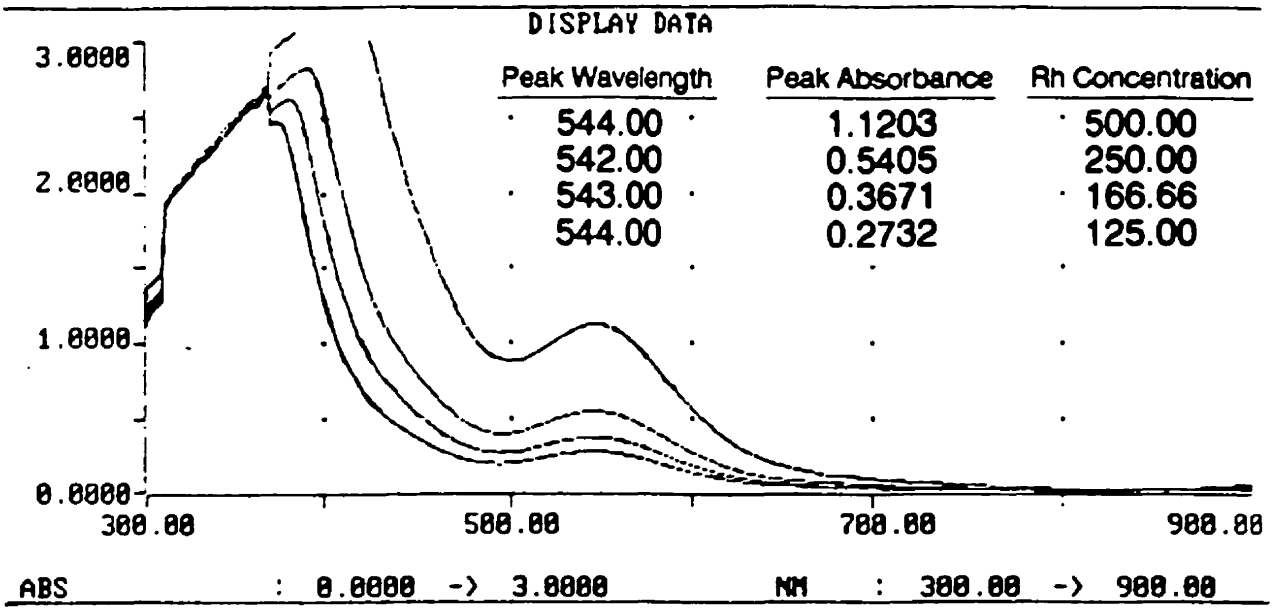

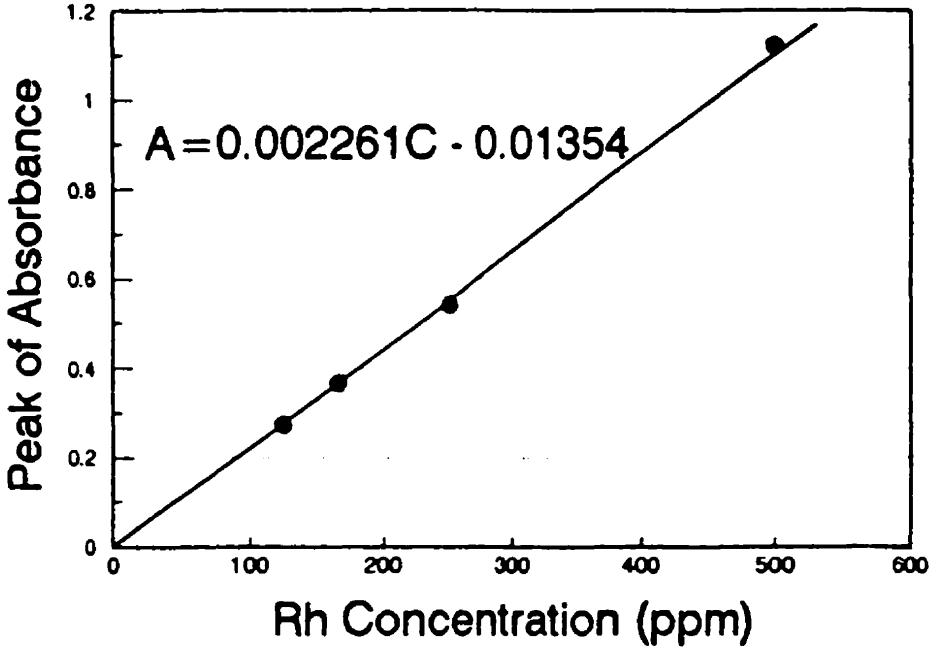

Figure 7.1: Absorption Spectra & Calibration Curve for Aged (Equilibrated) Rh Solutions of 1.5 M HBr

For the study of the formation of the $RhBr_{6-n}(H_2O)_n^{(3-n)-}$ complexes, the following procedure was adopted. Bromide solutions of Rh were prepared by dissolving Na_3RhCl_6 into hydrobromic acid solutions. During this dissolution process ligand exchange takes place and the chloride ions are replaced by the bromide ones. The feasibility of this *reversible* ligand exchange reaction and the formation of various $[RhCl_{6-n}Br_n]^{3-}$ complexes has been demonstrated in the literature (Mann and Spencer, 1983). It has also been shown that at elevated temperatures , i.e., 80 °C, the rate of this reaction is relatively fast and the system reaches its equilibrium in the order of several hours. However, no rate- and/or equilibrium-constants for this reversible reaction are available. Due to the significant impact such parameters may have on the separation process of Rh complexes, the latter exchange reaction was monitored through UV-Visible spectroscopy and SX experiments.

First, the substitution of bromide with chloride ligands at ambient temperature was investigated. As shown in Figure 7.2, the absorption spectrum of dissolved sodium hexachloro rhodate in 1.5 M HBr solution changes with time (Figure 7.2 (b)), and after about 5 hours (Figure 7.2 (c)) becomes almost identical with that of a pure solution of $RhBr_3$ in 1.5 M HBr (Figure 7.2 (a)). Second, in order to demonstrate the reversibility of this reaction (i.e., the chloride substitution with bromide where $RhBr_3$ is dissolved in HCl solution), the $RhBr_3$ salt was dissolved in a solution of 1.5 M HCl. In this case, only a modest change in the absorption spectrum was observed – and, that, only after 10 days of aging (compare Figure 7.3 (a) to Figure 7.2 (a)). However, when $RhBr_3$ was dissolved in 4 M HCl, the absorption spectrum of the solution (Figure 7.3 (b)) became very similar to that of rhodium chloride in 4 M HCl (Figure 7.3 (c)) after only a few hours of aging. This indicates that the exchange reaction is reversible to the extent that it depends on the relative concentration of each halide ion:

$$RhCl_6^{3-} + 6Br^- \leftrightarrow RhBr_6^{3-} + 6Cl^- \qquad (7.2)$$

By comparing Figures 7.2 (c) with 7.3 (a), one may infer that at 1.5 M HX the bromocomplex of Rh(III) dominates – i.e., the affinity of Br^- for Rh(III) is higher than that of Cl^-.

The aquation behavior of Rh(III) complexes in chloride/bromide media was investigated next. The aquation of the halocomplexes of Rh(III) was followed by monitoring the position of one of the characteristic UV-Visible absorption bands (λ_{max}) as it was discussed in Chapter 6. In Figure 7.4 the location of one of the absorption bands versus halogen concentration is presented. The solid line represents the chloride system and the dashed line represents the bromide system. As one may notice, there is a shift in the position of the band, in the case of chloride system, even at concentrations as high as than 6 M Cl^-. In other words, the aquation in chloride media is substantial and occurs even at high chloride concentrations. On the other hand, no shift in the absorption spectrum of the respective bromide solution is observed for bromide concentrations higher than 3-4 M Br^-. In other words, the aquation occurs only up to 3 M Br^- and the latter concentration is sufficient to suppress completely the aquation of the bromocomplexes of Rh(III). Moreover, judging from the magnitude of the shift it can be concluded that the extent of aquation is much lower in the bromide than in the chloride system.

As discussed earlier, aquation is held responsible for the failure of previous attempts of direct solvent extraction from chloride solutions. Since aquation of Rh(III) in bromide media proved to be much less prone to occur than in the respective chloride media, the possibility of successfully applying solvent extraction to bromide solutions of Rh(III) was examined.

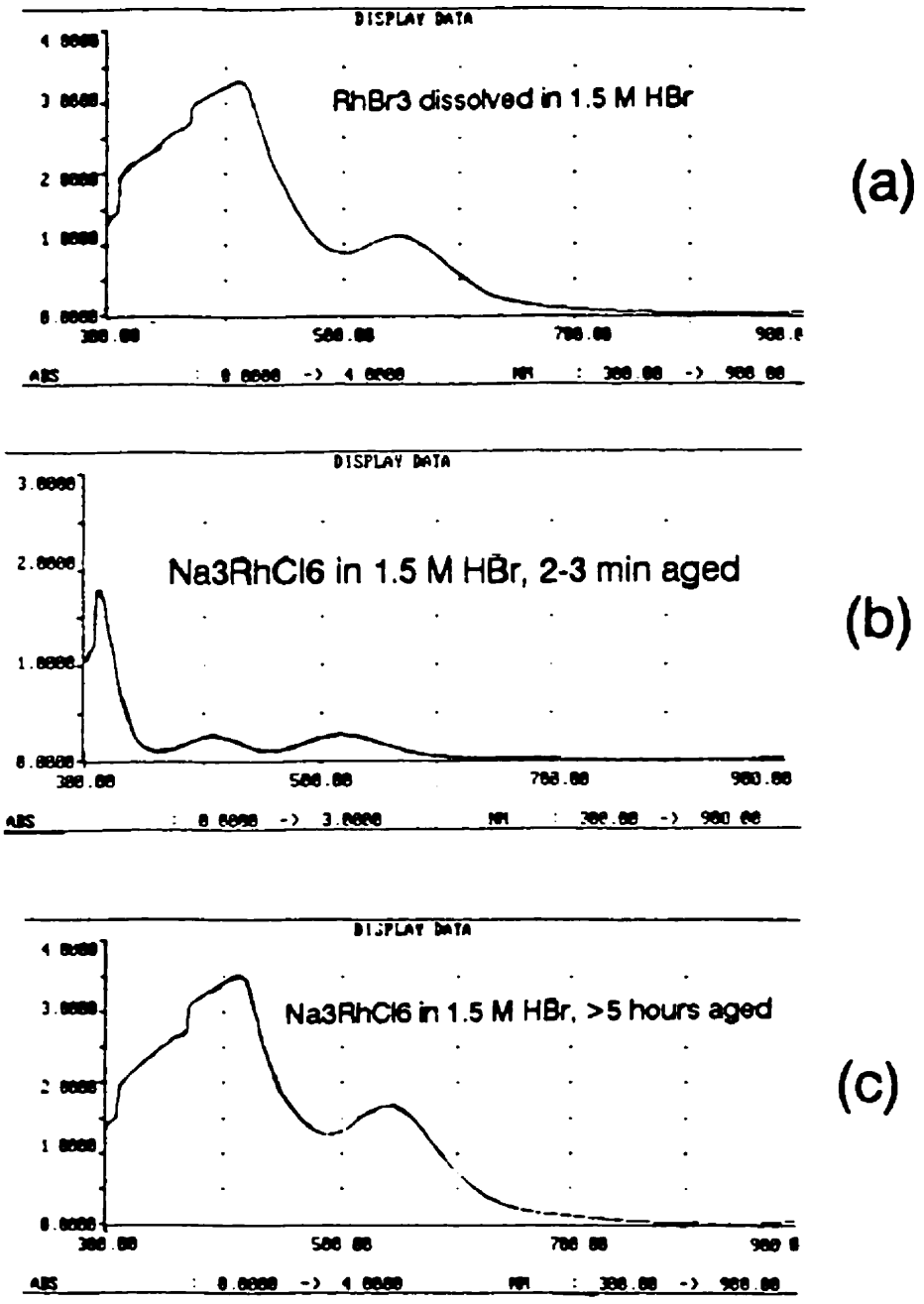

Figure 7.2: Monitoring of the Conversion of the Rh(III) Chlorocomplexes to Bromocomplexes with UV-Visible Spectroscopy

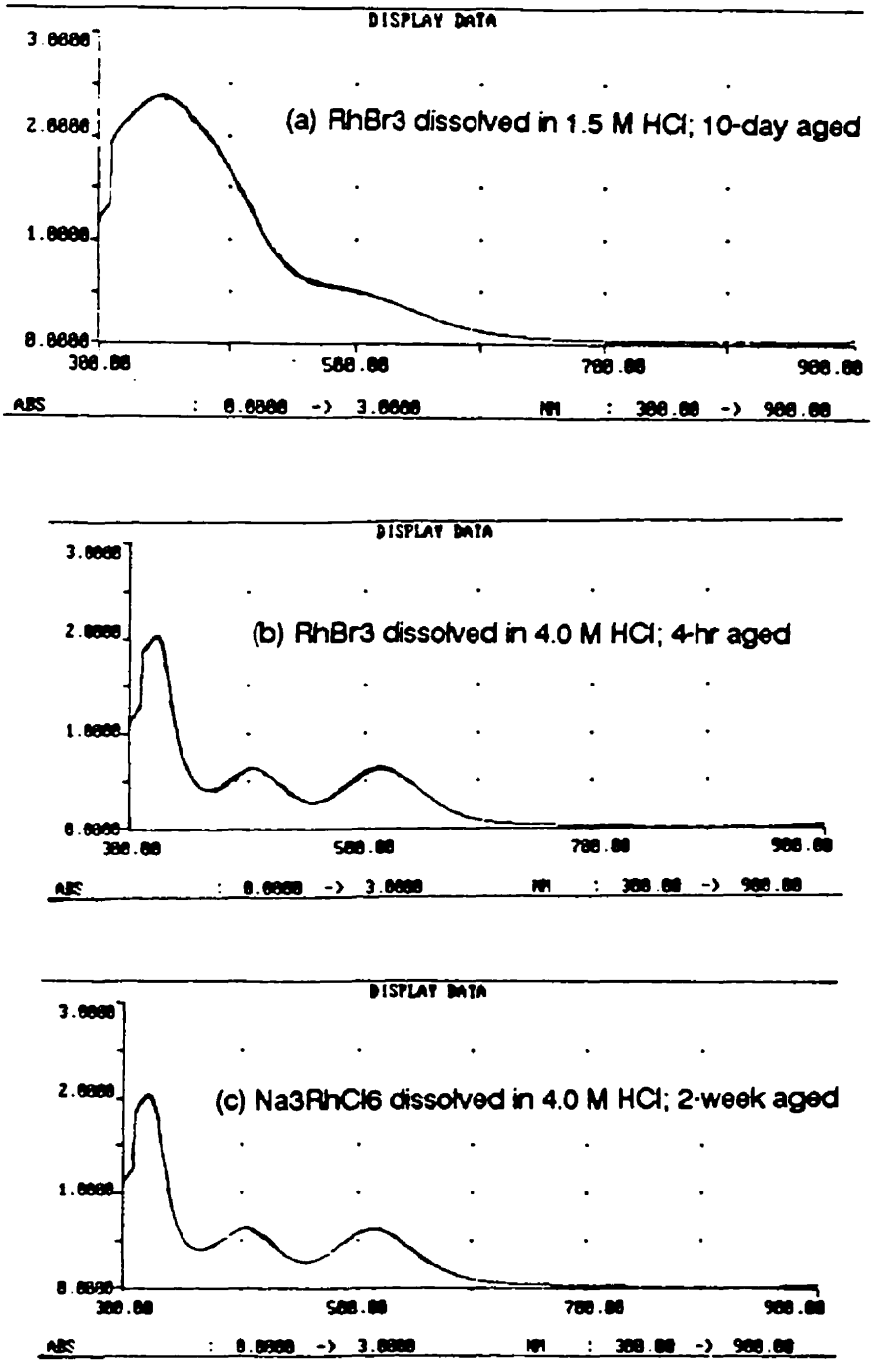

Figure 7.3: Monitoring of the Exchange of Cl^- with Br^- and Visible Spectrum Detection

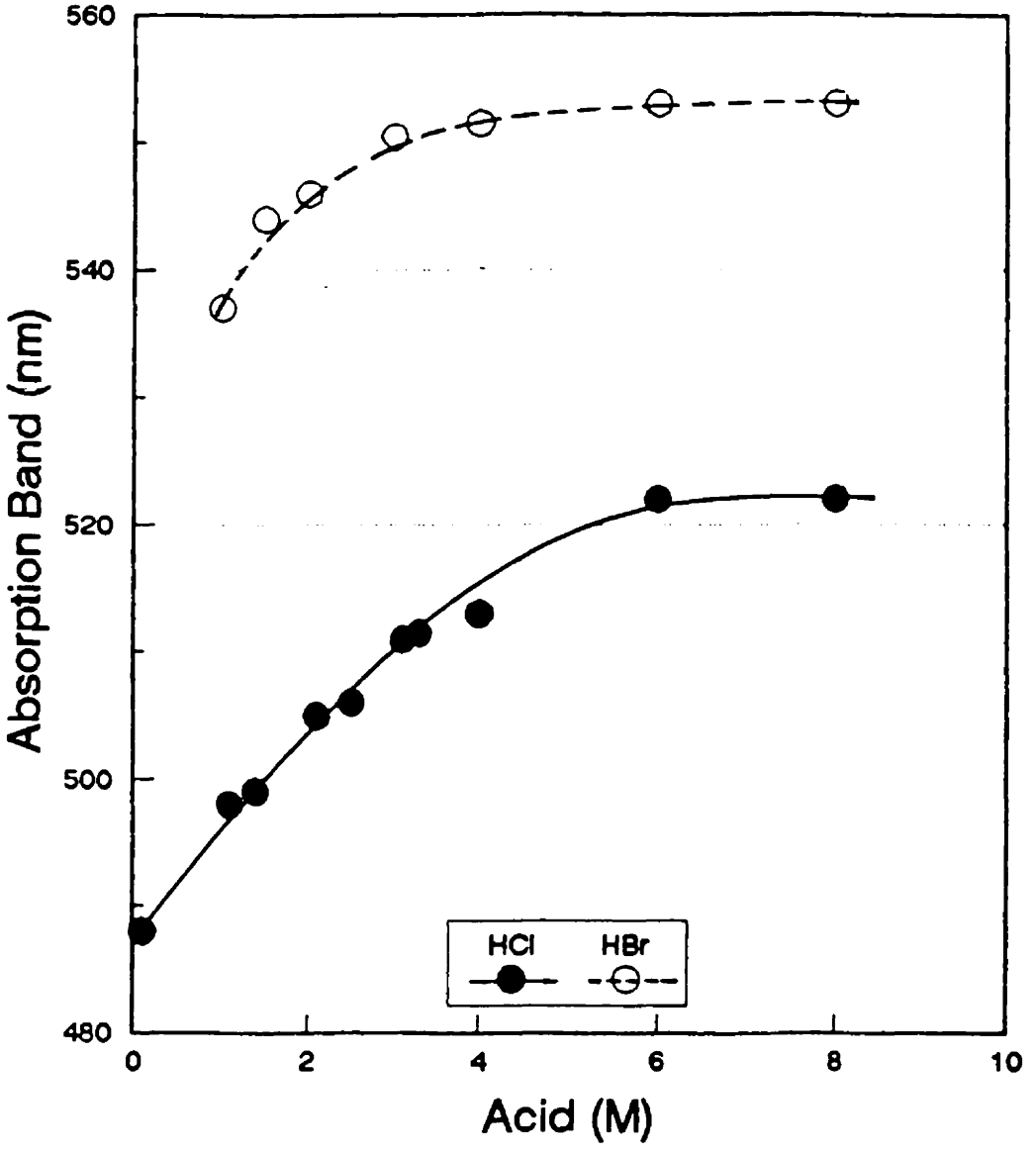

Figure 7.4: Monitoring of the Aquation of Rh Complexes in Chloride and Bromide Media with UV-Visible Spectra

(location of the absorption bands of two-week aged HCl & HBr solutions)

7.4 EXTRACTION

Aqueous bromide solutions of Rh(III) were prepared by dissolving Na_3RhCl_6 in HBr. The latter solutions of different ages were then subjected to extraction with Kelex 100. The results of these SX experiments, plotted in Figure 7.5, show the distribution coefficient to be limited to about one (under the applied conditions: 330 ppm Rh feed, 10 v/o Kelex 100, and 3 min CT) for the first 2-hour age period of the solution, but thereafter to increase, reaching nearly 9 after about 20 hours of equilibration time. The initial apparent drop of **D** (from 1.5 to 1) is attributed to the partial aquation of the hexachlorocomplex of Rh(III) to $RhCl_5(H_2O)^{2-}$ – the latter is not extractable with Kelex 100 – while the subsequent increase in extraction is attributed to the substitution of bromine into the inner coordination sphere of Rh(III) and, ultimately, to the conversion of the aquo/chloro complexes to bromocomplexes.

Meanwhile, as one may conclude from the ligand exchange reaction (i.e., eq. 7.2) that the extraction of Rh(III) would be expected to increase with a decrease in Cl^- concentration. Thus, while the level of extraction was about 90% (or **D** equal to 9) for the aged solution of 1.5 M HBr (see Figure 7.5), extraction dropped to 60% when a mixed solution of 0.75 M HCl and 0.75 M HBr was used (these results are not presented schematically). Following these preliminary tests it was decided thereafter to conduct the rest of the SX experiments with aqueous bromide solutions that have been aged at least 3 days, so as to ensure complete conversion of the chloro/aquo complexes to the extractable hexabromo complexes ($RhBr_6^{3-}$).

Having determined the required aging time for the rhodium(III) bromide feed solution, next, the effect of contact time (CT) on extraction was investigated. After performing experiments at different contact times, it became apparent that this variable had no significant effect on extraction; in other words, extraction equilibrium was reached very fast. Therefore, a contact time of 3 minutes was chosen for the rest of the extraction tests.

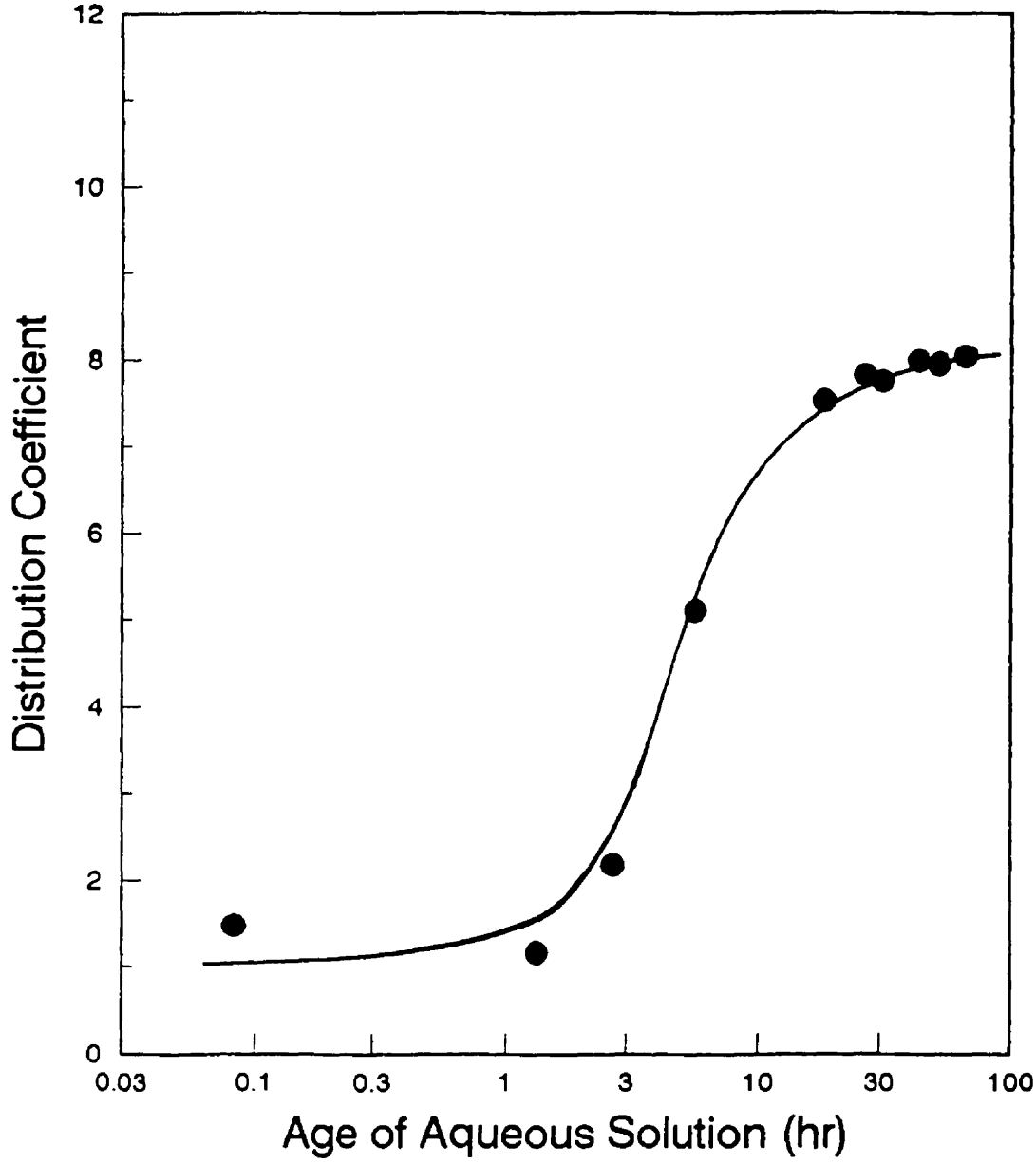

Figure 7.5: Distribution Coefficient of Rh vs Age of the Feed

(A: 330 ppm Rh, Na_3RhCl_6 dissolved in 1.5 M Hbr; A/O: 1;

O: 10 v/o Kelex 100 (0.28 M), 10 v/o tridecanol, 80 v/o kerosene; CT: 3 min)

To investigate the effect of feed acidity on Rh extraction, aqueous solutions with different HBr concentrations were contacted with 2 v/o Kelex 100 organic solutions (Figure 7.6). The amount of extraction or, equivalently, the distribution coefficient, was found to increase with acidity reaching a maximum at 1.5 M HBr and, subsequently, decreasing at higher acidities. This behavior, which is similar to that of HCl aqueous solutions, relates apparently to the protonation of the extractant at the lower acidity region (reaction (7.3)), and to the negative effect of Br^- on the ion-pair formation reaction at high Br^- concentrations (reaction (7.4)):

$$\overline{R-HQ} + HBr \leftrightarrow \overline{R-H_2Q^+Br^-} \tag{7.3}$$

$$RhBr_6^{3-} + 3\overline{R-H_2Q^+Br^-} \leftrightarrow \overline{RhBr_6^{3-}(R-H_2Q^+)_3} + 3Br^- \tag{7.4}$$

The latter effect was confirmed when another set of experiments was conducted with two aqueous solutions of 0.5 and 1 M of HBr, containing various amounts of NaBr. The results are shown in Figure 7.7. It is interesting to note that maximum extraction took place at a total Br^- concentration of 1.5 M.

The effect of Kelex 100 concentration on Rh extraction was investigated next. The amount of extraction or, equivalently, the distribution coefficient, as expected, was found to increase with Kelex 100 concentration as may be seen in Figure 7.8. The data of Figure 7.8 are re-plotted in Figure 7.9 as log **D** vs log[Kelex 100]. One may observe that log **D** shows a linear correlation with log[Kelex 100] with a slope of one. This was an unexpected result, as a slope of three was predicted by the stoichiometry of reaction 7.4.

In another series of tests, practically 100% extraction of Rh was obtained when the same aqueous solution was contacted in 3 consecutive contacts with fresh organic solutions of different Kelex 100 concentrations (Figure 7.10). On the other hand, the Rh extraction

was found to be independent of the modifier concentration within the range tested (Figure 7.11). Nevertheless a minimum alcohol concentration (at least 1 v/o per v/o Kelex 100) is needed to ensure satisfactory phase separation.

Finally, the extraction isotherms for two organic solutions of 5 and 15 v/o Kelex 100 are presented in Figures 7.12 and 7.13, respectively. These isotherms were prepared by contacting the corresponding aqueous and organic solutions at different volume ratios.

In connection to the rhodium extraction tests, the water uptake by the organic phase of Kelex 100 was monitored as well by contacting the latter with HBr solutions of different acidities. The results which are presented in Figure 7.14 exhibit a trend similar to that of Kelex 100 organic phase in contact with HCl solutions (see Chapter 4). In other words, the organic phase contains a substantial amount of water which, in principle, could have aquated the Rh(III) bromocomplexes transferred in the organic phase and suppressed their extraction. Nevertheless, the high degree of extraction achieved points to the fact that aquation is not as significant here as in the case of the chloride solutions.

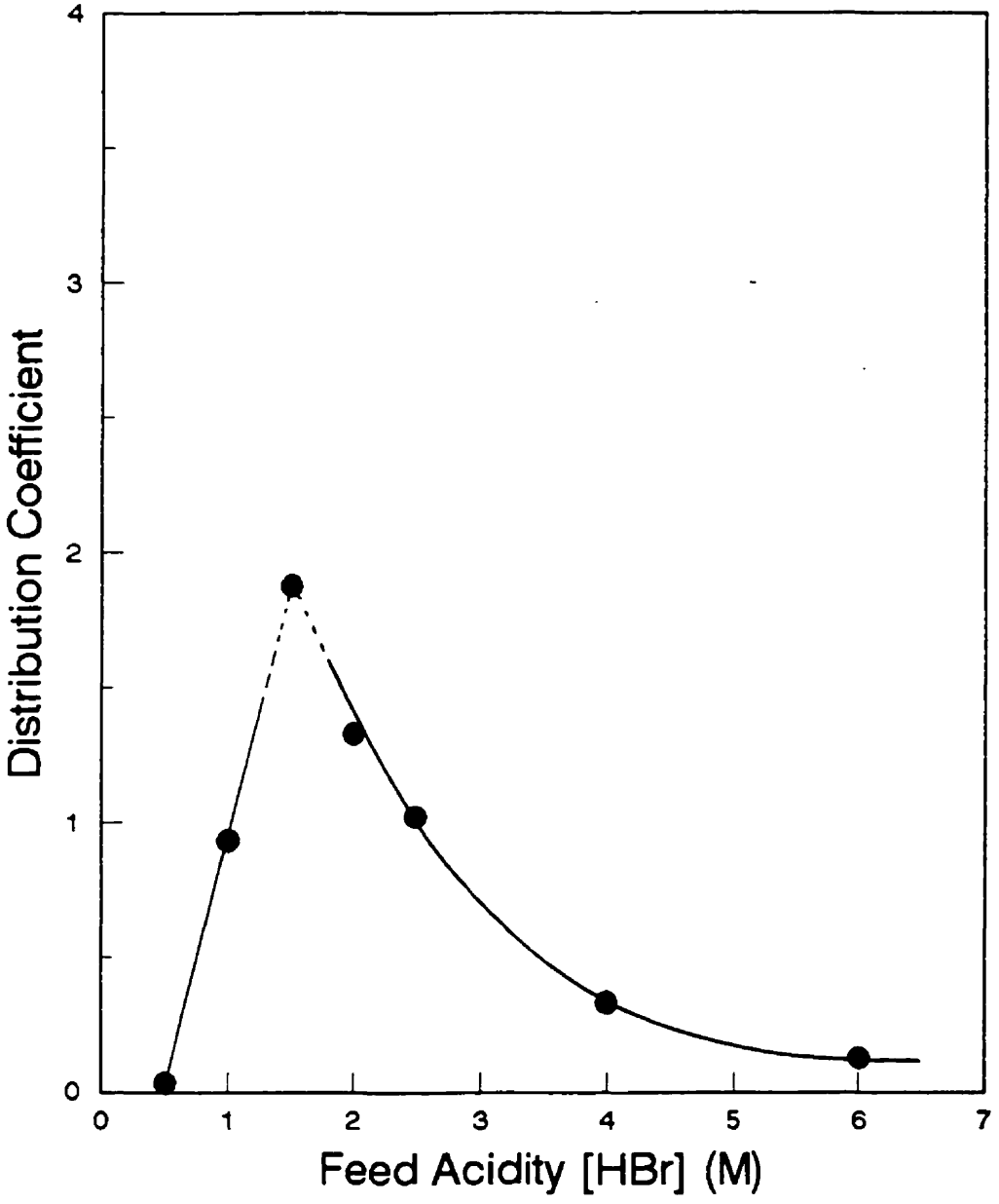

Figure 7.6: Distribution Coefficient of Rh vs Feed Acidity

(A: different acidity, 330 ppm Rh, 3-day aged; O: 2 v/o Kelex 100 (0.056 M), 5 v/o tridecanol, 93 v/o kerosene; CT: 3 min)

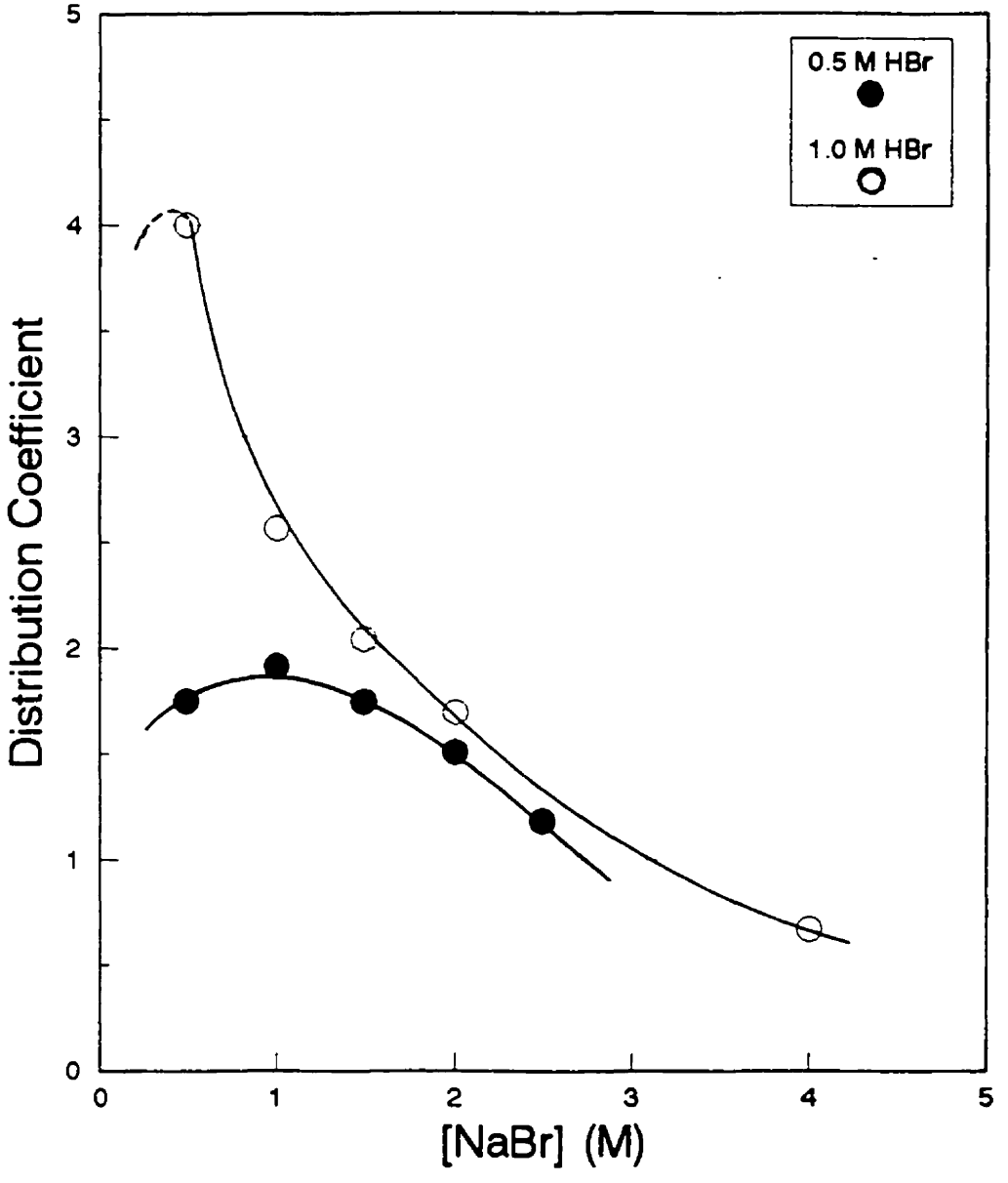

Figure 7.7: Effect of [Br⁻] on Distribution Coefficient of Rh

(A: 0.5/1 M HBr, different [NaBr], 300 ppm Rh, 3-day aged;

O: 5 v/o Kelex 100 (0.14 M), 5 v/o tridecanol, 90 v/o kerosene; CT: 3 min)

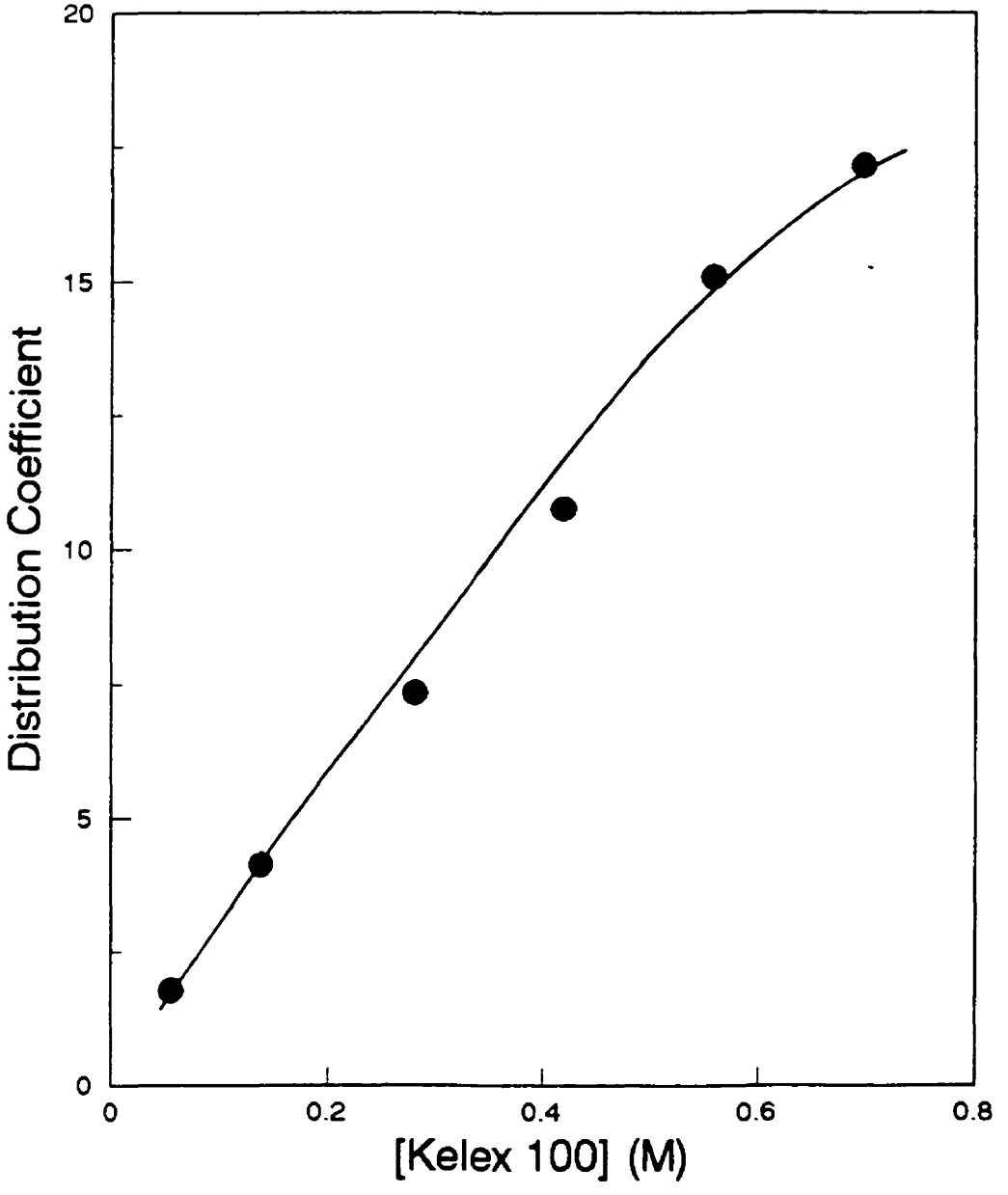

Figure 7.8: Effect of Kelex 100 Concentration on Distribution Coefficient of Rh

(A: 1.5 M HBr, 330 ppm Rh, 3-day aged; O: x v/o Kelex 100,
x v/o tridecanol, (100-2x) v/o kerosene; CT: 3 min)

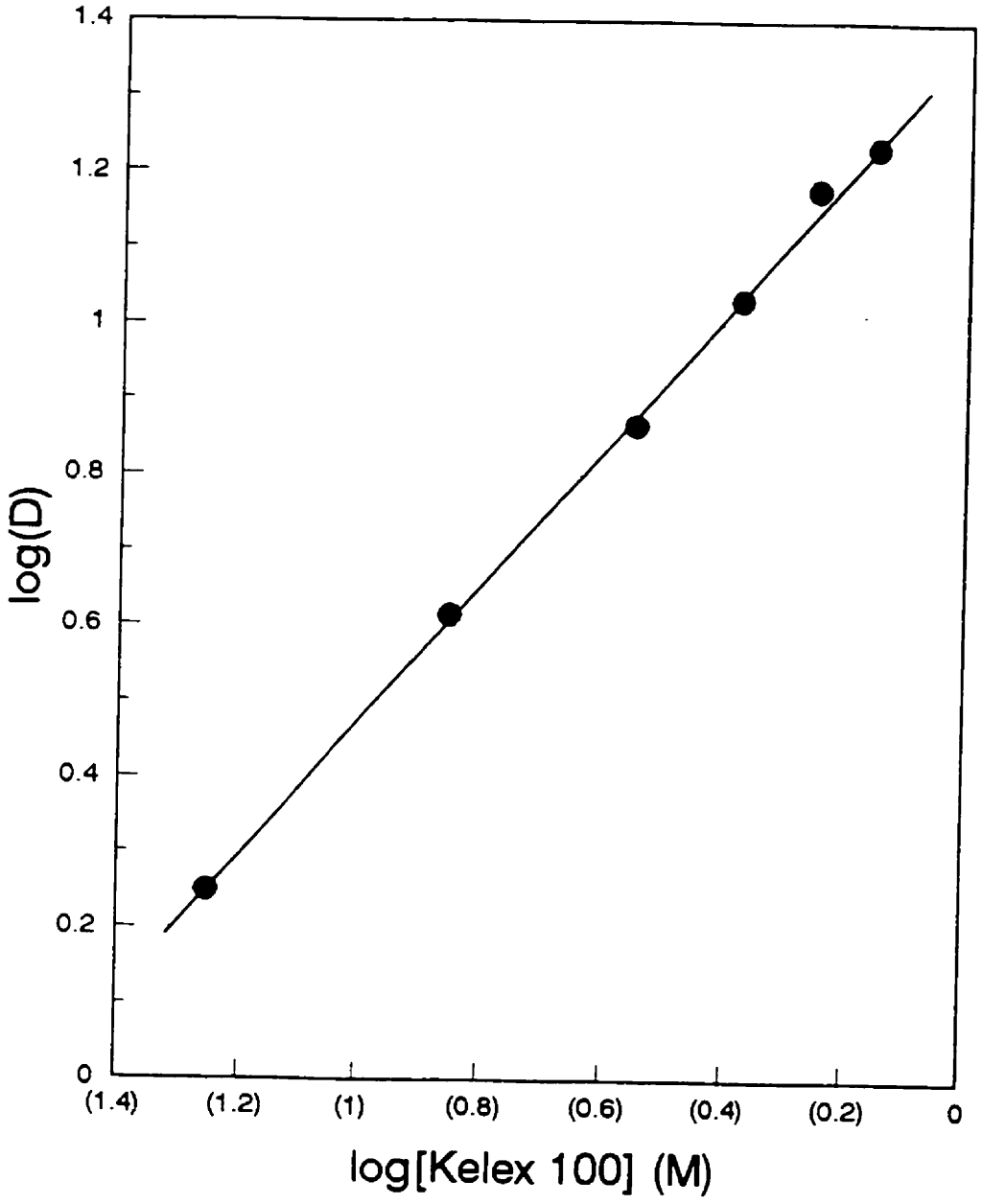

Figure 7.9: Plotting of the Data of Figure 7.8 as logD vs log[Kelex 100]

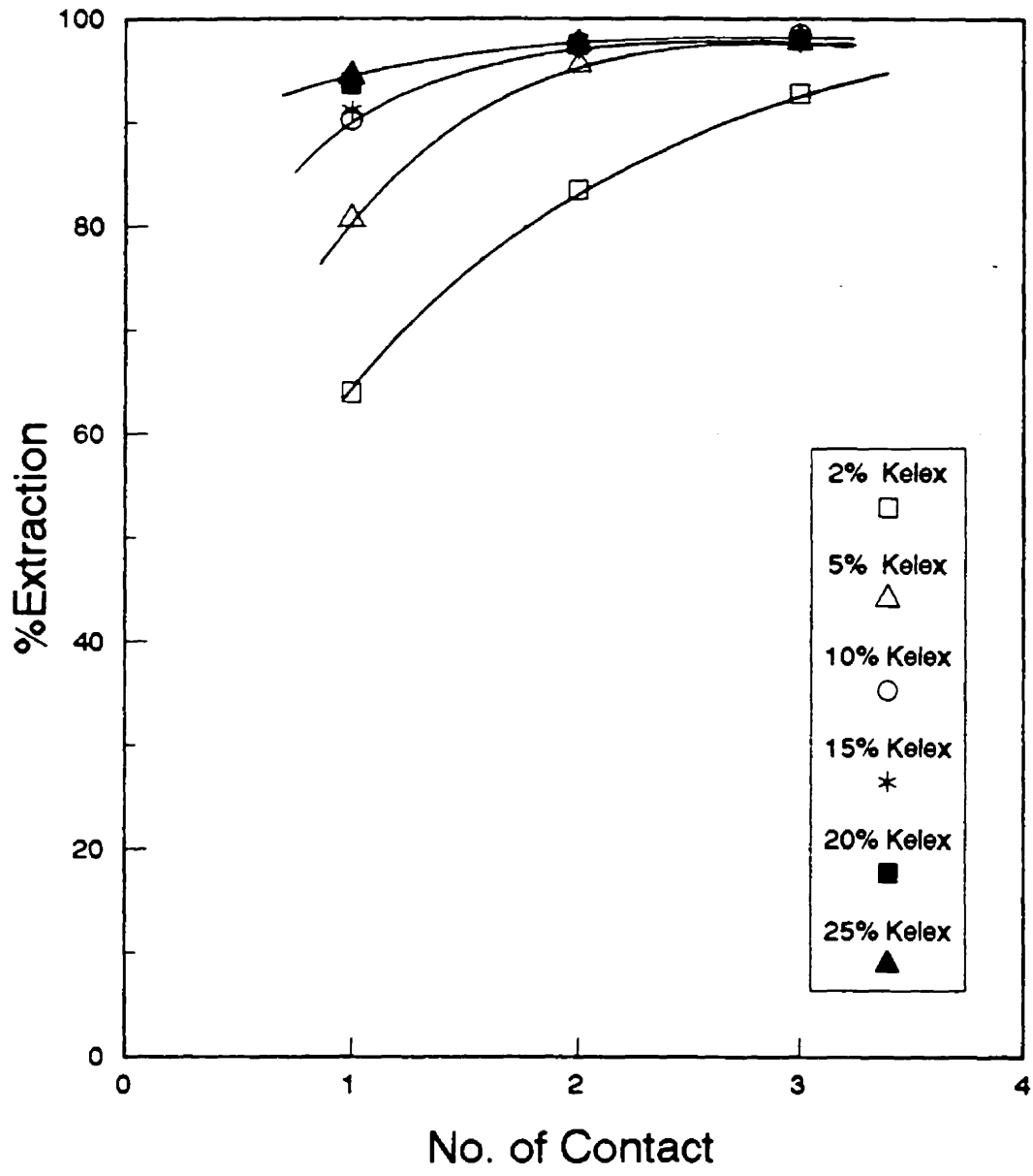

Figure 7.10: Extraction of Rh vs No. of Consecutive Contacts

(A: 1.5 M HBr, 330 ppm Rh, 3-day aged; O: x v/o Kelex 100,

x v/o tridecanol, (100-2x) v/o kerosene; CT: 3 min)

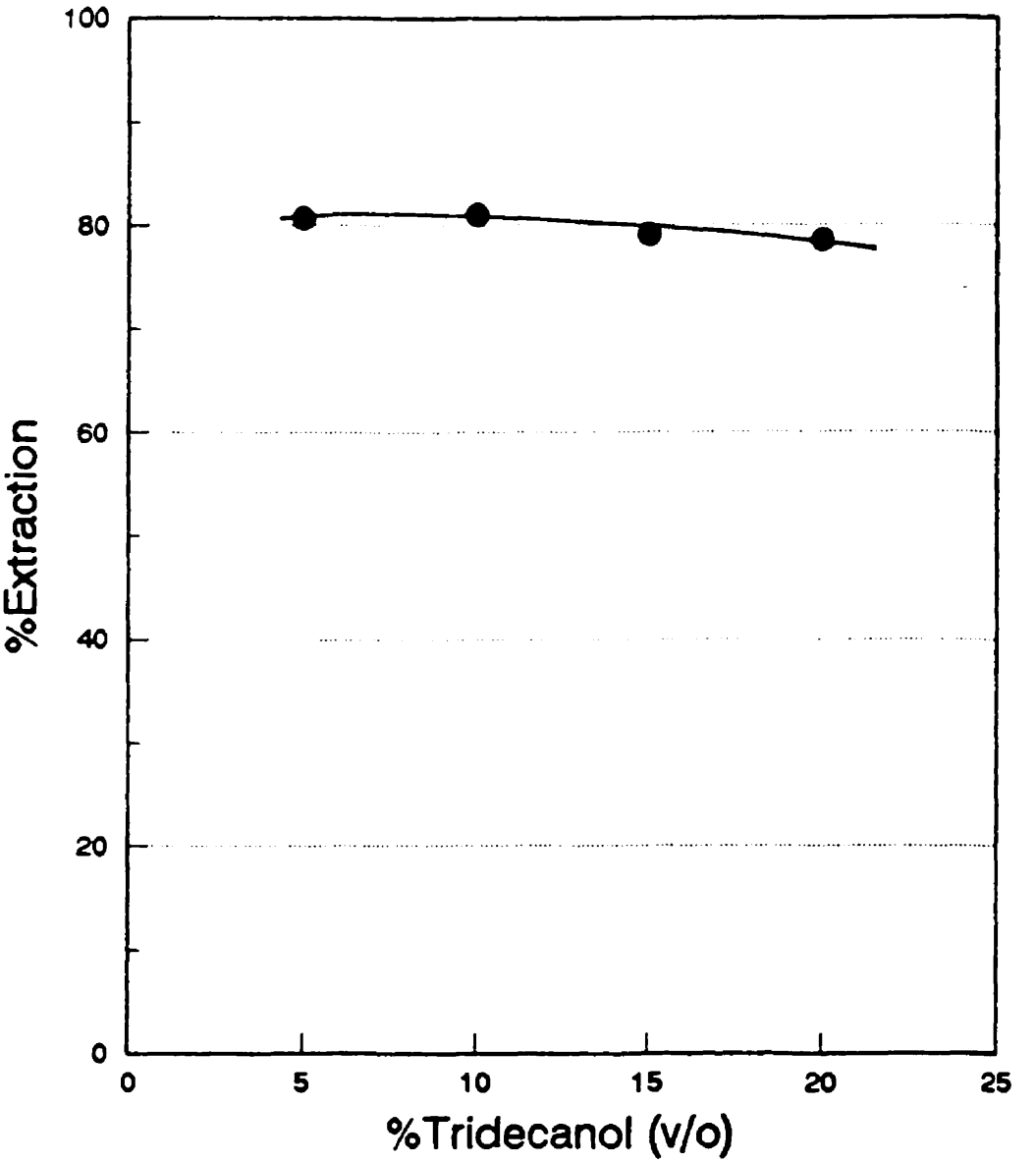

Figure 7.11: Effect of Alcohol Concentration on Rh Extraction

(A: 1.5 M HBr, 330 ppm Rh, 3-day aged; O: 5 v/o Kelex 100 (0.14 M), x v/o tridecanol, kerosene; CT: 3 min)

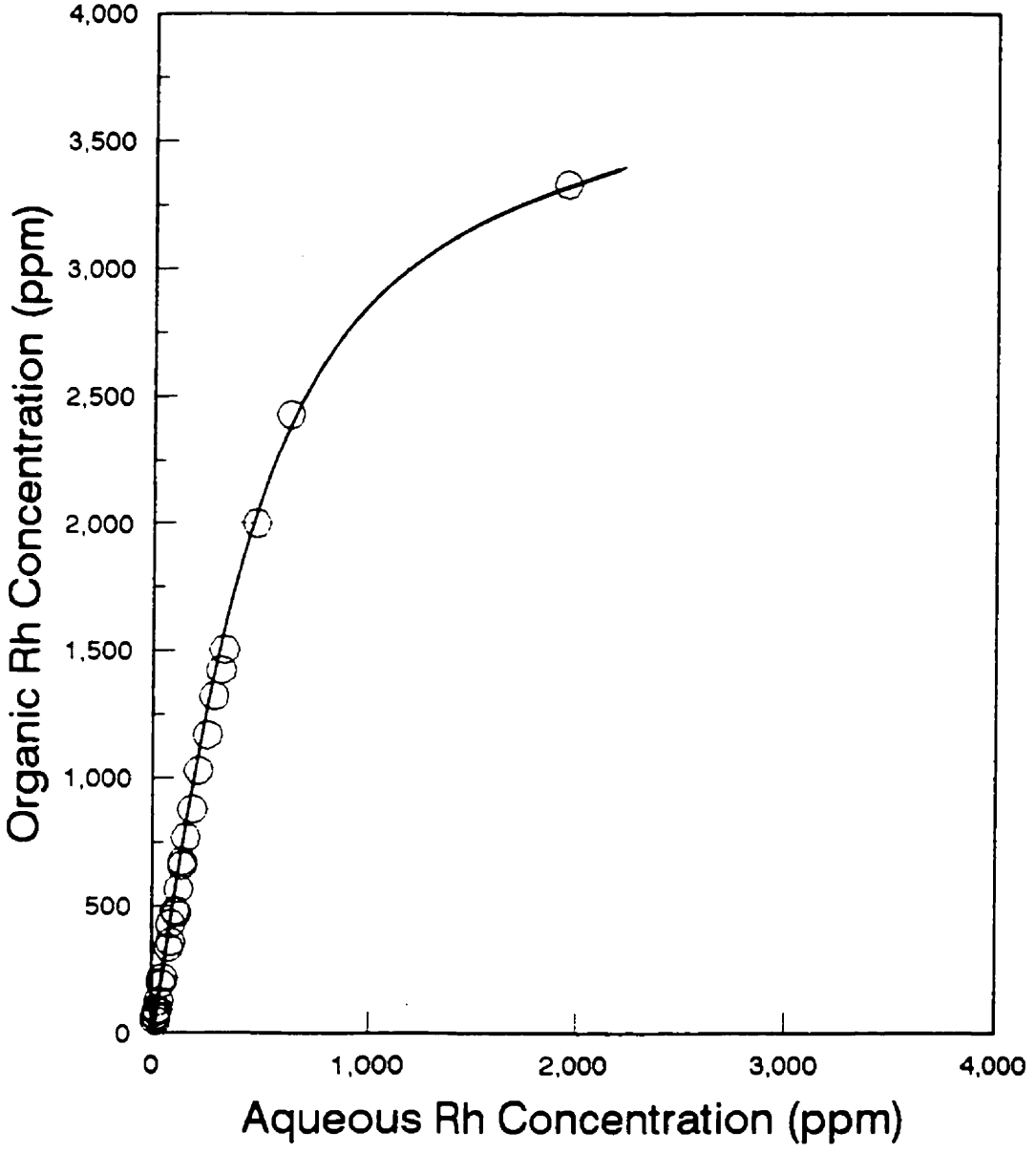

Figure 7.12: Rh Extraction Isotherm (5 v/o Kelex 100; 0.14 M)

(A: 1.5 M HBr, different Rh concentration, 3-day aged; O: 5 v/o Kelex 100, 5 v/o tridecanol, 90 v/o kerosene; Different A/O volume ratios; CT: 3 min)

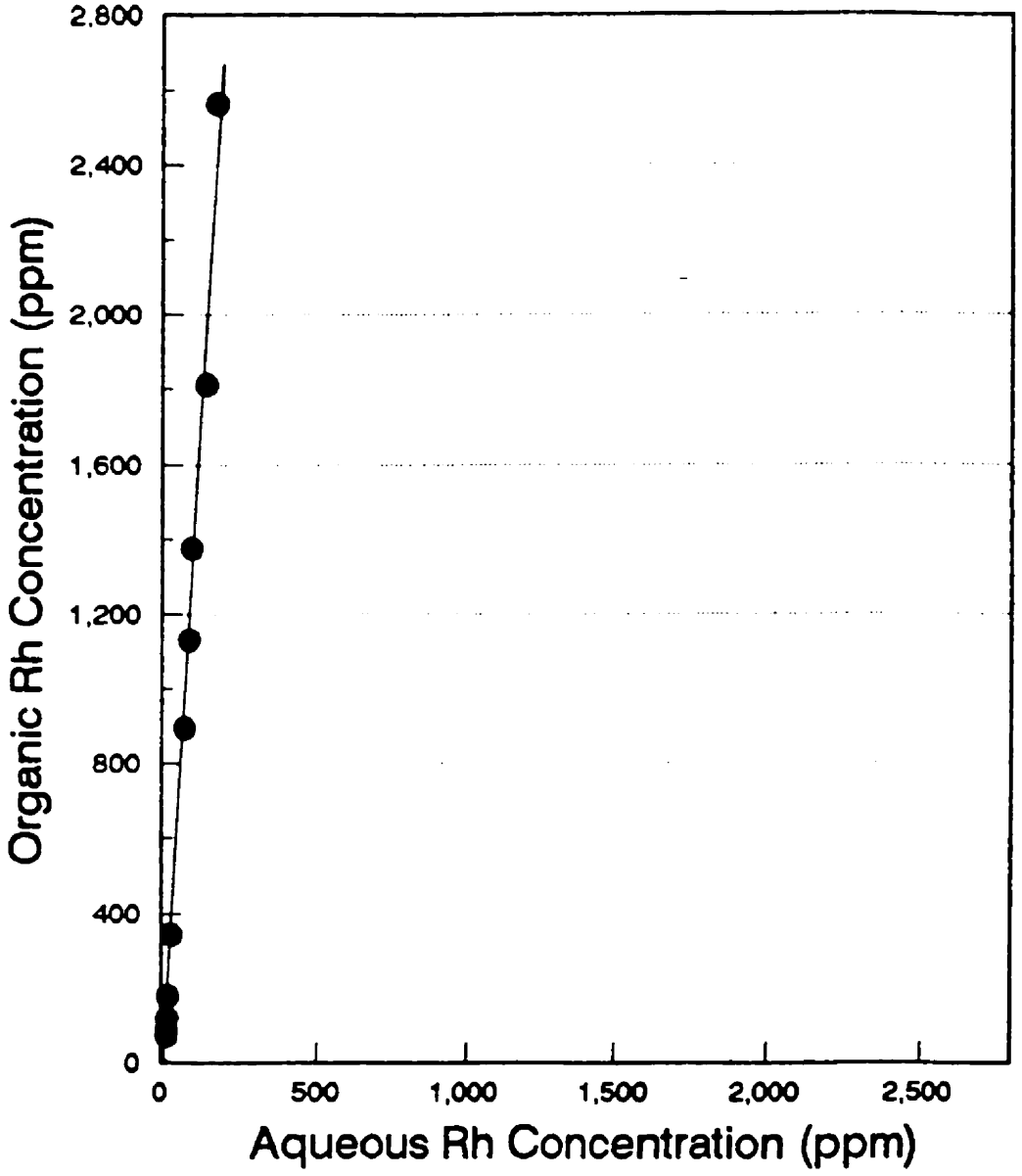

Figure 7.13: Rh Extraction Isotherm (15 v/o Kelex 100; 0.42 M)

(A: 1.5 M HBr, different Rh concentration, 3-day aged; O: 15 v/o Kelex 100, 15 v/o tridecanol, 70 v/o kerosene; Different A/O volume ratios; CT: 3 min)

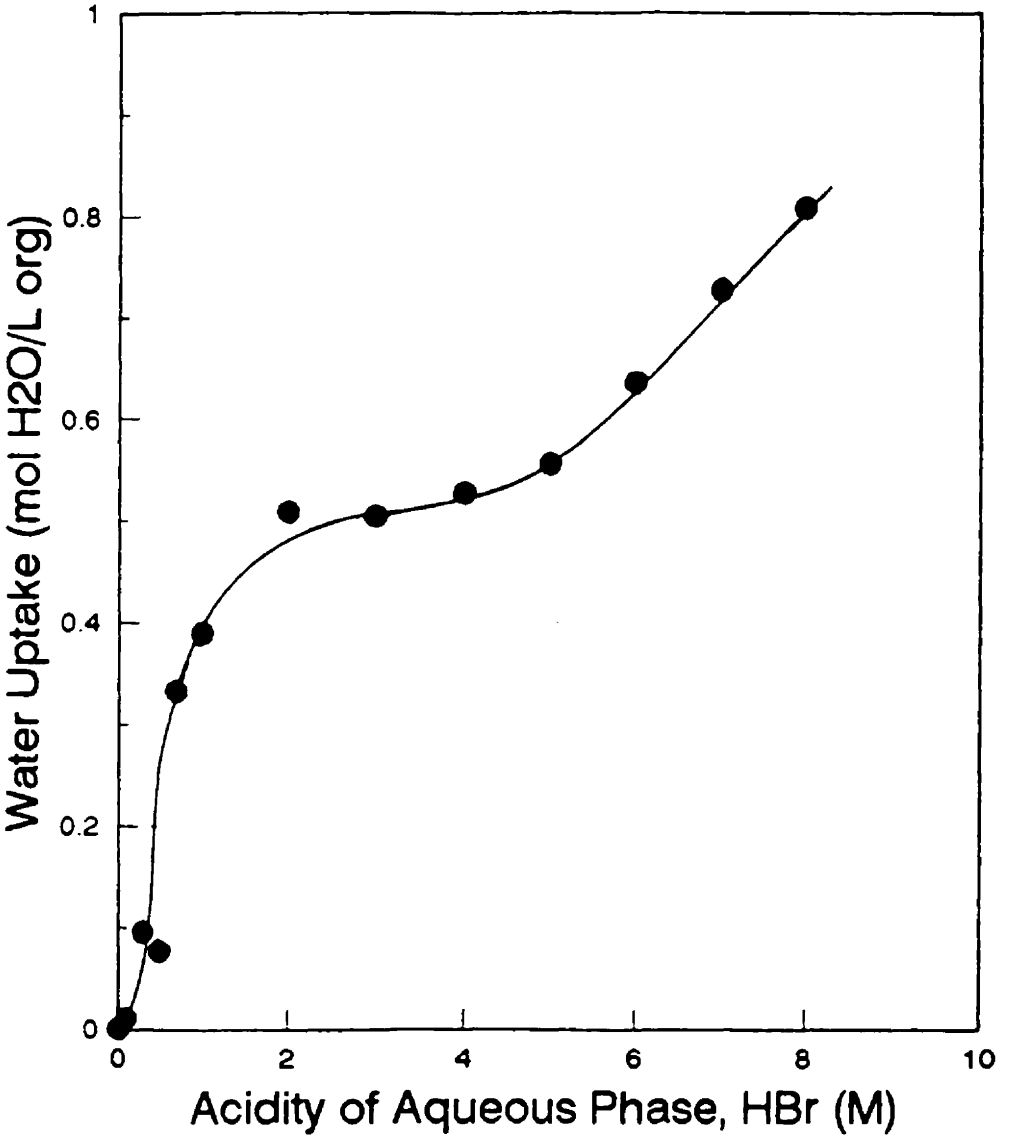

Figure 7.14: Effect of Acidity on Water Uptake

(A: 0-10 M HBr (no Rh); O: 5 v/o Kelex 100 (0.14 M),

5 v/o tridecanol, 90 v/o kerosene; CT: 3 min; A/O: 1)

7.5 STRIPPING

To find a suitable stripping medium, different solutions such as HCl, HBr, HNO_3, H_2SO_4, NaBr, NaCl, and H_2O were tried. Unfortunately, none of them were found to offer quantitative stripping, except HCl and water, both of which proved only partially successful in this respect. Here, it is worth mentioning that since the proposed mechanism of extraction is ion-pair formation (reactions (7.3) and (7.4)), it was expected that the loaded organic, upon contact with water (or more precisely a mild acidic solution – pH~2 – to prevent metal hydrolysis), would become fully stripped. However, this did not happen. It was also observed during these preliminary stripping tests that the color of the loaded organic phase changed with age (this happened over periods varying between a few hours and a few days). Thus the initial bright-yellow color of the organic phase was found to change gradually to dark-black, resulting, as it was recognized later, to metal lock-up. Further contacts of this organic with water or different acid solutions did not bring any improvement.

As mentioned before, the application of HCl did not yield satisfactory stripping results during the preliminary stage of this set of experiments. It became apparent later, though, that the contact time had a tremendous effect on the extent of stripping (Figure 7.15). As well, increasing HCl concentration was found to improve stripping (Figure 7.16). This observation led to the conclusion that the stripping mechanism is nothing else but the substitution of Cl^- with Br^- within the ion-pair of Rh complex and the protonated extractant (i.e., the reverse of reaction (7.2)). This confirms the previous observation (Figure 7.3) that the replacement of bromide with chloride ions is much easier when solutions of high HCl concentration are employed.

Having determined that concentrated HCl (i.e., 8 M) and long contact times (12 hours) are required to effect stripping of Rh, next the stripping isotherm was prepared (Figure 7.17). According to this strip isotherm, the complete removal of Rh from the loaded organic, and the production of a concentrated strip solution are possible with about two contact stages.

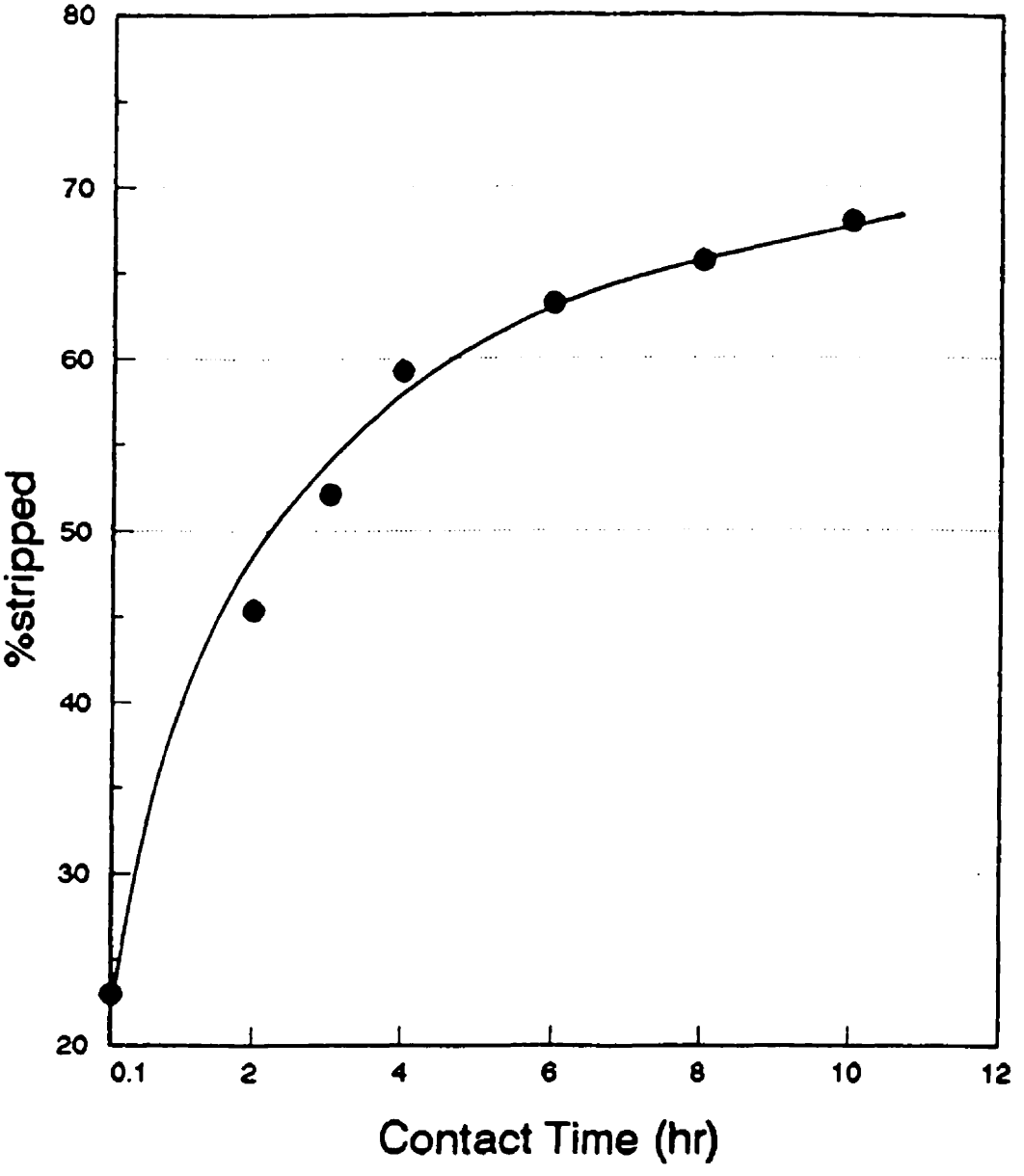

Figure 7.15: Effect of Contact Time on Stripping of Rh

(A: 6 M HCl; A/O: 1; O: 15 v/o Kelex 100 (0.42 M), 15 v/o tridecanol, 70 v/o kerosene, loaded 300 ppm Rh, Age of loaded organic: 5 min)

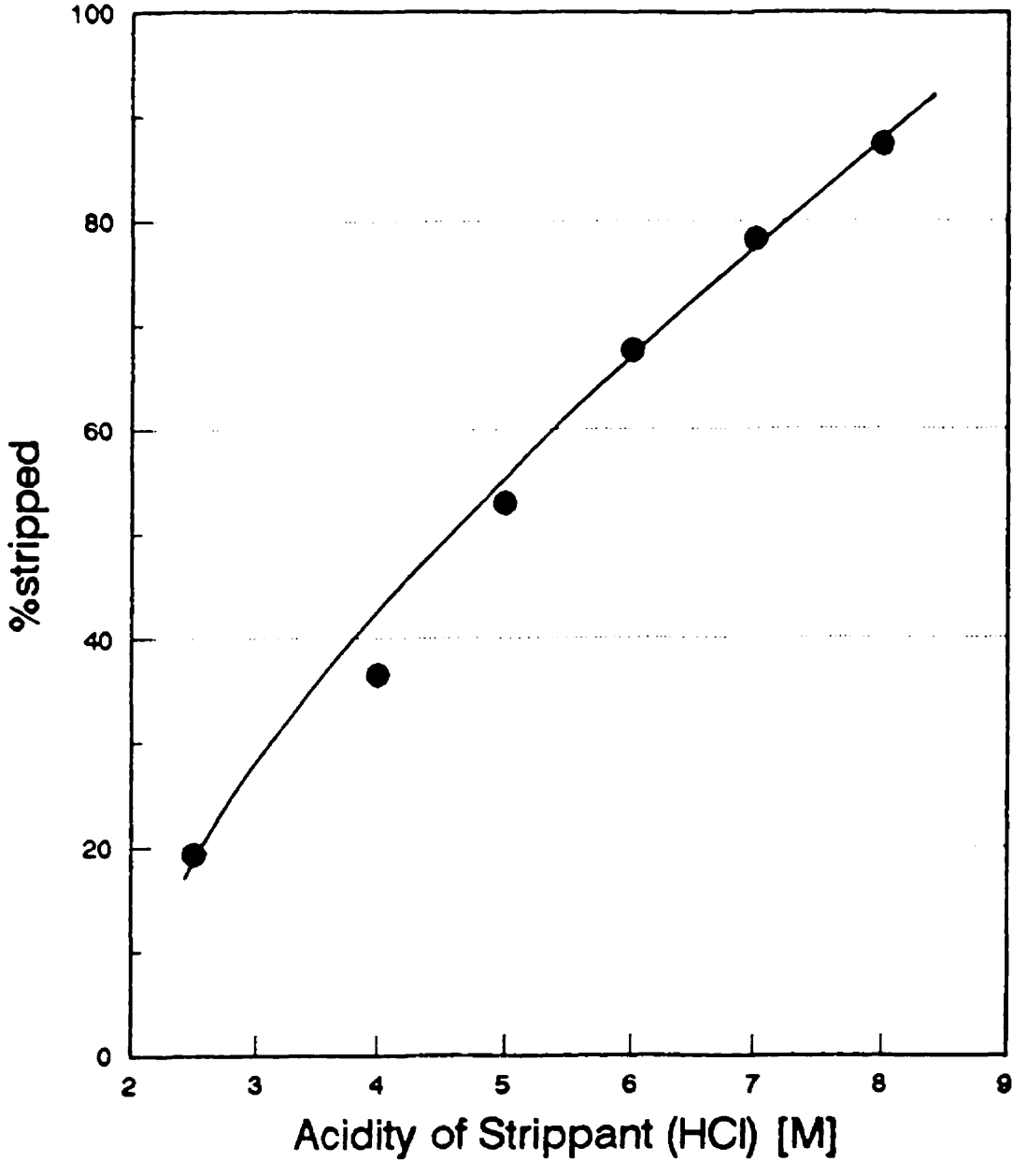

Figure 7.16: Effect of Acidity on Stripping of Rh with HCl (A: Different [HCl]; CT: 10 hr; A/O volume ratio: 1; O: 15 v/o Kelex 100; 15 v/o tridecanol; 70 v/o kerosene; loaded with 300 ppm Rh; Age of loaded organic: 5 min)

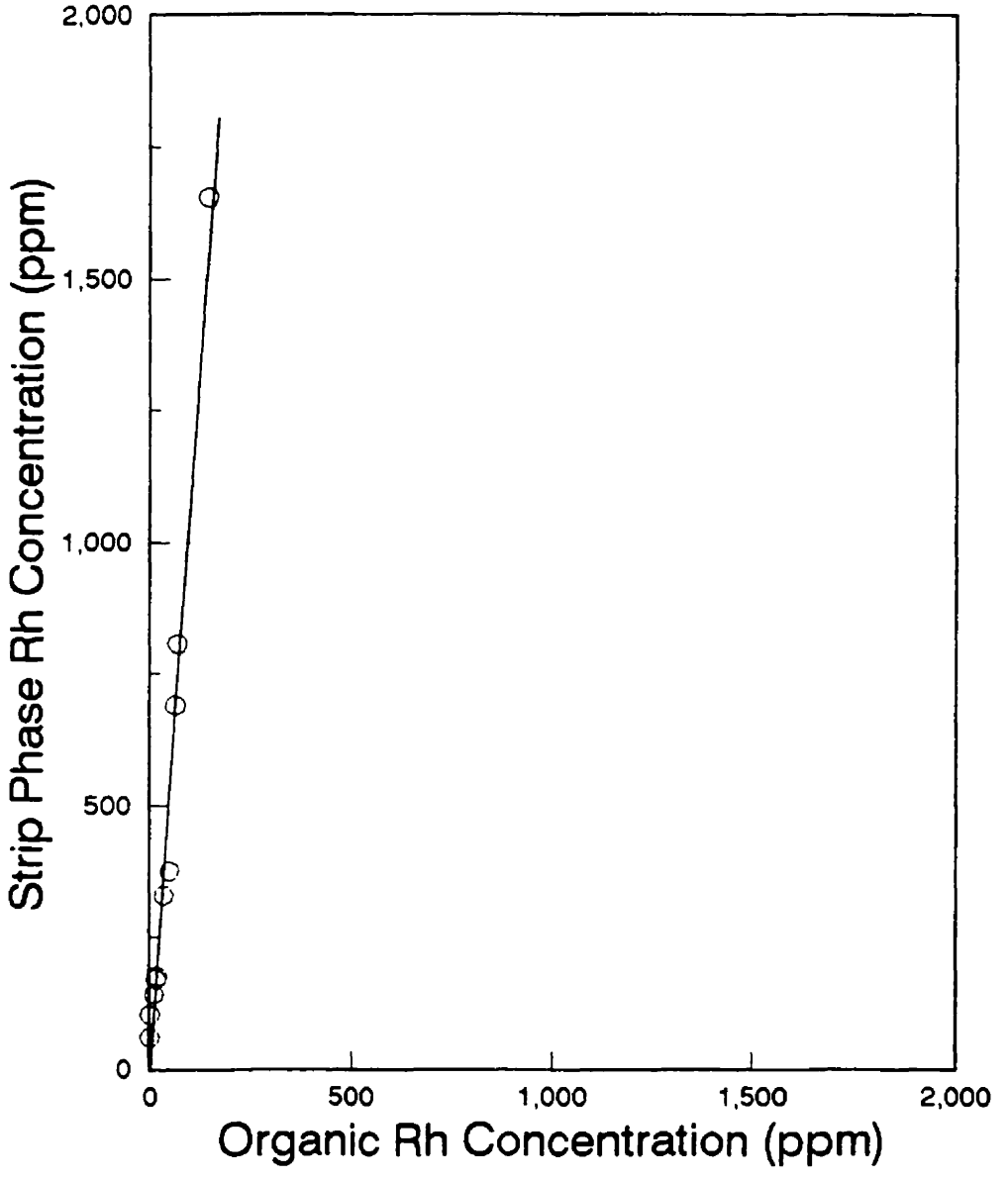

Figure 7.17: Stripping Isotherm of Rh with HCl (A: 8 M HCl; A/O: 1; CT: 12 hr; O: 5 v/o Kelex 100 (0.14 M), 5 v/o tridecanol, 90 v/o kerosene; loaded with 20-2000 ppm Rh; Age of loaded organic 5 min)

The stripping results of Figures 7.15 to 7.17 were obtained with freshly loaded organic phases (3 to 5 min age). However, when aged loaded organic phases were used, stripping performance was found to deteriorate (0.5% drop in stripping efficiency per hour of age) (Figure 7.18). This apparently relates to the color change of the loaded organic, as reported earlier, and implies that the extracted ion-pair undergoes certain transformation rendering rhodium unstrippable.

7.6 REGENERATION AND CHEMICAL STABILITY OF THE EXTRACTANT

To demonstrate that the freshly loaded organic phase of Kelex 100 can be stripped completely and reused for subsequent extraction cycles, a series of five recycle tests were conducted in which an organic phase of 15 v/o Kelex 100 was used. Upon extraction, the freshly (30-min aged) loaded organic was subjected to stripping with 6 M HCl at A/O volume ratio of 3, and then it was washed twice with water. The same "regenerated" organic was subsequently used in four extraction/stripping cycles. The results of these recycling tests are shown in Table 7.2. One will note from these data that the same level of extraction (93% in a single contact) was obtained in each cycle; while, in terms of stripping, all rhodium was stripped completely (again through a single contact) in each cycle. After this set of encouraging results a new series of tests was conducted to evaluate the long-term chemical stability of the extractant.

The chemical stability of the extractant in contact with concentrated HCl strip solution was tested by examining the loading capacity of the organic phase. This was measured via multiple contacts with a copper sulphate solution of pH 4 (De Schepper, 1989). The results are shown in Figure 7.19. As one may notice, no loss of loading capacity was observed after contacting the same organic phase (5 v/o Kelex 100) with 8 M HCl for 50 days.

Table 7.2: Consecutive Extraction/Stripping Cycles of Rh(III) Bromide Solutions with Kelex 100

Contact #	%Extraction	Raffinate (ppm)	Strippant (ppm)	%Rh left in Organic
1	93.0	28.7	126.3	0.56
2	92.5	30.8	126.7	0.00
3	94	24.6	126.7	1.32
4	93.5	26.7	130	-1.63

Feed: 410 ppm Rh (from Na_3RhCl_6), 1.5 M HBr, 3-day aged.

Org: 15 v/o Kelex 100, 15 v/o tridecanol, 70 v/o kerosene.

Ext: CT= 5 min; A/O = 1; one extraction stage.

Strip: CT = 12 hr; A/O = 3; Strip solution = 6 M HCl; one stripping stage.

In spite of this high stability of Kelex 100 against HCl media, which is known to be the most aggressive environment for the organic extractants, the non-efficient stripping of the metal species from the aged, loaded organic remains a problem. This loaded-organic aging phenomenon has not been studied in the present work.

7.7 PRECIPITATION-DISSOLUTION-EXTRACTION-STRIPPING CIRCUIT

Next it was decided to verify the effectiveness of the newly developed SX system by starting with a simulated (real) aged rhodium chloride solution instead of using a feed prepared artificially by dissolving Na_3RhCl_6 or $RhBr_3$ into HBr solution. The Rh chloride feed solution used had the following composition: 400 ppm Rh, 3-month age, 4 M HCl.

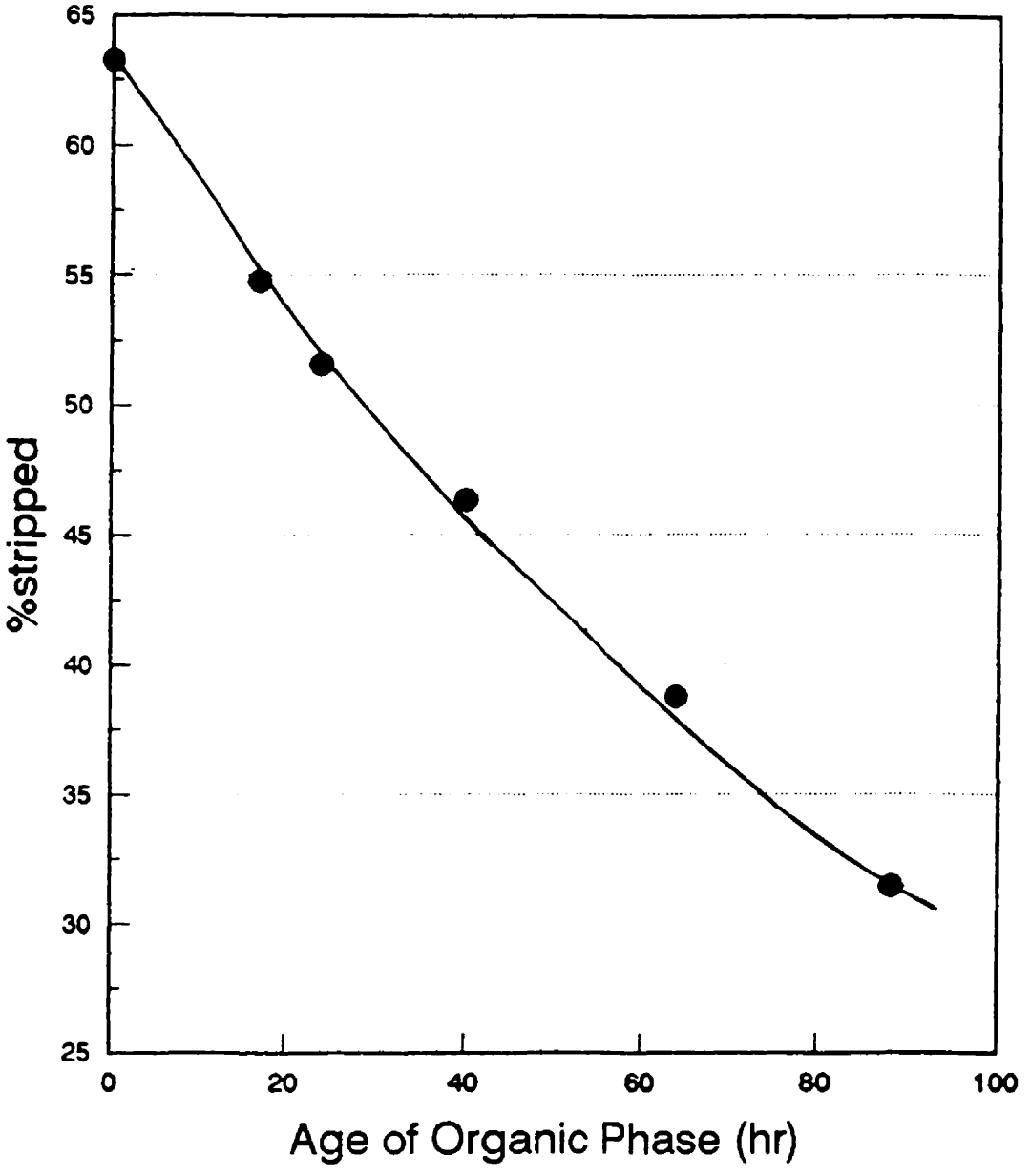

Figure 7.18: Effect of Aging of Loaded Organic on Stripping of Rh with HCl

(A: 6 M HCl; A/O volume ratio: 1; CT: 10 hr; O: 15 v/o Kelex 100, 15 v/o tridecanol, 70 v/o kerosene, loaded with 300 ppm Rh)

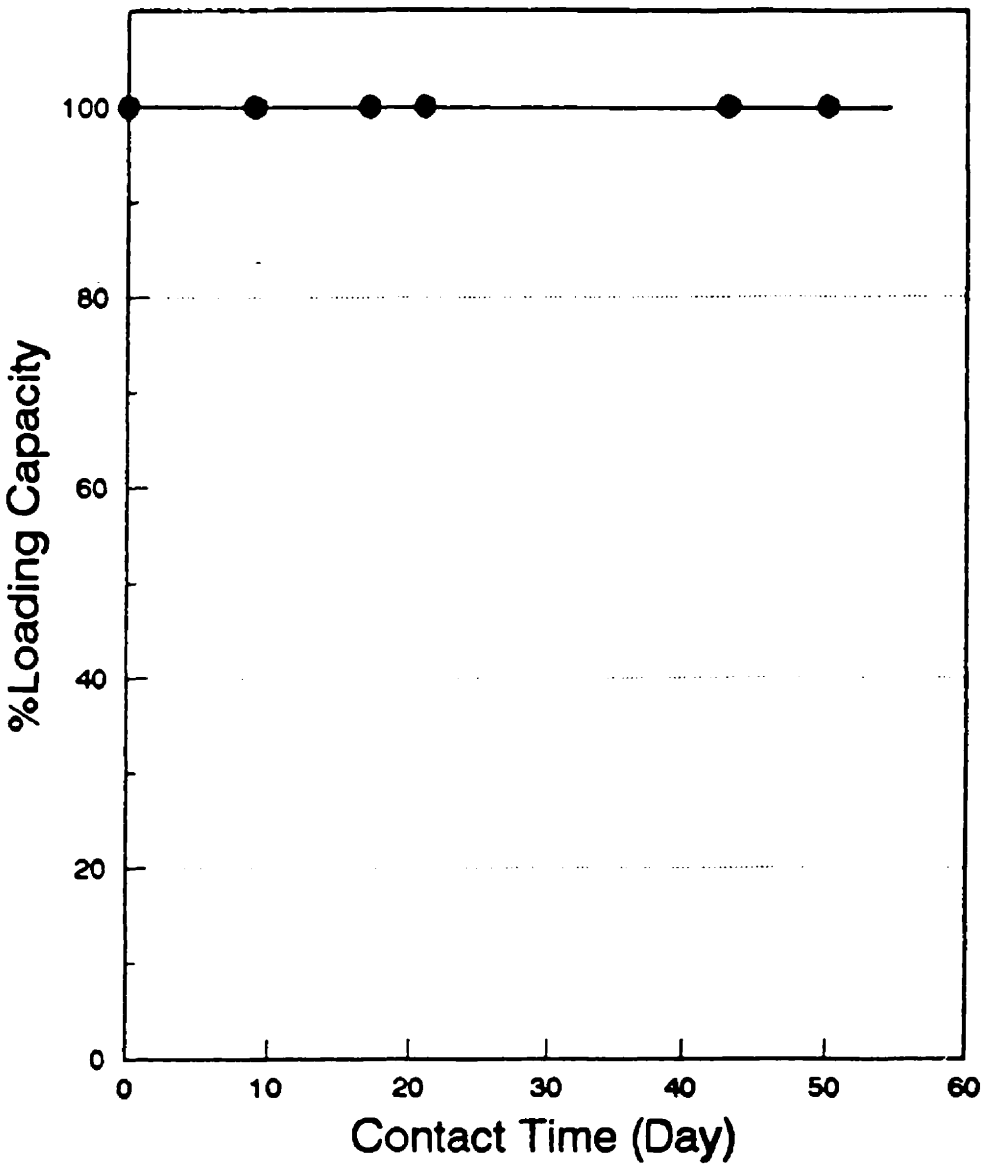

7.19: Long-Term Chemical Stability of Kelex 100

(A: 8 M HCl; O: 5 v/o Kelex 100, 5 v/o tridecanol, 90 v/o kerosene)

This aged chloride solution was first treated in the same manner as in the conventional Rh refining process (Figure 2.2). Thus, it was treated for 15 minutes with 3 M $NaNO_2$, while boiling at 105 °C, to convert the chlorocomplexes of Rh(III) to nitrite complexes (i.e., $Rh(NO2)_6^{3-}$), and then was allowed to cool to ambient temperature. After neutralizing the solution with NaOH to pH about 8, a concentrated NH_4Cl solution was added in order to precipitate the sodium ammonium salt of rhodium nitrite $Na(NH_4)_2[Rh(NO_2)_6]$. This precipitate, which forms in the course of minutes, would entirely precipitate the Rh values if a highly concentrated NH_4Cl solution is used (Grant, 1990). The precipitate was then readily dissolved in 1.5 M HBr solution at ambient temperature to produce a Rh(III) bromide solution of desired rhodium concentration. Apparently, the concentration of Rh in the final solution can be adjusted choosing the appropriate solid/solution volume ratio. The produced bromide solution of Rh(III) was allowed to age for 2-3 days, so that the bromocomplexes of Rh would have formed. As mentioned earlier, the solution could reach its equilibrium if heated at 80 °C for a few hours, however, the same results obtainable by aging over a period of 2-3 days under ambient temperature.

Subsequent to that, extraction/stripping experiments were performed using the produced 1.5 M HBr rhodium solution as the feed. In total, five complete extraction/stripping cycles were conducted with this feed, as done previously with the other artificially prepared solutions, presented in Table 7.2. Once more, identical results were obtained after each cycle (Table 7.3), proving the effectiveness of the new process. On the basis of these results, the flowsheet of Figure 7.20 is proposed as a totally new approach to refining of rhodium. Scrubbing of the loaded organic with a 1.5 M HBr solution prior to stripping with 6-8 M HCl is incorporated in the flowsheet as an additional means of improving the selectivity (impurity rejection) of the process.

Table 7.3: Consecutive Extraction/Stripping Cycles of Synthesized Rh(III) Bromide Solutions with Kelex 100

Contact #	%Extraction	Raffinate (ppm)	Strippant (ppm)	%Rh left in Organic
1	93.7	36.9	181.7	0.53
2	93.1	40.4	176.7	2.50
3	92.4	44.4	182.0	-0.92
4	94.1	34.5	181.0	1.28
5	93.5	38.0	182.2	0.00

Feed: 585 ppm Rh (from aged chloride solution), 1.5 M HBr, 3-day aged.
Org: 15 v/o Kelex 100, 15 v/o tridecanol, 70 v/o kerosene.
Extraction: CT: 5 min; A/O: 1; one extraction stage.
Strip: CT: 12 hr; A/O: 3; Strip solution: 6-8 M HCl; one stripping stage.

The new refining process offers several advantages. First, it has the potential of being considerably faster than the traditional one. Integration in the existing circuits should be rather straightforward, given the similarity of the front end of the new flowsheet (Figure 7. 20) to the conventional one (Figure 2.2). Impurity rejection is achieved by both the conventional NaOH hydrolysis step and the inherent selectivity of the solvent extraction step (enhanced further by the HBr scrubbing step – Figure 7.20). On the other hand, concentration of rhodium can be achieved via the HBr dissolving step (by choosing a high solid/solution ratio) as well as through the extraction and stripping stages (see respective isotherms).

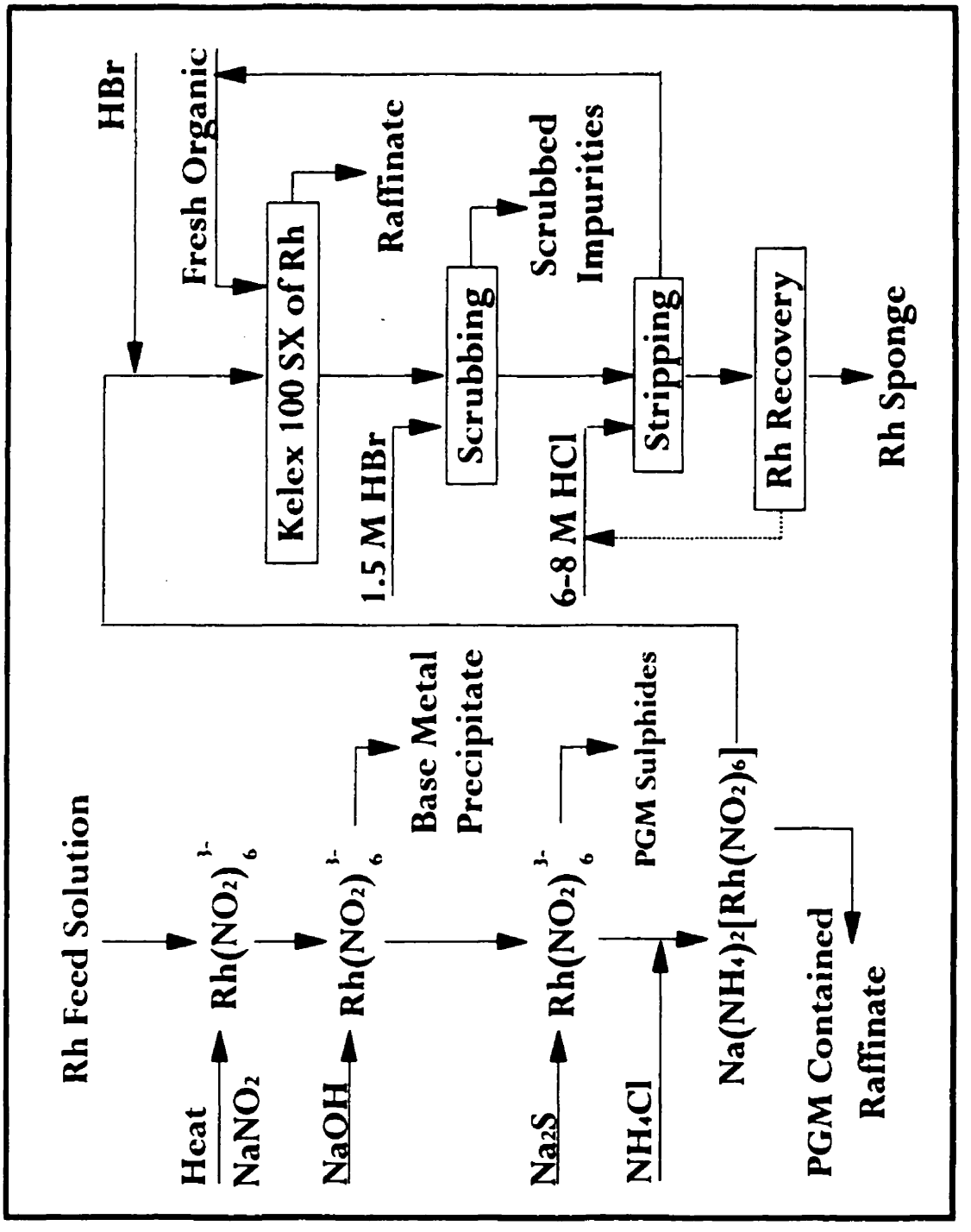

Figure 7.20: Proposed Rh Refining Flowsheet

7.8 SUMMARY

A novel SX-based separation scheme has been developed for the recovery of rhodium and its purification/concentration from chloride impure solutions. This new process consists of three steps: (i) precipitation of Rh from the chloride solution via the formation of $Na(NH_4)_2[Rh(NO_2)_6]$ salt as done in the front end of the conventional Rh refining process; (ii) dissolution of the Rh precipitate in an HBr solution (1.5 M) in which all rhodium species are converted upon 2-3 days aging (at ambient temperature or after a few hours heating at 80 °C) to bromocomplexes; (iii) solvent extraction of the latter with Kelex 100 and stripping with 6-8 M HCl. The new process scheme has the potential to offer simplicity and reduced processing times during which to achieve the concentration and purification of rhodium values, since it combines the benefits of the front end of the traditional refining process with the benefits of the modern solvent extraction technology. Further work, focusing both on the fundamental bromide chemistry of rhodium(III) in aqueous and organic solutions and on the development/optimization of the new process, is fully warranted.

CHAPTER 8

Conclusions

8.1 OVERALL CONCLUSIONS

1) The aquation of Rh(III) complexes in chloride media was confirmed experimentally through a series of extraction tests and UV-Visible spectroscopy investigations. The latter was found responsible for rendering Rh(III) which are not adequately extractable in conventional solvent contacting schemes. Even if Rh(III) is extracted from a fresh aqueous solution (i.e., from a solution not yet having undergone aquation), it still goes back into the aqueous phase. This unexpected behavior was found to be related to the presence of water inside the organic phase in the form of W/O microemulsions.

2) The formation of W/O microemulsions consisting of protonated Kelex 100-tridecanol-HCl-H_2O was confirmed experimentally through a variety of measurements such as Karl Fischer titration, viscosity, surfase tension, and light scattering measurements. The microemulsion water pools were found to have a 10-nm diameter and the ratio of H_2O/HCl/Kelex 100 to vary between 4/1/1 to 4.5/1.5/1. As a consequence of the aquation, which is catalyzed by microemulsion formation, a very low distribution coefficient for rhodium (i.e., 0.5) was obtained.

3) The use of a supported liquid membrane of Kelex 100 was found to overcome the limitations of the low distribution coefficient of Rh(III) permitting the quantitative transport-separation of the metal from a feed solution of 2.5 M HCl into a low-acidified HCl receiving phase at pH=1. The mechanism of extraction is via ion-pair formation between the protonated extractant molecules and the Rh chlorocomplexes ($RhCl_6^{3-}$), and the driving force for the permeation process is the acid activity gradient

across the membrane. As soon as $RhCl_6^{3-}$ species are withdrawn from the feed solution, the aquated chlorocomplexes, i.e., $RhCl_5(H_2O)^{2-}$, are converted to $RhCl_6^{3-}$ and extraction proceeds to completion. A Rh permeation rate in the order of 10^{-6} $mol.s^{-1}.m^{-2}$ was measured. This compares favorably with other analogous SLM systems. At the same time the Rh values were concentrated at least 10 times.

4) Acid (HCl) and water were found to be co-extracted along with the Rh(III) species via hydration of the extractant molecules and/or microemulsion formation. The rate of acid permeation was found to be about 100 times (in molar basis) that of Rh. The co-extraction of acid complicates the operation of the SLM and must be neutralized, or preferably, continuously removed from the receiving phase.

5) As a solution to the undesirable acid extraction in the SLM system, the co-extracted acid and Rh were separated through a SX process that involved co-extraction with trioctylamine (TOA) and differential stripping. The Rh(III) species are easily removed (extracted) from the freshly prepared SLM receiving solutions into the TOA organic phase, but not from the aged Rh solutions. The latter observation confirmed the previously claimed postulation that only the nonaquated Rh species ($RhCl_6^{3-}$) permeate through the SLM. UV-Visible observations verified that notion as well.

6) By combining SLM with SX it is possible to overcome the intrinsic drawbacks of both separation processes and design integrated separation circuits for metals like Rh(III), which are otherwise difficult to extract. Thus in the proposed combined SLM/SX circuit, Rh(III) is extracted due to the powerful driving force of SLM, which overcomes the low distribution coefficient of Rh (<0.5); while SX makes possible the operation of the SLM at its highest transfer (production) rate due to the continuous removal of HCl (and Rh(III)) from the receiving phase. In addition, the interfacing of the TOA solvent extraction process with the SLM system makes possible, in principle, the control of impurity carry-over through the downstream incorporation of scrubbing procedures.

7) Rh(III) species were found to undergo limited aquation in bromide media. This was confirmed with UV-Visible spectroscopic measurements and extraction tests. This property of Rh(III) in bromide solutions was used to design an altogether novel system of separation for rhodium(III). The main steps of this novel separation scheme are: (i) conversion of chlorocomplexes to bromocomplexes via precipitation of the $Na(NH_4)_2[Rh(NO_2)_6]$ salt; (ii) its subsequent dissolution into a HBr (1.5 M) solution; (iii) extraction of Rh(III) bromide species with Kelex 100, after the bromide-based solution has been aged for 3 days at ambient temperature, followed by stripping of the loaded organic with 6-8 M HCl. This newly identified scheme has the potential to develop into an attractive process from a practical implementation point of view.

8.2 ORIGINAL CONTRIBUTIONS TO KNOWLEDGE

1) The microemulsion structure of Kelex 100 organic phase was fully characterized for the first time. This helped to explain the low distribution coefficient of Rh(III) chlorocomplexes in conventional solvent extraction systems, and to figure out the mechanism of enhanced acid and water extraction into Kelex 100 organic phase.

2) The application of the supported liquid membrane (SLM) technique to the separation of Rh(III) from chloride solutions is a totally new contribution to knowledge. In particular, the demonstration that SLM systems can work in cases of metals with low distribution coefficients is a significant original finding.

3) The integration of SLM with conventional solvent extraction is another original conception in the search for systems that will overcome the shortcomings of each of these two processes.

4) The study of Rh(III) aquation in bromide media and the identification of a fully original approach to rhodium separation is yet another major contribution of this work.

8.3 SUGGESTIONS FOR FUTURE WORK

a. SLM Extraction of Rh(III)

The behavior of impurities and, in general, the selectivity of the SLM system should be investigated. In this regard, reagents other than Kelex 100, such as amines, may be used. The importance of precipitate formation and blockage of the pores of the membrane should be assessed. Those impurities which might block the membrane should be separated in advance, and separation of those which permeate the membrane should be carried out either through a scrubbing stage in TOA solvent extraction or through another process.

The design and testing of "SLM" systems with moving rather than stationary liquid membrane should be explored as a means of improving mass transfer rates and impurity rejection.

b. The Rh-HBr-Kelex 100 System

The bromide SX system shows great promise from a practical point of view. The process variables in all stages of the process – i.e., chloride/bromide conversion and extraction/stripping circuit – should be established in order to design a viable process flowsheet. In this regard, further investigations on the aging of the loaded organic are of vital importance.

The performance of the system against impurities and, in particular, against iridium is another important aspect that needs further investigation.

REFERENCES

Akiba, K., and Hashimoto, H., Extraction of Uranium by a Supported Liquid Membrane Containing Mobile Carrier, *Talanta*, **32(8B),** 824-826, 1985.

Al-Bazi, S.J., and Chow, A., Platinum Metals – Solution Chemistry and Separation Methods (Ion-Exchange and Solvent Extraction), *Talanta*, **31(10A),** 815-836, 1984.

Ashbrook, A.W., Commercial Chelating Solvent Extraction Reagents. IV. Alkenyl 8-Hydroxyquinoline. Spectra and Proton-Ligand Stability Constants, *Hydrometallurgy*, **1,** 93-96, 1975.

Ashbrook, A.W., Commercial Chelating Solvent Extraction Reagents. II. Purification and Properties of β-alkenyl-8-hydroxyquinoline, *J. Chromatogr.*, **105,** 151-156, 1975.

Ashrafizadeh, S.N., Cation Exchange with Reverse-Micelles, M.Eng. Thesis, McGill University, Montreal, 1992.

Ashrafizadeh, S.N., Weber, M.E., and Vera, J.H., Cation Exchange with Reverse Micelles, *Ind. Eng. Chem. Res.*, **32(1),** 125-132, 1993.

Ayres, G., and Tuffly, B., Spectrophotometric Determination of Palladium with Bromide, *Anal. Chem.*, **24,** 949-952, 1952.

Baird, R.S., Bunge, A.L., and Noble, R.D., Batch Extraction of Amines Using Emulsion Liquid Membranes: Importance of Reaction Reversibility, *AIChE J.*, **33(1),** 43-53, 1987.

Baker, R., and Blume, I., Coupled Transport Membranes, Handbook of Industrial Membrane Technology, M.C. Porter (ed.), Noyes, NJ, USA, 511-558, 1990.

Barnes, D.E., Marshall, G.D., and Van Staden, J.F., Rapid Optimization of Chemical Parameters Affecting Supported Liquid Membranes, *Sep. Sci. Technol.*, **30(5),** 751-776, 1995.

Bauer, D., Cote, G., Komornicki, J., and Mallet-Faux, S., Use of Microemulsions to Obtain Fast Kinetics in Extraction of Gallium(III) and Germanium(IV) by Kelex 100 in Acidic Medium, in Proc. 2nd Int. Conf. Sep. Sci. Technol., M.H.I. Baird and S. Vijayan (eds.), Can. Soc. Chem. Eng., Ottawa, Ont., Vol 2, p. 425-432, 1989.

Bauer, D., Fourré, P., and Lemerle, J., Existence d'une Microémulsion Dans les Systèmes d'Extraction du Gallium par la β-Dodécényl-7 Hydroxy-8 Quinoléine dite Kelex 100, *C .R. Acad. Sc. Paris*, **t. 292,** Série II, 1019-1022, 1981.

Beamish, F.E., A Critical Review of Methods of Isolating and Separating the Noble Metals -II Ion Exchange and Solvent Extraction, *Talanta*, **14**, 991-1009, 1967.

Benguerel , E., Demopoulos, G.P., Cote, G., and Bauer, D., An Investigation on the Extraction of Rhodium from Aqueous Chloride Solutions with 7-substituted 8-hydroxyquinolines, *Solvent Extr. Ion Exch.*, **12(3)**, 497-516, 1994.

Benguerel, E., and Demopoulos G.P., A Novel Solvent Extraction System for Rhodium, in Solvent Extraction in the Process Industries, Proc. ISEC'93, D.H. Logsdail and M.J. Slater (eds.), Elsevier Applied Sci., London, UK, p. 376-383, 1993.

Benguerel, E., Cote, G., Lautié, A., Demopoulos, G., and Bauer, D., Characterization of Extracted Complexes in Liquid-Liquid Extraction of Rhodium with Kelex 100 in the Presence of $SnCl_2$, *J. Chem. Tech. Biotechnol.*, **62**, 380-384, 1995.

Benguerel, E., Demopoulos, G. P., and Harris, G. B., Speciation and Separation of Rhodium (III) from Chloride Solutions: A Critical Review, *Hydrometallurgy*, **40**, 135-152, 1996.

Benguerel, E., Solvent Extraction of Rhodium from Chloride Solutions in the Presence of $SnCl_2$ with Kelex 100, Ph.D. Thesis, McGill University, Montreal, 1996.

Benner, L. S., Suzuki, T., Meguro, K., and Tanaka, S., Precious Metals Science and Technology, The International Precious Metals Institute, Allentown, PA, 1991.

Berne, B.J., and Pecora, R., Dynamic Light Scattering, Wiley, New York, USA, 1976.

Bhattacharyya, S.N., and Ganguly, B., Study of the Aggregation Behavior of Di(2-ethyl hexyl)Phosphoric Acid in Heptane in the Presence of Water, *J. Colloid Interface Sci.*, **118(1)**, 15-19, 1987.

Bock, J., and Valint, P.L., Uranium Extraction from Wet Process Phosphoric Acid. A Liquid Membrane Approach, *Ind. Eng. Chem. Fundam.*, **21**, 417-422, 1982.

Bockris, J. O'M., and Reddy, A.K.N., Modern Electrochemistry, Plenum Publishing Co., New York, USA, p. 461, 1970.

Bolinski, L., Platinum and Rhodium Recovery from Scrapped Automotive Catalyst by Oxidative Acid Chloride Leaching, M. Eng. Thesis, McGill University, Montreal, 1991.

Boumezioud, M., Derouiche, A., and Tondre, C., Solubilization versus Microemulsification of Extractant Molecules in Micellar Systems: Comparison between 8-Hydroxyquinoline and Kelex 100, *J. Colloid Interface Sci.*, **128(2)**, 422-426, 1989.

Boutonnet, M., Kizling, J., and Stenius, P., The Preparation of Monodisperse Colloidal Metal Particles from Microemulsions, *Colloids and Surfaces*, **5**, 209-225, 1982.

Boyadzhiev, L., Liquid Pertraction or Liquid Membranes-State of Art, *Sep. Sci. Technol.*, **25(3),** 187-205, 1990.

Boyadzhiev, L., Sapundzhiev, T., and Bezenshek, E., Modeling of Carrier-Mediated Extraction, *Separation Science*, **12(5),** 541-551, 1977.

Breuning, R.L., Izatt, S.R., and Griffin, L.D., Separation of Rh and/or Ir from Concentrated Precious and Base Metal Matrices Using SuperLig™ 1, in Precious Metals 1990, D.A. Corrigan (ed.), IPMI, Allentown, PA, p. 97, 1990.

Bridges, K.L., and Chang, J.C., The cis-trans Isomers of Tetrachlorodiaquorhodate(III) Anion, *Inorg. Chem.*, **6(3),** 619-620, 1967.

Bromberg, L., Levin, G., and Kedem, O., Transport of Metals through Gelled Supported Liquid Membranes Containing Carrier, *J. Membrane Sci.*, **71**, 41-50, 1992.

Bromley, L.A., Thermodynamic Properties of Strong Electrolytes in Aqueous Solutions, *AIChE J.*, **19**, 313-325, 1973.

Budde, W.M., and Hartlage, J.A., US Patent 3 637 711, 1972.

Butler, I.S., and Harrod, J.F., Inorganic Chemistry Principles and Applications, The Benjamin/Cummings Publishing Company, Inc., Redwood City, CA, p. 396, 1989.

Cabri, L.J., and Naldrett, A.J., The Nature of the Distribution and Concentration of Platinum-Group Elements in Various Geological Environments, Proc. 27th Int. Geol. Cong., V. 10, p. 17-46, 1984.

Cahn, R.P., and Li, N.N., Separation of Phenol from Waste Water by the Liquid Membrane Technique, *Separation Science*, **9(6),** 505-519, 1974.

Calvarin, L., Roche, B., and Renon, H., Anion Exchange and Aggregation of Dicyanocobalamin with Quaternary Ammonium Salts in Apolar Environment, *Ind. Eng. Chem. Res.*, **31**, 1705-1709, 1992.

Carr, C., Glaser, J., and Sandström, M., ^{103}Rh NMR Chemical Shifts of All Ten $[RhCl_n(OH_2)_{6-n}]^{3-n}$ Complexes in Aqueous Solution, *Inorg. Chim. Acta*, **131**, L53-L56, 1987.

Carson, N., Platinum-Supply, Demand and Outlook, in Precious Metals 1989, B. Harris (ed.), IPMI, Allentown, PA, p. 7-10, 1989.

Choppin, G.R., Solvation and Hydration in Solvent Extraction, in Solvent Extraction 1990, Proc. ISEC'90, T. Sekine (ed.), Elsevier Science Publishers, Amsterdam, The Netherlands, part A, p. 61-68, 1992.

Claassen, H.H., Selig,, H., Malm, J.G., Chernick, C.L., and Weinstock, B., Ruthenium Hexafluoride, *J. Am. Chem.*, **83**, 2390-2391, 1961.

Coté, B., and Demopoulos, G.P., New 8-Hydroxyquinoline Derivative Extractants for Platinum Group Metal Separation. Part I: Characterization and HCl Extraction, *Solvent Extr. Ion Exch.*, **11(2)**, 349-376, 1993.

Coté, B., and Demopoulos, G.P., New 8-Hydroxyquinoline Derivative Extractants for Platinum Group Metals Separation. Part 3: Pt(IV) Extraction Equilibria and Stripping, *Solvent Extr. Ion Exch.*, **12(3)**, 517-540, 1994.

Coté, B., and Demopoulos, G.P., New 8-Hydroxyquinoline Derivetive Extractants for Platinum Group Metals Separation. Part 2: Pd(II) Extraction Equilibria and Stripping, *Solvent Extr. Ion Exch.*, **12(2)**, 393-421, 1994.

Coté, B., Benguerel, E., and Demopoulos, G.P., Solvent Extraction Separation of Platinum Group Metals, in Precious Metals 1993, R.K. Mishra (ed.), IPMI, Allentown, PA, p. 593-617, 1993.

Coté, B., Solvent Extraction of Pt(IV) and Pd(II) with 7-Substituted 8-Hydroxyquinoline Derivatives, Ph.D Thesis, McGill University, Montreal, 1994.

Cote, G., and Bauer, D., Some Typical Behaviours of the β-Dodecenyl 8-Hydroxyquinoline–II Its Distribution Brtween Aqueous and Organic Phases, *J. Inorg. Nucl. Chem.*, **43**, 1023-1030, 1981.

Cotton, F.A., and Wilkinson, G., Advanced Inorganic Chemistry, A Comprehensive Text, John Wiley & Sons, Inc., New York, USA, 4th ed., 1980.

Cowley, A., Platinum 1995, Johnson Matthey, London, UK, 1995.

Cox, M., and Flett, D.S., Metal Extractant Chemistry, in Handbook of Solvent Extraction, T.C. Lo, M.H.I. Baird, C. Hanson (eds.), John Wiley & Sons, Inc., New York, USA, Chapter 2.2, p. 53-89, 1983.

Cozzi, D., and Pantani, F., A Polarographic and Spectrophotometric Investigation of Rhodium(III) Bromocomplexes, *J. Electroanal. Chem.*, **2**, 72-79, 1961.

Cozzi, D., and Pantani, F., The Polarographic Behavior of Rhodium(III) Chlorocomplexes, *J. Inorg. Nucl. Chem.*, **8**, 385-398, 1958.

Danesi, P.R., and Rickert, P.G., Some Observations on the Performance of Hollow Fiber Supported Liquid Membranes for Cobalt-Nickel Separations, *Solvent Extr. Ion. Exch.*, **4**, 149-164, 1986.

Danesi, P.R., Horwitz, E.P., Vandegrift, G.F., and Chiarizia, R., Mass Transfer Rate through Liquid Membranes: Interfacial Chemical Reactions and Diffusion as Simultaneous Permeability Controlling Factors, *Sep. Sci. Technol.*, **16(2),** 201-211, 1981.

Danesi, P.R., Separation of Metal Species by Supported Liquid Membranes, *Sep. Sci. Technol.*, **19(11&12),** 857-894, 1984/1985.

Danesi, P.R., Supported Liquid Membranes in 1986: New Technology or Scientific Curiosity?, in Proc. ISEC'1986, Society of the Chemical Industry, London, UK, Vol. 1, p. 527-536, 1986.

De Schepper, A.J.M., European Patent, 0 324 963 A1, 1989.

Deblay, P., Delepine, S., Minier, M., and Renon, H., Selection of Organic Phases for Optimal Stability and Efficiency of Flat-Sheet Supported Liquid Membrane, *Sep. Sci. Technol.*, **26(1),** 97-116, 1991.

Demopoulos, G.P., and Distin, P.A., On the Structure and Composition of Kelex 100, *Hydrometallurgy*, **11**, 389-396, 1983.

Demopoulos, G.P., Benguerel, E., and Harris, G.B., Solvent Extraction of Rhodium, US Patent 5 201 942, 1993.

Demopoulos, G.P., Kuyucak, N., Gefvert, D.L., and Richter, M.H., TN 1911: A New Hydroxyquinoline Extrctant for the Refining of Platinum Metals, in Precious Metals 1989, B. Harris (ed.), IPMI, Allentown, PA, p. 201-215, 1989.

Demopoulos, G.P., Pouskouleli, G., and Prud'homme, P.J.A., US Patent 4 654 145, 1987a.

Demopoulos, G.P., Pouskouleli, G., and Prud'homme, P.J.A., Canadian Patent 1 223 125, 1987b.

Demopoulos, G.P., Solvent Extraction in Precious Metals Refining, *J. Metals*, **38(6),** 13-17, 1986.

Dhara, S.C., Solvent Extraction of Precious Metals with Organic Amines, in Precious Metals: Mining, Extraction and Processing, V. Kudryk, D.A. Corrigan, W.W. Liang (eds.), TMS/AIME, Warrendale, PA, p. 199-226, 1984.

Dhara, S.C., The Application of Ion Exchangers in the Precious Metals Technology, in Precious Metals 1993, R.K. Mishra (ed.), IPMI, Allentown, PA, p. 375-410, 1993.

Dickson, R.S., Homogeneous Catalysis with Compounds of Rhodium and Iridium, D. Reidel Publishing Co., Dordrecht, Holland, 1985.

Draxler, J., and Marr, R., Emulsion Liquid Membranes Part I: Phenomenon and Industrial Application, *Chem. Eng. Process.*, **20**, 319-329, 1986.

Dziwinski, E., Cote, G., Bauer, D., and Szymanowski, J., Composition of Kelex 100, Kelex 100S, and Kelex 108: A Discussion on the Role of Impurities, *Hydrometallurgy*, **37**, 243-250, 1995.

Eyal, A.M., Arbel-Hadad, M., Hadi, S., Canari, R., Haringman, A., and Hazan, B., Extraction of Acids, Water and Hydrophilic Molecules by Amines and Amine Salts, in Solvent Extraction in the Process Industries, Proc. ISEC '93, D.H. Logsdail and M.J. Slater (eds.), Elsevier Applied Sci., London, UK, Vol 2, p. 723-730, 1993.

Fedorenko, N.V., and Ivanova, T.I., Extraction of Rhodium and Iridium from Hydrochloric Acid Solutions with Tri-n-Octylamine, *Russ. J. Inorg. Chem.*, **10(3)**, 387-389, 1965.

Fleming, C.A., Green, B.R., and Ashurst, K.G., in ISEC'80, Asso. Ing. Univ. Liege (eds.), Liege, Belgium, paper #80, p. 224-228, 1980.

Flett, D.S., Solvent Extraction and Membrane Processes in the Treatment of Metalliferous Effluents and Wastes, Proc. Int. Solvent Extraction Conf. 1990, T. Sekine (ed.), Elsevier Science Publishers, p. 1-22, 1992.

Fourré, P., Bauer, D., and Lemerle, J., Microemulsions in the Extraction of Gallium with 7-(1-ethenyl-3,3,5,5-tetramethylhexyl)-8-quinolinol from Aluminate Solutions, *Anal. Chem.*, **55**, 662-667, 1983.

Fu, J., Nakamura, S., and Akiba, K., Liquid Membrane Transport of Gold by a Trioctylamine Mobile Carrier, *Analytical Sciences*, **10**, 935-938, 1994.

Fu, J., Nakamura, S., and Akiba, K., Extraction of Platinum(IV) with Trioctylamine and Its Application to Liquid Membrane Transport, *Sep. Sci. Technol.*, **30(4)**, 609-619, 1995(a).

Fu, J., Nakamura, S., and Akiba, K., Separation and Recovery of Gold, Platinum and Palladium by a Trioctylamine Liquid Membrane, *Analytical Sciences*, **11**, 149-153, 1995(b).

Fu, J., Nakamura, S., and Akiba, K., Transport of Palladium(II) through Trioctylamine Liquid Membrane, *Sep. Sci. Technol.*, **30(5)**, 793-803, 1995(c).

Gareil, P., De Beler, S., and Bauer, D., Composition Analysis of Kelex 100, An Industrial Chelating Extractant, by Liquid Chromatography and Mass Spectrometry, *Hydrometallurgy*, **22**, 239-248, 1989.

Ginzburg, S. I., Ezerskaya, N.A., Prokof'eva, I.V., Fedorenko, N.V., Shlenskaya, V.I., and Bel'skii, N.K., Analytical Chemistry of the Platinum Metals, John Wiley & Sons, New York, USA, 1975.

Goklen, K.E., Liquid-Liquid Extraction of Biopolymers: Selective Solubilization of Proteins in Reverse Micelles, Ph.D. Thesis, Massachusetts Institute of Technology, Massachusetts, USA, 1986.

Goldschmidt, V.M., The Principles of Distribution of Chemical Elements in Minerals and Rocks, *J. Chem. Soc.*, **10**, 655-673, 1937.

Goto, M., Irie, J., Kondo, K., and Nakashio, F., Electrical Demulsification of W/O Emulsion by Continuous Tubular Coalescer, *J. Chem. Eng. Japan*, **22(4)**, 401-406, 1989.

Grant, R.A., The Separation Chemistry of Rhodium and Iridium, in Precious Metal Recovery and Refining, Proc. IPMI 1990, L. Manjiek (ed.), IPMI, Allentown, PA, p. 7-39, 1990.

Griffith, W.P., The Chemistry of the Rarer Platinum Metals, Interscience Publisher, London, UK, p. 13, 1967.

Haesebroek, G., Purity and Long-Term Stability of 8-Hydroxyquinoline-Based Metal Extractants, in: Non Ferrous Metallurgy-Present and Future, EMC'91, Elsevier Applied Science, London, UK, p. 301-304, 1991.

Hampel, C.A., Rare Metals Handbook, Reinhold, New York, Chap. 17, p. 304-335, 1954.

Haraguchi, K., and Freiser, H., Equilibrium and Kinetics of the Extraction of Nickel with 7-Dodecenyl-8-quinolinol (Kelex 100), *Inorg. Chem.*, **22**, 1187-1190, 1983.

Harris, G.B., A Review of Precious Metals Refining, in Precious Metals 1993, R.K. Mishra (ed.), IPMI, Allentown, PA, p. 351-367, 1993.

Hartlage, J. A., Cronberg, A. D., and Gefvert, D. L., Inst. Chem. Symp. Ser., 42 (Hydrometallurgy), 13, p. 7, 1975.

Ho, W.S.W., and Sirkar, K.K., Membrane Handbook, Van Nostrand Reinhold, New York, USA, p. 764-808, 1992.

Hollingshead, R. G. W., Oxine and Its Derivatives, I-IV, Buttersworth, London, UK, 1954.

Ichiishi, S., Griffin, L.D., and Breuning, R.L., The Recovery and Purification of Rhodium Using SuperLig™ Technology from a Platinum Group Metals Stream, in Rhodium/Sampling and Analysis, R.C. Kaltenbach and L. Manziek (eds.), IPMI, Allentown, PA, p. 159-163, 1992.

Inoue, K., Yoshizuka, K., Yamauchi, T., and Hudson, M. J., Separation of Rh(III) from Base Metals by Solvent Extraction with Pyridine Derivatives, in Solvent Extraction in the

Process Industries, Proc. ISEC'93, D.H. Logsdail and M.J. Slater (eds.), Vol 3, p. 1287-1294, 1993.

Ismael, M., and Tondre, C., Kinetically Controlled Separation of Nickel(II) and Cobalt(II) Using Micelle-Solubilized Extractant in Membrane Processes, *Langmuir*, **8**, 1039-1041, 1992.

Jansz, J.J.C., Estimation of Ionic Activities in Chloride Systems at Ambient and Elevated Temperatures, *Hydrometallurgy*, **11**, 13-31, 1983.

Jorgensen, C.K., Absorption Spectra and Chemical Bonding in Complexes, Pergamon Press, London, UK, Chapter 14, 262-283, 1962.

Jorgensen, C.K., Crystal Field Spectra of Rhodium(III) and Iridium(III), *Acta Chem. Scand.*, **10**, 500-517, 1956.

Kesting, R.E., Synthetic Polymeric Membranes, John Wiley & Sons, Inc., New York, 1985.

Khan, M.A., and Morris, D.F.C., Application of Solvent Extraction to the Refining of Precious Metals. I. Purification of Rhodium, *J. Less-Common Met.*, **13**, 53-61, 1967.

Khattak, M.A., and Magee, R.J., Extraction of Platinum Metals by High-Molecular-Weight Amines. Rhodium(III) Systems, *Anal. Chim. Acta*, **45**, 297-304, 1969.

Khoshkbarchi, M.K., and Vera, J.H., Formation of Water in Oil Microemulsions with Three Dialkyl Sodium Phosphinates in Alcohol/Isooctane Mixtures, *J. Colloid Interface Sci.*, **170**, 562-568, 1995.

Khoshkbarchi, M.K., and Vera, J.H., Measurement and Correlation of Ion Activity Coefficients in Aqueous Single Electrolyte Solutions, *AIChE J.*, **42**, 294-258, 1996.

Kiani, A., Bhave, R.R., and Sirkar, K.K., Solvent Extraction with Immobilized Interfaces in a Microporous Hydrophobic Membrane, *J. Membrane Sci.*, **20**, 125-145, 1984.

Kim, H.S., and Tondre, C., Kinetics of Complexation of Ni^{2+} with 8-Hydroxyquinoline and a C_{11}-Alkylated Analogue in Cetyltrimethylammonium Bromide Micellar Solutions, *Langmuir*, **5**, 395-397, 1989.

Klein, W., and Schneider, K., Exchange Processes Using Impregnated Membrane with Maintenance of Impregnant on Membrane, US Patent 4 659 473 21, 1987.

Knothe, M., Study of Rhodium-Platinum Separation with Solid and Liquid Cation Exchangers, *J. Radioanal. Chem.*, **52(2),** 335-341, 1979.

Kotlarchyk, M., Chen, S., and Huang,, J.S., Temperature Dependence of Size and Polydispersity in a Three-Component Microemulsion by Small-Angle Neutron Scattering, *J. Phys. Chem.*, **86(17),** 3273-3276, 1982.

Krei, G.A., and Hustedt, H., Extraction of Enzymes by Reverse Micelles, *Chem. Eng. Sci.*, **47(1),** 99-111, 1992.

Kremesec, V.J., Modeling of Dispersed-Emulsion Separation Systems, *Sep. Purif. Methods*, **10(2),** 117-157, 1981.

Leung, R., and Shah, D.O., Solubilization and Phase Equilibria of Water-in-Oil Microemulsions II. Effects of Alcohols, Oils, and Salinity on Single-Chain Surfactant Systems, *J. Colloid Interface Sci.*, **120(2),** 330-344, 1987.

Li, N. N., US patent 3 410 794, 1968.

Lide, D.R., CRC Handbook of Chemistry and Physics, CRC Press, Inc., New York, 76th Edition, 1993.

Lloyd, D.R., Materials Science of Synthetic Membranes, American Chemical Society, Washington, D.C., 1985.

Loebenstein, J.R., Mineral Facts and Problems, US Bureau of Mines, Bulletin 675, p. 595, 1985.

Mann, B. E., and Spencer, C. M., ^{103}Rh Chemical Shifts of $[RhCl_{6-n}Br_n]^{3-}$, *Inorg. Chim. Acta*, **76**, L65-L66, 1983.

Mann, B.E., and Spencer, C., The Identification of All Ten $[Rh(OH_2)_{6-n}Cl_n]^{3-n}$ Isomers by ^{103}Rh NMR Spectroscopy, *Inorg. Chim. Acta*, **65**, L57-L58, 1982.

Mann, B.E., The University of Sheffield, Sheffield, UK, private communication to Ashrafizadeh, S.N., 1995.

Marr, R., Bart, H.J., and Draxler, J., Liquid Membrane Permeation, *Chem. Eng. Process.*, **27**, 59-64, 1990.

Martell, A.E., Coordination Chemistry, Vol. 1, Van Nostrand Reinhold Co., New York, USA, p. 397, 1971.

Matulevicius, E.S., and Li, N.N., Facilitated Transport through Liquid Membranes, *Sep. Purif. Methods*, **4(1),** 73-96, 1975.

Meissner, H.P., and Kusik, C.L., Activity Coefficients of Strong Electrolytes in Multicomponent Aqueous Solutions, *AIChE J.*, **18(2),** 294-298, 1972.

Meissner, H.P., Prediction of Activity Coefficients of Strong Electrolytes in Aqueous Systems, in Thermodynamics of Aqueous Systems with Industrial Applications, ACS Symposium Series 133, p. 495-511, 1980.

Miesiac, I., Schügerl, K., Szymanowski, J., and Sobczynska, A., Physicochemical Approach to Emulsifier Selection for Emulsion Liquid Membranes, in Solvent Extraction in the Process Industries, Proc. ISEC'93, D.H. Logsdail and M.J. Slater (eds.), Elsevier Applied Science, London, UK, Vol. 2, p. 903-908, 1993.

Mihailov, M.H., A Correlation Between the Overall Stability Constants of Metal Complexes -I, Calculation of the Stability Constants Using the Formation Function n, *J. Inorg. Nucl. Chem.*, **36**, 107-113, 1974.

Mihailov, M.H., Mihailov, V.Ts., and Khalkin, V.A., A Correlation Between the Overall Stability Constants of Metal Complexes -II, Application of Data Obtained by the Polarographic Method for Metal-Inorganic Ligand Systems, *J. Inorg. Nucl. Chem.*, **36**, 115-120, 1974.

Mihaylov, I.O., Gallium Solvent Extraction from Sulphate Solutions Using Organophosphoric Acid Reagents (D2EHPA, OPAP), Ph.D. Thesis, McGill University, Montreal, 1991.

Milanova, M., Horozov, T., Nikolov, A., and Todorovsky, D., On the Liquid Membrane Extraction of Lanthanum and Neodymium, *Sep. Sci. Technol.*, **28(8)**, 1641-1646, 1993.

Mooiman, M. B., The Solvent Extraction of Precious Metals - A Review, Precious Metals 1993, R.K. Mishra (ed.), IPMI, Allentown, PA, p. 411-434, 1993.

Morrison, R.T., and Boyd, R.N., Organic Chemistry, 6th edition, Prentice Hall, Englewood Cliffs, NJ, 1992.

Nai-Fu, Z., Jinguang W., Partha K., Sarathy, Fuan, L., and Neuman, R.D., Comparison of Aggregates Formed by Acidic Organophosphorus Extractants and Metals (Ni and Co) in Solvent Extraction, in Solvent Extraction 1990, Proc. ISEC'90, T. Sekine (ed.), Elsevier Science Publishers, Amsterdam, Netherlands, part A, p. 165-170, 1992.

Nakano, M., Takahashi, K., and Takeuchi, H., A Method for Continuous Operation of Supported Liquid Membranes, *J. Chem. Eng. Japan*, **20(3)**, 326-328, 1987.

Nakashio, F., Goto, M., and Kondo, K., New Surfactants for Metal Extraction by Liquid Surfactant Membranes, in Solvent Extraction 1990, Proc. ISEC'90, T. Sekine (ed.), Elsevier Science Publishers, Amsterdam, The Netherlands, p. 1459-1468, 1992.

Neplenbroek, A.M., Bargeman, D., and Smolders, C.A., Nitrate Removal Using Supported Liquid Membranes: Transport Mechanism, *J. Membr. Sci.*, **67**, 107-119, 1992a.

Neplenbroek, A.M., Bargeman, D., and Smolders, C.A., Supported Liquid Membranes: Instability Effects, *J. Membr. Sci.*, **67**, 121-132, 1992b.

Neplenbroek, A.M., Bargeman, D., and Smolders, C.A., Mechanism of Supported Liquid Membrane Degradation: Emulsion Formation, *J. Membr. Sci.*, **67**, 133-148, 1992c.

Neplenbroek, A.M., Stability of Supported Liquid Membranes, Ph.D. Thesis, University of Twente, The Netherlands, 1989.

Noble, R.D., An Overview of Membrane Separations, *Sep. Sci. Technol.*, **22(2&3)**, 731-743, 1987.

Ohrbach, K.H., Kettrup, A., and Matuschck, G., Calcination of Platinum Group Complexes to Form Pure Metal, in Precious Metals 1988 (R.M. Nadkarni, ed.), IPMI, Allentown, PA, p. 117, 1988.

Osseo-Asare, K., Aggregation, Reversed Micelles, and Microemulsions in Liquid-Liquid Extraction: The Tri-n-Butyl Phosphate-Diluent-Water-Electrolyte System, *Adv. Colloid Interface Sci.*, **37**, 123-173, 1991.

Palmer, D.A., and Harris, G.M., Kinetics, Mechanism, and Stereochemistry of the Aquation and Chloride Anation Reactions of fac- and mer- Trichlorotriaquorhodium(III) Complexes in Acidic Aqueous Solution. A Complete Reaction Scheme for Complex Ions of the General Formula $[RhCl_n(OH_2)_{6-n}]^{3-n}$, *Inorg. Chem.*, **14(6)**, 1316-1321, 1975.

Pavelich, M.J., and Harris, G.M., Kinetics, Mechanism, and Stereochemistry of Chloride Anation of Chloropentaaquorhodium(III) Complex Ion in Aqueous Solution. An Approach for Distinguishing Between the Five-Coordinate-Intermediate and Ion-Pair-Interchange Mechanisms for Octahedral Complexes Containing at Least Two Water Ligands, *Inorg. Chem.*, **12(2)**, 423-431, 1973.

Postle, J.T., Roscoe, W.E., Watanabe, R.Y., and Martin, P.S., Review of Platinum Group Element Deposits in Ontario, Ministry of Northern Development and Mines, Ontario, 1986.

Pouskouleli, G., and Demopoulos, G.P., Direct Recovery of Precious Metals by Integration of Solvent Extraction and Hydrogen Reduction Techniques, in Precious Metals 1984, T.P. Mohide (ed.), IPMI, Allentown, PA, p. 189, 1985.

Pouskouleli, G., Kelebek, S., and Demopoulos, G. P., Recovery and Separation of Platinum and Palladium by Co-Extraction and Differential Stripping, in Separation

Processes in Hydrometallurgy, G.A. Davies (ed.), Ellis Harwood, Cheschiter, UK, p. 174-188, 1987.

Prasad, R., and Sirkar, K.K., Hollow Fiber Solvent Extraction: Performances and Design, *J. Membrane Sci.*, **50**, 153-175, 1990.

Prasad, R., Kiani, A., Bhave, R.R., and Sirkar, K.K., Further Studies on Solvent Extraction with Immobilized Interfaces in a Microporous Hydrophobic Membrane, *J. Membr. Sci.*, **26**, 79-97, 1986.

Read, M. C., Glaser, J., and Sandström, M., A ^{103}Rh Nuclear Magnetic Resonance Study of Rhodium(III) Bromide Complexes in Aqueous Solution, *J. Chem. Soc. Dalton Trans.*, 233-240, 1992.

Robb, W., and Harris, G.M., Some Exchange and Substitution Reactions of Hexachloro-rhodium(III) and Pentachloroaquorhodium(III) Ions in Aqueous Acid Solutions, *J. Amer. Chem. Soc.*, **87**, 4472-4476, 1965.

Robb, W., and Steyn, M.M. de V., Kinetics of Aquation of Aquopentachlororhodium(III) and Chloride Anation of Diaquotetrachlororhodium(III) Anions, *Inorg. Chem.*, **6(3),** 616-619, 1967.

Robinson, R.A., and Stokes, R.H., Electrolyte Solutions, Butterworth & Co., London, UK, 1959.

Ruppert, M., Draxler, J., and Marr, R., Liquid-Membrane-Permeation and Its Experiences in Pilot-Plant and Industrial Scale, *Sep. Sci., Technol.*, **23 (12&13),** 1659-1666, 1988.

Ryan, W., Non-Ferrous Extractive Metallurgy in the United Kingdom, IMM, London, UK, 1968.

Saito, T., Deterioration of Liquid Membrane and Its Improvement in Permeation Transport of Zn(II) Ion through a Supported Liquid Membrane Containing a Bathocuproine, *Sep. Sci. Technol.*, **27(1),** 1-9, 1992.

Saito, T., Selective Transport of Alkali and Alkaline Earth Metallic Ions through a Supported Liquid Membrane Containing Tripentyl Phosphate as a Carrier, *Sep. Sci. Technol.*, **28(8),** 1629-1640, 1993.

Saito, T., Transport of Cadmium(II) Ion through a Supported Liquid Membrane Containing a Bathocuproine, *Sep. Sci. Technol.*, **26(12),** 1495-1506, 1991.

Sato, Y., Kondo, K., and Nakashio, F., A Novel Membrane Extractor Using Hollow Fibers for Separation and Enrichment of Metal, *J. Chem. Eng. Japan*, **23(1),** 23-29, 1990.

Shukla, J.P., Kumar, A., and Singh, R.K., Macrocycle-Mediated Selective Transport of Plutonium(IV) Nitrate through Bulk Liquid and Supported Liquid Membranes Using Dicyclohexano-18-crown-6 as Mobile Carrier, *Sep. Sci. Technol.*, **27(4),** 447-465, 1992.

Sidgwick, N.V., The Chemical Elements and Their Compounds, Vol. II, Oxford, London, UK, p. 1511-1529, 1950.

Sillen, L.G., and Martel, A.E., Stability Constants of Metal-Ion Complexes, Special Publication No 25, The Chemical Society, London, UK, 1979.

Sillen, L.G., Stability Constants of Metal-Ion Complexes, Supplement No. 1, Part 1, Inorganic Ligands, The Chemical Society, London, UK, 1971.

Sillen, L.G., Stability Constants of Metal-Ion Complexes, The Chemical Society, London, UK, 2nd ed., 1964.

Stern, E.W., in Symp. on Recovery, Reclamation and Refining of Precious Metals, G. Foo, and M.E. Browing (Eds.), IPMI, Allentown, PA, p. 1-7, 1981.

Swaminathan, K., and Harris, G.M., Kinetics and Mechanism of the Reaction of Chloride Ion with Hexaaquorhodium(III) Ion in Acidic Aqueous Solution, *J. Amer. Chem. Soc.*, **88**, 4411-4414, 1966.

Szymanowski, J., and Sobczynska, A., Emulsifier Selection for Liquid Membrane System, Proc. Second Int. Conf. on Hydrometallurgy, ICHM'92, C. Jiayong (ed.), Changsha, China, p. 641-646, 1992.

Tanigaki, M., Ueda, M., and Eguchi, W., Facilitated Transport of Zinc Chloride through Hollow Fiber Supported Liquid Membranes. Part 2. Membrane Stability, *Sep. Sci. Technol.*, **23**, 1161-1169, 1988.

Teramoto, M., and Tanimoto, H., Mechanism of Copper Permeation through Hollow Fiber Liquid Membranes, *Sep. Sci. Technol.*, **18(10)**, 871-892, 1983.

Teramoto, M., Takihana, H., Shibutani, M., Yuasa, T., Miyake, Y., and Teranishi, H., Extraction of Amine by W/O/W Emulsion System, *J. Chem. Eng. Japan*, **14(2)**, 122-128, 1981.

Thorpe, T.E., Thorpe's Dictionary of Applied Chemistry, 4th edition, Longmans Green, London, Vol. X, p. 535, 1937/1956.

Tondre, C., and Boumezioud, M., Microemulsions as Model Systems to Study the Kinetics and Mechanism of Reactions Occurring in the Extraction of Metal Ions by Lipophilic Extractants: Complexation of Nickel(II) by 8-Hydroxyquinoline and Kelex 100, *J. Phys. Chem.*, **93**, 846-854, 1989.

Tondre, C., and Canet, D., On the Problem of Reaction Site in Biphasic Extraction of Metal Ions: NMR versus Spectrophotometric Evidence in Micellar Model Systems, *J. Phys. Chem.*, **95**, 4810-4813, 1991.

Tondre, C., Claude-Montigny, B., Ismael, M., Scrimin, P., and Tecilla, P., Copper(II) Complexation by Micelle-Solubilized Long-Chain Complexing Agents: Unusually Slow Reaction Rates, *Polyhedron*, **10(15),** 1791-1798, 1991.

Wang, X., Jiang, M., Liu, X., and Liu, Y., A New Process for Separating and Purifying Rhodium and Iridium from Concentrate Liquors, in Proc. First Intr. Conf. on Hydromet. (ICHM '88), Beijing, International Academic Publishers, p. 279-288, 1988.

Wiencek, J. M., and Qutubuddin, S., Microemulsion Liquid Membranes. I. Application to Acetic Acid Removal from Water, *Sep. Sci. Technol.*, **27(10),** 1211-1228, 1992a.

Wiencek, J. M., and Qutubuddin, S., Microemulsion Liquid Membranes. II. Copper Ion Removal from Buffered and Unbuffered Aqueous Feed, *Sep. Sci. Technol.*, **27(11),** 1407-1422, 1992b.

Wijers, M.C., Bargeman, D., Van den Boomgaard, Th., Leese, T.A., Tasker, P.A., and Thorp, D., Extraction of Copper from Dilute Solutions Using Acorga P50 Oxime in Hollow Fiber and Flat Sheet Supported Liquid Membranes, in Proc. Int. Symp. on Impurity Control and Disposal in Hydrometallurgical Processes, B. Harris and E. Krause (eds.), CIM, Toronto, p. 137-151, 1994.

Wilkinson, G., Gillard, R.D., and McCleverty, J.A., Comprehensive Coordination Chemistry, Vol. 4, Pergamon Press, Oxford, UK, 1987.

Wolsey, W.C., Reynolds, C.A., and Kleinberg, J., Complexes in the Rhodium(III)-Chloride System in Acid Solution, *Inorg. Chem.*, **2(3),** 463-468, 1963.

Work, R.A., and Good, M.L., Structural and Spectroscopic Characteristics of the Nonachlorodirhodate(III) Anion, *Inorg. Chem.*, **9(4),** 956-958, 1970.

Yamada, E., and Freiser, H., Mixed Ligand Chelate Extraction of Lanthanide Ions in Systems Involving 7-(1-Vinyl-3,3,6,6-tetramethylhexyl)-8-quinolinol, 8-Quinolinol, and 1, 10-Phenanthroline, *Anal. Chem.*, **53**, 2115-2117, 1981.

Zemaitis, J.F., Clark, D.M., Rafal, M., and Scrivner, N.C., Handbook of Aqueous Electrolyte Thermodynamics, AIChE, New York, USA, 1986.

Zha, F.F., Fane, A.G., and Fell, C.J.D., Liquid Membrane Processes for Gallium Recovery from Alkaline Solutions, *Ind. Eng. Chem. Res.*, **34**, 1799-1809, 1995.

Zha, F.F., Fane, A.G., and Fell, C.J.D., Phenol Removal by Supported Liquid Membranes, *Sep. Sci. Technol.*, **29(17),** 2317-2343, 1994.

Zha, F.F., Fane, A.G., Fell, C.J.D., and Schofield, R.W., Critical Displacement Pressure of a Supported Liquid Membrane, *J. Membrane Sci.*, **75**, 69-80, 1992.

APPENDIX A

UV-Visible Absorption Spectra and Calibration Curves for Aged Rh Solutions

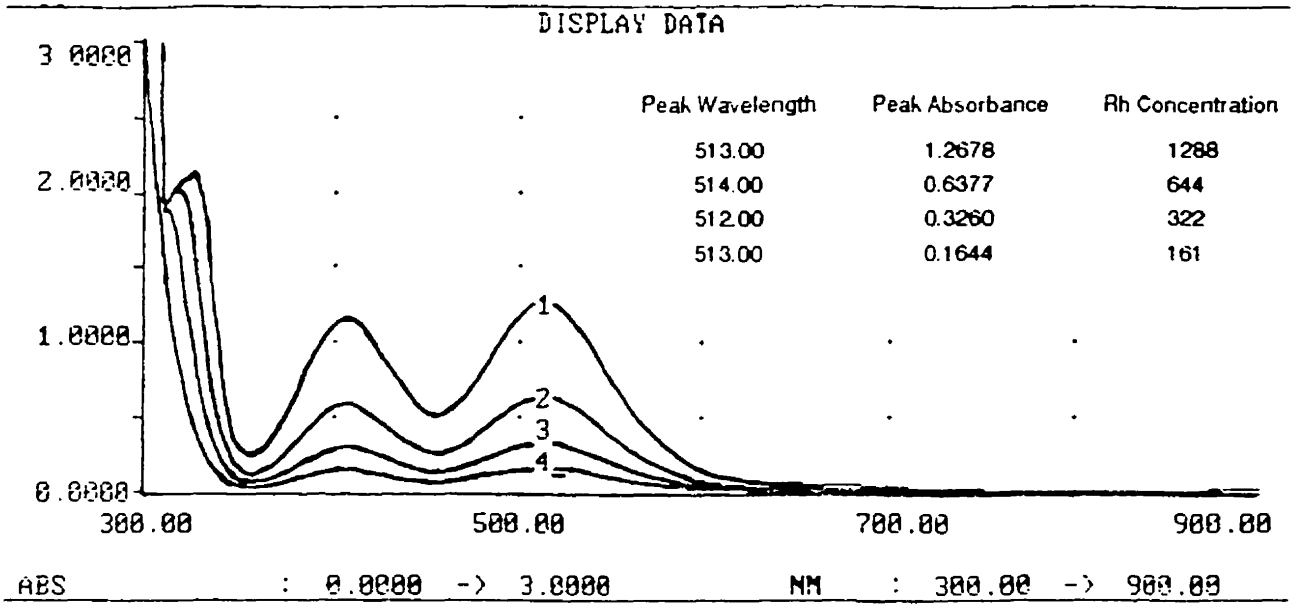

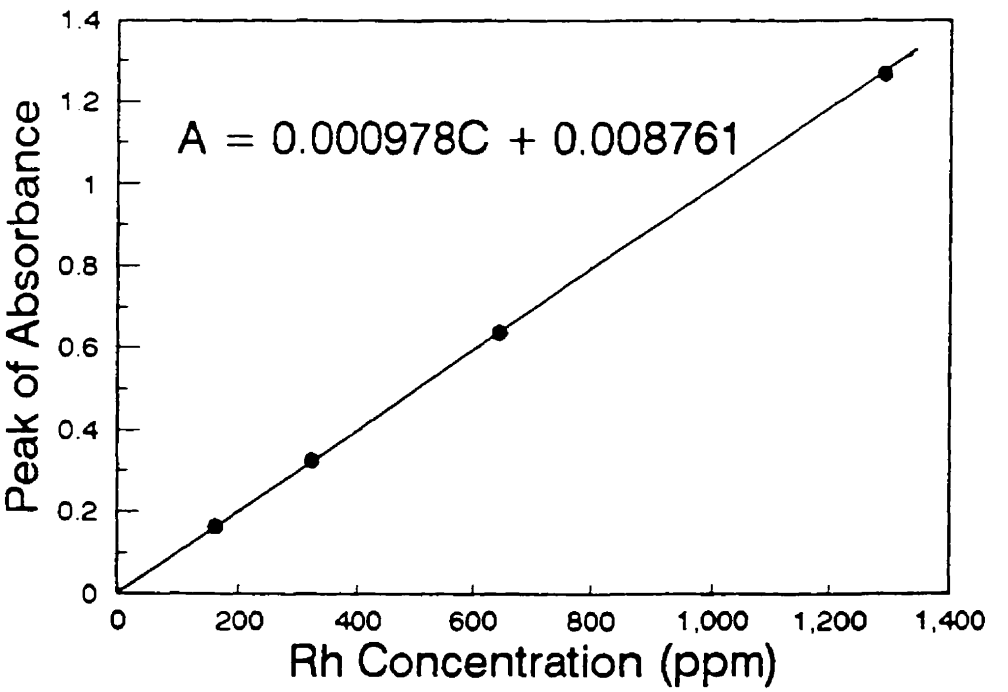

Figure A.1: Absorption Spectra and Calibration Curve for Aged Rh Solutions of 4.0 M HCl

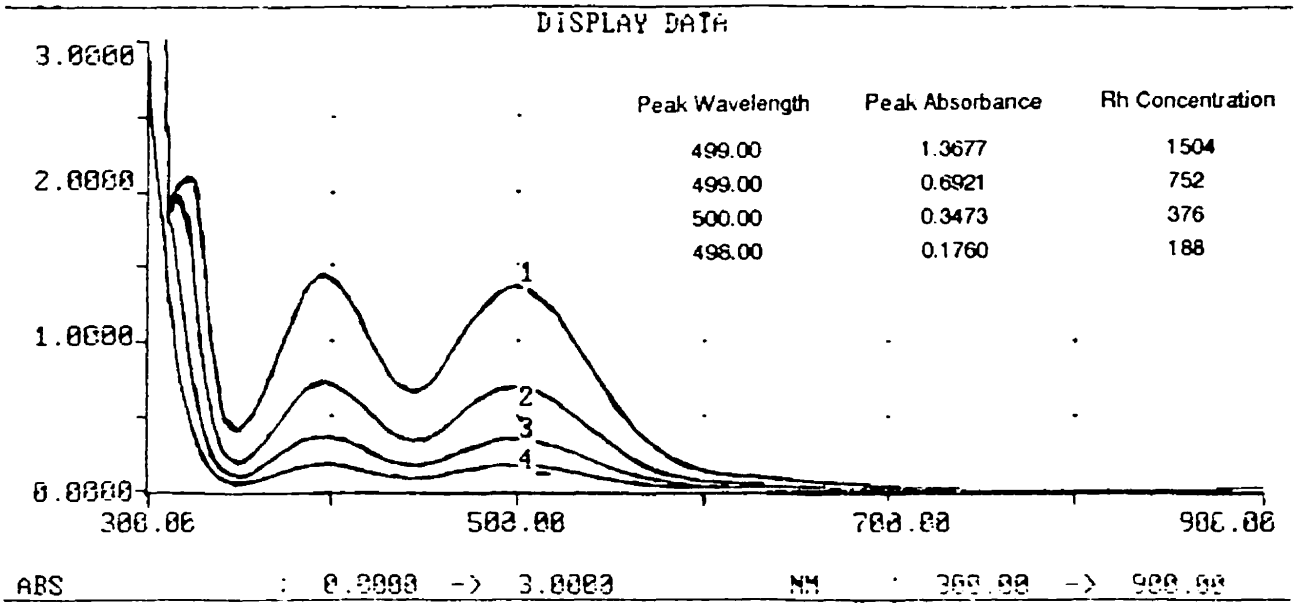

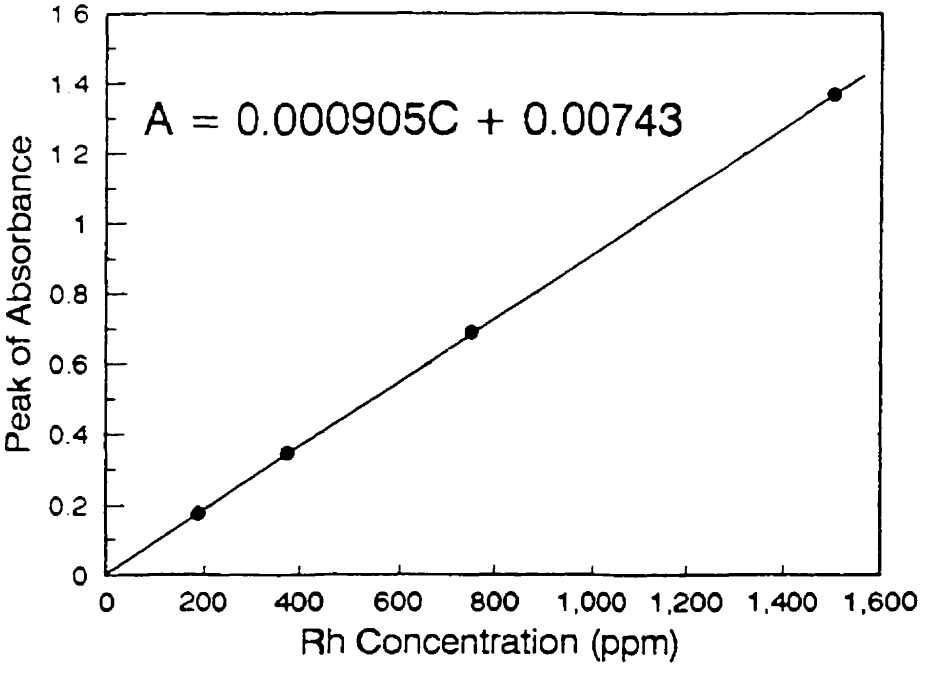

Figure A.2: Absorption Spectra and Calibration Curve for Aged Rh Solutions of 1.4 M HCl

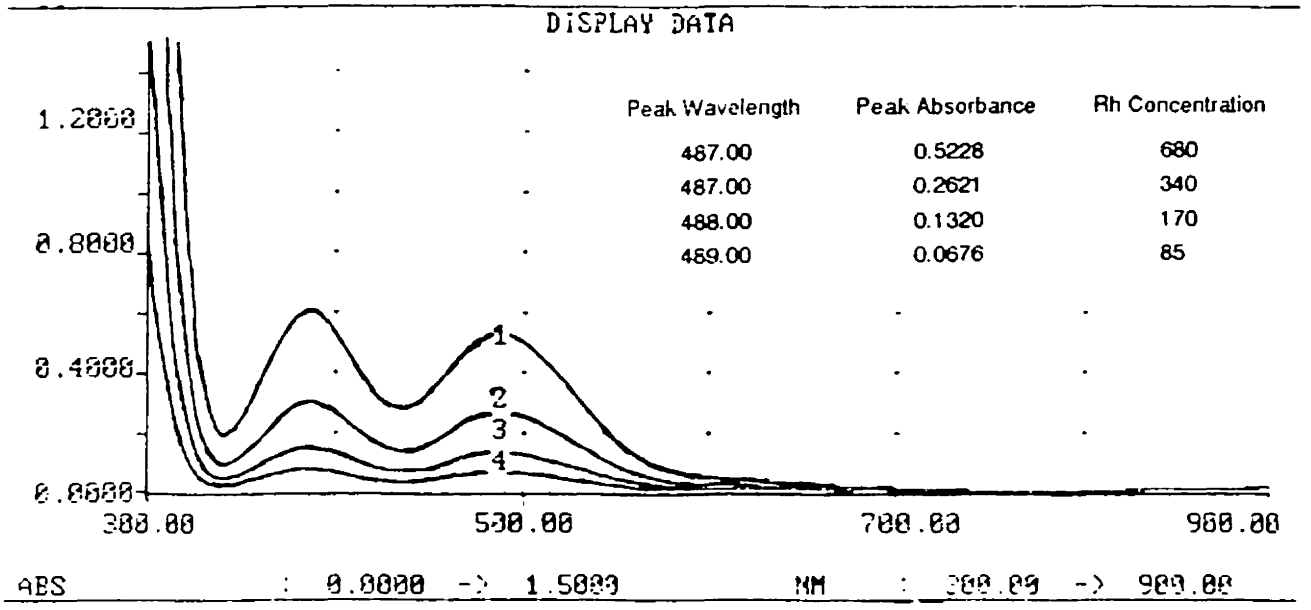

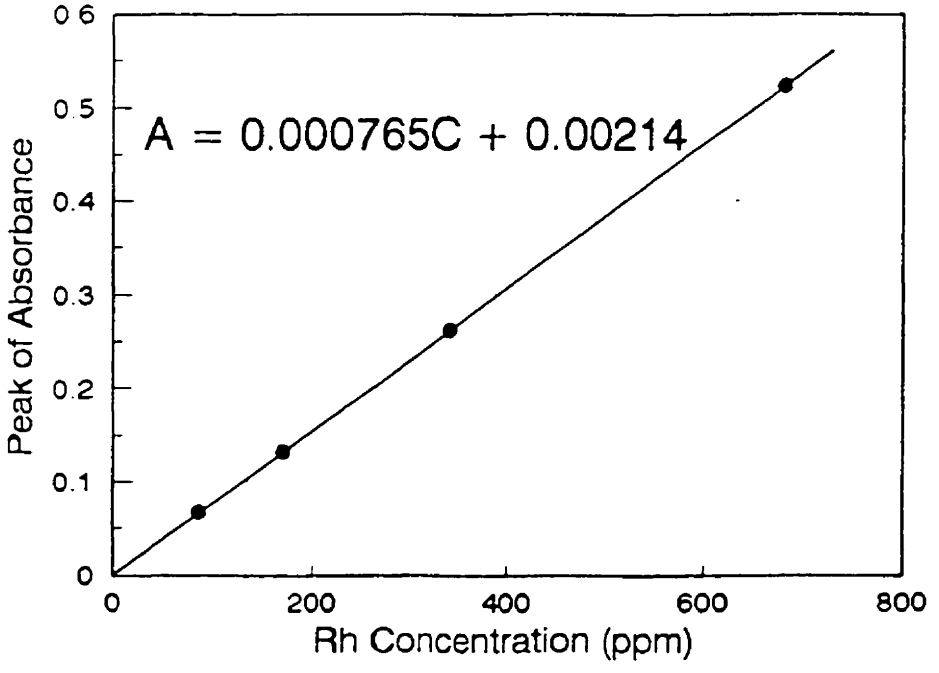

Figure A.3: Absorption Spectra and Calibration Curve for Aged Rh Solution of 0.1 M HCl

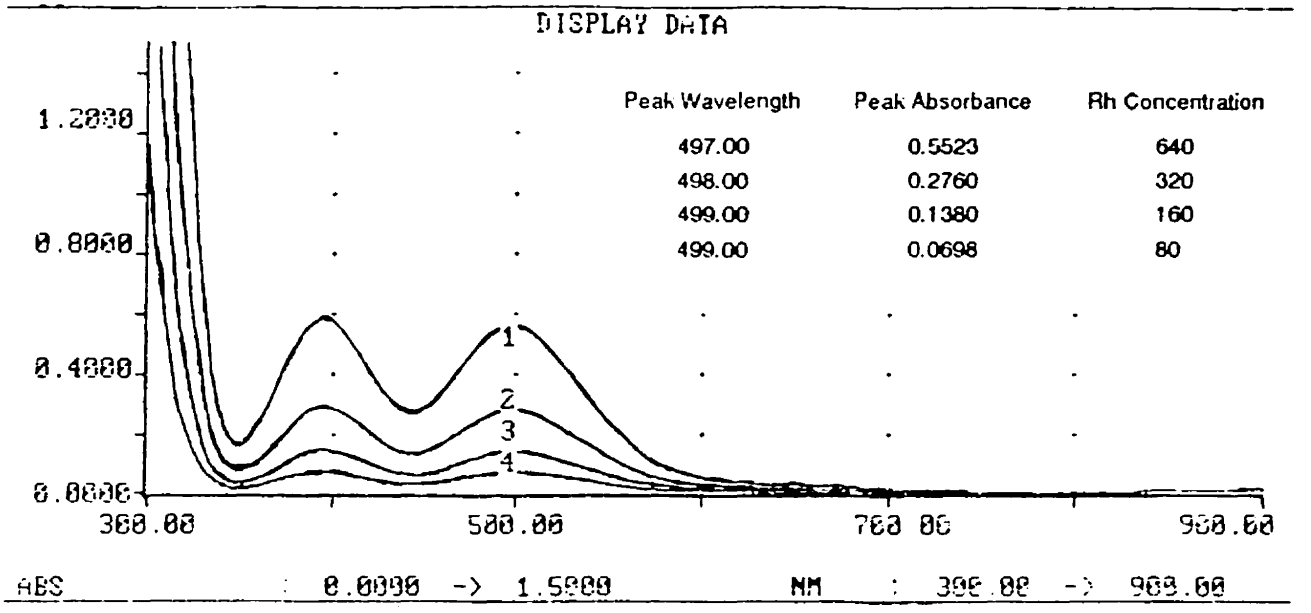

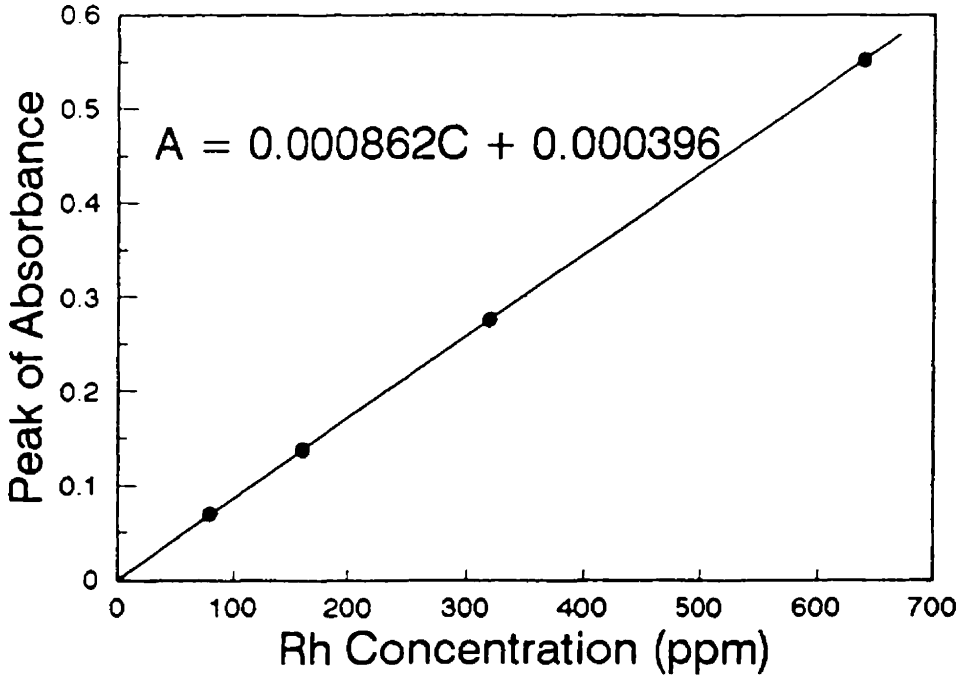

Figure A.4: Absorption Spectra and Calibration Curve for Aged Rh Solutions of 0.1 M HCl & 1 M NaCl

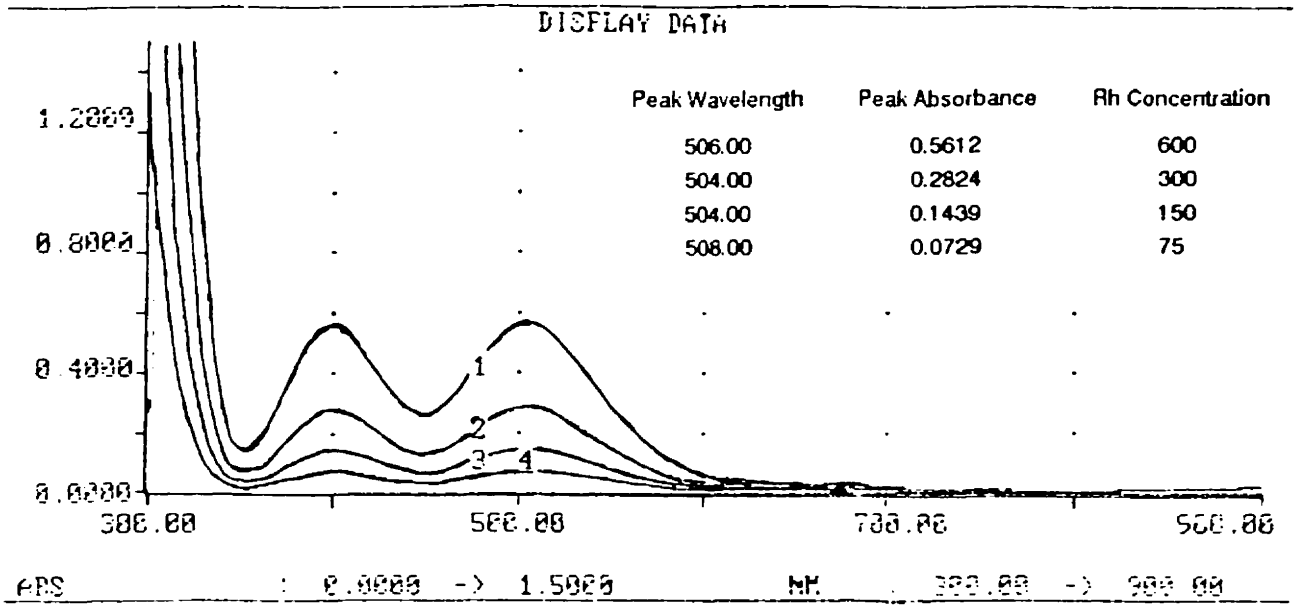

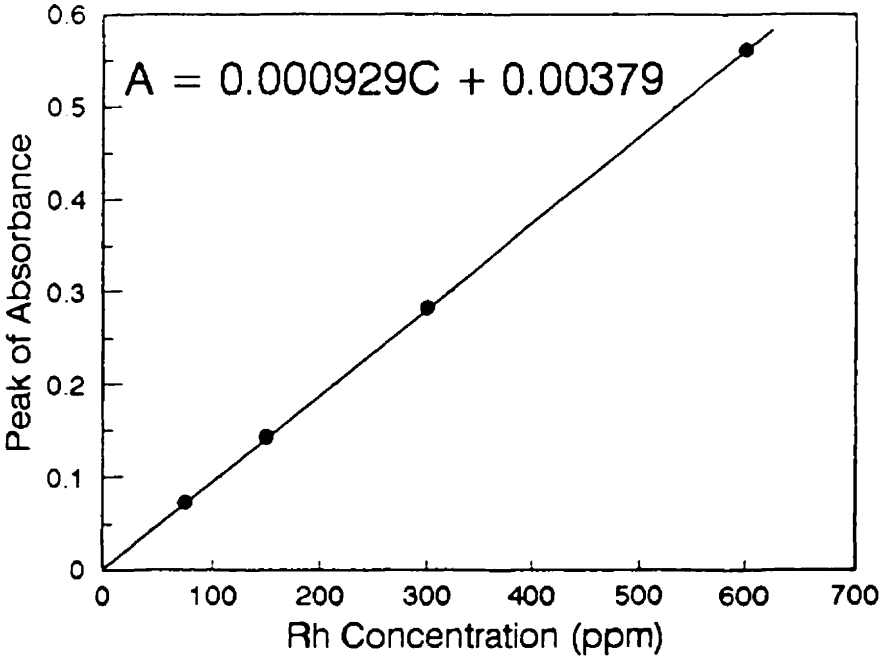

Figure A.5: Absorption Spectra and Calibration Curve for Aged Rh Solutions of 0.1 M HCl & 2 M NaCl

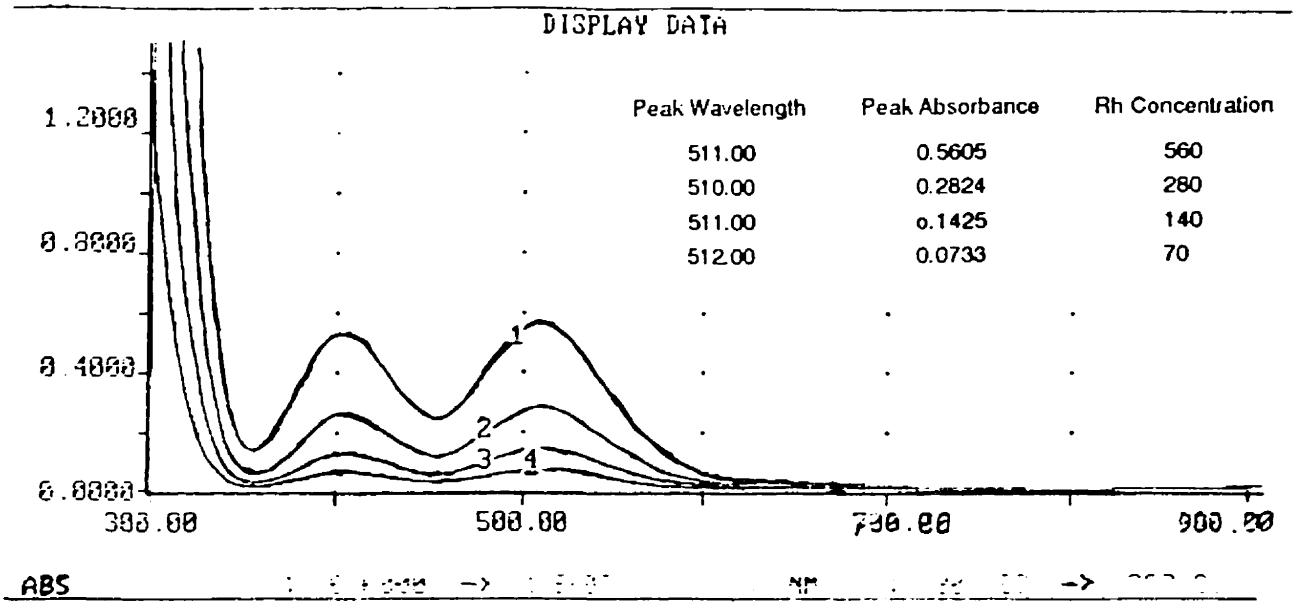

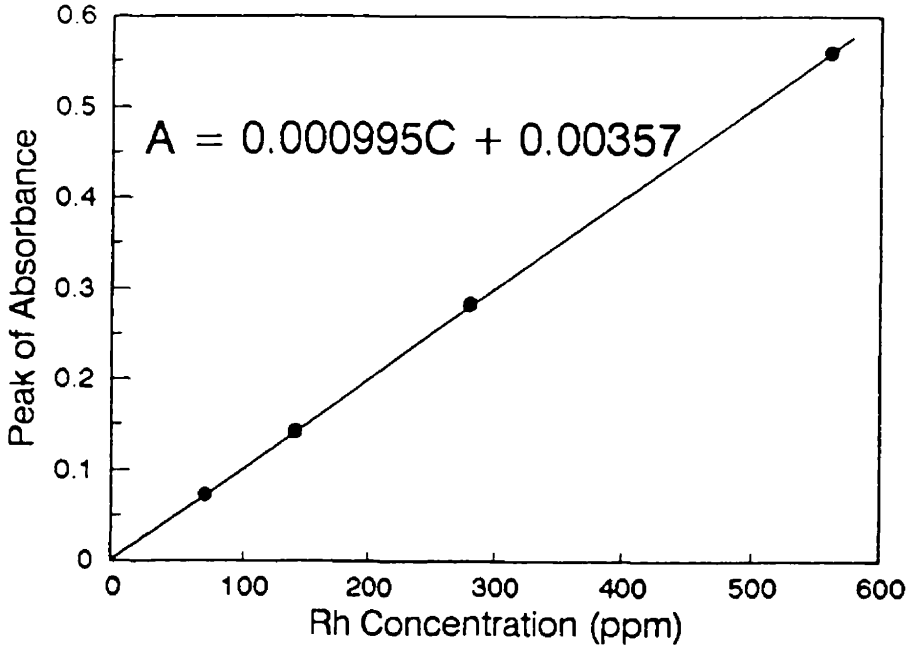

Figure A.6: Absorption Spectra and Calibration Curve for Aged Rh Solutions of 0.1 M HCl & 3 M NaCl

APPENDIX B

Estimation of HCl Activities

B.1 Single HCl Solutions

The activity of acid ($\mathbf{a}_{HCl}$), as the main driving force for SLM permeation process, has been calculated using the following equations (Zemaitis et al., 1986). For a 1:1 electrolyte such as HCl or NaCl:

$$\mathbf{a} = \mathbf{a}_+ \mathbf{a}_- = \mathbf{a}_\pm^2 \tag{B.1}$$

$$\gamma_\pm^2 = \gamma_+ \gamma_- \tag{B.2}$$

$$m_\pm^2 = m_+ m_- = m^2 \qquad \Rightarrow \qquad m_\pm = m \tag{B.3}$$

$$\gamma_\pm = \frac{\mathbf{a}_\pm}{m_\pm} = \frac{\mathbf{a}_\pm}{m} \tag{B.4}$$

where $\boldsymbol{a}$, m, and γ denote activity, molality, and activity coefficient, respectively. The subscripts + and - refer to the cation and anion of the electrolyte, while subscript ± refers to the mean activity ($\mathbf{a}_\pm$), molality ($m_\pm$), and activity coefficient ($\gamma_\pm$) of the solute. Therefore, the following relations hold for HCl in single or mixed electrolyte solutions:

$$\mathbf{a}_{H^+} = \gamma_{H^+} m_{H^+} \tag{B.5}$$

$$\mathbf{a}_{Cl^-} = \gamma_{Cl^-} m_{Cl^-} \tag{B.6}$$

$$\mathbf{a}_{HCl} = \gamma_{H^+} m_{H^+} \gamma_{Cl^-} m_{Cl^-} \tag{B.7}$$

$$\mathbf{a}_{HCl} = \gamma_\pm^2 m_{H^+} m_{Cl^-} \tag{B.8}$$

Meanwhile, the molality and molarity of electrolytes are related via following equation:

$$m_i = \frac{M_i}{\rho - 0.001 \sum_i M_i W_i} \tag{B.9}$$

where W_i is the molar weight of the solute i, ρ is the density of the solution, M is the concentration of solute in molarity units (moles per liter solution), and m is the concentration of solute in molality units (moles per kilogram water).

The data for a number of HCl solutions (Zemaitis et al., 1986) are tabulated in Table B.1.

Table B.1: Activity of HCl vs Acid Concentration (Bromley, 1973)

m_{HCl}	density* (g/mL)	M_{HCl}	$\gamma_{\pm HCl}$	a_{HCl}
0.1	0.997	0.0993	0.799	0.0064
0.2	0.999	0.1984	0.773	0.0239
0.3	1.000	0.2967	0.764	0.0525
0.4	1.002	0.3950	0.762	0.0930
0.5	1.003	0.4925	0.765	0.1464
0.6	1.005	0.5901	0.771	0.2141
0.7	1.006	0.6866	0.780	0.2978
0.8	1.008	0.7835	0.790	0.3992
0.9	1.009	0.8792	0.802	0.5210
1.0	1.011	0.9754	0.815	0.6642
1.5	1.018	1.4477	0.900	1.8237
2.0	1.026	1.9124	1.013	4.1028
2.5	1.033	2.3666	1.152	8.2930

* Density data taken from Robinson and Stokes (1959).

Using the activity data provided in Table B.1 the activity gradient of $(a_{HCl})_f$-$(a_{HCl})_s$ for a feed solution of varying HCl concentrations from 0.1 to 0.7 M HCl and a strip solution of 0.1 M HCl was calculated. These data were presented in Figure 5.8. In a similar fashion the activity of HCl for strip solutions with varying acidities from 0.1 M to 0.6 M HCl was calculated. The data were presented in Figure 5.9.

B.2 Binary HCl-NaCl Solutions

To investigate further the driving force for the permeation process it was necessary to estimate acid and proton activities in the presence of NaCl. The estimation of activities in this case was made with the aid of the Meissner's method (Meissner and Kusik, 1972; Meissner, 1980). The parameters and equations used in the method are:

$q_{HCl} = 6.69$

$q_{NaCl} = 2.23$

$$q_{mix} = \frac{I_{H^+}}{I_{tot}} q_{HCl} + \frac{I_{Na^+}}{I_{tot}} q_{NaCl} + \frac{I_{Cl^-}}{I_{tot}} q_{HCl} \qquad \text{(B.10)}$$

$$B = 0.75 - 0.065q \qquad \text{(B.11)}$$

$$C = 1 + 0.055q \times \exp(-0.023 I^3) \qquad \text{(B.12)}$$

$$\log \Gamma^* = \frac{-0.5107\sqrt{I_{tot}}}{1 + C\sqrt{I_{tot}}} \qquad \text{(B.13)}$$

$$\Gamma_{HCl} = [1 + B(1 + 0.1 I_{tot})^q - B]\Gamma^* \qquad \text{(B.14)}$$

$$\Gamma_{HCl} = \gamma_{\pm}^{\nu/z_+ z_-} \quad \text{;for HCl} \quad z_+ = z_- = 1 \quad \Rightarrow \quad \Gamma_{HCl} = \gamma_{\pm HCl} \qquad \text{(B.15)}$$

$$\mathbf{a}_{HCl} = \gamma_{\pm HCl}^2 m_{H^+} . m_{Cl^-} \qquad \text{(B.16)}$$

where q_{HCl} and q_{NaCl} are the characteristic parameters of HCl and NaCl; I_H, I_{Na}, and I_{Cl} are fractions of the ionic strengh due to specific individual ions and I_{tot} is the total ionic strength; Γ is the reduced activity coefficient, $\gamma_{\pm}$ mean activity coefficient, and **a** is the activity of HCl. The description of the method is beyond the scope this thesis.

The activity of HCl for two different sets of solutions, i.e., of 0.1 and 0.7 M HCl containing various amounts of NaCl, was calculated through the above method and the calculated results are tabulated in Tables B.2 and B.3. This was done to correlate the activity of HCl with the rate of acid permeation (re Figures 5.5 and 5.6). To simplify this comparison, the data of the latter two tables are also presented in Figures B.1 and B.2. As shown, the acid activity for the solution of 0.1 M HCl increases with the salt concentration, with a similar trend as the rate of acid permeation decreases (Figure 5.5). Similarly, the increase in acid activity versus salt concentration for a feed solution of 0.7 M HCl follows the same trend as that of the rate of acid permeation, depicted in Figure 5.6. However, the latter correspondence holds only for the low acid region, i.e., for the region at which Kelex 100 is not yet fully protonated. Upon fully protonation of the extractant, there is no further increase in the rate of acid permeation. This is another manifestation of the fact that the transport of Rh is coupled to that of HCl.

Table B.2: Activity of HCl in mixed HCl/NaCl Strip Solutions

$M_{HCl} + M_{NaCl}$ (mol/L)	density* (g/mL)	m_{HCl} (mol/kg H_2O)	m_{NaCl} (mol/kg H_2O)	I_{total}	$\gamma_{\pm HCl}$	a_{HCl}
0.1 + 0.0	0.9979	0.1006	0.000	0.1006	0.788	0.0063
0.1 + 0.5	1.0178	0.1015	0.5077	0.6092	0.721	0.0321
0.1 + 1.0	1.0376	0.1025	1.0251	1.1276	0.753	0.0656
0.1 + 1.5	1.0559	0.1037	1.5550	1.6587	0.8133	0.1138
0.1 + 2.0	1.0739	0.1049	2.0978	2.2027	0.8912	0.1835
0.1 + 2.5	1.0916	0.1062	2.6540	2.7605	0.984	0.2838

*Density of the solutions was measured using picnometers. A thermostated bath was used to keep the temperature of the solutions at 25 °C during the volumetric measurements.

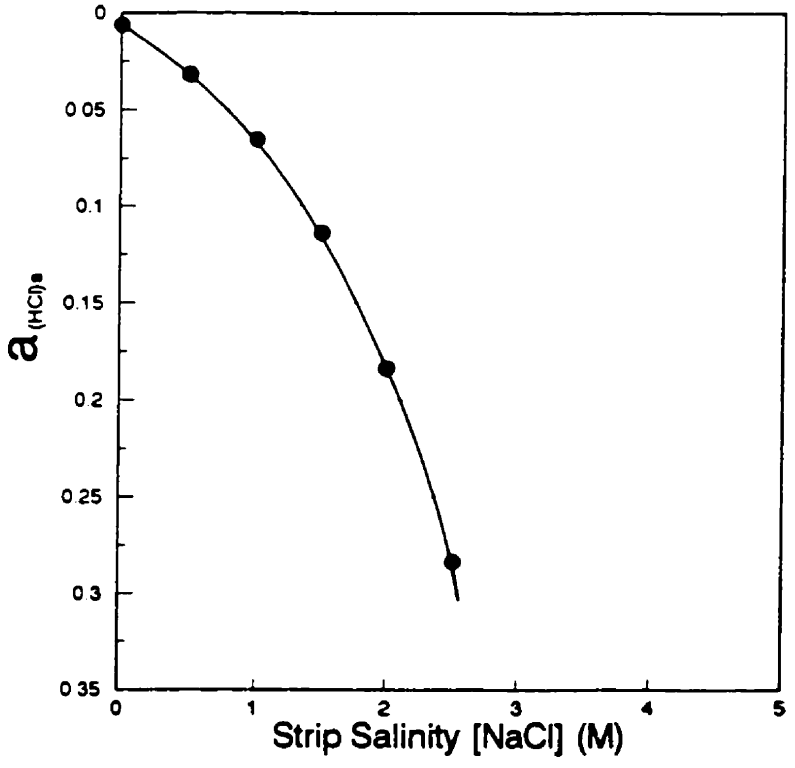

Figure B.1: Activity of HCl in SLM Strip Phase vs Strip Salinity

Table B.3: Activity of HCl in Mixed HCl/NaCl Solutions

$M_{HCl} + M_{NaCl}$ (mol/L)	density* (g/mL)	m_{HCl} (mol/kg H_2O)	m_{NaCl} (mol/kg H_2O)	I_{total}	$\gamma_{\pm HCl}$	a_{HCl}
0.7 + 0.0	1.006	0.714	0.000	0.7140	0.747	0.2844
0.7 + 0.5	1.026	0.7208	0.5149	1.2357	0.797	0.5659
0.7 + 1.0	1.045	0.7282	1.0404	1.7685	0.870	0.9752
0.7 + 1.5	1.064	0.7365	1.5783	2.3148	0.961	1.5729
0.7 + 2.0	1.082	0.7452	2.1291	2.8743	1.066	2.4325
0.7 + 2.5	1.099	0.7548	2.6956	3.4504	1.188	3.6745

*Density of the solutions was measured using picnometers. A thermostated bath was used to keep the temperature of the solutions at 25 °C during the volumetric measurements.

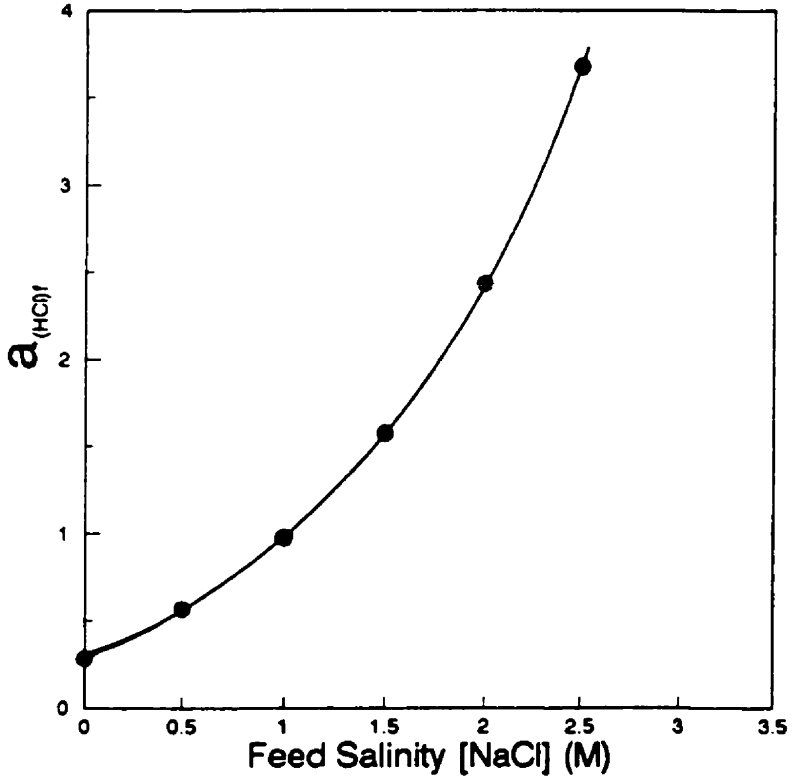

Figure B.2: Activity of HCl in SLM Feed Phase vs Feed Salinity

APPENDIX C

A UV-Visible Investigation of the Aquation of Rh(III) Chlorocomplexes

Rh(III) in chloride solutions is known to undergo aquation resulting in the formation of mixed aquo-chloro complexes; $RhCl_{6-n}(H_2O)_n^{(3-n)+}$. The relevant literature on the subject has been critically reviewed by Benguerel et al. (1996). Due to the possession of unfilled "d" orbitals, all of the ten isomers of Rh(III) aquo-chlorocomplexes (Mann and Spencer, 1982) exhibit absorption bands at the visible region (Butler and Harrod, 1989) and, thus their aqueous solutions are colored. This property of the aquo-chlorocomplexes of Rh(III) was used to monitor the aquation process via the use of UV-Visible spectroscopy. The UV-Visible absorption spectrum of an aged (i.e., equilibrated) Rh(III) solution is shown in Figure C.1 (this is Fig. 3.3 reproduced here for the purpose of completeness). The presence of two characteristic absorption bands at approximately 400 and 500 nm, respectively, is evident. The position of the two bands was found to shift with HCl (Figure C.1) or Cl^- concentration (Table C.1). The observed shift in the wavelengths of the absorption peaks (Figure C.1 and Table C.1) was associated with the changes in the color of the solution, from orange-peach to cherry-red with increasing HCl/Cl^- concentration, which, in turn, reflect the variable degree of aquation (Benguerel et al., 1996). The observed shift of one of the characteristic absorption peaks of aged (equilibrated) Rh(III) solutions with Cl^- concentration is illustrated in Figure C.2. As one can see, a shift towards higher wavelengths occurs with increasing the chloride ion concentration. No shift occurs beyond 6 M. This implies that aquation is effectively stopped beyond that concentration level.

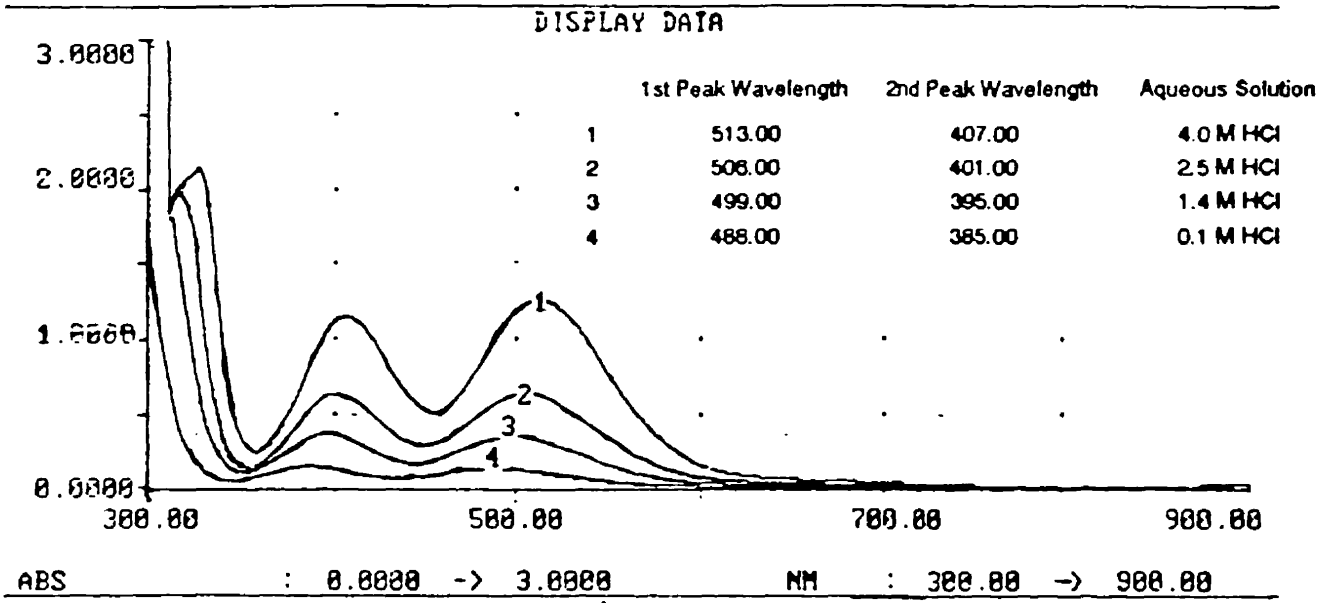

Figure C.1: Absorption Spectra for Aged Rh Solutions at Different HCl Concentrations

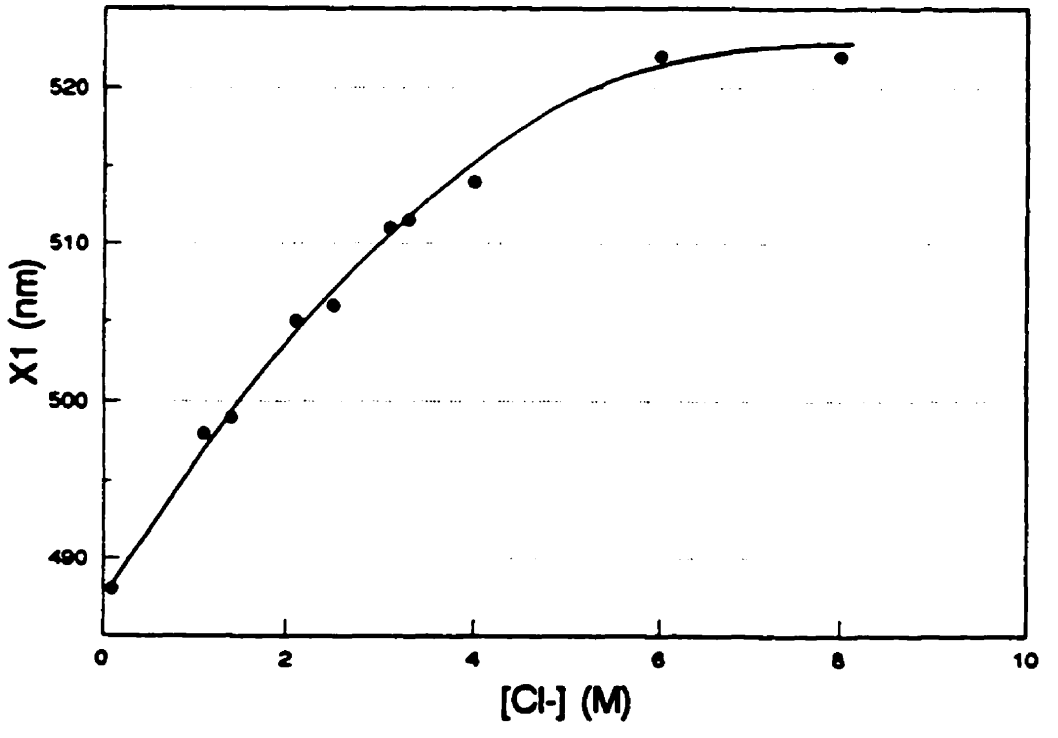

Figure C.2: The Shift of One of the Absorption Bands (500 nm) with Cl⁻ concentration
(Aqueous Solution: 0.1 M HCl, 400 ppm Rh, 3-week aged)

Table C.1: Location of the Absorption Bands as a Function of [Cl⁻] for 3-week Aged (equilibrated) Solutions

$[Cl^-]$ (M)	X_1 (nm)	X_2 (nm)
0.1	488.00	385.00
1.1	498.00	394.50
1.4	499.00	395.00
2.1	505.00	401.00
2.5	506.00	401.00
3.1	511.00	404.00
3.3	511.50	405.00
4.0	513.00	407.00
6.0	522.00	--
8.0	522.00	--

The solution always contained 0.1 M HCl, & 400 ppm Rh, 3-week aged. Proper amounts of NaCl was added to adjust $[Cl^-]$.

The shift of the absorption bands was used to monitor the progress of aquation (aging) in a freshly-prepared, and low in Cl^- concentration (0.1 M HCl), Rh(III) solution prepared using Na_3RhCl_6. The results of this investigation are presented in Table C.2. Comparison of these measurements with those of equilibrated (aged) Rh(III) solutions (Table C.1) reveals the 5-min solution to be practically free of aquation (its absorption bands correspond to an equilibrated solution of ≥ 4 M Cl^-, i.e., the dominant rhodium complex in this solution is $RhCl_6^{3-}$ and this explains its high extraction degree (re data of Table 6.4)). On the other hand, the spectrum of the 100-hr aged solution has the same peaks with the 3-week equilibrated solution of the same Cl^- concentration (i.e., 0.1 M HCl; Figure C.1).

The equilibration time can be shorten if the Rh(III) solution is subjected to heating. The effect of heating on equilibration was studied from both sides of the equilibrium position, i.e., aquation (forward direction of eq. (6.3)) and anation (backward direction of eq. (6.3)). The UV-Visible spectroscopic measurements are summarized in Table C.3. As

shown, the equilibrium was reached within 4 hours, where heating at 70 °C was applied. The obtained results of this investigation are in agreement with previously published NMR data (Mann and Spencer, 1982).

Table C.2: Monitoring of Aquation

Age of Solution	Absorption Peak Location	
	X_1 (nm)	X_2 (nm)
5 min	515.00	407.00
4 hr	499.00	393.50
8.5 hr	494.00	391.00
24 hr	492.50	390.00
48 hr	491.00	388.50
75 hr	488.00	387.00
100 hr	487.00	385.50

The solution was 0.1 M HCl and contained 400 ppm Rh.

Table C.3: Effect of Temperature on Aquation-Anation of Rh(III) Solutions

Initial Rh Solution	Fresh		4 hr Heated at 70 °C Prior to Measurement		Reaction Direction
	X_1 (nm)	X_2 (nm)	X_1 (nm)	X_2 (nm)	
1.4 M NaCl + **A**	511.00	405.00	499.00	395.00	Aquation
1.4 M NaCl + **B**	488.00	385.00	499.00	395.00	Anation
2.0 M NaCl + **A**	512.00	405.00	505.00	401.00	Aquation
2.0 M NaCl + **B**	488.00	385.00	505.00	401.00	Anation

A: 0.1 M HCl fresh Rh solution of 400 ppm.
B: 0.1 M HCl 2-week aged solution of 400 ppm.